Biomolecular Materials Principal Investigators' Meeting–2013

August 19–21, 2013

Hilton Washington DC North/Gaithersburg, Gaithersburg, MD

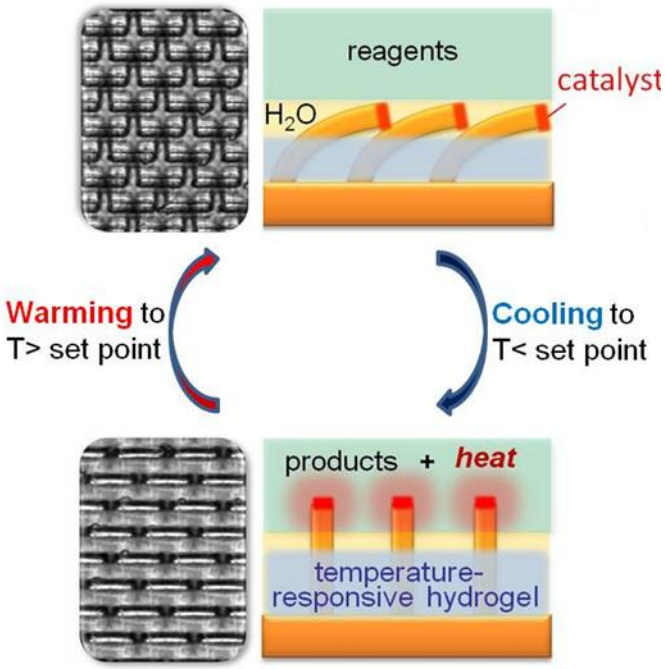

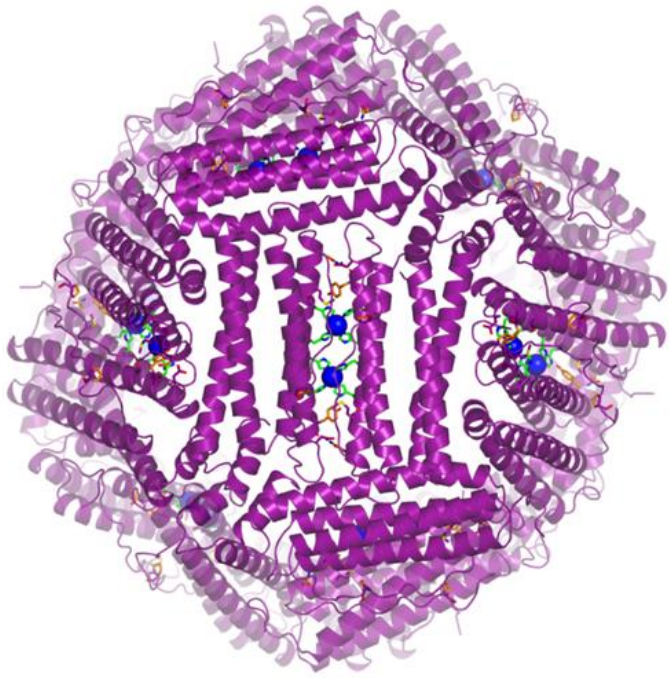

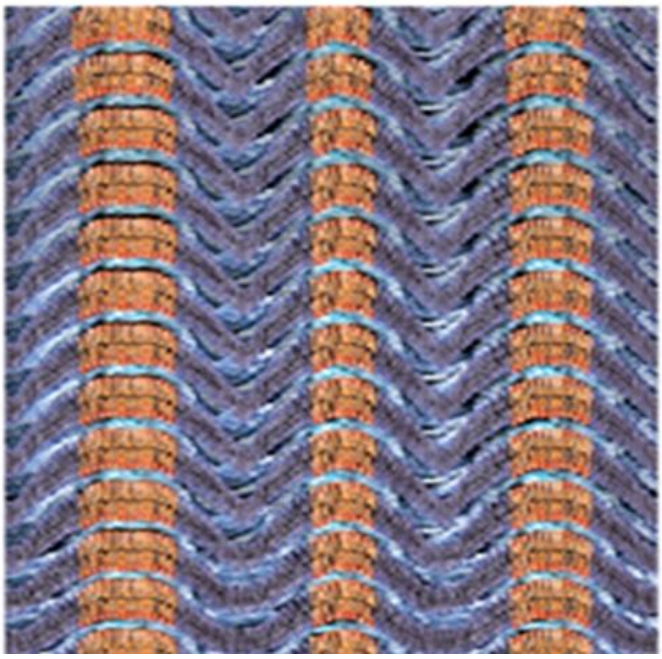

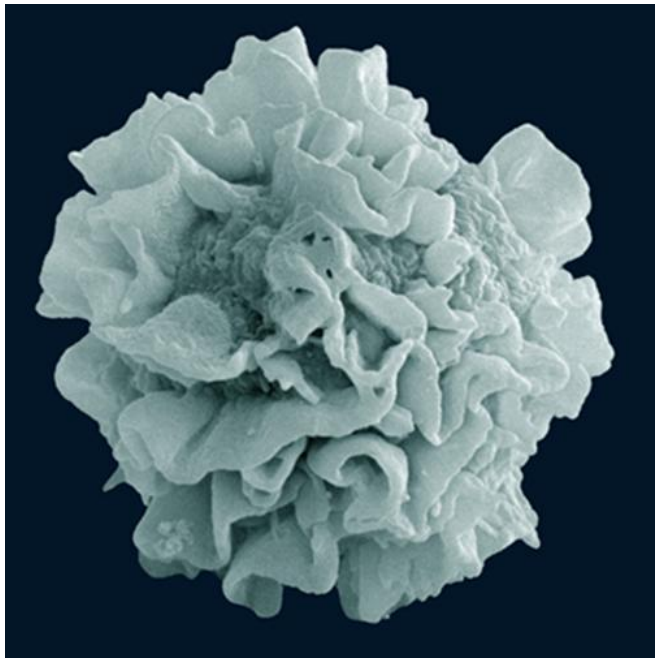

U.S. DEPARTMENT OF ENERGY | Office of Science

Office of Basic Energy Sciences
Materials Sciences and Engineering Division

On the Cover

Top Left: Schematic of the temperature-regulating bioinspired homeostatic material showing a feedback loop, in which mechanical action of temperature-responsive gel is coupled with an exothermic reaction.
Courtesy: *Dr. Joanna Aizenberg, Harvard University*

Top Right: Crystal structure of cage-like protein ferritin formed using reverse metal-templated interface redesign (rMeTIR) process, which transforms a natural protein-protein interface into one that only engages in selective response to a metal ion (interfacial copper coordination sites are highlighted as blue spheres).
Courtesy: *Dr. F. Akif Tezcan, University of California, San Diego*

Bottom Left: A schematic depiction of mesoscale ordering of liquid-ordered domains in liquid-disordered surroundings in co-existing lipid phases in membrane multilayers.
. ` ***Courtesy***: *Dr. Atul Parikh, University of California, Davis*

Bottom Right: Scanning electron micrograph of a surface ruffled 10 μm diameter silica particle synthesized from an RBL-2H3 cell using the silica cell replication (SCR) process.
Courtesy: *Dr. Jeffrey Brinker, Sandia National Laboratories*

This document was produced under contract number DE-AC05-06OR23100 between the U.S. Department of Energy and Oak Ridge Associated Universities.

The research grants and contracts described in this document are supported by the U.S. DOE Office of Science, Office of Basic Energy Sciences, Materials Sciences and Engineering Division.

Foreword

This volume comprises the scientific content of the 2013 Biomolecular Materials Principal Investigators' Meeting sponsored by the Materials Sciences and Engineering (MSE) Division in the Office of Basic Energy Sciences (BES) of the U. S. Department of Energy (DOE). The meeting, held on August 19–21, 2013 at the Hilton Washington DC North/Gaithersburg in Gaithersburg, Maryland, is the fifth such meeting on this topic, and is one of several research theme-based Principal Investigators' Meetings conducted by BES. The meeting's focus is on research at the intersection of materials sciences and biology, and the agenda at this year's meeting is representative of many of the major scientific areas supported by the Biomolecular Materials program. In addition, this meeting will provide an opportunity to consider how this program may continue to evolve over the next ten years to support DOE's mission. As has been the case for other BES Principal Investigators' Meetings, previous meetings have been highly valued and cherished by the participants for the opportunity to see the entire research program, learn about the latest results/advances, develop new ideas, and forge new collaborations. The meeting will also help MSE in assessing the state of the program, identifying new research directions and recognizing programmatic needs.

The Biomolecular Materials Core Research Activity (CRA) formally came into existence following the recommendations of a workshop sponsored by the Basic Energy Sciences Advisory Committee (BESAC) in 2002. In addition, recent BES workshops and The National Academies' reports have clearly identified mastering the capabilities of living systems as a Grand Challenge that could provide the knowledge base to discover, design, and synthesize new materials with totally new properties for next-generation energy technologies. To address these goals, the Biomolecular Materials program supports fundamental research in the discovery, design and synthesis of functional materials and complex structures based on principles and concepts of biology. The major programmatic focus is on the design and scalable creation of robust energy-relevant materials and systems with collective behavior, which rival or exceed biology's extraordinary effectiveness for controlling matter, energy, and information.

I genuinely look forward to this meeting and hope that it will be as fruitful as past BES Principal Investigators' Meetings. It is a great pleasure to express my sincere thanks to all of the attendees for their active participation and sharing their ideas and new research results. The advice and help of Meeting Chairs, Monica Olvera de la Cruz and Igor Aronson, in organizing this meeting are deeply appreciated. My hearty thanks also go to Teresa Crockett in MSE and Tammy Click and her colleagues at the Oak Ridge Institute for Science and Education (ORISE) for their outstanding work in taking care of all the logistical aspects of the meeting.

Mike Markowitz
Program Manager, Biomolecular Materials
Materials Sciences and Engineering Division
Office of Basic Energy Sciences
U.S. Department of Energy

Agenda

2013 Biomolecular Materials
Principal Investigators' Meeting Agenda

Meeting Chairs: **Igor Aronson** and **Monica Olvera de la Cruz**
Argonne National Laboratory / Northwestern University

Monday, August 19, 2013

7:15 – 8:15 am	***** **Breakfast*****
8:15 – 9:00 am	*Introductory Remarks* **Arvind Kini** Team Lead for Materials Discovery, Design and Synthesis, Materials Sciences & Engineering Division, Basic Energy Sciences
9:00 – 9:15 am	**Mike Markowitz**, Program Manager, Biomolecular Materials Meeting Chairs: **Igor Aronson** and **Monica Olvera de la Cruz** Argonne National Laboratory / Northwest University
Session 1	**Materials and Systems with Programmable Function** Chair: **Igor Aronson**, Argonne National Laboratory
9:15 – 10:00 am	**Zhibin Guan,** University of California, Irvine *Adaptive and Self-Healing Materials via Dynamic Non-covalent and Covalent Interactions*
10:00 – 10:30 am	***** **Break** *****
10:30 – 11:15 am	**George Whitesides,** Harvard University *Dynamic Self-Assembly, Emergence, and Complexity*
11:15 – 12:00 pm	**Paul Chaikin,** New York University *Self-Assembly and Self-Replication of Novel Materials from Particles with Specific Recognition*
12:00 – 1:30 pm	***** **Working Lunch/ Poster Introductions** *****
1:30 – 3:30 pm	***** **Poster Session 1** *****
Session 2	**How Will Biomolecular Materials Continue to Evolve Over the Next 10 Years?** Chair: **Monica Olvera de la Cruz**, Northwestern University
3:30 – 3:50 pm	**Mike Markowitz,** Program Manager, Biomolecular Materials *Where We Started, How We Have Grown, and Things to Consider Going Forward*
3:50 – 4:10 pm	**Sharon Glotzer,** University of Michigan *Computational Materials Science and Chemistry: Accelerating Discovery and Innovation through Simulation-Based Engineering and Science (BESAC Report)*
4:10 – 4:30 pm	**Roger French,** Case Western Reserve University *From Quanta to the Continuum: Opportunities for Mesoscale Science (BESAC Report)*
4:30 – 4:50 pm	**Anna Balazs,** University of Pittsburgh *Materials Council Workshop on Dissipative Assembly*
4:50 – 5:30 pm	**General Discussion**
5:30 – 7:00 pm	***** **Poster Session 1 (Continued)*****
7:00 – 8:30 pm	**Dinner and Meeting Discussions**

Tuesday, August 20, 2013

7:00 – 8:00 am	***** **Breakfast*****
Session 3	**Science Driven by New Tools and Computational Modeling** Chair: **David Erickson**, Cornell University
8:00 – 8:45 am	**Tanya Prozorov,** Ames Laboratory *Emergent Atomic and Magnetic Structures*
8:45 – 9:30 am	**Jim De Yoreo,** Pacific Northwest National Laboratory *Directed Organization of Functional Materials at Inorganic-Macromolecular Interfaces*
9:30 –10:00 am	*****Break*****
10:00 – 10:45 am	**Adrian Parsegian,** University of Massachusetts-Amherst *Long Range van der Waals-London Dispersion Interactions for Biomolecular and Inorganic Nanoscale Assembly*
10:45 – 11:30 am	**Anna Balazs,** University of Pittsburgh *Integrating Modeling and Experiments to Design Robust Self-Healing Materials*
11:30 – 1:00 pm	***** **Working Lunch/ Poster Introductions** *****
1:00 – 3:00 pm	***** **Poster Session 2** *****
Session 4	**Synthesis and Dynamic Assembly: Cellular Templates, Artificial Cells, and Capsules** Chair: **Sarah Heilshorn**, SLAC National Accelerator Laboratory
3:00 – 3:45 pm	**Jeff Brinker,** Sandia National Laboratories *Complex Nanocomposites Directed by Cells*
3:45 – 4:30 pm	**Daniel E. Morse,** University of California, Santa Barbara *Enzymatic Synthesis of Semiconductors: Directed Evolution of Silicatein, the Silica-Synthesizing Enzyme (and Advantages of Kinetically Controlled Catalytic Synthesis)*
4:30 – 5:15 pm	**Daniel Hammer**, University of Pennsylvania *Designing Smart, Responsive Communicating Microcapsules from Polymersomes*
5:15 – 7:00 pm	***** **Poster Session 2 (Continued)*****
7:00 – 8:30 pm	**Dinner and Meeting Discussions**

Wednesday, August 21, 2013

7:15 – 8:15 am	***** **Breakfast** *****
Session 5	**Materials for Energy Conversion** Chair: **Samuel I. Stupp**, Northwestern University
8:15 – 9:00 am	**Donald A. Bryant,** Pennsylvania State University *A Hybrid Biological/Organic Photochemical Half-Cell for Generating Dihydrogen*
9:00 – 9:45 am	**Trevor Douglas,** Montana State University *Multicomponent Protein Cage Architectures for Photocatalysis*
9:45 – 10:30 am	**Michael Strano,** Massachusetts Institute of Technology *A Plant Nanobionic Approach to Enhance Solar Energy Conversion of Extracted Chloroplasts using Spontaneously Assembled Nanoparticles*

10:30 – 11:00 am	*****Break*****
11:00 – 12:00 pm	*Remarks, Concluding Comments* **Igor Aronson** and **Monica Olvera de la Cruz**, Meeting Chairs **Mike Markowitz**, Program Manager, Biomolecular Materials
12:00 – 1:00 pm	**Lunch, Open Discussions, and Adjourning Comments** (Optional Box Lunches Available)

Table of Contents

Table of Contents

University Grant Projects

LABORATORY PROJECTS

Program Title: Dynamics of Active Self-Assembled Materials

Principal Investigator: Igor S. Aronson, Co-Investigator: Alexey Snezhko
Mailing Address: Materials Science Division, Argonne National Laboratory, 9700 South Cass Avenue, Argonne, IL60439
E-mail: aronson@anl.gov

Program Scope

Self-assembly, a natural tendency of simple building blocks to organize into complex architectures, is a unique opportunity for materials science. The in-depth understanding of self-assembly paves the way for the design of tailored smart materials for emerging energy technologies, such as materials that can self-heal, regulate porosity, strength, water or air resistance, viscosity, or conductivity. However, self-assembled materials pose a formidable challenge: they are intrinsically complex, with often-hierarchical organization occurring on many nested length and time scales. Our approach is a combination of in-depth theoretical and experimental studies of the dynamics of active self-assembled material for the purpose of control, prediction, and design of novel bio-inspired materials for emerging energy applications.

In the past three years our program yielded discoveries of self-assembled magnetic swimmers and robots, drastic reduction of viscosity in suspensions of swimming bacteria, extraction of useful energy from chaotic movement of microswimmers. For all these systems we have developed theoretical descriptions leading to prediction and control of the emergent self-assembled structures. In the next three years we will explore new approaches to synthesis and discovery of a broad range of self-assembled bio-inspired materials stemming from the advances of our program: functional 2D and 3D tunable colloidal networks built from elementary functionalized sub-units, design of bio-mechanical hybrids such as living liquid crystals.

The project synergistically integrates theory, simulations, and experiments, and focuses on the fundamental issues at the forefront of contemporary materials science. On the theoretical side we consider a theory and large-scale molecular dynamics simulations, implemented on Graphic Processing Units (GPU), of active self-assembly in the systems of magnetic nano- and microparticles, swimming microorganisms, and a mesoscale description (phase field models) of self-organization in active biological systems. We actively use unique fabrication, characterization, and computational user facilities in Argonne National Laboratory: Center for Nanoscale Materials, Advance Photon Source, and Leadership Computing Facility.

Recent progress

Viscosity controls the dynamic self-assembly in ferromagnetic suspension. Studies of dynamic self-assembly in ferromagnetic colloid suspended in liquid-air or liquid-liquid interfaces revealed a rich variety of dynamic structures ranging from linear snakes to axisymmetric asters, which exhibit novel morphology of the magnetic ordering accompanied by large-scale hydrodynamic flows. Based on controlled experiments and

first principles theory, we demonstrate that the transition from snakes to asters is governed by the viscosity of the suspending liquid where less viscous liquids favor snakes and more viscous, asters, see Figure 1. By obtaining analytic solutions of the time-averaged Navier-Stokes equations, we gain insight into the role of mean hydrodynamic flows and an overall balance of forces governing the self-assembly. Our results illustrate that the viscosity can be used to control the outcome of the dynamic self-assembly in magnetic colloidal suspensions. Our observations provide a nontrivial insight into how the long-range hydrodynamic forces, usually assumed to be unimportant in colloidal self-assembly, become critical players determining the shape and organization of the emergent dynamic structures.

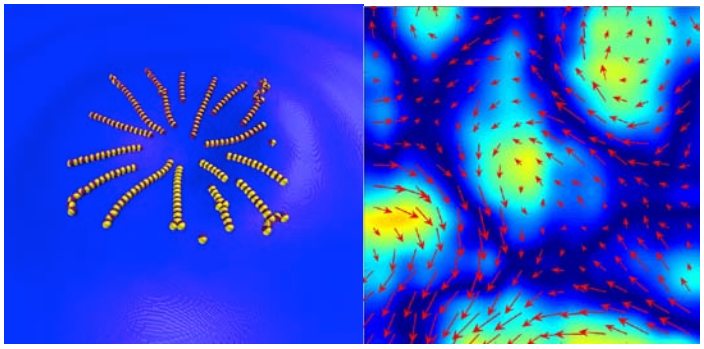

Figure 1. *Left:* Magnetic aster formed via an axisymmetric ordering of ferromagnetic chains aligned along the induced surface elevation, simulation performed on the GPU cluster in ANL [1]. *Right:* Self-organized vortices formed by bacteria swimming together in water, arrows show the direction of swimming, and colors depict the strength of vortices created by the bacteria [2].

Properties of collective motion in suspensions of self-propelled particles. Novel experiments on suspensions of swimming bacteria *Bacillus subtilis* produced a puzzling result: the amount of energy injected by bacteria into the liquid increases with the increase in the number of bacteria and their swimming speed, which intuitively presumes more intensive stirring of the liquid, see Figure 1. However, our experiments show that the bacteria self-organize into large vortices and swirls whose size does not depend on the number of bacteria or how fast they swim. This discovery highlights two fundamental mechanisms of bacterial self-organization: hydrodynamic interactions and collisions; for both of these mechanisms, the change of the swimming speed or number of bacteria alters only the overall time scales of the collective motion. A suspension of microswimmers, the simplest realization of active matter, exhibits novel material properties: emergence of a collective motion, reduction in viscosity, increase in diffusivity, and extraction of a useful energy. These findings are crucial for further development of biomechanical systems utilizing the collective motion of subunits to achieve useful functions.

Future Plans

Self-assembled tunable colloidal networks. Surfaces decorated with dense arrays of microscopic fibers exhibit unique materials properties, including superhydrophobicity and low friction. Nature relies on "hairy" surfaces to protect blood capillary from wear and infections (endothelial glycocalyx). We initiated studies of self-assembled tunable networks of microscopic polymer fibers formed by sticky colloidal particles. Preliminary studies revealed a large variety of self-assembled networks, ranging from dense colloidal "fur" to highly interconnected gels, see Figure 2. The networks emerge via dynamic self-assembly in the alternating electric field from a non-aqueous suspension of "sticky"

polymeric colloidal particles with a controlled degree of polymerization. The resulting architectures can be further tuned by the frequency and amplitude of the electric field and surface properties of the particles. We demonstrate, by coating the fibers with a thin layer of SnO_2 using atomic layer deposition, that the networks can serve as templates for transparent conductor. These self-assembled tunable materials are promising candidates for large surface area electrodes in batteries and organic photovoltaic cells, as well as for microfluidic sensors and filters.

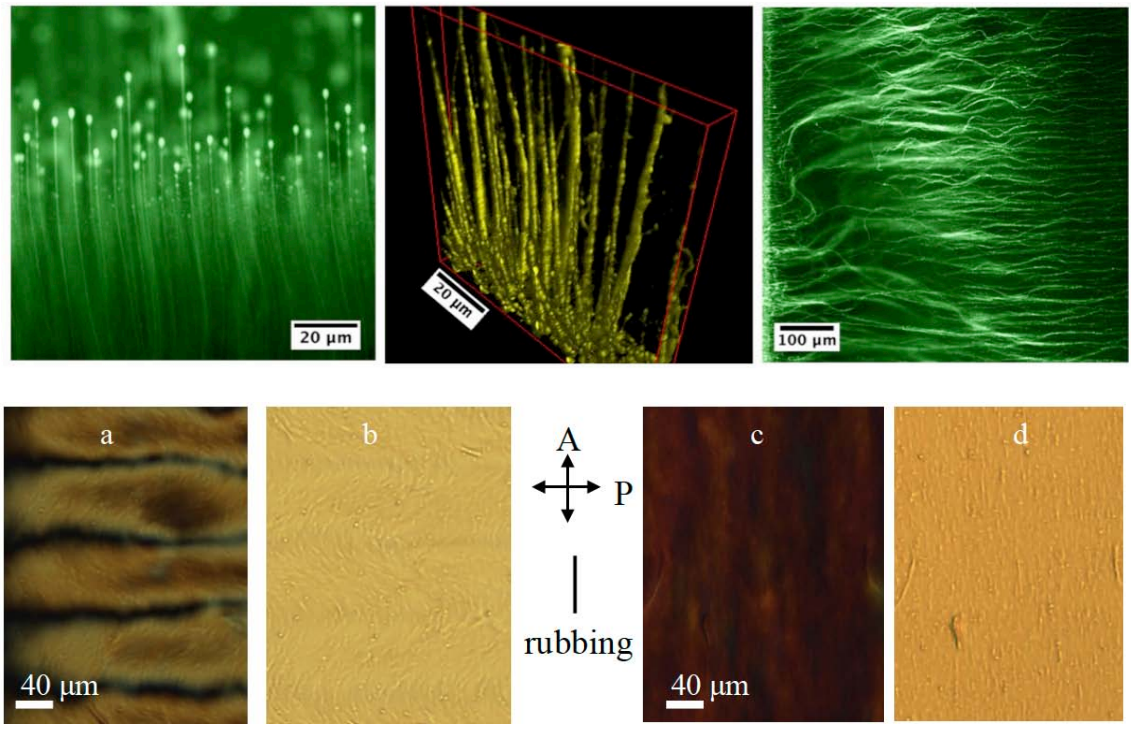

Figure 2. *Top row***:** Examples of self-assembled colloidal networks. Fibers-mushrooms formed at a low degree of polymerization; 3D reconstruction of a permanent self-assembled array of polymer fibers from the stacks of 2D confocal images. Colloidal fur is formed from highly polymerized colloidal epoxy particles. *Bottom row:* Living liquid crystal. Set of cross-polarized and bright-field images (P indicates the polarizer angle) for living (a-b) and dead bacteria (c-d) in LC. Individual bacteria are seen as short rods in the bright-field images (b,d). While living bacteria form wavy periodic patterns in the LC, dead bacteria align along the rubbing direction.

Biomechanical hybrid materials are an emerging class of engineered soft composites with the ability to move and reconfigure their structure and properties in response to external stimuli. Similar to their biological counterparts, they can transduce energy stored in the environment to drive systematic movements. We are exploring these biomechanical hybrid materials by combining two seemingly incompatible concepts: living swimming bacteria and inanimate but highly structured lyotropic liquid crystal – living liquid crystal (LLC). LLC can be actuated and controlled by the amount of oxygen available to bacteria, by the concentration of ingredients or by the temperature. We are exploring the simplest

representative of a LLC - a living nematic, see Figure 2. Our preliminary studies revealed a wealth of intriguing phenomena, caused primarily by the coupling between the activity-triggered flows and LC director reorientations. Among these are spontaneous formations of pairs of topological point defects in the LLC with degenerate and weak surface anchoring, stripe instabilities of the director in strongly surface anchored samples, broken chiral symmetry of the director patterns in the wake of moving bacteria, coupling between the LLC orientational order and the trajectory of the bacteria, and even local nematic-isotropic phase transition triggered by the shear flows produced by the bacteria. LLC makes possible a direct visualization of micro-flows excited by the nanometers-wide bacterial flagella. Due to hydrodynamic coupling between the nematic director and the flagella beating we were able to observe the flagella's pitch and rotation rate. Our work suggests an unorthodox design concept of reconfigurable microfluidic chambers for control and manipulation of individual bacteria. Besides an obvious importance to active matter, our studies can result in valuable biosensing and biomedical applications.

References (which acknowledge DOE support)

1. Piet, D. L., Straube, A. V., Snezhko, A., & Aranson, I. S. (2013). Viscosity control of the dynamic self-assembly in ferromagnetic suspensions. *Physical Review Letters*, **110**(19), 198001.
2. Sokolov, A., & Aranson, I. S. (2012). Physical properties of collective motion in suspensions of bacteria. *Physical Review Letters*, **109**(24), 248109.
3. Peshkov, A., Aranson, I. S., Bertin, E., Chaté, H., & Ginelli, F. (2012). Nonlinear field equations for aligning self-propelled rods. *Physical Review Letters*, **109**(26), 268701.
4. Harvey, C. W., Du, H., Xu, Z., Kaiser, D., Aranson, I., & Alber, M. (2012). Interconnected Cavernous Structure of Bacterial Fruiting Bodies. *PLoS computational biology*, **8**(12), e1002850.
5. Melhus, M. F., & Aranson, I. S. (2012). Effect of vibration on solid-to-liquid transition in small granular systems under shear. *Granular Matter*, **14**(2), 151-156.
6. Harvey, C. W., Alber, M., Tsimring, L. S., & Aranson, I. S. (2013). Continuum modeling of myxobacteria clustering. *New Journal of Physics*, **15**(3), 035029.
7. Dobnikar, J., Snezhko, A., & Yethiraj, A. (2013). Emergent colloidal dynamics in electromagnetic fields. *Soft Matter*, **9**, 3693-3704 , *invited review*
8. Kokot, G., Snezhko, A., & Aranson, I. S. (2013). Emergent coherent states and flow rectification in active magnetic colloidal monolayers. *Soft Matter*. **9**, 6757-6760
9. Ziebert, F., Swaminathan, S., & Aranson, I. S. (2012). Model for self-polarization and motility of keratocyte fragments. *Journal of The Royal Society Interface*, **9**(70), 1084-1092.
10. Ziebert, F., & Aranson, I. S. (2013). Effects of Adhesion Dynamics and Substrate Compliance on the Shape and Motility of Crawling Cells. *PloS one*,**8**(5), e64511.
11. Aranson, I. S. (2013). Collective behavior in out-of-equilibrium colloidal suspensions. *Comptes Rendus Physique*, *invited review*
12. Potomkin, M., Gyrya, V., Aranson, I., & Berlyand, L. (2013). Collision of microswimmers in a viscous fluid. *Physical Review E*, **87**(5), 053005.
13. Aranson, I.S. (2013) Active Colloids, *Phys. Usp.* **56,** 79-92**,** *invited review*
14. Kolmakov, G. V., Schaefer, A., Aranson, I., & Balazs, A. C. (2012). Designing mechano-responsive microcapsules that undergo self-propelled motion. *Soft Matter*, **8**(1), 180-190.

Active Assembly of Dynamic and Adaptable Materials: Active Protein Assemblies

Principal Investigator: George D. Bachand
Co-Investigators: Erik Spoerke, Mark Stevens, and Darryl Sasaki
Mailing Address: Nanosystems Synthesis & Analysis Department, Sandia National Laboratories, PO Box 5800, MS 1303, Albuquerque, NM 87185
Email: gdbacha@sandia.gov

Program Scope

The *Active Assembly of Dynamic and Adaptable Materials* research program examines fundamental materials science issues at the intersection of biology, nanomaterials, and hybrid interfaces. The overall program goal is to understand nature's strategies for non-equilibrium materials assembly, and apply these principles in hybrid or composite materials whose assembly and organization can be programmed, and/or "self-directed." More specifically, we are exploring materials systems that exhibit adaptive behaviors based on the use of energy consuming proteins and/or synthetic analogs capable of removing the constraints imposed by diffusion and chemical equilibria. Research tasks are focused on (1) the active assembly of hybrid nanomaterials based on motor protein-driven transport and dynamic polymerization of cytoskeletal filaments, and (2) the design and exploration of "artificial microtubules" that can mimic the dynamic, non-equilibrium behaviors of the natural filaments in synthetic systems

Many of unique behaviors found in living systems (e.g., self-replication, adaptivity) are commonly associated with dynamic self-assembly processes.[1] The interactions responsible for such self-assembly depend strongly on the dissipating of energy, commonly through enzymatic reactions that alter biomolecular interactions. Our program has focused on the components involved in one of nature's active transport systems, specifically microtubules (MTs) and their associated motor proteins (Fig. 1). MTs are hollow filaments composed of αβ tubulin dimers whose energy-dissipative assembly is used to push, pull, or rearrange the cell's cytoskeleton. These filaments also serve as "train tracks" for the bidirectional transport of macromolecules and organelles by the motor proteins kinesin and dynein through the conversion of chemical energy into mechanical work. Living organisms use the concerted and dynamic interactions between kinesin and MTs for physiological processes ranging from chromosomal segregation at the cellular level to macroscopic color changing behaviors at the organismal level.[2] Thus, learning to exploit, mimic, and/or translate the role of active proteins in emergent biological behaviors represents an opportunity to dramatically advance nanomaterials assembly.

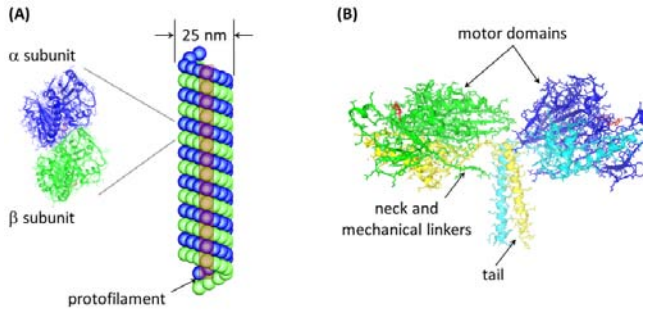

Fig. 1. (A) Crystal structures of tubulin and diagram showing an assembled microtubule (MT) filament. (B) Crystal structure of a kinesin motor protein.

Recent Progress

This abstract will highlight on the recent progress on program's work in the active assembly of hybrid nanomaterials based on kinesin-driven transport and dynamic assembly of MTs.

MT Filament Growth via Fusion

MT polymerization proceeds through a spontaneous nucleation and growth process.[3] However, we recently characterized a new growth mechanism in which MT length increased significantly over extended periods of time (i.e., days to weeks). In contrast to increased length based on dimer addition during polymerization, we observed end-to-end self-organization of stabilized MT filaments, leading to the formation of extended 1D structures with lengths up to 200 μm. In our proposed mechanism, MT polymerization proceeds through dimer addition until the dimer concentration reaches a sub-critical concentration at which time a phase transition occurs, and the self-organization and "fusion" of MT becomes the dominate growth mechanism. Fusion of tubules was first observed as part of molecular dynamics simulations of artificial MT assembly (Fig. 2). Here, wedge-shaped monomers initially assembled into of rings that stacked to form short tubules. Fusion and annealing of tubules was occasionally noted.[4] Additional simulations suggest that fusion occurs when the vertical interaction strength is ~7 k_BT, which is similar to the published value of ~9.5 k_BT for natural tubulin dimers.[5] Coincident with these simulations, we experimentally observed that the length taxol-stabilized MTs increased significant over the course of weeks, while the number of MTs decreased. Together these results raised the question: "do actual MTs self-organize and fuse to form extended structures?"

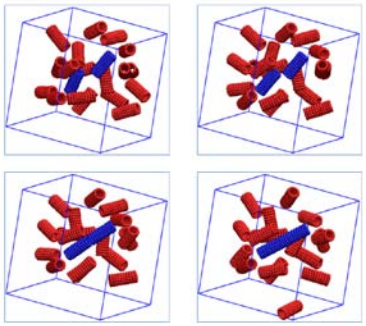

Fig. 2. Time-lapse frames from a molecular dynamic simulation showing the self-organization and fusion of two tubules (blue).

To address this issue, we assembled mixtures of green-(HiLyte Fluor™ 488 dye) fluorescently labeled MTs and free, red-(rhodamine dye) labeled αβ tubulin dimers. If growth was solely due to polymerization, only green MTs with red ends would have been expected based on the nucleated polymerization with free tubulin. Alternatively, self-organization and fusion should result in alternating green segments separated by short red segments. Fusion of MT should also result in an overall decrease in the total number of MTs over time, whereas the population would remain constant if nucleated polymerization occurred. As shown in Fig. 3, the predominance of MTs with alternating green segments separated by smaller red segments strongly supports the hypothesized self-organization and fusion of MTs. Increases in MT length over time followed a one-half power-law function, while the number of MT per field of view followed a first-order exponential decay. As noted above, the inverse correlation between MT length and the number of MTs in the population is consistent with the proposed fusion mechanism.

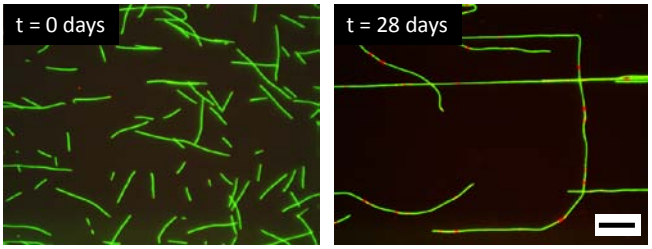

Fig. 3. Fluorescence images of MT self-organization and fusion in which red-tubulin dimers function as glue between annealed green MT filaments. Scale bar = 10 μm.

Active Assembly of Lipid Transport Network

Intracellular membranous networks formed by the endoplasmic reticulum (ER) and Golgi apparatus play a critical role in the compartmentalization of eukaryotic cells, and are sites of

important physiological processes (e.g., protein synthesis). Moreover, motor protein-based transport and spatial reorganization of these organelles enable a cell to adapt to and meet the changing physiological needs.[6, 7] As a means of mimicking the organization of organelles such as the ER, we explored a system in which the gliding motility of MTs coupled with large multilamellar liposomes composed DOPC lipids was used to fabricate interconnected lipid nanotube networks with total lengths *exceeding 10 mm* (Fig. 4A).[8] The total size of these nanofluidic networks is only limited by MT surface density, molecular motor energy source (ATP) and total amount and physical properties of lipid source material. A valuable biomimetic aspect of these lipid networks is their ability to "self-heal;" new pathways are continuously being generated as failures occur (i.e., branches collapse) in the larger network.

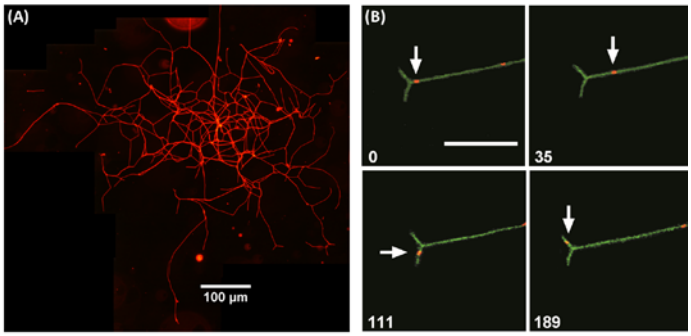

Fig. 4. (A) Fluorescence images of a continuous network of lipid nanotubes with a total length of ~10 mm. (B) Time-lapse images (time in seconds, lower left corner) of a red-QD "surfing" on the outer leaflet of a green lipid nanotube. Scale bar = 10 µm. From Bouxsein *et al*.[9]

These networks may also be used as "highways" for mass transport of nanomaterials based on the fluidity of the building blocks (i.e., lipid molecules), which maintain fluidity in these structures. To demonstrate this effect, quantum dots (QDs) were attached to lipids on the outer surface of the lipid nanotubes and their diffusive transport was characterized by single-particle tracking. As show in Fig. 4B, QDs are able to "surf" along membrane nanotubes, including through bifurcate junctions simply based on diffusive motion. We observed that transport followed normal 1D diffusion models when the QD concentration was relatively low (as in Fig. 4B). The diffusion coefficient was estimated as $D = 2.278 \pm 0.36\ \mu m^2\ s^{-1}$, which is about four-times slower than the rate reported for DOPC membranes. At high densities, QD transport is characterized by single file diffusion in which transport is confined by near-neighbors.

Future Plans

MT Filament Growth via Fusion

Future work with MT fusion will focus on developing a more comprehensive understanding of the phase behavior and thermodynamics underlying this process. Specifically, we intend to characterize the role of GTP-tubulin in the transition from nucleated polymerization to MT fusion. As part of this work, we will also develop an understanding of whether MT fusion is driven by entropic and/or enthalpic effects. The role of taxol-induced changes in MT dynamics and physical properties in the fusion process will be also investigated. Finally, methods for selective mineralization of multifunctional MTs formed through fusion will be developed and applied as a means of fabricating heterostructured nanocomposites.

Active Assembly of Lipid Transport Network

Future work with the motor-driven assembly of lipid nanotube networks will concentrate on increasing the complexity of the system as a model for primitive, biomolecular communication networks. As our prior work relied on networks formed from individual, isolated liposomes, we will begin investigating the behaviors of multi-vesicle networks including characterization of

lipid network connectivity, nanotube junction morphology, and self-healing properties. In addition, the ability to transport nanomaterials on the surface and in the interstitial space will be evaluated with these multi-vesicle networks. Lastly, we intend to use protein-ligand pairs to study multi-material transport and biomolecular communication within these networks.

Acknowledgment

This research was supported by the U.S. Department of Energy, Office of Basic Energy Sciences, Division of Materials Sciences and Engineering, Project KC0203010. Sandia National Laboratories is a multi-program laboratory managed and operated by Sandia Corporation, a wholly owned subsidiary of Lockheed Martin Corporation, for the U.S. Department of Energy's National Nuclear Security Administration under contract DE-AC04-94AL85000.

Abstract References

1. Fialkowski, M.; Bishop, K. J. M.; Klajn, R.; Smoukov, S. K.; Campbell, C. J.; Grzybowski, B. A. *J. Phys. Chem. B* **2006,** 110, (6), 2482-2496.
2. Goldstein, L. S. B.; Yang, Z. H. *Annu. Rev. Neurosci.* **2000,** 23, 39-71.
3. Fygenson, D. K.; Braun, E.; Libchaber, A. *Phys. Rev. E.* **1994,** 50, (2), 1579-1588.
4. Cheng, S. F.; Aggarwal, A.; Stevens, M. J. *Soft Matter* **2012,** 8, (20), 5666-5678.
5. Gardner, M. K.; Charlebois, B. D.; Janosi, I. M.; Howard, J.; Hunt, A. J.; Odde, D. J. *Cell* **2011,** 146, (4), 582-592.
6. Wozniak, M. J.; Bola, B.; Brownhill, K.; Yang, Y. C.; Levakova, V.; Allan, V. J. *J Cell Sci* **2009,** 122, (12), 1979-1989.
7. Lippincottschwartz, J.; Cole, N. B.; Marotta, A.; Conrad, P. A.; Bloom, G. S. *J Cell Biol* **1995,** 128, (3), 293-306.
8. Bouxsein, N. F.; Carroll-Portillo, A.; Bachand, M.; Sasaki, D. Y.; Bachand, G. D. *Langmuir* **2013,** 29, (9), 2992-2999.

DOE-Sponsored Publications (2011-2013)

- Gough, D.V., Wheeler, J.S., and Spoerke, E.D., Supramolecular assembly of asymmetric self-neutralizing amphiphilic peptide wedges. *Soft Matter* **9**, (in press) (2013).
- Spoerke, E.D., Boal, A.K., Bachand, G.D., and Bunker, B.C., Biodynamic assembly of nanocrystals on artificial microtubule asters. *ACS Nano* **7**, 2012-2019 (2013).
- Bouxsein, N.F., Carroll-Portillo, A., Bachand, M., Sasaki, D.Y., and Bachand, G.D., A continuous network of lipid nanotubes fabricated from the gliding motility of kinesin powered microtubule filaments. *Langmuir* **29**, 2992-2999 (2013).
- Liu, H. and Bachand, G.D., Effects of confinement on molecular motor-driven self-assembly of ring structures. *Cell. Mol. Bioeng.* **6**, 98-108 (2013).
- Cheng, S.F., Aggarwal, A., and Stevens, M.J., Self-assembly of artificial microtubules. *Soft Matter* **8**, 5666-5678 (2012).
- Bachand, M. and Bachand, G.D., Effects of potential environmental interferents on kinesin-powered molecular shuttles. *Nanoscale* **4**, 3706-3710 (2012).
- Polaske, N.W., McGrath, D.V., and McElhanon, J.R., Thermally reversible dendronized linear AB step-polymers via "click" chemistry. *Macromolecules* **44**, 3203 (2011).

Molecular Nanocomposites − Complex Nanocomposites

Principle Investigator: Jeff Brinker; Program Manager: Paul Clem; Co-PIs Bryan Kaehr, Hongyou Fan, Eric Carnes, Andrew Dattelbaum (Los Alamos)
Mailing Address: Sandia National Laboratories, Advanced Materials Lab, 1001 University Blvd, SE, Albuquerque, NM 87106

Program Scope

The goal of the Complex Nanocomposite task is the discovery and understanding of new chemically- and physically-based synthesis and assembly methodologies to construct and integrate complex porous and composite materials, which exhibit structure and function across multiple length scales. A significant aim is to establish processing-structure-property relationships for new nanocomposites prepared by self-assembly, directed assembly and templating procedures pioneered by the team members through over a decade of DOE support.

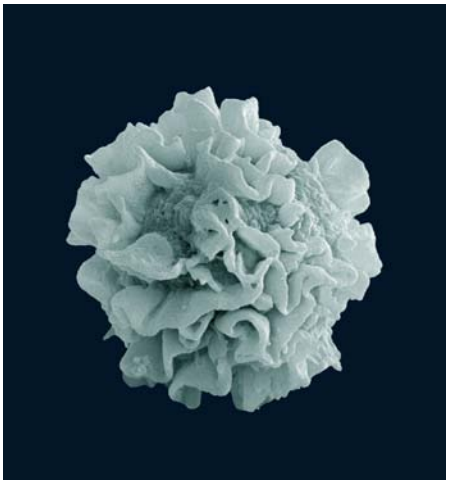

Fig 1. Scanning electron micrograph of a surface ruffled 10 μm diameter silica particle synthesized from an RBL-2H3 cell following surface activation via DNP-BSA crosslinking of anti-DNP-IgE primed IgE receptors (*PNAS* 2012).

Emphasis is on construction of 2- and 3D nanocomposites with dimensional scales and interfacial behaviors designed to allow energy conversion, transduction, or storage and/or enable development of life-like structure and functionality. An example of a complex structure formation, where a biological response is used to program an inorganic material, is shown in **Figure 1**. The idea of using the responsiveness of living, energy dissipating cells or organisms to program the formation of synthetic materials is a representative theme of our program.

This project employs self-assembly, in particular evaporation-induced self-assembly and cell-directed assembly, in combination with top-down directed assembly procedures like bio-compatible multi-photon lithography, pressure-directed assembly, and atomic layer deposition to create model composite materials, which can be further chemically or physically 'adjusted' at the nm to μm scale. Further we use and develop advanced *in situ* scattering and diffraction methodologies along with electron and probe microscopies to characterize the formation and structures of the complex composites and probe their collective properties deriving from hierarchical organization.

Recent Progress

We recently reported our discovery of silica cell replication (SCR; published in *PNAS 2012*[1] and re-reported *Nature Nanotechnology News & Views 2012*[2]) as a means to form an exact silica replica of cells (and now organisms) with preservation of shape and feature dimensions to over 550˚C. The simplicity of the process and its seeming extendibility to virtually any cell type (**Figures 1 and 2**) provides exciting opportunities to understand and exploit the biotic/abiotic interface in the development of complex nanocomposites. SCR can capture directed dynamic behaviors, such as apoptotic blebbing, the crenate response of red blood cells to osmotic stress,

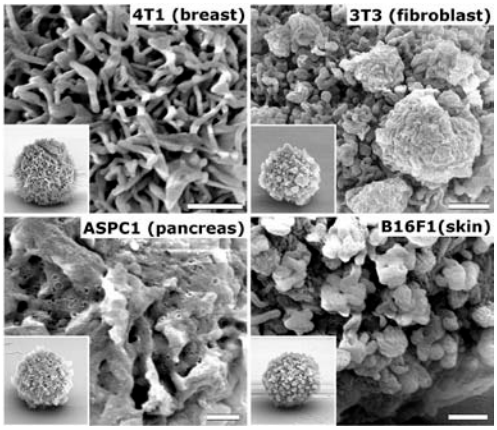

Fig. 2 Conversion of mammalian cells into inorganic silica replicas allows access to a range of surface morphologies. Scale bars, 1 µm.

and cell ruffling upon antigen binding to basophile immune cells (**Figure 1)**. We aim to understand and develop SRC as a simple and general approach to maintain the complex structure and function of biomolecular components under extreme environmental conditions, and potentially across multiple length scales, as well as develop new functions via transformative chemistries. Along these lines, we recently have demonstrated that this approach can be extended to replicate tissues and whole organisms in silica. Further, silica stabilization allows shape-preserving high temperature transformation of cells and tissues into electrically conductive materials (**Figure 3)**. A practical outcome of this advance is the ability to image complex specimen using high resolution electron microscopies without sputtering conductive coatings (e.g., Au). Thus, single cells could be sectioned in situ (using a focused ion beam) without loss of resolution as each sectioned plane maintains consistent conductivity. Ultimately, we envision the development of SCR as an alternative room temperature approach to cryo-preservation of cellular function.

Future Plans

Investigate the self-limiting molecular mechanisms underlying SCR - Our current hypothesis is that at its isoelectric point (pH~3) silicic acid molecules (similar to water) diffuse throughout the fixed cell via molecular channels, diffusion through membranes, and/or alcohol induced membrane permeability. Silicic acid then displaces/replaces bound water at biomolecular interfaces and is amphoterically catalyzed by proximal proteins and other membrane components to form a self-limiting, self-supporting, nm-thick silica 'encasement' that pervades the complete crowded biomolecular space. This 'silica replacement hypothesis' is based on the fact that the tetrahedral symmetry and hydrogen bond strength of silanols in silicic acid are strikingly similar to water (Leung and Rempe (SNL), unpublished). We will test this hypothesis using quantitative calorimetric studies of cell/silica/water interactions[3] (with C. Perry, Nottingham, UK) complemented with molecular dynamics and *ab initio* MD calculations of a model water/silicic acid/protein system[4] (with L. Ciacchi, University of Bremen).

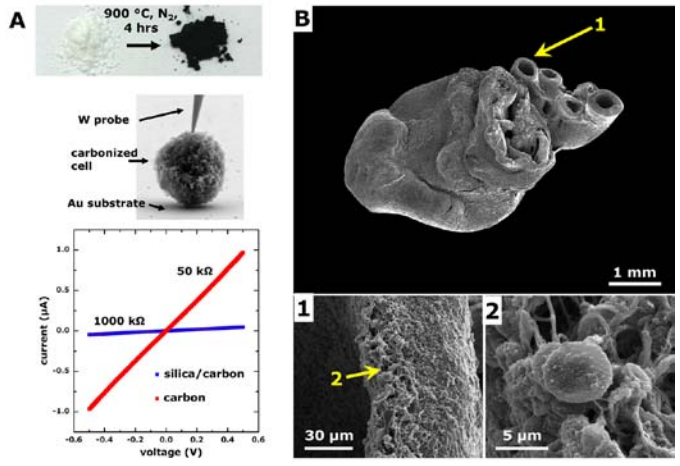

Figure 3 (A) Shape-preserving carbonization of silica replicated cells yields conductive particles. (B) Extension of SCR to a chicken embryo heart allows multi-scale electron microscopy imaging without the need for sputtered conductive coatings.

Optimize SCR procedures for retained biofunctionality - Activity of subclasses

of enzymes will be evaluated in fixed cells, silicified cells, and silicified cells after varying stages of desilicification. Based on our model, we anticipate that gradual de-silicification should 'thaw' the system and allow recovery of biofunctionality. Importantly, we envision that by preserving the native molecularly crowded environment of the cell, which evolved to conduct biomolecular chemistry, we should be able to perform coupled chemical reactions using a partially desilicified cellular platform. Biofunction will also be assessed following environmental challenges (e.g., chemical, temperature) versus non-silicified controls.

Customize SCRs using genetic and chemical engineering Having demonstrated retention of enzyme activity, we can contemplate metabolic 'priming' of the cells prior to silicification to effect overexpression of desired enzymes and direct function. In principle, any enzyme, including those that are otherwise difficult to express in bacterial systems due to post-translational modifications, could be concentrated in SCRs.

Transform silica cell replicas into other chemistries - We expect to be able to transform cellular designs into a spectrum of other chemistries. In our preliminary work, we demonstrated transformation of silicified protein scaffolds into silicon, and cell silica composites into inverse carbon replicas, both with preservation of shape and high Ohmic electrical conductivity. Starting with silica cell replicas we will employ reactive transformation chemistries to convert the replicas into new chemistries (MgO, Al_2O_3, Si, TiO_2, etc). Compared to the conversion of diatoms into Si, TiO_2, etc. as pioneered by Sandhage[5], the idea of programming silica cell shape prior to conversion will provide a new ability to create customized materials. In addition the thinness of the silica features in cell replicas may allow density (and therefore volumetric) changes to be accommodated by changes in thickness, while preserving the shape and macroscopic dimensions of the parent cell.

Acknowledgements

This research was supported by the Division of Materials Science and Engineering in the Department of Energy Office of Basic Energy Sciences. Sandia National Laboratories is a multi-program laboratory managed and operated by Sandia Corporation, a wholly owned subsidiary of Lockheed Martin Corporation, for the U.S. Department of Energy's National Nuclear Security Administration under contract DE-AC04-94AL85000

References cited

1. Kaehr, B.; Townson, J. L.; Kalinich, R. M.; Awad, Y. H.; Swartzentruber, B. S.; Dunphy, D. R.; Brinker, C. J.: Cellular complexity captured in durable silica biocomposites. *Proceedings of the National Academy of Sciences* **2012**, *109*, 17336-17341.
2. Ying, J. Y.: Cells made of silica. *Nature Nanotechnology* **2012**, *7*, 777-778.
3. Patwardhan, S. V.; Emami, F. S.; Berry, R. J.; Jones, S. E.; Naik, R. R.; Deschaume, O.; Heinz, H.; Perry, C. C.: Chemistry of Aqueous Silica Nanoparticle Surfaces and the Mechanism of Selective Peptide Adsorption. *Journal of the American Chemical Society* **2012**, *134*, 6244-6256.
4. Schneider, J.; Colombi Ciacchi, L.: Specific Material Recognition by Small Peptides Mediated by the Interfacial Solvent Structure. *Journal of the American Chemical Society* **2011**, *134*, 2407-2413
5. Sandhage, K.: Materials "alchemy": Shape-preserving chemical transformation of micro-to-macroscopic 3-D structures. JOM 2010, 62, 32-43.

Publications (selected from 22 2011-2013 publications that acknowledge DSME support)

1. Xiong, S.; Dunphy, D. R.; Wilkinson, D. C.; Jiang, Z.; Strzalka, J.; Wang, J.; Su, Y.; de Pablo, J. J.; Brinker, C. J.: Revealing the Interfacial Self-Assembly Pathway of Large-Scale, Highly-Ordered, Nanoparticle/Polymer Monolayer Arrays at an Air/Water Interface. *Nano Letters* **2013**, *13*, 1041-1046.
2. Chou, S. S.; Kaehr, B.; Kim, J.; Foley, B. M.; De, M.; Hopkins, P. E.; Huang, J.; Brinker, C. J.; Dravid, V. P.: Chemically exfoliated MoS2 as near-infrared photothermal agents. *Angew Chem Int Ed Engl* **2013**, *52*, 4160-4.

3. Zhang, H.; Dunphy, D. R.; Jiang, X.; Meng, H.; Sun, B.; Tarn, D.; Xue, M.; Wang, X.; Lin, S.; Ji, Z.; Li, R.; Garcia, F. L.; Yang, J.; Kirk, M. L.; Xia, T.; Zink, J. I.; Nel, A.; Brinker, C. J.: Processing Pathway Dependence of Amorphous Silica Nanoparticle Toxicity: Colloidal vs Pyrolytic. *Journal of the American Chemical Society* **2012**, *134*, 15790-15804.
4. Zarzar, L. D.; Swartzentruber, B. S.; Harper, J. C.; Dunphy, D. R.; Brinker, C. J.; Aizenberg, J.; Kaehr, B.: Multiphoton Lithography of Nanocrystalline Platinum and Palladium for Site-Specific Catalysis in 3D Microenvironments. *Journal of the American Chemical Society* **2012**, *134*, 4007-4010.
5. Kaehr, B.; Townson, J. L.; Kalinich, R. M.; Awad, Y. H.; Swartzentruber, B. S.; Dunphy, D. R.; Brinker, C. J.: Cellular complexity captured in durable silica biocomposites. *Proceedings of the National Academy of Sciences* **2012**, *109*, 17336-17341 (Commentary: Ying, J.Y., Cells made of silica. *Nature Nanotechnology News & Views* **2012**, 7, 777-778).
6. Harper, J. C.; Edwards, T. L.; Savage, T.; Harbaugh, S.; Kelley-Loughnane, N.; Stone, M. O.; Brinker, C. J.; Brozik, S. M.: Orthogonal Cell-Based Biosensing: Fluorescent, Electrochemical, and Colorimetric Detection with Silica-Immobilized Cellular Communities Integrated with an ITO-Glass/Plastic Laminate Cartridge. *Small* **2012**, *8*, 2743-2751 (Cover).
7. Harper, J. C.; Brozik, S. M.; Brinker, C. J.; Kaehr, B.: Biocompatible Microfabrication of 3D Isolation Chambers for Targeted Confinement of Individual Cells and Their Progeny. *Analytical Chemistry* **2012**, *84*, 8985-8989.
8. Ashley, C. E.; Carnes, E. C.; Epler, K. E.; Padilla, D. P.; Phillips, G. K.; Castillo, R. E.; Wilkinson, D. C.; Wilkinson, B. S.; Burgard, C. A.; Kalinich, R. M.; Townson, J. L.; Chackerian, B.; Willman, C. L.; Peabody, D. S.; Wharton, W.; Brinker, C. J.: Delivery of Small Interfering RNA by Peptide-Targeted Mesoporous Silica Nanoparticle-Supported Lipid Bilayers. *ACS Nano* **2012**, *6*, 2174-2188 (COVER).
9. Zarzar, L. D.; Kim, P.; Kolle, M.; Brinker, J.; Aizenberg, J.; Kaehr, B.: Direct Writing and Actuation of Three-Dimensionally Patterned Hydrogel Pads on Micropillar Supports. *Angewandte Chemie-International Edition* **2011**, *50*, 9356-9360.
10. Xiong, S.; Molecke, R.; Bosch, M.; Schunk, P. R.; Brinker, C. J.: Transformation of a Close-Packed Au Nanoparticle/Polymer Monolayer into a Large Area Array of Oriented Au Nanowires via E-beam Promoted Uniaxial Deformation and Room Temperature Sintering. *Journal of the American Chemical Society* **2011**, *133*, 11410-11413.
11. Luk, T. S.; Xiong, S.; Chow, W. W.; Miao, X.; Subramania, G.; Resnick, P. J.; Fischer, A. J.; Brinker, C. J.: Anomolous Enhanced Emission from PbS Quantum Dots on a Photonic-Crystal Microcavity. *J. Opt. Soc. Am. B* **2011**, *28*, 1365-1373.
12. Khripin, C. Y.; Pristinski, D.; Dunphy, D. R.; Brinker, C. J.; Kaehr, B. J.: Protein-Directed Assembly of Arbitrary Three-Dimensional Nanoporous Silica Architectures. *ACS Nano* **2011**, *5*, 1401-1409.
13. Ashley, C. E.; Dunphy, D. R.; Jiang, Z.; Carnes, E. C.; Yuan, Z.; Petsev, D. N.; Atanassov, P. B.; Velev, O. D.; Sprung, M.; Wang, J.; Peabody, D. S.; Brinker, C. J.: Convective Assembly of 2D Lattices of Virus-like Particles Visualized by In-Situ Grazing-Incidence Small-Angle X-Ray Scattering. *Small* **2011**, *7*, 1043-1050.
14. Ashley, C. E.; Carnes, E. C.; Phillips, G. K.; Padilla, D.; Durfee, P. N.; Brown, P. A.; Hanna, T. N.; Liu, J.; Phillips, B.; Carter, M. B.; Carroll, N. J.; Jiang, X.; Dunphy, D. R.; Willman, C. L.; Petsev, D. N.; Evans, D. G.; Parikh, A. N.; Chackerian, B.; Wharton, W.; Peabody, D. S.; Brinker, C. J.: The targeted delivery of multicomponent cargos to cancer cells by nanoporous particle-supported lipid bilayers. *Nat Mater* **2011**, *10*, 389-397 (COVER with commentary: Irvine, D. J., One nanoparticle, one kill. *Nature Materials News & Views* **2011**, 10, 342).

Task Title: Protein Biotemplates for Self-Assembly of Nanostructures

Investigators: Sarah Heilshorn, Nicholas Melosh, Seb Doniach, and Andrew Spakowitz
476 Lomita Mall, McCullough 246, SLAC National Accelerator Laboratory & Stanford University, Stanford, CA 94305. Heilshorn@stanford.edu

Program Scope: The focus of this multi-disciplinary research program is to characterize and exploit the tailored molecular interactions inherent in biological systems. Such understanding will enable deterministic formation of complex organic/inorganic constructs and engineering of responsive, biomimetic materials that exhibit self-healing and self-regulating transformations. These materials will lead to fundamentally new designs in biomimetic organic/inorganic devices for energy storage, catalysis, solar cells, and fuel cells. The team integrates a wide range of experimental and theoretical approaches to assemble, characterize, and model dynamic assembly. Our recent collaborative effort has focused on experimental and theoretical insights into the fundamentals of biomimetic self-assembly in two and three dimensions, investigating the effects of multivalency on hierarchical assembly processes, extending our strategy for non-covalent, site-specific functionalization of clathrin protein assemblies to template multiple inorganic species simultaneously on the same protein particle, and developing advanced x-ray characterization techniques for atomic scale resolution of assembled structures.

Recent Progress:

Kinetics of three-dimensional (3D) protein self-assembly assembly.

To compare simulation of 3D clathrin assembly with experimental assembly triggered by a change in pH, we have developed a 3D model that examines the driving forces that dictate the dynamic pathways of clathrin self-assembly as well as their resulting equilibrium structures. Our clathrin triskelia model compared to experimental light scattering and TEM data, suggests there is internal order within aggregated species that may act as nucleation sites for remodeling into fully ordered structures, an important insight that would have been difficult to gain solely through experimental study. By integrating further experimental light scattering and cryo-electron microscopy results with these computational data, we have shown that competition between weak nonspecific interactions and site-specific molecular recognition events can dictate initial pathways of biomolecular self-assembly, yet the final structure is formed robustly along each kinetic pathway even when the initial state is a disordered protein aggregate (**Figure 1**). This suggests that weak nonspecific interactions can be used in a *de novo* self-assembling system as an aid in assembly rather than being considered only as a route to kinetically trapped disordered structures. Future work will exploit this insight to design novel biomimetic systems that robustly self-assemble into 3D structures.

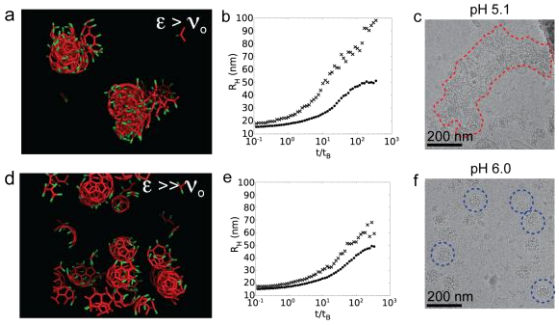

Figure 1. a, d) Snapshots of simulations show formation of disordered aggregates when nonspecific interactions are on the order of thermal energy (v_o = 1 kBT) and ordered cages when they are negligible (v_o = 0.1 kBT). **b, e)** Hydrodynamic radii calculations of simulated clusters at v_o = 1 kBT (b) and v_o = 0.1 kBT (e). The dots on each plot correspond to clusters defined by a group of triskelia that are specifically bound through leg-leg interactions, and the crosses correspond to clusters defined by triskelia whose hubs are separated by less than 1.25 leg lengths from at least one other triskelion hub in the cluster. **c, f)** Cryo-TEM of clathrin assemblies at pH 5.1 (c) and 6.0 (f) after 20 minutes of assembly. Aggregates and cages are outlined in red and blue, respectively.

Responsiveness of two-dimensional protein assemblies on deformable membranes.

We have developed a model of clathrin lattices that are self-assembling on deformable cell membranes. Through Monte Carlo simulations, we find that large out-of-plane membrane fluctuations cause otherwise crystalline lattices to become disordered. Membranes at high tension have small out-of-plane fluctuations, while low tension membranes exhibit large fluctuations. Clathrin systems that are otherwise crystalline on

high tension membranes decay to a disordered state at low tension (**Figure 2**). Comparison with experimental 2D clathrin assembly at lipid interfaces is currently underway. Experiments and modeling will investigate the response of clathrin lattices to locally curved membrane deformations, similar to those experienced during endocytosis. Preliminary results show that these deformations are accommodated more easily by fluid rather than crystalline lattices. Hemispherical indentations are made on elastic membranes within the regions circled in white (**Figure 3**). Highly ordered lattices respond to these indentations by localizing defects and void spaces on or near the deformations. However, fluid lattices that are induced through large out-of-plane membrane fluctuations in the bulk exhibit relatively continuous coated networks around the indentations. We will explore the impact of local curvatures on the large-scale reorganization of clathrin lattices in conjunction with the thermodynamic modeling. Further experimental study into 2D assembly measurements focuses on a surface tension measurement system to evaluate the impact of DNA-lipid constructs that have been designed as clathrin mimics. The goal of this system is to macroscopically measure the impact of a surface-assembled network of DNA on an oil-water interface and the dynamic modulation of the surface tension via self-assembly. Objective benchmarks include the programming of an algorithm to fit a pendant-drop surface tension measurement method. Further progress is being made on the experimental set-up, which includes thermal control for self-assembly. TEM characterization of assembled DNA-lipid constructs is currently undergoing optimization and development while collected tension data is being analyzed.

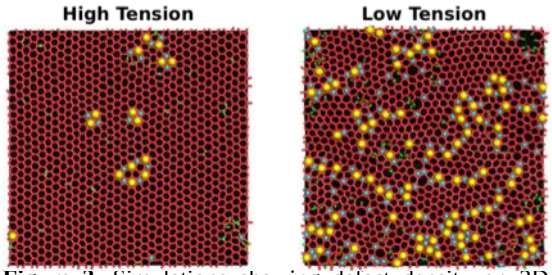

Figure 2. Simulations showing defect density on 2D membranes at different tensions.

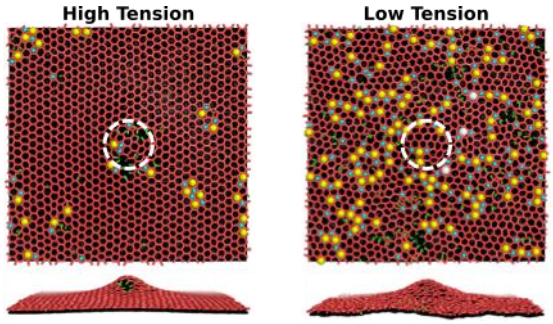

Figure 3. Simulations showing defect density upon indentration of the membrane at different tensions.

Inorganic templating using multiple epitopes on protein scaffolds.

In earlier templating studies, the Heilshorn group focused on the clathrin box or "C-box" epitope binding site to nucleate and grow inorganic particles within the clathrin protein cage template using our Template Engineering Through Epitope Recognition (TEThER) strategy. Two additional binding sites on the clathrin protein have been investigated: the W-box and the Huntington Interacting Protein 1 (HIP1) sites. We have confirmed that all three epitope sites are independent of each other and binding to one does not interfere with binding to the others. The W-box, like the C-box site, facilitates inorganic templating within the clathrin cage, and these two sites in combination have been used for synthesis of particles with nanoscale domains of gold and silver intermixed within the clathrin cages (**Figure 4 a – c**). The HIP1 site, located on the outside of assembled clathrin cages, enables synthesis of inorganic material coating the protein templates. Templating reactions with clathrin cages functionalized with HIP1-Au (outside of cage) and W-box-Ag peptides (inside of the cage) resulted in core (silver)-shell (gold) composite

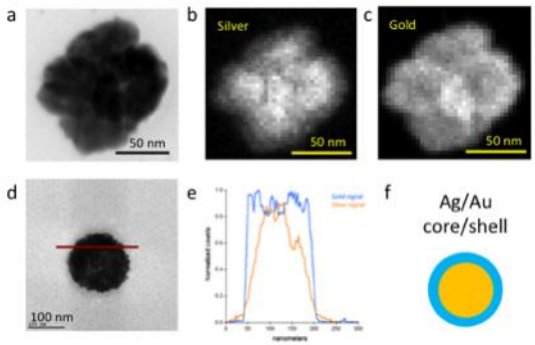

Figure 4. (a) TEM of composite Ag-Au nanoparticle formed using C-box and W-box binding sites. (b, c) scanning EDS of (a) showing location of silver (b) and gold (c) within the particle. (d) TEM of core-shell Ag-Au nanoparticle formed using W-box and HIP1 binding sites. (e) Line scans showing elemental composition as a function of location on the particle (red line in (d)). Overlapping gold and silver signals for each scan show Au intensity surrounding "cage" while Ag signal is found in the core of the nanoparticle. (f) Schematic of core-shell nanoparticle.

particles (**Figure 4 d – f**). This work shows that the site-specificity of the engineered peptides binding to the clathrin scaffold can be exploited to direct the structure of the synthesized material in predictable ways. Future work will include investigation into the functional properties of the nanoparticles.

Multivalent, peptide-mediated hierarchical assembly.

In collaboration with the Mirjam Leunissen group at FOM Institute AMOLF (Amsterdam), we have demonstrated the use of leucine zipper peptides to achieve specific association of micron-sized colloidal building blocks. Confocal microscopy is used to visualize colloidal assemblies of polystyrene beads coated with engineered peptide sequences that are able to form molecular bridges between beads through specific dimer interactions. While an increase in temperature up to the measured melting temperature of the peptide dimers in solution is not able to dissociate the peptide-coated beads, assembly can be controlled at room temperature by titrating in freely soluble peptide binding partners (**Figure 5**). This reduces the number of binding events between particles and effectively lowers the valency of the beads. This approach offers specific and tunable control over the highly multivalent particle interactions compared to global inputs such as temperature, pH, or ionic strength. Integration of these engineered peptide sequences with our previously developed biotemplating strategy may enable the hierarchical organization of nanoscale protein scaffolds through specific molecular recognition. Further studies will provide insight into the nature of multivalent interactions and their potential for fine-tuning hierarchical assembly in *de novo* assembly systems.

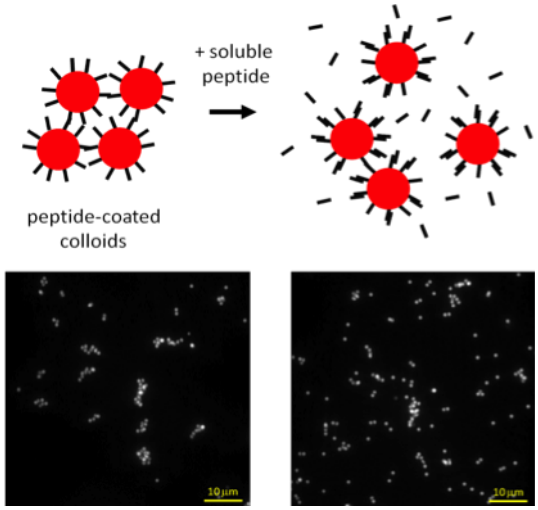

Figure 5. (top) Schematic of colloidal assembly controlled by titrating in freely soluble peptide. **(bottom)** Confocal microscopy images of peptide-coated colloids at room temperature with no soluble peptide (left) and 1 micromolar soluble peptide (right).

Development of advanced X-ray scattering techniques.

We have been focusing on correlated x-ray scattering (CXS) studies of ordered particles and molecules in disordered substrates. This technique permits study of ordered species such as clathrin cage assemblies without requiring crystallization of the protein assemblies. Two sets of data have been taken on the SSRL microfocus beamline 12-2 and one set of data on the LCLS CXI beamline. Data on 20 nm silver nanoparticles from SSRL beamline 12-2 have been analyzed for angular correlations. We have resolved a fundamental problem in the interpretation of CXS arising from "psuedo-correlations". In these scattering events, two scatterings from *different* particles are recorded which happen to have the same scattering vectors as those of the set of molecular correlation events in which two scattering events are registered from the *same* molecule. By cross-correlating events from different shots, we can measure the background due to the psuedo-events since, by definition, the molecular orientations in two different shots cannot have the same ensemble of orientations. These "inter-shot" correlations show a different distribution of PC1 amplitudes, clustering around zero correlation, from those seen for the "intra-shot" correlations (**Figure 6**). After correction for polarization, a histogram of the 1st Principle Component of the correlators measured

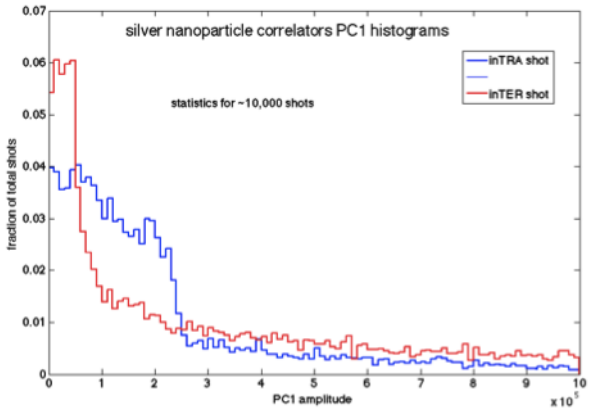

Figure 6. "Inter" and "intra" shot correlations for CXS analysis of silver nanoparticles.

for some 10,000 individual x-ray shots, each from a different part of the sample, showed a marked deviation from a simple Gaussian expected for a monodisperse system of ideal nanoparticles. This is interpreted as being due to lattice imperfections in each nanoparticle coupled with a distribution of particle sizes; this interpretation has been verified with traditional TEM analysis.

Future Plans:

- Design novel clathrin-mimetic systems that robustly self-assemble into 3D structures based on insights from kinetic studies of clathrin assembly
- Compare model of 2D self-assembly on deformable membranes to experimental measurements
- Develop DNA-lipid constructs as clathrin mimics and study their effect on membrane tension
- Study the catalytic properties of nanoscale composite and core/shell nanoparticles synthesized with clathrin scaffolds
- Utilize peptides for hierarchical assembly in templating strategy to generate templates with 3D order.

Publications Resulting from DOE Support (previous two years):

Primary DOE support:

1. Schoen AP, Cordella N, Mehraeen S, Arunagirinathan MA, Spakowitz AJ, Heilshorn SC. *Dynamic remodeling of disordered protein aggregates is an alternative pathway to achieve robust self-assembly of nanostructures*. **Soft Matter**, 2013, accepted, DOI:10.1039/C3SM50830G.
2. VanDersarl JJ, Xu AM, Melosh NA, *Nanostraws for Direct Fluidic Intracellular Access*. **Nano Letters**, 2012, 12:3881-3886.
3. Schoen AP, Schoen DT, Huggins KNL, Arunagirinathan MA, Heilshorn SC. *Engineered protein templates synthesize inorganic nanomaterials*. **Chemical Engineering Progress**, 2012, 108:47-50.
4. Huggins KN, Schoen AP, Arunagirinathan MA, Heilshorn SC. *Molecular recognition enables biotemplating at distinct protein sites.* **American Chemical Society Proceedings, Division of Polymeric Materials Science and Engineering**, 2012, 106 PMSE-125.
5. Schoen AP, Schoen DT, Huggins KN, Arunigirinathan MA, Heilshorn SC. *Template Engineering Through Epitope Recognition: A modular, biomimetic strategy for inorganic nanomaterial synthesis*. **Journal of the American Chemical Society**, 2011, 133:18202-18207.
6. VanDersarl JJ, Xu AM, Melosh NA. *Rapid spatial and temporal controlled signal delivery over large cell culture areas*. **Lab on a Chip**, 2011, 11:3057-3063.

Collaborative DOE support:

7. Schoen AP, Hommersom B, Heilshorn SC, Leunissen M. *Tuning colloidal association with specific peptide interactions*. **Soft Matter**, 2013, 9:6781-6785.
8. Hong AH, Toro E, Mortenson KI, Diaz de la Rosa MA, Doniach S, Shapiro L, Spakowitz AJ, McAdams HH. *Caulobacter chromosome in vivo configuration matches model predictions for a supercoiled polymer in a cell-like confinement*. **Proceedings of the National Academy of Sciences USA**, 2013, 110:1674-1679.
9. Sim AYL, Lipfert J, Herschlag D, Doniach S. *Salt dependence of the radius of gyration and flexibility of single-stranded DNA in solution probed by small-angle x-ray scattering*. **Physical Review E**, 2012, 86.
10. Anthony PC, Sim AYL, Chu VB, Doniach S, Block SM, Herschlag D. *Electrostatics of Nucleic Acid Folding under Conformational Constraint*. **Journal of the American Chemical Society**, 2012, 134: 4607-4614.
11. Almquist BD, Melosh NA. *Molecular structure influences the stability of membrane penetrating biointerfaces.* **Nano Letters**, 2011, 11:2066-2070.
12. Kwiatkowski JJ, Jimison LH, Salleo A, Spakowitz AJ. *A Boltzmann-weighted hopping model of charge transport in organic semicrystalline films.* **Journal of Applied Physics**, 2011, 109:113720.

Program Title: Solid-State NMR of Complex Materials

Principal Investigator: Klaus Schmidt-Rohr; Co-PI: Mei Hong and Evgenii M. Levin
Mailing Address: Department of Chemistry and Ames Laboratory, Gilman 1605, Iowa State University, Ames IA 50011
Email: mhong@iastate.edu

Program Scope

We develop and apply solid-state nuclear magnetic resonance (ssNMR) methods to study the structure-function relationship of complex materials. In the arena of biomaterials, we investigate the structure and dynamics of plant cell walls (CWs), organic-inorganic nanocomposites, and a protein involved in nucleating ferromagnetic nanocrystals in magnetotactic bacteria. Part of this work (1-3) is tightly integrated with the FWP on *Bioinspired Materials* led by Dr. Surya Mallapragada. Other parts of this ssNMR FWP involve studies of the nanostructures of thermoelectric tellurides, carbon materials, and Nafion fuel-cell membranes. In this abstract, we focus on the biomaterials components of this program.

Recent Progress

1. Structure determination of plant cell walls

Background: Plant cell walls (CWs) provide mechanical strength to plant cells and allow plant growth. The energy-rich polysaccharides in the CWs make plant CWs important sources of energy in the modern bio-economy. For decades, plant CW structures have been studied based on chemical extraction and enzymatic hydrolysis, which perturb the integrity of the CW. Microscopy and X-ray diffraction have been used to obtain ultrastructural details of the CW, but they primarily focus on the crystalline cellulose while neglecting the amorphous matrix polysaccharides such as hemicellulose and pectins. As a result, matrix polysaccharides' interactions with and proximity to cellulose microfibrils are poorly understood.

Major findings: We have developed a multidimensional solid-state NMR strategy, in conjunction with isotopic labeling of whole plants, to determine the molecular structure, dynamics, and intermolecular interactions of polysaccharides in the primary CWs of model flowering plants (dicots) and grasses (monocots). Since 2011, we have published and submitted 5 papers in this area, which are the very first 2D and 3D high-resolution magic-angle-spinning (MAS) solid-state NMR studies of intact plant CWs. So far we have focused on *Arabidopsis thaliana,* the model organism of dicots, but a study of the model grass organism, *Brachypodium*, is ongoing.

By uniformly labeling entire plants with ^{13}C and carrying out 2D and 3D ^{13}C-^{13}C correlation experiments at NMR field strengths of 600 to 900 MHz (14 – 21 Tesla), we have resolved and assigned the ^{13}C resonances of cellulose, hemicellulose, and pectins in the *Arabidopsis* primary CW. These assignments showed that cellulose microfibrils have significant spatial interactions with pectins, while the main hemicellulose, xyloglucan, exhibited relatively few cellulose cross-peaks (4). The latter suggests that xyloglucan, instead of covering the cellulose surface extensively, may be trapped in the microfibrils at a limited number of locations. Site-resolved ^{13}C T_1 and ^{1}H $T_{1\rho}$ relaxation times indicate that xyloglucan mobility is intermediate between the mobility of cellulose and pectins. By comparing the spectra of wild-type and a xyloglucan-deficient mutant, we found that the remaining polysaccharides in the mutant CW undergo much faster motions than in the wild-type CW. These results suggest that load bearing in plant CWs is accomplished by a single network of all three types of polysaccharides instead of a cellulose-xyloglucan network that is separate from the xyloglucan-pectin network, which revises the conventional model of CW structure.

We further characterized the pectin-cellulose interactions by comparing the dynamics of intact and partially depectinated CWs (5). The latter showed higher spectral intensities and longer ^{1}H T_{1r} and ^{13}C T_1 relaxation times, indicating higher rigidity and denser packing of the remaining wall polysaccharides. These data confirm that pectins endow the polysaccharide network of the CW with mobility and flexibility, which is opposite to the function of hemicellulose.

By measuring cross peak intensities as a function of spin diffusion mixing time, we obtained semi-quantitative information about the spatial proximity between different wall polysaccharides (6). Interestingly, the intensity buildup is only modestly slower for cellulose-pectin cross peaks than for interior-surface cellulose cross peaks, suggesting that pectins come into direct spatial contact with cellulose microfibrils. About 25-50% of the cellulose chains exhibit close contact with pectins. However, the ^{13}C magnetization of the wall polysaccharides is not fully equilibrated by 1.5 s, indicating that pectins and cellulose are not homogeneously mixed on the molecular level.

In collaboration with Professor Seth DeBolt at the University of Kentucky, we investigated the mechanism of cellulose biosynthesis in *Arabidopsis* through a combination of chemical genetics approaches and ssNMR (7). The question of interest is how cellulose synthase (CESA) catalyzes the polymerization of cellulose microfibrils. Mutations in the C-terminal transmembrane domain of CESA1(A903V) and CESA3(T942I) in *Arabidopsis thaliana* produced altered growth phenotypes. ^{13}C NMR spectra showed that the mutant cellulose microfibrils have reduced width and different crystallinity from wild-type cellulose, suggesting that the mutations caused different glucan chain associations during microfibril formation. These results suggest that it may be possible to modify plant CWs to facilitate cellulose extraction.

With the knowledge of polysaccharide chemical shifts, we recently carried out a novel study to determine the binding target of a protein, expansin, in the CW (8). Expansin loosens CWs during acid-stimulated plant growth by weakening the non-covalent network formed by cellulose, hemicellulose and pectins. Although crystal structures of expansins became available recently, the functional binding site of expansins in the CW has remained elusive. We combined ssNMR with the sensitivity-enhancing technology of dynamic nuclear polarization (DNP) to show that expansin binds specific domains in cellulose microfibrils in the *Arabidopsis* CW to carry out its function. By transferring the electron polarization of a paramagnetic dopant to the nuclei, DNP allowed the selective detection of the trace concentration of ^{13}C, ^{15}N-labeled expansin in the CW and the observation of protein-to-polysaccharide ^{13}C spin diffusion. We found that a hyper-active expansin mutant binds more cellulose than the wild type and an inactive mutant, while pectin binding does not correlate with activity. Molecular dynamics simulations indicate short ^{13}C-^{13}C distances of 4-6 Å between a hydrophobic surface of the cellulose microfibril and an aromatic motif on the expansin surface, consistent with the observed NMR signals. DNP-enhanced 2D ^{13}C correlation spectra indicate that the cellulose binding site of expansin is enriched in xyloglucan and has altered cellulose conformation, suggesting that expansin loosens the wall by targeting rare cellulose-xyloglucan sites.

2. Composition and nanostructure of bone

The stiff and tough load-bearing material in bone is a nanocomposite of calcium phosphate (apatite) nanocrystals imbedded in a matrix of the fibrous protein collagen, at a 45:45 volume ratio; water accounts for the remaining 10 vol%. As a target for biomimetic materials synthesis, this nanocomposite needs to be characterized more accurately. We have shown that multinuclear (^{13}C, ^{1}H, ^{31}P) NMR with direct polarization and spectral editing can provide the mole fractions of anions such as OH^-, CO_3^{2-}, PO_4^{3-}, HPO_4^{2-}, citrate, and water of crystallization, while energy-dispersive X-ray analysis (EDX) quantifies Ca^{2+}, Mg^{2+}, Na^+, and P. On this basis, an accurate charge-balanced composition of bone apatite in terms of 8 components has been obtained (e.g. $Ca_{7.6}Mg_{0.3}Na_{0.4}(PO_4)_{4.5}(HPO_4)_{0.5}(CO_3)_{0.7}(OH)_{0.3}(H_2O)_{0.55}$ for bovine bone). Quantification of the 5- to 8-fold reduced concentration of OH^- (relative to $Ca_{10}(PO_4)_6(OH)_2$) has been obtained by selective $^{1}H\{^{31}P\}$ REDOR

experiments, and the invisibility of OH^- in vibrational spectra of bone has been explained. The presence of carbonate inside bone apatite is proved by $^{13}C\{^1H\}$ REDOR NMR, and the substitution of one out of every 8 phosphates by carbonate demonstrated. ^{31}P spin-diffusion NMR showed that ordered and disordered phosphates are not in different phases but in close proximity forming core and surface layers, respectively, of the apatite nanocrystals. The concentrations of HPO_4^{2-} and structurally bound H_2O were determined by $^1H\{^{31}P\}$ REDOR and ^{31}P chemical-shift anisotropy measurements. The data confirm that the nanocrystals have a large fraction of phosphate groups at the surface (around 30%), consistent with the small crystal thickness of ca. 2.5 nm.

Various bone structural models assume that the bone apatite nanocrystals are concentrated in the "gap" regions of the collagen fibrils. This would require the presence of thick collagen layers in the apatite-poor regions. We are testing these models by probing the thickness of the collagen layers in bone by long-range $^{13}C\{^{31}P\}$ NMR, where thick layers produce a nearly constant intensity at long dephasing times. The data indicate a locally inhomogeneous distribution of collagen layers, which would also explain the lack of a correlation peak in small-angle scattering in bone.

3. Structure of the nanocrystalline-Fe_2O_3 promoting Mms6 protein

Magnetotactic bacteria tightly control the size and morphology of $\gamma-Fe_2O_3$ nanoparticles that they synthesize at ambient temperature and close to neutral pH. The 61-residue protein Mms6 was found to be tightly associated with the nanocrystals within the magnetosome of *Magnetospirillum magneticum* and has been shown to promote formation of iron oxide nanocrystals in vitro. The recombinant purified protein forms tightly bound micelles, consisting of 20-40 monomers, which could be attributed to hydrophobic interactions between the Gly-rich N-termini with $(Gly\text{-}Leu)_5$ segments in their center. The micellization also interferes with solution-NMR or X-ray structure determination, and consequently little is known about the secondary or tertiary structure of Mms6. In collaboration with Dr. Marit Nilsen-Hamilton and coworkers in the FWP *Bioinspired Materials*, we have studied the secondary structure of ^{13}C- and ^{15}N-enriched Mms6 by solid-state NMR. Due to the lack of crystallinity, line broadening is quite severe. However, the resulting peak overlap can be alleviated by spectral editing techniques that we have developed (9), and this enables us to selectively observe the signals of five types of amino-acid residues (Asp, Glu, Ile, Val, and Leu).

Our NMR data show that Mms6 is not unstructured but contains both β-sheets and α-helices. More than half of the 21 Gly, one third of the Ala, and at least a third of Leu residues are found in β-sheets, while several Val, at least one Ile, and another third of the Ala residues are located in α-helices.

Future Plans

Grass cell wall structure. We will investigate the CW polysaccharide structure and dynamics of the model grass organism, *Brachypodium*. Grasses have great potential as a source of renewable bioenergy. Grass CW differs from dicot CW and even less structural information is available for grass CW. We have obtained ^{13}C-labeled *Brachypodium* and will complete ^{13}C chemical shift assignment. These chemical shifts will allow us to investigate how the matrix polysaccharides in the grass CW are organized spatially with respect to cellulose and how the three-dimensional network of grass CWs differs from that of dicots, as represented by *Arabidopsis*.

Secondary structure of Mms6. We will explore whether the NMR-derived distribution of amino-acid residues associated with the secondary structure elements can be used to localize the β-sheets and α-helices in Mms6. In particular, while it may be proposed that the $(Gly\text{-}Leu)_5$-containing N-termini aggregate just due to hydrophobic interactions, our data indicate that these segments form β-sheets. We will test this hypothesis by 2D NMR with spin diffusion from β-sheet Gly, selected by N-C cross polarization before evolution. Cross-peaks between β-sheet Gly and Leu would confirm the presence of β-sheets involving the $(Gly\text{-}Leu)_5$ segments.

Relevant Publications with DOE Support in 2011-2013

1. Liu XP, Ge QW, Rawal A, Parada G, Schmidt-Rohr K, Akinc M, Mallapragada SK, 2013. Templated and Bioinspired Aqueous Phase Synthesis and Characterization of Mesoporous Zirconia. ***Science of Advanced Materials*** 5:354-65
2. Ma X, Klosterman L, Hu YY, Liu XP, Schmidt-Rohr K, Mallapragada SK, Akinc M, 2012. Aqueous Route Synthesis of Mesoporous ZrO_2 by Agarose Templation. ***J. Am. Ceramic Soc.*** 95:3455-62
3. Hu YY, Liu XP, Ma X, Rawal A, Prozorov T, et al. 2011. Biomimetic Self-Assembling Copolymer-Hydroxyapatite Nanocomposites with the Nanocrystal Size Controlled by Citrate. ***Chem. Mat.*** 23:2481-90
4. Dick-Pérez M, Zhang Y, Hayes J, Salazar A, Zabotina OA, Hong M. 2011. Structure and interactions of plant cell-wall polysaccharides by two- and three-dimensional magic-angle-spinning solid-state NMR. ***Biochemistry*** 50:989-1000
5. Dick-Pérez M, Wang T, Salazar A, Zabotina OA, Hong M. 2012. Multidimensional Solid-State NMR Studies of the Structure and Dynamics of Pectic Polysaccharides in Uniformly 13C-Labeled Arabidopsis Primary Cell Walls. ***Magn. Reson. Chem.*** 50:539-50
6. Wang T, Zabotina O, Hong M. 2012. Pectin-cellulose interactions in the Arabidopsis primary cell wall from two-dimensional magic-angle-spinning solid-state nuclear magnetic resonance. ***Biochemistry*** 51:9846-56
7. Harris DM, Corbin K, Wang T, Gutierrez R, Bertolo AL, et al. 2012. Cellulose microfibril crystallinity is reduced by mutating C-terminal transmembrane region residues CESA1A903V and CESA3T942I of cellulose synthase. ***Proc. Natl. Acad. Sci. U. S. A.*** 109:4098-103
8. Wang T, Park YB, Caporini MA, Rosay M, Zhong L, et al. 2013. Sensitivity-Enhanced Solid-State NMR Elucidation of Protein Binding to Cell Walls. ***submitted***
9. Schmidt-Rohr K, Fritzsching KJ, Wang T, Liao SY, Hong M. 2012. Spectral Editing of Two-Dimensional Magic-Angle-Spinning Solid-State NMR Spectra For Protein Resonance Assignment and Structure Determination. ***J. Biomol. NMR*** 54:343-53

Plus 4 other DOE-supported publications, in Advanced Functional Materials, Physical Review B, and Solid State NMR.

Molecular Nanocomposites—Adaptive and Reconfigurable Nancomposites Subtask

Principal Investigator: Dale L. Huber; Program Manager: Paul Clem; Co-PIs: Darryl Y. Sasaki, Mark J. Stevens, Carl C. Hayden, Amalie L. Frischknecht.

Mailing Address: Sandia National Laboratories, PO Box 5800, Albuquerque, NM 87185

Program Scope

The goal of the Adaptive and Reconfigurable Nanocomposites subtask is to explore the basic science associated with the use of energy consuming, switchable, and responsive components to create programmable and reconfigurable nanocomposites. We take much of our inspiration for these functional hierarchical assemblies from biology, and can make an illustrative analogy with the programmable molecules and assemblies present in a cell. The complex responsive behaviors of a cell are the result of a wide range of individual molecules present in a fluid matrix that allows them to maintain their own distinct responsive behaviors.

So, to construct molecular nanocomposites that are truly adaptable and configurable, we must have two classes of building blocks. First are elements that can be programmed using energy sources such as heat, light, or magnetic fields, and the second set of building blocks are mobile hosts that allow components to reconfigure themselves in response to applied stimuli.

We have been exploring programmable species whose size, shape, charge, hydrophilicity, and/or interaction potentials can be switched in a reversible fashion between at least two distinct states. A significant amount of effort is geared towards new synthetic methods for making responsive materials. With regard to responsive hosts, we are exploring fluid or viscous phases ranging from aqueous solutions to lipid bilayers to polymeric liquids and liquid crystals. For composite materials, we are investigating using the programmable elements to functionalize both hosts and active materials that can be inserted into the hosts such as optically, electrically, or magnetically active nanoparticles. Finally, in terms of behavior, we are observing how programming controls the size, shape, agglomeration, transport, and phase behavior of nanoscale assemblies.

Recent Progress

While we aim to produce some of the complex behaviors seen in living systems, we are making assemblies from fairly simple components that can be reliably synthesized. One of the primary motifs we are exploring look very similar to traditional surfactants, though with responsive endgroups. Specifically, the molecules we have designed and synthesized have one or two alkyl chains of similar length to natural phospholipids, and a polar, responsive headgroup that is of similar size as the hydrophobic tail. These molecules have the advantage of being quickly and easily inserted into either supported or free-standing bilayers, a feature that is utilized extensively for programmable assemblies. A multitude of responsive behaviors can be built into a molecule with this basic structure, and we have investigated host-guest interactions, thermally responsive behaviors, charge, and other responsive behaviors. One class of molecules we have been investigating are surfactants based upon poly(N-isopropylacrylamide) or polyNIPAM. PolyNIPAM has a lower critical solution temperature (LCST) below which it is freely soluble in water, and above which it collapses and precipitates from aqueous solutions[1]. While this material has been extensively studied as a high molecular weight polymer, a bulk gel, and a polymer monolayer, little work has been done on this molecule on the size range of interest to us (a size that is comparable to the length of an 18 carbon chain). Initial explorations of these oligomeric NIPAM molecules demonstrated to us that the phase behavior was more complex

than one may have predicted, and there was a lack of fundamental understanding of the molecular underpinnings of the phase behavior. Molecular Dynamics (MD) simulations of isolated molecules of low molecular weight polyNIPAM were conducted to provide this fundamental understanding. The results of these simulations are summarized in Fig.1. In short, very small oligomers such as an 8-mer have a weak or non-existent thermal transition. When we reach sizes such as an 18-mer, the change is more significant, while a 30-mer is reminiscent of the behavior of high molecular weight polymers where a coil-to-globule transition is observed. This molecular level understanding of the behavior of the polymer allows us to design systems where oligomeric NIPAM can perform a useful function. For example, it would be futile to design a system where isolated 8-mers were relied upon to change their molecular dimensions to alter steric crowding, while an isolated 30-mer could perform that function well. Alternatively, an 8-mer could be used in a more concentrated system, where it could rely on ensemble behaviors to alter the sterics of the system. Detailed simulations will be performed on these types of ensemble behaviors in the near future.

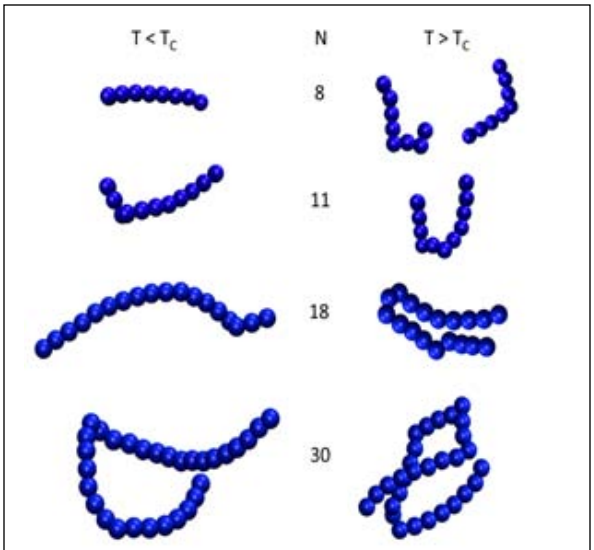

Figure 1. Simulated conformation of polyNIPAM molecules of varying number of repeat units (N) both below (left) and above (right) the LCST.

We have also applied a similar approach to functionalizing nanoparticles with a lipid bilayer, into which a responsive molecule can be inserted. We view this as a powerful new motif for nanoparticle functionalization, where multiple functionalities can be easily inserted into a fluidic coating. The only requirement for the functional molecules is that they have a substantial alkyl chain that is capable of inserting into a lipid bilayer. We have demonstrated the utility of this approach using the polyNIPAM surfactant molecule, which was easily inserted into lipid bilayers coating gold spheres and nanorods. The polyNIPAM based surfactant then imbued the particles with the temperature responsive behavior of the polymer itself. Heating stable dispersions of the nanoparticles past the polymer's LCST caused immediate, wholesale agglomeration leading to rapid precipitation of the aggregates. While the study described demonstrated only a single responsive behavior, multiple responsive behaviors can be programmed by the insertion of additional responsive molecules. The ease of insertion into the lipid bilayer, and the fluidity of the matrix which allows for the extreme responsiveness makes this system an outstanding alternative to traditional chemical modification approaches.

While certainly useful for nanocomposite formation, polyNIPAM surfactant molecules themselves have complex and sometimes unexpected, phase behavior. An interesting example of unexpected phase behavior of these molecules is the temperature sensitivity of the critical micellar concentration (CMC) of these molecules. The CMC is a fundamental property of surfactants, and typically varies an insignificant amount with temperature, though one would obviously expect a more significant effect from a polyNIPAM based molecule. Since the CMC is the concentration where addition of more molecules into solution causes the formation of micelles, instead of more individually solvated molecules, a low CMC is indicative of a low solubility while a high CMC is indicative of a high solubility. Decreasing the solubility of the

polyNIPAM section of a polyNIPAM surfactant would then be reasonably expected to decrease the solubility of the molecule, lowering its CMC. In fact, what is observed is the exact opposite (see Fig. 2). The high temperature CMC is three times the value of the low temperature CMC. One interesting impact of this work is that we see in Fig. 2 that there is a fairly broad concentration range where we can cross the CMC by altering only temperature (and only by a few degrees). This is an unusual responsive behavior that could have interesting and useful applications. For example, molecules could be shuttled in micelles then released on command by increasing the temperature a few degrees until all micelles are dissolved. Releasing emulsified molecules is typically much more difficult than this.

Future Plans

An increase in CMC with increasing temperature has been previously reported in the literature for a high molecular weight diblock material, though it has not been explained[2]. Since the molecular weights of the polyNIPAM and the attached alkyl chain in our surfactant are similar to each other, the molecules we are investigating could be considered extremely low molecular weight diblock copolymers. We believe that the behaviors in the literature and reported here occur for the same reason, and we will explore the reasons using Molecular Dynamics (MD) simulations and complimentary experimental studies.

It stands to reason that the increase in CMC above the polymer's LCST is caused by something that either stabilizes the individually solvated molecules, destabilizes the micellar form, or some combination of the two. Preliminary MD simulations are presented in Fig. 3, and show representative conformations for the surfactant molecules above and below the LCST. A comparison of these structures shows that the high temperature forms are less elongated and have a lower surface area exposed to the solvent (water). The shape change from elongated to more spherical would have the effect of destabilizing micelles above the LCST. The decreased exposure to the aqueous environment, particularly for the alkyl chain, will also have the effect of stabilizing the individually solvated form. These simulations certainly give us interesting clues to the unexpected behavior, but to be certain we must do further simulations. Specifically, we could calculate the relative energies of an individually solvated molecule versus a molecule in a micelle as a function of temperature. An alternative approach would be to allow individually solvated molecules and micelles to equilibrate at a variety of temperatures to see the shifting CMC values. Either approach will push the envelope of what is achievable today using MD simulations. The first due to conceptual issues with calculating and comparing absolute energies, and the second due to the size, complexity, and required time scale of equilibration in a calculation of this nature. We will choose between the two alternatives after completing the simulations of isolated molecules, and regardless of the choice, expect to make valuable contributions to Molecular Dynamics technique development in addition to the fundamental scientific understanding that is yielded.

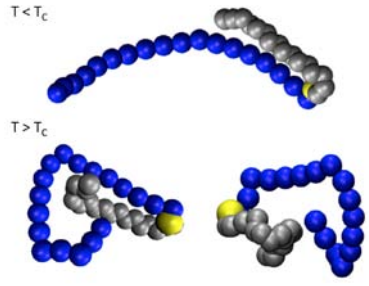

Figure 3. Conformations calculated for polyNIPAM-based surfactants below (top) and above the LCST. Grey regions are the alkyl chain, blue in polyNIPAM, and yellow is the bridging thioether.

In addition to thermally responsive molecules, we have been developing light responsive molecules and particles, magnetically responsive particles, and electrochemically active species,

as well as methods for integrating these materials into nanocomposites.

Acknowledgements

This research was supported by the Division of Materials Science and Engineering in the Department of Energy Office of Basic Energy Sciences. Sandia National Laboratories is a multi-program laboratory managed and operated by Sandia Corporation, a wholly owned subsidiary of Lockheed Martin Corporation, for the U.S. Department of Energy's National Nuclear Security Administration under contract DE-AC04-94AL85000.

References

1. Heskins, M. and Guillet, J.E., *Solution Properties of Poly(N-isopropylacrylamide).* Journal of Macromolecular Science: Part A - Chemistry, 1968. **2**(8): p. 1441-1455.
2. Kelarakis, A., Tang, T., Havredaki, V., Viras, K., and Hamley, I.W., *Micellar and surface properties of a poly(methyl methacrylate)-block-poly(N-isopropylacrylamide) copolymer in aqueous solution.* Journal of Colloid and Interface Science, 2008. **320**(1): p. 70-73.

Publications (2011-2013)

1. Stachowiak, J.C., Hayden, C.C., Sanchez, M.A.A., Wang, J., Bunker, B.C., Voigt, J.A., and Sasaki, D.Y., *Targeting Proteins to Liquid-Ordered Domains in Lipid Membranes.* Langmuir, 2011. **27**(4): p. 1457-1462.
2. Zendejas, F.J., Meagher, R.J., Stachowiak, J.C., Hayden, C.C., and Sasaki, D.Y., *Orienting lipid domains in giant vesicles using an electric field.* Chem Comm, 2011. **47**(26): p. 7320-7322, (Journal Cover).
3. Lee, S.E., Sasaki, D.Y., Park, Y., Xu, R., Brennan, J.S., Bissell, M.J., and Lee, L.P., *Photonic Gene Circuits by Optically Addressable siRNA-Au Nanoantennas.* ACS Nano, 2012. **6**(9): p. 7770-7780.
4. Stachowiak, J.C., Schmid, E.M., Ryan, C.J., Ann, H.S., Sasaki, D.Y., Sherman, M.B., Geissler, P.L., Fletcher, D.A., and Hayden, C.C., *Membrane bending by protein-protein crowding.* Nat Cell Biol, 2012. **14**(9): p. 944-9.
5. Tucker, A.K. and Stevens, M.J., *Study of the Polymer Length Dependence of the Single Chain Transition Temperature in Syndiotactic Poly(N-isopropylacrylamide) Oligomers in Water.* Macromolecules, 2012. **45**(16): p. 6697-6703.
6. Monson, T.C., Ma, Q., Stevens, T.E., Lavin, J.M., Leger, J.L., Klimov, P.V., and Huber, D.L., *Implication of Ligand Choice on Surface Properties, Crystal Structure, and Magnetic Properties of Iron Nanoparticles.* Particle & Particle Systems Characterization, 2013. **30**(3): p. 258-265, (Journal Cover).
7. Monson, T.C., Rodriguez, M.A., Leger, J.L., Stevens, T.E., and Huber, D.L., *A simple low-cost synthesis of brookite TiO2 nanoparticles.* J Mat Res 2013. **28**(3): p. 348-353.
8. Monson, T.C., Venturini, E.L., Petkov, V., Ren, Y., Lavin, J.M., and Huber, D.L., *Large enhancements of magnetic anisotropy in oxide-free iron nanoparticles.* Journal of Magnetism and Magnetic Materials, 2013. **331**: p. 156-161.
9. Ogunyankin, M.O., Huber, D.L., Sasaki, D.Y., and Longo, M.L., *Nanoscale Patterning of Membrane-Bound Proteins Formed through Curvature-Induced Partitioning of Phase-Specific Receptor Lipids.* Langmuir, 2013. **29**(20): p. 6109-6115.
10. Price, A.D. and Huber, D.L., *Controlled polymer monolayer synthesis by radical transfer to surface immobilized transfer agents.* Polymer Chemistry, 2013. **4**(5): p. 1565-1574.

Program Title: Bioinspired Magnetic Nanomaterials (Bioinspired Materials FWP)

PIs: Surya Mallapragada (FWP leader), Mufit Akinc, Dennis Bazylinski (UNLV), David Vaknin, Marit Nilsen-Hamilton, Alex Travesset, Monica Lamm, Ruslan Prozorov and Tanya Prozorov. Collaborator: Klaus Schmidt-Rohr, Tanya Prozorov
Mailing Address: Division of Materials Sci. and Eng., Ames Laboratory, Ames, IA 50011
Email: suryakm@iastate.edu

Program Scope: Nature is replete with hierarchically assembled hybrid materials where the multi-scale structures confer unique properties and functions. The objective of the Bioinspired Materials FWP is to explore biomimetic pathways for design and synthesis of hierarchically self-assembled functional materials with controllable properties for energy applications. Our approach uses organic templates coupled to mineralization proteins to control the growth of the inorganic phases to form self-assembled nanocomposites. Magnetotactic bacteria with chains of magnetic nanocrystals serve as inspiration and sources of mineralization proteins. We are developing methods to create dynamic tunable nanostructures using reversible linkages for assembly/disassembly of inorganic nanocrystals in response to environmental conditions.

The synergistic combination of synthesis, molecular biology, microbiology, materials characterization and theory provides a powerful approach for understanding mineralization processes in Nature and for expanding on these processes to grow novel nanocrystals in organic matrices *in vitro*. This controlled bottom-up approach for materials design aligns well with DOE's proposed directions in "control science", allowing for the synthesis of nanostructures such as complex magnetic nanocrystals with potential energy relevance. Our future directions in the FWP are to build on our current successes to fabricate nanocomposites with complex inorganic nanocrystals of energy relevance, and to control the hierarchical assembly/disassembly process to create nanocomposites with dynamic nanostructures.

Recent Progress:
Background In the past two years, we have synthesized biomimetic nanocrystals and nanocomposites by hierarchical assembly, developed and used new characterization techniques to investigate these materials and processes, and used computational methods for hierarchical and dynamical self-assembly to help guide the design of the experiments [1-20]. Focus has been on self-assembling nanocomposites with three different inorganic phases - calcium phosphate, magnetite and zirconia. The initial approach was developed using bone as inspiration for the development of calcium phosphate nanocomposites, and most of the recent work has focused on magnetic nanocomposites inspired by magnetotactic bacteria. Characterization techniques such as solid-state NMR and X-ray and neutron scattering methods, coupled with molecular biology techniques, have been developed to elucidate the hierarchical assembly and to understand the role of the mineralization proteins. The experimental techniques were complemented with computational methods to model dynamic self-assembly processes and help guide the experimental efforts.

We have developed a novel, room-temperature bioinspired route to create nanostructured magnetic materials, using the recombinant protein, Mms6 (Fig. 1), found in the magnetotactic bacteria, that promotes shape-specific magnetite nanocrystal growth. We have been able to synthesize not just magnetite nanocrystals similar to those found in Nature, but also cobalt and manganese ferrites as well as gadolinium doped multiferroic materials at room temperature synthesis conditions in the presence of Mms6. To investigate the mineralization mechanism to be able to design more robust synthetic analogs, mutants of Mms6 were developed, and characterized using a variety of techniques.

Discussion of Findings Control samples synthesized without protein, as well as those prepared in the presence of mutants of the wild-type Mms6, m2Mms6 and m3Mms6, featuring changes to the C-terminus of the protein, which we have demonstrated to be the active site of the protein for mineralization, showed only the small ill-shaped, poorly crystalline nanoparticles, while all of the Mms6-templated samples showed larger well-defined superparamagentic properties (Fig. 2).

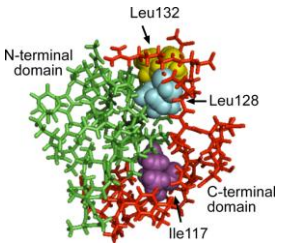

Fig. 1. Proposed structure of Mms6 mineralization protein

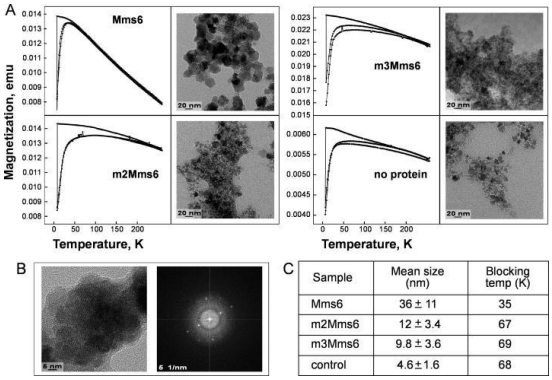

Sample	Mean size (nm)	Blocking temp (K)
Mms6	36 ± 11	35
m2Mms6	12 ± 3.4	67
m3Mms6	9.8 ± 3.6	69
control	4.6±1.6	68

Fig. 2. TEM images and magnetic measurements showing the ability of Mms6 to promote the formation of super-paramagnetic magnetite nanoparticles *in vitro*, while the two C-terminal mutants of the protein do not [9].

We have systematically established solid-state NMR as a tool for characterizing hierarchically assembled nanocomposites. We have introduced several NMR methods (in collaboration with the *Solid State NMR* FWP) for proving the presence of a nanocomposite where standard electron microscopy fails to provide a specific signature. To understand the role of mineralization proteins, we have developed surface sensitive synchrotron X-ray scattering and also used small angle X-ray scattering (SAXS) studies for determination of ion-specific distributions on molecular length scales at the surface of soft-matter templates and to investigate changes in the structure of Mms6 in the presence of iron (Fig. 3). This protein structural rearrangement does not occur in the case of the mutants, emphasizing the importance of this rearrangement in the mineralization process. We have shown that Mms6 binds iron very tightly stoichiometrically and then binds large amounts of iron at lower affinity to a limiting amount of ~18:1 (iron:protein). The SAXS studies have also been complemented by surface-sensitive X-ray and spectroscopy studies that allow us to take advantage of the fact that Mms6 forms a stable monolayer at the air-buffer interface, facilitating X-ray reflectivity studies on Mms6 template films. We developed and employed surface sensitive X-ray scattering and spectroscopy techniques to explore these thin protein films and also of lipids, or polymers at liquid/vapor interfaces and their interactions with ions and other organic solutes. X-ray reflectivity and grazing angle X-ray diffraction (GIXD) are used to determine the films structure, and X-ray fluorescence spectroscopy near-total-reflection (XNTRF) is used to determine surface ionic excess specifically, and surface X-ray absorption near-edge spectroscopy (SXANES) is used to probe the valence state of surface-bound ions, Fe(II) and Fe(III) in particular (Fig. 4). These experiments have been conducted on the Liquid Surface Spectrometer (LSS) at Sector 9 at the Advanced Photon Source at Argonne National Laboratory and also on a home based LSS using a rotating anode X-ray generator source.

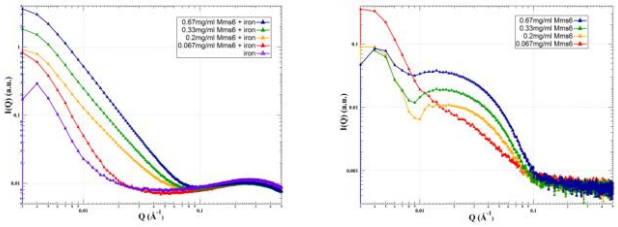

Fig. 3. SAXS studies show a change in Mms6 structure in the presence of iron, leading to disk-like structures

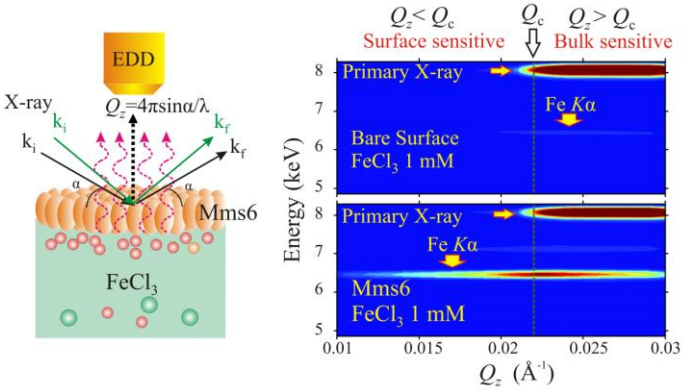

Fig. 4. (Left) Schematic illustration of X-ray fluorescence set up from the protein film on buffer solution with Fe ions in solution. **(**Right) Spectra from iron solutions of bare surfaces showing a weak signal from iron above the critical angle. Below, spectra on the same solution now covered by Mms6 protein, showing a strong signal below and above critical angle, evidence for strong accumulation of iron at the protein template [15].

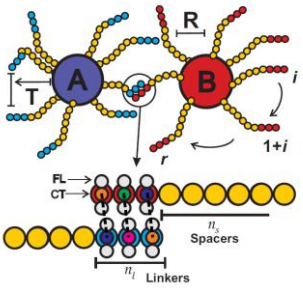

Fig. 5. Coarse grained models of DNA programmed self-assembly of nanoparticles [3].

Besides Mms6, we are investigating other mineralization proteins, especially from strains of magnetotactic bacteria that produce magnetic nanocrystals with various morphologies besides cubo-octahedral, such as bullet-shaped nanocrystals etc. In this regard, we have identified MamC biomineralization protein, originally obtained from the *Magnetococcus marinus*, a magnetotactic coccus (MC-1), to be one of the promising candidates for the bioinspired magnetite synthesis. We also continue work on a variety of magnetotactic bacteria, probing the incorporation of dopant cations into the magnetosome magnetite crystal. The experimental studies are being complemented with predictive theoretical studies that involve coarse-grained molecular dynamics simulations of programmed DNA self-assembly of inorganic nanoparticles, and the dynamics of crystallization of DNA programmed self-assembly (Fig. 5). This work will help guide the future directions of the project involved DNA strands attached to self-assembling polymer templates for biomineralization, as described below.

Importance of Findings The ability to synthesize a variety of uniform magnetic nanoparticles under ambient synthesis conditions through the use of biomimetic approaches involving self-assembling polymers and mineralization proteins, opens up new possibilities for green synthetic approaches. In addition, these approaches allow for the ability to pattern arrays of nanocrystals on surfaces, and create dynamic nanostructures with reversible assembly/disassembly. This provides a lot of versatility for the creation of hierarchically self-assembled structures using bottom-up approaches.

Future Plans:

We have already demonstrated how to produce nanostructured inorganic materials and control their placement in an organic matrix through self-assembly. In the next phase of this work, we will fabricate *dynamic* structures with reversible assembly/disassembly of arrangements of the magnetic nanocrystals on surfaces (Fig. 6). This will enable the formation of tunable and dynamic "smart" structures with different hierarchical and magnetic properties in response to different environmental stimuli. It will further impart a new degree of functionality that cannot be obtained with materials fabricated using top-down approaches. Immobilizing and patterning the Mms6 on hydrophobic surfaces (such as octadecane thiol (ODT) monolayers on gold) using reversible or irreversible linkages, provides an opportunity to create nanowires and other assemblies of magnetic nanocrystals. Using the templates and mineralization proteins similar to those outlined above, we are using complementary DNA strands attached to the ends of self-assembling polymers to guide the assembly and provide reversible linkages to create dynamic nanostructures (Fig. 7).

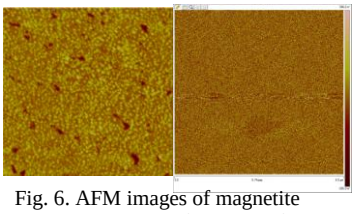

Fig. 6. AFM images of magnetite nanoparticles on (left) gold surface with ODT and Mms6 and absence of nanoparticles on (right) gold surface with ODT and no Mms6.

Computational studies will guide the design of these experiments. Based on our previous theoretical work, we have provided a detailed theoretical understanding for the complementary DNA based experiments predicting a new class of materials that consist of hybridization of nanoparticles with grafted ssDNA and linkers attached to hydrophobic blocks. Combinations of templating methods on mineralization proteins and nanocrystal systems are being explored. We will continue to develop novel methods for comprehensive characterization of both inorganic and organic components of the nanocomposites and probe structure, composition and function, as well as mechanisms of biomineralization. The computational and theoretical challenges address the problems of characterizing the design rules of polymer nanocomposites as well as the challenge to simulate biomineralization processes. The goal

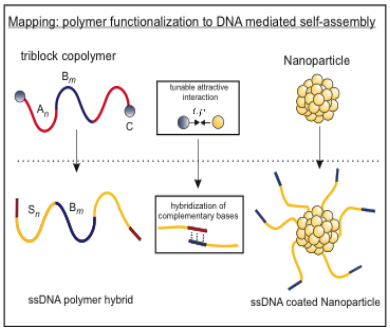

Fig. 7. Mapping polymer functionalization to ssDNA mediated self-assembly [5]

is to provide a theoretical framework for the proposed experiments and build upon the success of the models developed in this program.

References (which acknowledge DOE support; from 2011 to 2013)

1. Self-Assembly Enters the Design Era, Travesset, A., *Science*, **334**, 183-184 (2011).
2. A Cultured Greigite-Producing Magnetotactic Bacterium in a Novel Group of Sulfate-Reducing Bacteria. Lefevre, C. T., Menguy, N., Abreu, F., Lins, U., Mihaly, P., Prozorov, T., Pignol, D., Frankel, R. B., and Bazylinski, D. A., *Science.* **334**, 1720-1723 (2011).
3. Dynamics and Statics of DNA-Programmable Nanoparticle Self-Assembly and Crystallization, Knorowski, C., Burleigh, S., and Travesset, A., *Phys. Rev. Lett.*, 106215501-215504 (2011).
4. Biomimetic Self-assembling Copolymer - Hydroxyapatite Nanocomposites with the Nanocrystal Size Controlled by Citrate, Hu, Y., Liu, X., Ma, X., Rawal, A., Prozorov, T., Akinc, M., Mallapragada, S., Schmidt-Rohr, K., *Chem. Mater.*, **23**, 2481-2490 (2011).
5. Materials Design by DNA Programmed Self-assembly, Knorowski, C., and Travesset, A., *Curr. Opin. Solid State and Mater. Sci*., **15**, 262 – 270 (2011).
6. Ionic Specificity in pH Regulated Charged Interfaces: Fe^{3+}versus La^{3+}, Wang, W., Park, R., Meyer, D., Travesset, A., and Vaknin, D., *Langmuir*, **27**, 11917-11924 (2011).
7. Ion-Specific Induced Charges at Aqueous Soft Interfaces, Wang, W., Park, R., Travesset, A., and Vaknin, D., *Phys. Rev. Lett.*, 106056102 (2011).
8. Bioinspired Synthesis of Organic/Inorganic Nancomposite Materials Mediated by Biomolecules, Liu, X., and Mallapragada, S.K., in On Biomimetics, Pramatarova (Ed.) InTech Publishers, pp. 229-251 (2011).
9. Self-Assembly and Biphasic Iron-Binding Characteristics of Mms6, a Bacterial Protein that Promotes the Formation of Superparamagnetic Magnetite Nanoparticles of Uniform Size and Shape, Wang, L. J., Prozorov, T., Palo, P. E., Liu, X. P., Vaknin, D., Prozorov, R., Mallapragada, S., and Nilsen-Hamilton, M., *Biomacromolecules*, **13**, 98-105 (2012).
10. Dynamics of DNA-Programmable Nanoparticle Crystallization: Gelation, Nucleation and Topological Defects, Knorowski, C., and Travesset, A., *Soft Matter*, **8**, 12053-12059 (2012).
11. X-ray Diffraction and Spectroscopic Techniques for Liquid Surfaces and Interfaces, Vaknin, D., Characterization of Materials (Edited by E. N. Kaufmann) **2**, 1393-1423 (2012).
12. Amorphous Iron-(hydr)-oxide Networks at Liquid/Vapor Interfaces: In situ X-ray Scattering and Spectroscopy Studies, Wang, W., Pleasants, J., Bu, W., Park, R. Y., Kuzmenko, I. and Vaknin, D., *J. Colloid Inter. Sci.*, **384**, 45-54 (2012).
13. Nanorods in Functionalized Block-Copolymer gels: Flexible Ladders and Liquid Crystalline Order in Curved Geometries Knorowski, C., and Travesset, A., *EPL*, 10056004 (2012).
14. Regulation of the Electric Charge in Phosphatidic Acid Domains, Wang, W., Anderson, N. A., Travesset, A., and Vaknin, D., *J. Phys. Chem. B*, **116**, 10406-10406 (2012).
15. Interfacial Properties and Iron Binding to Bacterial Proteins That Promote the Growth of Magnetite Nanocrystals: X-ray Reflectivity and Surface Spectroscopy Studies, Wang, W., Bu, W., Wang, L. –J., Palo, P. E., Mallapragada, S., Nilsen-Hamilton, M., and Vaknin, D., *Langmuir*, **28**, 4274-4282 (2012).
16. Klostermann, L., Ma, X., Hu, Y.-Y., Liu, X.P., Mallapragada, S.K., Schmidt-Rohr, K., and Akinc, M.A., "Aqueous Route Synthesis of Mesoporous Zirconia by Agarose Templation", *J. Am. Ceram. Soc.*, **95**, 3455-62 (2012).
17. Surface Nano-crystallization of an Ionic Liquid, Jeon, Y., Vaknin, D., Bu, W., Sung, J., Ouchi, Y., Sung, W., and Kim, D., *Phys. Rev. Lett.*, **108**, 055502/1-5 (2012).
18. Different Adsorption Behavior of Rare Earth and Metallic Ion Complexes on Langmuir Monolayers Probed by Sum-Frequency Generation Spectroscopy, Sung, W., Vaknin, D., and Kim, D., *J. Opt. Soc. Korea*, **17**, 10-13 (2013).
19. Bioinspired Synthesis and Characterization of Mesoporous Zirconia Templated by Cationic Block Copolymers in Aqueous Media, Liu, X., Ge, Q., Rawal, A., Parada, G., Schmidt-Rohr, K., Akinc, M., and Mallapragada, S.K., *Sci. Adv. Mater*., **5**, 1-12 (2013).
20. Novel Magnetic Nanomaterials Inspired by Magnetotactic Bacteria: Topical Review, Prozorov, T., Bazylinski, D., Mallapragada, S.K., and Prozorov, R., *Matl. Sci. Eng. R.*, **74,** 133-172 (2013).

Molecularly Engineered Biomimetic Nanoassemblies

Jennifer S. Martinez (jenm@lanl.gov), **Hsing-Lin Wang** (hwang@lanl.gov), Srinivas Iyer (siyer@lanl.gov), Reginaldo Rocha (rcrocha@lanl.gov), Los Alamos National Laboratory;
Andrew P. Shreve (shreve@unm.edu), University of New Mexico;
James Brozik (brozik@wsu.edu), Washington State University;
Darryl Sasaki (dysasak@sandia.gov), Sandia National Laboratories;
Atul N. Parikh (anparikh@ucdavis.edu), University of California, Davis;
Sunil K. Sinha (ssinha@physics.ucsd.edu), University of California, San Diego.

Program Scope

The program aims to develop self-assembly and biologically-assisted assembly methods for the control of functional responses in complex, multi-component materials. The overall motivation is derived from an examination of natural systems that demonstrate exquisite manipulation and transduction of optical energy. We are interested in developing assemblies of nanomaterials that mimic two particular functions of natural systems, photo-induced charge separation and control of light-harvesting (or manipulation of electromagnetic fields). In natural systems, control over these functions is achieved through a dynamic hierarchical organization, which allows for control and manipulation of energy across multiple length scales in a spatially directed manner. In many cases, this hierarchical organization is associated with complex membrane assemblies. Thus, within the past period we have also explored the integration of functional synthetic nanomaterials with complex membrane-based architectures in order to generate materials with energy-relevant functions that demonstrate larger-scale organization similar to that found in natural systems. Functionally active synthetic materials under study include conjugated polymers and polyelectrolytes, carbon-based nanomaterials, and luminescent noble-metal nanoclusters. Approaches used include a combination of material synthesis and fabrication, static and time-resolved spectroscopies, optical and scanning probe microscopies, X-ray and neutron scattering, structural characterization, and modeling and analysis.

Recent progress

We highlight here three areas of recent work that will form the basis of presentations. Progress in other areas related to the program scope is represented in the publication list.

Fluorescent metal nanoclusters (Martinez, Shreve, Rocha, Sinha) Fluorescent metal nanoclusters are collections of small numbers of gold or silver atoms (2-31 atoms, $\leq$ 1 nm) with tunable fluorescence emission, single-timescale photoblinking, and high quantum yields (Fig. 1). These nanoclusters are a missing link between the atomic and nanoparticle behavior of noble metals – exhibiting fluorescence emissions spanning the UV to near IR range. Recently, we have synthesized and photophysically characterized a palette of Ag-nanoclusters (AgNCs), templated on DNA, with distinct and narrow excitation and emission profiles tuned to common laser lines, and with high quantum yields.[R1] These two-photon active clusters,[5] templated within individual DNA, have been shown by photon antibunching to exist as single quantum systems. For the first time in the literature we have definitively shown that these "fluorescent clusters" are truly *clusters* through Extended X-ray Absorption Fine Structure (EXAFS) analysis of each AgNC within the palette of fluorescent

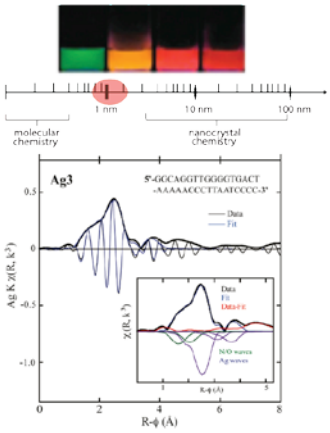

Fig. 1 EXAFS determination of the cluster-nature of DNA-AgNC

clusters (Fig. 1 EXAFS spectra of a red cluster).[2] We found that the number of nearest neighbors in the first AgAg shell is small and variable among the optically different clusters, with cluster size ranging from 8-31 atoms and with Ag-Ag bonds at distances contracted from Ag metal, consistent with the presence of small clusters. Most recently, we have learned to evolve DNA AgNC templating sequences so as to dramatically increase the time, temperature, and oxidative stability of the resultant AgNC,[4] leading to better stability within assemblies.

Conjugated polymers and oligomers (Wang, Shreve). While conjugated polymers have proven invaluable for applications in optical, electronic, sensing, and photovoltaic devices, in many respects the optical properties of a conjugated polymer can be regarded as the collective properties of an ensemble of conjugated oligomers.[R2] Because conjugated oligomers can be self-assembled into hierarchical structures, whose optical and electronic properties are strongly related to the interactions between oligomer molecules, we have synthesized a series of PPVO (p-phenylene vinylene oligomer) derivatives, with functional groups of varying electronegativity, via the Horner-Wadsworth-Emmons reaction.[20] We found that subtle changes in the end group functionality significantly impact the molecular electronic and optical properties of the PPVOs, resulting in broadly tunable and efficient UV absorption and photoluminescence spectra (Fig. 2), with similar properties observed in OLED devices. Experimental and theoretical results for the NH_2-, H-, and NO_2-substituted PPVOs suggest that the stabilization of ground or excited state dipoles leads to a blue or red shift of the optical spectra. Of particular interest is the NO_2-PPVO, which exhibits strong solvatochromism with photoluminescence color ranging from the blue to the red, resulting from formation of aggregates and strong dipole-dipole solute-solvent interactions. Toward creating stimuli-responsive and dynamic assemblies, COOH-PPVO has been positionally conjugated to PNIPAM (poly(N-isopropylacrylamide)) and genetically engineered elastin polymers,[22] whose conjugates show increased fluorescence intensity, in response to stimuli, resulting from rigidchromism of the PPVO.

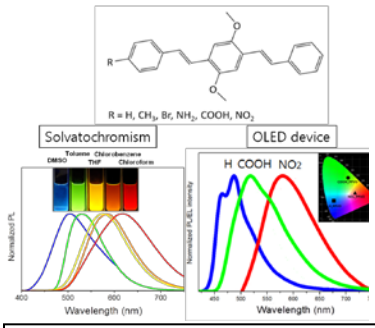

Fig. 2 Suites of PPVO with optical activities tuned for molecular assembly and OLED devices

Lipid-based assembly of conjugated polymers. (Sasaki, Wang, Shreve, Parikh)**.** Toward integrating electrically and optically active components within a membrane scaffold, we have been tuning membrane properties to develop methods for spatial control over interfacial organization of conjugated polymers. Both single lipid bilayers and multicomponent membranes are explored. Using single supported lipid bilayers we examined the use of phase-separating lipid membranes as a means to direct and reprogram organization of associating conjugated PPV-P2, (poly{2,5-bis[3-(*N*,*N*,*N*-triethylammonium bromide)-1-oxapropyl]-1,4-phenylenevinylene}).[R3] Phase separation of a gel phase anionic lipid and fluid phase phosphocholine lipid allowed the formation of negatively charged domain assemblies that selectively adsorbed the cationic PPV-P2. Spectroscopic studies found the adsorption of P2 to negatively charged membranes resulted in minimal structural change of the solution phase polymer, but yielded an enhancement in fluorescence intensity (~50%) due to loss of quenching pathways (Fig. 3).[15] In addition to randomly formed circular gel phase domains we also showed

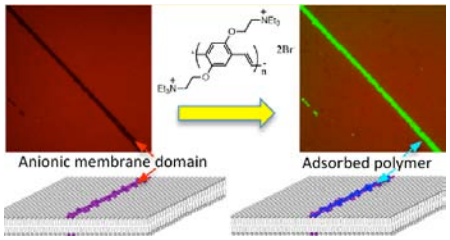

Fig. 3 Phase separating lipids can assemble conducting polymers

that predefined features, such as straight lines of polymers, can be directed to form upon etched patterns within the substrate thus providing potential routes towards the self-organization of optoelectronic architectures.[15] Inspired by these findings, we explored if the same mixture of phase separating lipids could be organized into three-dimensional (3D) assemblies. We have found that negatively-enriched domains in the parent bilayer template the nucleation of higher ordered lamellae, simply by thermal annealing,[26] originating from an interplay between height mismatch in co-existing domains and headgroup electrostatics, producing novel multilamellar stacks exhibiting pyramidal staircase topography. In addition to height and electrostatic mismatches, we find that proteins such as BSA and the lipid binding transmembrane protein Annexin V can order and assemble lipid domains.[6,17]

Future Plans

In the future we focus our effort on creating environmentally tunable fluorescent silver and gold nanoclusters and conjugated oligomers that are optimized for integration within biomolecular assemblies; develop DNA and computationally designed peptide components with predictable assembly properties that can be used to produce functional optical materials; and finally use of a suite of advanced characterization tools to better understand the effect of dynamics in controlling the structure and functionality of complex biomolecular assemblies.

References

R1. Yeh, H.-C., Sharma, J., Martinez*, J.S., Werner*, J.H. "A DNA−Silver Nanocluster Probe That Fluoresces upon Hybridization," *Nano Letters* 10(8), 3106-3110 (2010). Sharma, J., Yeh, H.-C., Yoo, H., Werner, J.H., Martinez, J.S. "A complimentary palette of fluorescent silver nanoclusters," *Chemical Communications* 46, 3280 (2010).
R2. Hu, D.; Yu, J.; Wong, K.; Bagchi, B.; Rossky, P. J.; Barbara, P. F., "Collapse of stiff conjugated polymers with chemical defects into ordered, cylindrical conformations." *Nature*, 405, 1030, (2000).
R3. Gao Y.; Wang C. C; Wang L.; Wang H. L., "Conjugated polyelectrolytes with pH-dependent conformations and optical properties" *Langmuir*, 23, 7760, (2007).

Publications supported by BES (July 2011-July 2013)

1. Yoo, H, Sharma, J., Kim, J.K., Shreve, A.P., Martinez, J.S. "Tailored Microcrystal Growth: A Facile Solution-Phase Synthesis of Gold Rings," *Advanced Materials* 23, 4431 (2011). *(highlighted in ACS Noteworthy Chemistry: Oct 17, 2011)*
2. Neidig, M.L., Sharma, J., Yeh, H.-C., Martinez, J.S., Conradson, S.D., Shreve, A.P. "Ag K-edge EXAFS analysis of DNA-templated fluorescent silver nanoclusters: insight into the structural origins of emission tuning by DNA sequence variations" *Journal of the American Chemical Society* 133, 11837 (2011).
3. Wang, H.-L., Xu, P., Akhadov, E., "Sequential deposition of Ag/Au alloys with Jelly fish morphology" *Chemical Comm*unications 47, 10764 (2011).
4. Sharma, J.K., Phipps, M.L., Yeh, H.-C., Werner, J.H., Martinez, J.S., "A DNA-templated fluorescent silver nanocluster with enhanced stability " *Nanoscale*, 4, 4107(2012) .
5. Yeu, S.H., Abeyasinghe, N., Orr, M., Yeh, H.-C., Sharma, J.K., Werner, J.H., Shreve, A.P., Varnavski, O., Martinez, J.S., Goodson, T. III, "Bright two-photon emission and multi-atom excitation in a DNA-templated fluorescent silver nanoclusters investigated by ultra-fast spectroscopy" *Nanoscale*, 4, 4247(2012).
6. Poudel, K.R., Keller, D.,J., Brozik, J.A., "The Effect of a Phase Transition on Single Molecule Tracks of Annexin V in Cushioned DMPC Assemblies", *Soft Matter,* 8, 11285 (2012).
7. Cotlet, M, Wang, H.-L., Xu, Z., "Transparent light harvesting polymer films' *McGrawHill Yearbook of Science and Technology*, 278-282 (2012).
8. Huang, Y.-F., Xu, P., Wang, H.-L., "Low temperature synthesis of PANI/Au nanocomposites: Toward controlled formation of Au nanoparticle size, nanocomposite morphology, and size dispersity" *Journal of Physical Chemistry C.* 116, 11272 (2012).

9. Huang, Y.-F., Shih, H.-H., Ramos, K., Hooks, D., Xu, P., Wang, H.L., "Morphology Control of Cu Crvstals on Modified Conjugated Polymer Surfaces" *Crystal Growth and Design,* 12, 1778 (2012).
10. Duque, J.G., Telg, H., Chen,H., Swan, A.K., Shreve, A.P., Tu, X., Zheng, M., Doorn, S.K., "Quantum interference between the third and fourth excitonic states in semiconducting carbon nanotubes," *Physical Review Letter,* 108, 117404 (2012)
11. Parikh A. N., Allara, D. L.,"Self-Assembled Monolayers: A Versatile Tool for Biofunctionalization of Surfaces," Handbook of Biofunctionalization of Surfaces (Ed., Knoll, W.), Pan Stanford Press, in press (2012)
12. Yan, J., Han, S., He, J., Kang, L., Zhang, B., Du, Y., Zhao, H., Dong, C., Wang, H.-L., Xu, P., "Highly Sensitive SERS Platforms Based on Silver Nanostructures Fabricated on Polyaniline Membrane Surfaces" *ACS Applied Materials & Interfaces*, 4, 2752 (2012).
13. He, J., Han, X., Yan, J., Kang, L., Zhang, B., Du, Y., Dong, C., Wang, H.-L., Xu, P., "Fast fabrication of homogeneous silver nanostructures on hydrazine treated polyaniline films For SERS applications" CrystEngComm, 14, 4952 (2012).
14. Han, J.J., Shreve, A.P., Werner, J.H., "Super-resolution optical microscopy," in Characterization of Materials, 2nd Edition, Ed. E.N. Kaufmann (Wiley: 2012)
15. Sasaki, D.Y., Zawada, N., Gilmore, S. F., Narasimmaraj, P., Sanchez, M.A.A., Stachowiak, J.C., Hayden, C. C., Wang, H.-L., Parikh, A. N., Shreve, A. P., "Lipid Membrane Domains for the Selective Adsorption and Surface Patterning of Conjugated Polyelectrolyes," *Langmuir 29*, 5214 (2013).
16. Babayco, C., Chang, P., Land, D.P., Kiehl, R.A., Parikh, A.N., *"Evolution of Conformational Order During Self-Assembly of n-Alkanethiols on Hg Droplets: An Infrared Spectro-microscopy Study," Langmuir*, 2013, 29, 8203
17. Silva-Lopez, E.I., Barden, A.O., Brozik, J.A., "Near Native Binding of a Fluorescent Serotonin Conjugate to Serotonin Type-3 Receptors", *Bioorganic and Medicinal Chemistry Letters,* 23, 773 (2013).
18. Xu, P., Chang, K., Park, Y.I., Zhang, B., Kang, L., Du, Y., Iyer, R.S., Wang , H.-L.,"Conjugated polymer mediated synthesis of nanoparticle clusters and core/shell nanoparticles *Polymer,* 54, 485 (2013).
19. Li, S., Xu, P., Ren, Z., Mack, N.H., Wang, H.-L., "The Fabrication of Thorny Au Nanostructures on Polyaniline Surfaces for Sensitive Surface Enhanced Raman Spectroscopy" *ACS Applied Materials and Interfaces,* 5, 49 (2013).
20. Wang, H.-L., Park, Y.I., Kuo, C.-Y., Tretiak, S., Martinez, J.S., Zhugayevych, A., Postupna, O., "Tailored electronic structure and optical properties of conjugated systems through aggregates and dipole-dipole interactions" *ACS Applied Materials and Interface,* 5, 4685 (2013).
21. Xu, P., Li, Q., Zheng, S., Wu, G., Wang, J., Wang, H.-L., "Facile Synthesis and Structure-Dependent Electrocatalvtic Properties of Cu_2O Nanocrystals for Oxygen Reduction" *Journal of Physical Chemistry C.,* (2013). DOI: 10.1021/jp403655y
22. Park, Y.I., Zhang, B., Mallapragada, S., Martinez, J.S., Park, Y.W., Wang, H.-L., "Stimuli Responsive Poly-N-isopropylacrylamide- polyphenylene vinylene Oligomer Conjugate" *Journal of Physical Chemistry C*. 117, 7757 (2013).

23. Kang, L., Xu, P., Zhang, B., Tsai, H., Han, X., Wang, H.-L., "Laser wavelength- and power-dependent plasmon-driven chemical reactions by single particle surface enhanced Raman spectroscopy" *Chemical Comm*unications, 49, 3389 (2013). (featured cover article)
24. Xu, P., Zhang, B., Wu, G., Fu, E., Han, X., Li, Q., Wang, H.-L., "A Novel Synthesis of Pt Nanoassemblies *via* Galvanic Replacement from Cu_2O for Oxygen Reduction and Methanol Oxidation" *Nanoscale,* accepted (2013).
25. Kuo, C.-Y., Rwei, S.-P., Wang, H.-L., Wang, L., "Effect of chain architecture of side group on the optical and crystalline properties of two-dimensional polythiophenes" *Macromolecules,* accepted in revision (2013).
26. Gilmore, S.F., Sasaki, D.Y., Parikh, A.N., "Thermal annealing triggers collapse of biphasic supported lipid bilayers into multilayer islands," *Soft Matter*, in review, (2013).

Program Title: Directed Organization of Functional Materials at Inorganic-Macromolecular Interfaces

PI: ***Aleksandr Noy*[1]; Co-Is:** ***Jim De Yoreo*[2], *Tony Van Buuren*[1], *George Gilmer*[1] *and Matt Francis*[3]**

Mailing address: [1]Physical & Life Sciences Directorate, Lawrence Livermore National Laboratory, Livermore, CA; [2] MS[3], Pacific Northwest National Laboratory, Richland, WA; [3]Univiersity of California Berkeley, Berkeley, CA

E-mail: noy1@llnl.gov

PROGRAM SCOPE

The purpose of this project is to develop a quantitative physical picture of macromolecular organization and its relationship to function, and to use macromolecular organization to derive new functionality. The research is divided into several tasks. In the first, we are fabricating bio-nanoelectronic devices in which phospholipids bilayers assembled on 1D Si nanowires create an impermeable barrier against solution species transport to the nanowire surface. The bilayers serve as artificial environments for membrane pore proteins and creating a versatile assembly for biomimetic control of ion transport to and from the nanowire surfaces. Significantly, these devices can function as a versatile interface between biological objects and electronic circuits. In the second task, we are creating artificial light harvesting complexes using virus-DNA origami arrays assembled on 2D chemical templates. MS2 viral capsids functionalized on their exterior surfaces with DNA linkers are modified to include light adsorbing centers. These are either assembled with capsids functionalized with complementary strands to form FRET pairs, or assembled with Au nanoparticles at nm-scale using DNA origami tiles to achieve plasmonic enhancement of fluourescence. In the final task, we are investigating the mechanistic controls on formation of extended 2D macromolecular structures, in which conformational transformations are an inherent feature of assembly and multiple order parameters evolve on distinct timescales. Using two self-organizing systems — S-layer tetramers and collagen triple helices — we are determining the dependence of assembly pathway, kinetics and morphology on the intermolecular and substrate interactions. Two complementary characterization efforts cut across these tasks. First effort involves atomic-scale characterization using small-angle x-ray scattering (SAXS) and imaging (STXM), and a recently introduced effort uses high-speed atomic force microscopy imaging to capture real-time dynamics of biomolecular assembly on planar and curved templates.

RECENT PROGRESS

(1) Bionanoelectronic devices controlled by a light-activated protein pump. We have been developing 1D bilayer bioelectronic transistors in which nanowires and nanotubes are covered by a lipid bilayer that contains different membrane proteins (Fig. 1A). In the past we built prototype devices that incorporate self-assembled active and passive membrane proteins as integral parts of the circuit. In this cycle we have demonstrated devices that use photoactivated proton pump bacteriorhodopsin (Fig. 1A) as a biological gate for a nanowire transistor. Upon green light illumination devices show a response that is stronger and markedly different from the small photocurrent response exhibited by the control devices without bR protein. (Fig. 1B). Light intensity dependence of the device response is also consistent with the protein activity (Fig. 1C).

Furthermore, we have investigated a possibility of using other biological molecules to tune the device characteristics. In particular we found that incorporation of other biological pores and transporters into the system can enhance the device response or device relaxation time. Specifically, addition of nigericin that neutralizes the charge under the bilayer enhances the device efficiency, and addition of non-specific GramA pores enhances the proton leakage rate

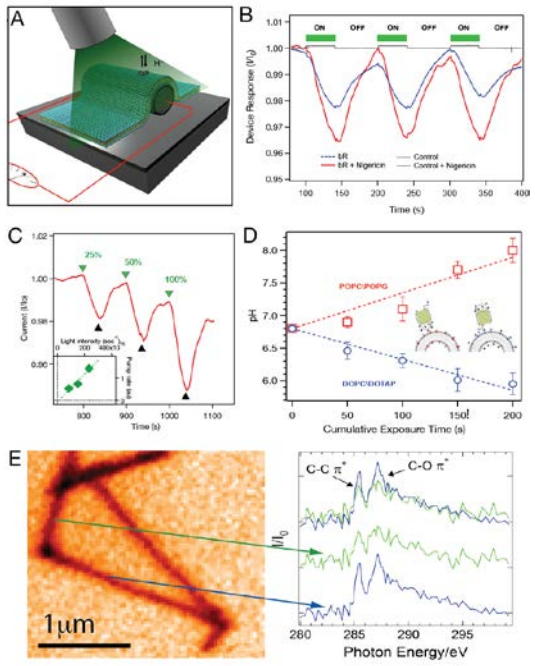

Fig. 1. Bionanoelectronic transistor gated by a photoactivated proton pump. (A) Schematic of the experiment showing a nanowire device covered with lipid bilayer incorporating bacteriorhodopsin (bR) protein pump. (B) Time traces of normalized device conductance recorded for the device incorporating bR protein (blue), bR protein and ionophore nigericin (red) and a control experiment that did not have proteins in the lipid bilayers (grey). (C) Time traces of normalized conductance of the bR-controlled device recorded at different light levels. Inset shows the dependence of the pump rate on light intensity. (D) Orthogonal protein activity controlled by oriented insertion of proteorhodopsin (pR) into lipid bilayers. (E): STXM stack plot analysis of phospholipid bilayer-coated SiNWs. Angular dependence in the C K-edge NEXAFS arises from ordering in the 1-D lipid. bilayer on two orthogonal SiNWs.

and produces faster relaxation times. In a parallel effort we explored different strategies for oriented insertion of membrane proteins into the lipid bilayer and showed that controlling bilayer charge could be an effective means to achieve strong preferential insertion of asymmetric membrane proteins (Fig 1D).

We have also been using SAXS and STXM to determine the orientation and structure of the phospholipid bilayers. Analysis of STXM data recorded for isolated Si wires with orthogonal spatial orientations (e.g. one wire perpendicular to the x-ray field vector and one parallel (Fig. 1E) reveals angular dependent NEXAFS resonance intensities for the C-C and C-O π*-orbitals of the phospholipid molecules. This statistically averaged anisotropy in the electronic density of states indicates that the phospholipid layers formed on the wires are ordered and exhibit a preferred orientation of the aromatic groups contained within them. SAXS measurements on lipid coated SiNW reported the electron density of the lipid coating, which turned out to be different from that of the isolated lipid vesicle. This result indicates that the nanowire surface may influence lipid packing.

(2) High-speed AFM investigations of biomolecular assembly on lipid templates. Ability to monitor biological molecules with high spatial and temporal resolution would be a tremendous asset to unraveling the physics of biomolecular assembly. During the project period our team acquired a high-speed atomic microscope (funded by a BES equipment grant) that speeds up the traditional AFM imaging by several orders of magnitude and permits direct *in-situ* observation of dynamics on millisecond time scale. Our initial activities with this instrument are focused on studying of the protein assembly on flat and curved membrane surfaces and, in particular, we are looking at assembly of dynamin, one of the key players in clathrin-mediated endocytosis. Initial movies of dynamin assembly revealed dynamics of the transient formation of rings composed of protein dimers and tetramers (Fig. 2). Researchers previously observed such rings with cryo-TEM and postulated that the assembly proceeds through the association of tetramers; our initial observations of the assembly dynamics suggest that dynamin dimers play a key role in the process.

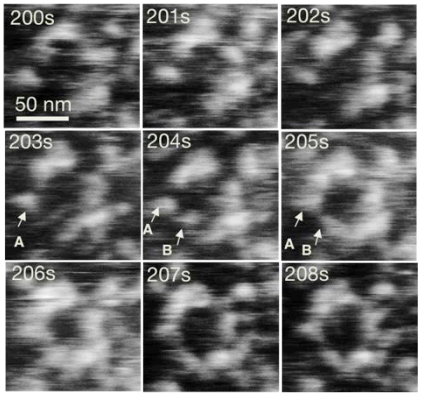

Fig. 2. Snapshots from a high-speed AFM movie showing the formation of a transient ring assembly of dynamin proteins.

(3) Immobilization and organization of optically-active virus capsids with nanoscale precision using DNA origami. Virus capsids present a high density of equivalent positions that

can be exploited to make molecular-density arrays of precisely-defined active sites. Previously we demonstrated labeling of the interior of MS2 capsids with Oregon Green maleimide fluorescent dye and of the exterior with a 20-nt poly-T DNA sequence. Moreover, we showed the capsids could be bound to DNA origami tiles bearing complementary probe strands for both 90x60 nm^2 rectangles and 120 nm equilateral triangles. Recently, we have used these heterostructures as a platform to achieve plasmonic enhancement of fluorescence by attaching Au nanoparticles (AuNP) onto the origami tiles. The virus capsid creates a scaffold for control over the three dimensional arrangement of the chromophores, whereas the origami provides precise control over the distance between the capsid and the AuNP. Using finite-difference time-domain numerical simulations and multimodal single-particle imaging measurements of fluorescence intensity vs. capsid-AuNP spacing, we showed that the judicial design of these structures places the dye molecules near the hot spot of the AuNP. This geometry increases the fluorescence intensity in what would normally be the quenching regime of the AuNP, with an enhancement factor that increases with increasing AuNP size (Fig. 3). This strategy of using biological scaffolds to control fluorescence paves the way for exploring plasmonic fluorescence parameters. It may lead to a better understanding of the antenna effects of photon absorption and emission, enabling the construction of multicomponent plasmonic systems.

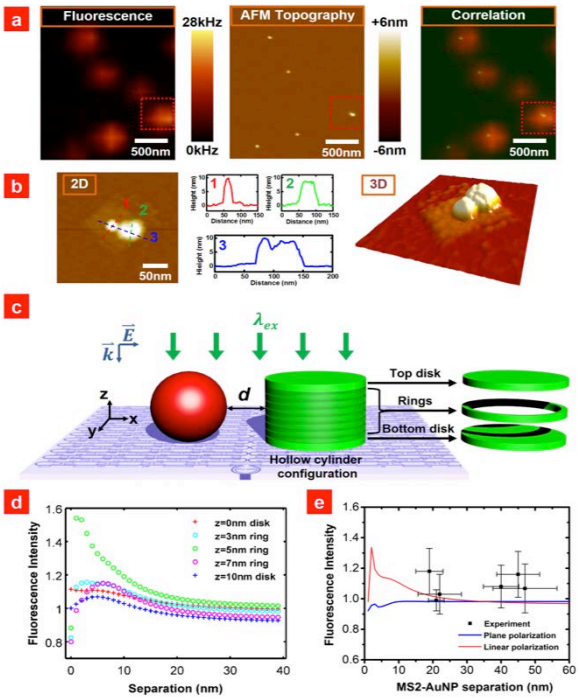

Fig. 3. Multimodal single-particle imaging and numerical simulation of individual capsid-AuNP-origami plasmonic heterostructures. (A) Correlation between fluorescence and position. (B) Non-contact mode AFM images of capsid-AuNP pair on DNA origami and profiles of an AuNP (red), capsid (green), and capsid-NP pair (blue). (C) Schematic of geometric model used to calculate the ensemble fluorescence intensities of the entire dye molecule distribution on the capsid as a function of distance from the AuNP. The arrays of dye molecules on the top and bottom surfaces were treated as disks, and the dye molecules on the side of the cylinder were treated as stacking rings sandwiched between the top and bottom surfaces. (D) Fluorescence intensities of disks and rings as a function of separation are. (E) Ensemble fluorescence intensity of the entire hollow cylinder distribution of the dye molecules was obtained from the calculations for disks and rings along with the experimental data.

(4) Protein self-assembly with conformational transitions and substrate interactions. Collagen is a fibrillar protein that consists of three polypeptide chains wrapped around one another to form triple helices approximately 300 nm in length. The helices are arranged in a quasi-hexagonal five-helix bundle in which the individual collagen molecules overlap and intertwine to form microfibrils containing "hole zones", where there is a gap between the end of one helix and the start of another. We have found that we can use variations in pH and K^+ concentration to direct assembly of collagen on mica into structures ranging from disordered monolayers, to monolayers of co-aligned helices to 3D bundles of co-aligned helices, to ordered 2D matrices. Dynamic force spectroscopy measurements show that the K^+-induced transition from co-aligned fibrils to 3D bundles is due to an inversion of the dominant binding free energy from collagen-substrate to collagen-collagen. Moreover, Raman and IR spectra demonstrate that this increase in collagen-collagen interaction strength is accompanied by a release of water from ice-like to liquid likes states and a reduction in hydrogen bonding, indicating that 3D assembly is driven by solvent exclusion.

MD and kMC models of interacting "beads-on-a-string" with a mix of weakly and strongly interacting beads can reproduce this morphological evolution through variations in a qualitative sense, but the lack of specificity in bond orientations and conformational transitions prevents an accurate description of assembly into the ordered state.

FUTURE PLANS

Our work on lipid-nanowire bioelectronics devices will focus on assembling multicomponent bionanoelectronic devices by inserting multiple membrane protein species into the 1D lipid bi-layer platform, demonstrating enhanced control over device functionality resulting from such co-assembly, and exploring new nanomaterials components. In our research on virus-origami plasmonic arrays, we plan to move to a design based on cylindrical capsids and gold nano-posts. Based on our numerical simulations, we conclude that this design will optimize the enhancement factor. Multi-modal single particle imaging will again test the model predictions. Finally, we will explore the source of specific-ion effects in collagen assembly by correlating assembly dynamics and morphology with IR and Raman spectra for a range of ions (Na^+, K^+, Ca^{2+}), as well as in situ STXM analysis of K^+ binding. We will modify our molecular models to incorporate the specificity of collagen-collagen bond orientation and conformational ordering.

PUBLICATIONS.

R. Tunuguntla, M. Bangar, K. Kim, P. Stroeve, C.M. Ajo-Franklin, A. Noy, Lipid Bilayer Composition can Influence the Orientation of Proteorhodopsin in Artificial Membranes, *Biophys. J.*, in press (2013).

A. Noy, R.W. Friddle, Practical Single Molecule Force Spectroscopy: How to determine fundamental thermodynamic parameters of intermolecular bonds with an atomic force microscope, *Methods*, v.60, p.142–150 (2013).

A. Noy, Kinetic Model of Gas Transport in Carbon Nanotubes, *J. Phys. Chem. C.*, v. 117(15), p. 7656–7660 (2013).

J.J. De Yoreo, S. Chung, and R.W. Friddle, "*In situ* AFM as a tool for investigating interactions and assembly dynamics in biomolecular and biomineral systems" (**Invited Review**) *Adv. Func. Mat., in press* (2013) DOI: 10.1002/adfm.201203424, **Inside Cover Article**.

S.L. Capehart, M.P. Coyle, J.E. Glasgow, M.B. Francis, Controlled Integration of Gold Nanoparticles and Organic Fluorophores Using Synthetically Modified MS2 Viral Capsids. *J. Am. Chem. Soc.*, **135** 3011-6 (2013).

L.R. Comolli, C.E. Siegerist, S-H. Shin, C.R. Bertozzi, W. Regan, A. Zettl and J.J. De Yoreo, Conformational transitions at an S-layer growing boundary resolved by cryo-TEM *Agew. Chem. Int. Ed., in press*, **Inside Cover Article** (2013).

J.J. De Yoreo, S. Chung and M.H. Nielsen, The dynamics and energetics of matrix assembly and mineralization, *Cal. Tiss. Int., in press* (2013) DOI 10.1007/s00223-013-9707-9 (**Invited Review**).

L.R. Comolli, S-H. Shin, J.J. De Yoreo, C.R. Bertozzi, R., C.E. Siegerist, A. Hexemer, K.T.Nam, C. Wang, and R. Tscheliessnig, "Discovery of "S-bilayers", a step toward expanding the dimensionality of S-layer assemblies" *ACS Nano, in press* (2013) **Cover Article**.

R.W. Friddle, A. Noy, J.J. DeYoreo "Interpreting the widespread non-linear force spectra of intermolecular bonds", *Proc. Natl. Acad. Sci. USA* **109**, 13573-13578 (2012).

S-H. Shin, S. Chung, B. Sanii, C.R. Bertozzi and J.J. De Yoreo, "Direct observation of kinetic traps associated with structural transformations leading to multiple pathways of S-layer assembly" *Proc. Nat'l. Acad. Sci.* **109**, 12968-12973 (2012).

J.E. Glasgow, S.L. Capehart, M.B. Francis, D. Tullman-Ercek, Osmolyte-Mediated Encapsulation of Proteins inside MS2 Viral Capsid. *ACS Nano.*, **6**, 8658-64 (2012).

J-B.In, C.P. Grigoropoulos, A. Chernov, A. Noy "Growth Kinetics of Vertically Aligned CNT Arrays in Clean Oxygen-Free Conditions", *ACS Nano* v.**5, p.**9602-9610. (**2011**)

R.W. Friddle, K. Battle, V. Trubetskoy, J. Tao, E.A. Salter, J.J. De Yoreo, A. Wierzbicki, "Single-Molecule Determination of the Face-Specific Adsorption of Amelogenin's C-terminus on Hydroxyapatite", *Angew. Chem. Int. Ed.* **50**, 7541 –7545 (2011).

Wang, X., Wang, Y., Åberg, D., Erhart, P., Misra, N., Noy, A., Hamza, A.V., Yang, J., Batteryless chemical detection with semiconducting nanowires, *Advanced Materials*, 23, 117–121 (2011). Inside front cover article.

R.W. Meulenberg, T.M. Willey J. R. I. Lee, L. J. Terminello and T. van Buuren, Erbium doping effects on the conduction band edge in germanium nanocrystals " *Applied Physics Letters"* **98**, 203107 (2011).

T. M. Willey, M. Bagge-Hansen, J. R. I. Lee, R. W. Call L. Landt, T. van Buuren, C. Colesniuc, C. Monton, I. Valmianski, Ivan K. Schuller, Electronic Structure Differences Between H2-, Fe-, Co-, and Cu-Phthalocyanine Highly Oriented Thin Films Observed Using NEXAFS Spectroscopy, *J. Chem. Phys.* **139**, 034701 (2013)

J. R. I. Lee, M. Bagge-Hansen, T. M. Willey, R. W. Meulenberg, M. H. Nielsen, I. C. Tran, T. van Buuren, X-ray Absorption Spectroscopy for the Structural Investigation of Self-Assembled-Monolayer-Directed Mineralization, *In press Methods Enzymol.* (2013)

J. R. I. Lee, T. Han, T. Willey, M. Nielsen, L. Klivansky, Y. Liu, S.W. Chung, L. Terminello, T. van Buuren, J. De Yoreo, Cooperative Reorganization of Mineral and Template during Directed Nucleation of Calcium Carbonate, *Journal of Physical Chemistry C*, **117** 11076-11085 (2013) .

X.L He, I.N Demchenko, W.C. Stolte, A. van Buuren, H. Liang, Synthesis and Transformation of Zn-Doped PbS Quantum Dots *J. Phys. Chem. C*, **116**, 22001-22008 (2012)

Soft-Matter Physics: Directed Self-Assembly of Soft-Matter and Biomolecular Materials

Benjamin Ocko (ocko@bnl.gov), Antonio Checco (checco@bnl.gov) & Masa Fukuto (fukuto@bnl.gov), Brookhaven National Laboratory, Upton, NY 11973

Program Scope: The primary goal of the group is to understand the effects of nanoscale confinement and the role of self-assembly in soft and biomolecular materials through the use of patterned templates and well-defined interfaces. We use synchrotron x-ray scattering, scanning probe and optical microscopy techniques to study fundamental properties of complex fluids, simple liquids, macromolecular assemblies, liquid crystals, polymers, and biomolecular materials. The challenges are (1) to understand the behavior and structure of liquids under nano-confinement, (2) how templates and confinement can be used to direct the assembly of soft and biomolecular materials (3) to gain a fundamental understanding of interactions which give rise to similar self-assembly behavior for a wide variety of systems, (4) how the order correlates with function. Understanding structural aspects of self-assembly at interfaces and in thin organic films underlies many emerging organic based devices and energy technologies. Our approach uses complementary structural probes, x-ray scattering and AFM. An important aspect of our approach is the use of nanopatterned surfaces to confine liquids and complex fluids. To accomplish this, we are using polymer based self-assembly techniques, AFM based local-oxidation nanolithography and e-beam lithography.

A. Biomolecular materials: A key challenge in directed assembly is to understand and exploit the effects of anisotropy, an issue of increasing importance due to the recent progress in the synthesis of anisotropic nanoparticles. Arrays of biomolecular nanoparticles (BNPs), i.e., proteins and viruses, formed at the lipid membrane-aqueous solution interface are well suited for investigating the effects of anisotropy since BNPs' topographical and chemical heterogeneities can often be deduced from their known atomic coordinates and since the lipid-coated aqueous interface provides a means to impose a specific particle orientation. Our recent progress in this area includes improved understanding of anisotropy effects in 2D crystals of icosahedral viruses. Specifically, we have investigated the 2D assembly of turnip yellow mosaic virus (TYMV) on cationic lipid monolayers at the aqueous solution-vapor interface (Fig. 1). The 2D crystallization of TYMV has been achieved by enhancing electrostatically induced interfacial adsorption, an approach we recently demonstrated for another virus [Kewalramani et al., Soft Matter (2011)]. In situ x-ray scattering (Fig. 1) reveals two close-packed 2D crystalline phases of TYMV that are distinct from the previously reported hexagonal and centered square arrays of TYMV. This finding points to structural diversity in the 2D arrays of icosahedral particles. TYMV's anisotropy attributes and numerical

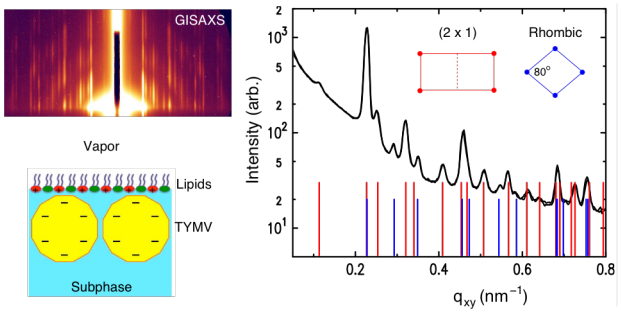

Fig. 1: (Bottom left) Schematics for electrostatic 2D assembly of viruses on a cationic lipid monolayer. (Top left and right) GISAXS pattern from 2D crystals of TYMV.

analysis of 2D arrays of virus-shaped particles have been used to derive a model for the newly observed rhombic crystal. In this model, the particle orientation is consistent with the electrostatic lipid-TYMV attraction and the interparticle contacts exhibit steric complementarity. The contrast between the rhombic and centered square crystals highlights how the high symmetry and subtle asphericity of icosahedral particles enrich the variety and complexity of ordered 2D structures that can be generated through self-assembly. We have recently established collaboration with BNL Center for Functional Nanomaterials to investigate the lipid-mediated 2D assembly of DNA-functionalized gold nanoparticles (DNA-NPs) at liquid interfaces. Having already succeeded in forming ordered 2D arrays of DNA-NPs, we are currently studying the effects of salt- and pH-induced DNA hybridization on the 2D assembly behavior.

B. Nanoliquids: We have continued investigating the wetting behavior of simple liquids and polymers on chemical and topographical nanopatterns. The effects of confinement and long-range interactions between the liquid and the nanostructured substrate may lead to substantial deviations from macroscopic wetting behavior or direct the phase separation in polymer films. In situ X-ray scattering and AFM are then used to study the morphology of the confined nanoliquids and the experimental results are compared to recent theoretical models. Recent progress follow:

• *Thin film dewetting on chemical patterns.* We have studied the morphology and stability of thin volatile wetting films on model chemically patterned surfaces composed of periodic arrays of alternating completely and partially wettable nanostripes using noncontact AFM. Films spanning the entire pattern are found to be stable only for thicknesses in excess of a critical value whereas thinner films spontaneously dewet the partially wettable regions of the substrate. This behavior originates from the competition of long range (stabilizing) and capillary (destabilizing) forces. It can be accurately modeled by accounting for the effect of long-range forces using microscopic density functional theory.

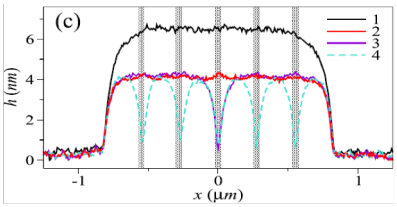

Fig. 2: Noncontact AFM profiles of a thin film of octane wetting a chemically patterned substrate. Films thicker than ~ 4nm are stable whereas thinner films break into array of "liquid nanostripes".

• *Directed assembly of polymer thin-film blends using chemical nanopatterns.* Using chemical patterns similar to those above with different widths, we have investigated the directed assembly of poly(3-hexylthiophene):phenyl-C61-butyric acid methyl ester (P3HT:PCBM) blends. Tapping-, contact-, and current-sensing AFM studies demonstrated that chemical patterns were effective at directing the 3D morphology of P3HT:PCBM blends at dimensions of >200 nm. As the dimensionality of domains approached 100 nm, the chemical patterns were no longer able to direct phase segregation, evidence that a directed spinodal decomposition mechanism was responsible for the observed morphology.

• *Forced water infiltration into hydrophobic nanotextures.* We have carried out highly sensitive measurements of pressure-induced infiltration of water into hydrophobic nanotextures with various geometries (posts, lamellae, or tapered cones) using transmission small angle x-ray scattering. Above a critical pressure, significant infiltration occurs irreversibly where the specifics depend on the texture's size and

geometry. The sorption isotherms are well modeled by accounting for the geometry.

C. Interfacial Freezing*:* Understanding interface-induced freezing is relevant to many fields including molecular electronic and photovoltaic devices. One of the most elegant examples is the surface freezing of alkanes at the liquid/vapor interface, discovered by our group, where a crystalline phase forms up to 3˚C above the bulk melting transition. Related phenomena is now observed at the solid/liquid and solid/vapor interfaces:

• *Surface freezing of long-chain alcohols at solid interface:* X-ray reflectivity measurements have been carried out to determine the density profiles at the solid/liquid (*s/l*) interface between a bulk alcohol (octadecanol: C18OH) and the native oxide that forms on silicon. Over a range of temperature (~ 10 ˚C) above the freezing point of C18OH (59 ˚C) an extremely well defined monolayer is stable at the solid interface with surface-normal molecules. This reversible formation of an interfacial monolayer is reminiscent of surface freezing at the liquid/vapor (*l/v*) interface where the much larger temperature range for the solid interface is consistent with the much stronger surface interaction. In addition to the *s/l* studies we have also carried out investigations at the solid/vapor (*s/v*) interface for the same system where a reservoir of the C18OH is maintained at the sample temperature just below the sample. At the *s/v* interface, similar reversible interfacial freezing is found except that in-plane x-ray studies are feasible. Despite the hexagonal crystalline order in-plane, our investigations show that the molecules are not crystalline along their entire length, rather only about half the molecular length contributes to the in-plane hexagonal order, hence the molecules must exhibit a degree of Gauche configurations. Additional studies on other molecular layers suggest that this behavior is universal.

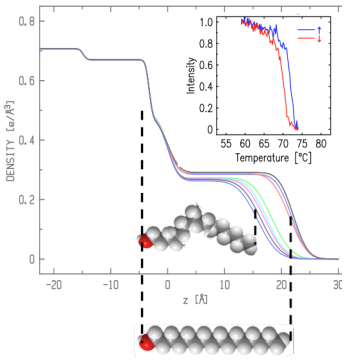

Fig. 3: C18OH on SiO_2 real space profiles show a sharp melting transition around 70C.

D. Liquid-Liquid Interfaces: The oil/water interface is deceptively simple. These liquids do not mix and their interface-normal density profile has long been considered to vary monotonically between the two bulk densities, over a width dictated by capillary-wave theory (CWT). CWT assigns the width to roughness due to thermally-excited capillary waves, the amplitudes of which are dictated by the interfacial tension. Yet, a number of studies indicate that this simple picture may be incomplete. Recent measurements on hydrophobic/hydrophilic interfaces find *a non-monotonic* interfacial profile, including a density depletion layer between the two bulks. The exact nature, and origin, of this layer is, however, controversial, with the layer assigned either to water depletion or to a lower-density, hydrogen-rich terminal monolayer. To gain new insight into the nature and origin of the depletion layer we have carried out preliminary XR measurements on the arch-typical hydrophobic/hydrophilic interface, the liquid alkane/water interface, reported in early studies to exhibit a monotonic, depletion-layer-devoid interface, rougher than predicted by CWT. Our measurements find roughness conforming to CWT and support the monotonicity of the alkane/water interface with no evidence for a depletion layer.

E. New x-ray surface scattering method: We have developed a new x-ray scattering technique for probing the molecular structure of interfaces. This method is much more direct than the widely used Grazing Incidence Small Angle X-ray Scattering (GISAXS)

approach since the latter can ben severely complicated & compromised by distortions and multiple scattering effects. Our new method, which we refer to as Grazing Transmission Small Angle X-ray Scattering (GTSAXS), not only simplifies the analysis it also allows for considerably more detailed and quantitative results. With GTSAXS the scattered beam is transmitted through the sample's edge rather than reflected as with GISAXS. Our work appeared on the cover of the Journal of Applied Crystallography in 2013.

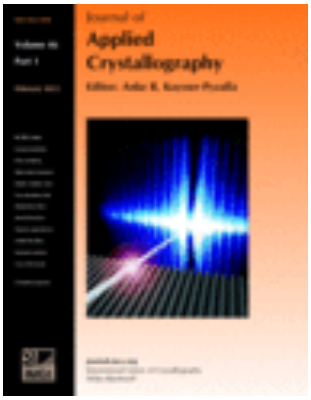

Future Plans In addition to the projects discussed above, many of which are ongoing, we highlight some additional research plans below. In the area of biomolecular materials, we will continue to extend the approach of the lipid-mediated 2D assembly to water-soluble nanoparticles at both the vapor and liquid/liquid interfaces and to graphoepitaxial assembly at chemically patterned substrate-liquid interfaces. In the area of nanoliquids, we will continue to explore the role of nanotopography on the wetting properties and fluid slippage. We will continue recently initiated measurements of Casimir forces in binary critical fluids using environmental AFM. The studies on the effect of lateral confinement on spreading will be extended to complex liquids where anomalous behavior is expected. In the area of surface induced ordering, we intend to continue to studies on solid surfaces, both with long chain alcohols, fatty acids and amines and to extend our studies to liquid/liquid interfaces. Measurements of the nature of the oil/water interface will be extended to branched alkanes. The Group has spearheaded the proposal for the Soft Matter Interfaces (SMI) undulator beamline at NSLS II and continues in advisory capacities. This facility will be vital for the Group's future plans once the existing synchrotron is shuttered.

Publications (2011-2013) 25 Articles (4. Phys. Rev. Lett, 3 Proc. Nat Acad., 3 ACS Nano, 1 Nano Lett., 1 Nat. Comm., 1 Adv. Mat.) & 2 Book Chapters

Selected Publications:

Directed Assembly of P3HT: PCBM Blend Films Using A Chemical Template with Sub-300 nm Features, D.S. Germack, A. Checco, B.M. Ocko, ACS Nano 7, 1990-1999 (2013).

Grazing-incidence transmission X-ray scattering: surface scattering in the Born approximation, X. Lu, K.G. Yager, D. Johnston, C.T. Black, B.M. Ocko, J. App. Crys. 46, 165-172 (2013).

Stability of thin wetting films on chemically nanostructured surfaces, A. Checco, B.M. Ocko, M. Tasinkevych, S. Dietrich, Phys. Rev. Lett. 109, 166101 (2012).

Lattice Deformation and Domain Distortion in the Self-Assembly of Block Copolymer Thin Films on Chemical Patterns, J. Xu, T. P. Russell, A. Checco, Small 9, 779–784 (2013)

Bilayer order in a polycarbazole-conjugated polymer, X. Lu, H. Hlaing, D.S. Germack, J. Peet, W.H. Jo, D. Andrienko, K. Kremer, B.M. Ocko, Nat. Comm. 3, 795 (2012).

Role of Electrostatic Interactions in Two-Dimensional Self-Assembly of Tobacco Mosaic Viruses on Cationic Lipid Monolayers, ST Wang, M. Fukuto, A. Checco, Z. Niu, Q. Wang, and L. Yang, J. Coll. Int. Sci. 358, 497 (2011).

Unifying Interfacial Self-Assembly and Surface Freezing, B.M. Ocko, H. Hlaing, P.N. Jepsen, S. Kewalramani, A. Tkachenko, D. Pontoni, Phys. Rev. Lett. 106 (13), 13780 (2011).

Systematic Approach to Electrostatically Induced 2D Crystallization of Nanoparticles at Liquid Interfaces, S. Kewalramani, S.T. Wang, Y. Lin, H.G. Nguyen, Q. Wang, M. Fukuto, and L. Yang, Soft Matter 7, 939 (2011).

Project Title: Emergent Atomic and Magnetic Structures (Early Career Project)

PI: Tanya Prozorov

Collaborators: Surya K. Mallapragada, Marit Nilsen-Hamilton, Ruslan Prozorov, Dennis A. Bazylinski, Monica Lamm, David Vakhnin, Damien Faivre, Michael Winklhofer, Rafal Dunin-Borkowski, Richard B. Frankel, Mihály Pósfai, Arash Komeili, Concepcion Jiménez-Lopez, Alejandro Rodríguez-Navarro, Marcin Konczykowski

Mailing Address: Division of Materials Science and Engineering, Ames Laboratory, Ames, IA 50011

Email: tprozoro@ameslab.gov

Project Scope:

The objective of the newly formed *Emergent Atomic and Magnetic Structures Group* is to deploy *new* characterization techniques based on the real time high-resolution TEM imaging of the individual nanocrystals at various stages of their formation. Our research is focused on direct visualization of *in-situ* growth of the protein-templated magnetic nanocrystals from the incipient nuclei to the fully developed crystalline and magnetic structures, by using continuous fluid flow sample holder.

The controlled, low-temperature chemical synthesis of uniform magnetic nanoparticles with narrow size distribution is of significant importance [1]. Magnetotactic bacteria, present in many natural aquatic environments, produce uniform, structurally perfect magnetic nanocrystals under a strict biological control over the mineralization process. As a result, the biomineralization of magnetotactic bacterial magnetite nanoparticles is a topic of intense research, with several bacterial recombinant proteins used in biomimetic synthesis [1]. Bio-inspired synthetic routes offer room-temperature pathways to the production of a variety of functional magnetic nanostructures with the exceptional control over nanoparticles nucleation and growth. For example, using the iron-binding protein, Mms6, and corresponding peptides, well-formed nanocrystals of magnetite and cobalt ferrite can be synthesized in a process mimicking the growth of magnetite in live magnetotactic bacteria [1-3]. However, despite the significant effort, the structure of Mms6, as well as the detailed process of protein-assisted nanoparticle nucleation and growth, remains largely unexplained [4]. The major issue is that common characterization techniques only work with large, macroscopic assemblies of nanoparticles, so that interactions and collective effects mask the behavior of individual nanoparticles. Our research is aimed at determining the nature of macromolecule-mediated *individual magnetic nanoparticle formation* by utilizing advanced electron microscopy techniques. We are working on a real-time in-situ investigation of individual magnetic nanoparticle nucleation, growth, crystallization and development of the long-range order, as well as clustering and development of collective interactions. Our approaches include:

- labeling and characterization of the specific biomineralization proteins using their iron-binding ability, and utilizing the iron self-staining for direct visualization of protein-rich areas of the macromolecular specimens;

- employing the in-situ synthesis of nanocrystals as a tool of direct evaluation of nucleation and growth of nanocrystalline materials under precise temperature control, using various biomacromolecules;

- using magnetotactic bacteria in its native environment as model system for the *in-situ* visualization of magnetite biomineralization;

- extending the developed methods to a real-time study of magnetic nanocrystal growth, utilizing the integrated microfluidics system, developed for the nanometer scale imaging of materials in fluid environments, and advanced analytical EM tools, such as high angle annular dark field (HAADF) imaging in STEM mode for obtaining compositional and morphological information of the sample (Z-contrast imaging), and analytical spectroscopy for probing the chemical environment of the specimen.

Our findings are applicable to the fabrication of various bio-compatible magnetic nanomaterials with controlled and well-defined properties relevant to the DOE's mission.

Recent Progress:

We tested the *on-the-EM-window* synthesis of biomacromolecule-templated magnetic nanocrystals and by adapting the existing *in-vitro* bulk synthesis protocol. After establishing the initial experiment parameters, we proceeded with chemical functionalization of the surface of the silicon nitride window membranes to allow for the immobilization of the macromolecular templating agents, using the (3-aminopropyl)-triethoxysilane (APTES) as the model protein linker. Analysis of both the static cell regime and the fluid flow experiments is indicative of the ferric iron highly localized in the micellar corona, with a partial diffusion into the surrounding liquid (**Figure 1 (a)**) [5,6]. Mid-reaction images (**Figure 1 (b)**) revealed formation of a depletion zone, corresponding to chemical binding of the surface-bound ferric iron to the hydroxyl ion moieties. The nanoparticles formation is observed in a close proximity to the surface of iron-incubated proteinaceous micelles, as shown in **Figure 1(c)**. The protein-iron bonding stability and dynamics were probed via the *in-situ* Electron Energy Loss Spectroscopy.

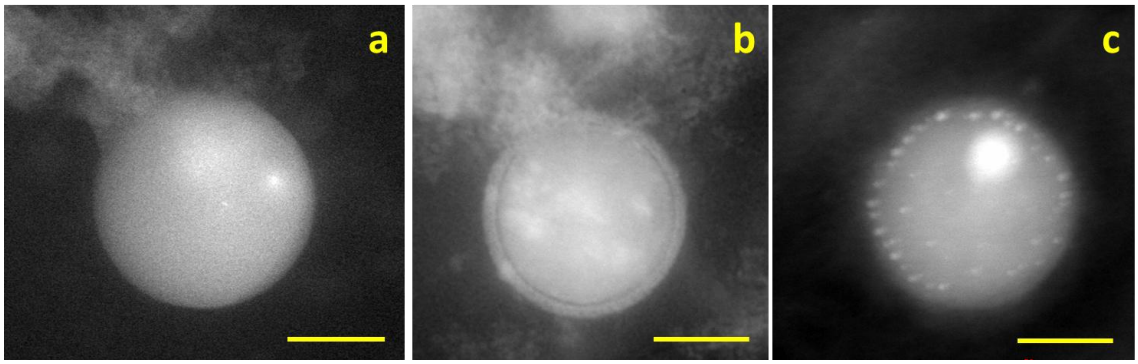

Figure 1. STEM HAADF image of iron-incubated proteinateous micelles on the functionalized silicon nitride window membrane taken in a fluid flow mode: (a) proteinaceous micelle incubated with ferric iron; (b) formation of a depletion zone as a result of chemical binding of the surface-localized ferric iron to the hydroxyl moieties; and (c) iron oxide nanoparticls form *in-situ* on the surface of the Mms6- micells after delivering the dilute NaOH solution to the fluid cell. Scale bar: 50 nm.

Using the liquid cell holder, we tested the liquid cell for the imaging of the magnetotactic bacteria in their native environment *in-situ*, with the encouraging preliminary results **(Figure 2 (a, b))** [7].

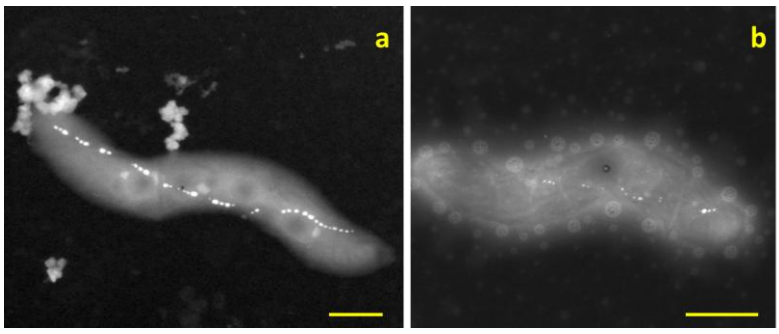

Figure 2. STEM HAADF image of magnetotactic bacteria in liquid, taken in a static cell mode: (a) wild-type AMB-1 bacterium, with the fully formed magnetosome chain; (b) bacterium of the mutated culture, AMB1 ΔMamS, with the distinctively visible cell components. The mutation leads to the biomineralization of significantly smaller, imperfect magnetosomes crystals. Scale bar: 500 nm.

Due to the dynamic nature of the features of interest, their detailed characterization and statistical analysis rely on extensive data acquisition and specimen cross-examination [5-7].

Future Plans:

1) Visualization of the Magnetosome Magnetite Crystal Formation *In-Vivo*.

The initial attempt to visualize the magnetotactic bacteria in their native environment were successful, however the extent of the radiation damage and viability of the bacterial cells has to be carefully investigated. We are working on adjusting the imaging conditions to effectively minimize the electron bean damage, as to allow the *in-situ* imaging of *live* magnetotactic bacteria. Current effort is aimed at the *in-vivo* visualization of iron uptake by the non-magnetic magnetotactic bacteria culture grown in the absence of iron, and identifying the different stages of formation of the magnetosome magnetite nanocrystals, working under the hypothesis that the *magnetosome magnetite biomineralization only takes place in live bacterial cells*. For this purpose, we are preparing to carry out the unprecedented series of induction experiments: using the fluid flow holder, the iron-containing growth medium is delivered directly to the non-magnetic bacterial microorganisms confined within the liquid cell. Iron uptake and magnetosome formation is monitored in the STEM mode, as demonstrated in **Figure 3 (a, b)**. Such an approach will rely on fast imaging using the direct imaging camera, currently available at the Center for Functional Nanomaterials, Brookhaven National Laboratory, and we will utilize the facilities at CFN BNL for these experiments, which will be expanded to a variety of *in-vivo* biomineralization processes [8].

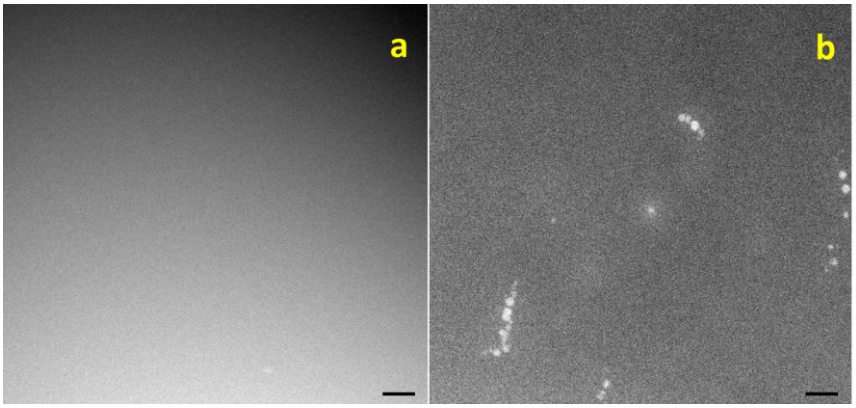

Figure 3. STEM HAADF characterization of the magnetotactic bacteria in liquid: (a) non-magnetic MSR-1 bacterial culture grown without the source of iron, with the thick, fully hyrdated, organic specimen, comprised of predominantly light elements, leadint to poor contrast; (b) active magnetosome biomineralization seen during the induction experiment 140 minutes after the iron-containing growth medium is delivered into the fluid cell. Scale bar: 200 nm.

Magnetosome magnetite nanocrystals produced by the magnetotactic bacteria serve as model biomineralization system, thus permitting establishing the reliable modes of imaging and spectral analysis of bio-templated nanoparticles. The ability to visualize the magnetosome formation by the magnetotactic bacteria provides the invaluable information about the magnetite biomineralization process, deepening the understanding of the biomineralization in general, and, thus, enabling a better control of biomimetic synthesis. This, in turn, will bring the field closer to rational design and fabrication of the more complex bioinspired magnetic nanomaterials of potential energy relevance, in line with DOE's vision of controlling the properties of matter.

2) Towards the Visualization of Magnetic Response of Magnetic Nanoparticle.

Normally, the magnetic properties of either the individual nanoparticles, or small assemblies of nanoparticles, cannot be measured due to the extremely low amount of the material. We are attempting to use the electron holography to establish magnetic signatures of the individual bacterial magnetosome nanocrystals in magnetosome chains *in-situ*. One of our future directions is to explore utilization of the

phase contrast (electron holography) and to visualize magnetic fields to study evolving ferromagnetism in a single nanocrystalline particle as it grows, as well as spatial characterization (electron tomography) to understand the growth process, with the emphasis of characterization at the particle-protein interface. In a close collaboration with the Hummingbird Scientific, we are going to design and test a magnetizable fluid cell holder capable of localized application of magnetic fields, to exert an additional control over the magnetic nanocrystals formation, growth, and ordering. Therefore, the project is strongly aligned with the energy mission the DOE.

References:

[1] Prozorov, T.; Bazylinski, D. A.; Prozorov, R.; Mallapragada, S. M.; "Novel Magnetic Nanomaterials Inspired by Magnetotactic Bacteria: Topical Review", *Mater. Sci. Eng. R. 173*, 133 (2013).

[2] Prozorov, T.; Mallapragada, S. M.; Narasimhan, B.; Wang, L.; Palo, P.; Nilsen-Hamilton, M.; Williams, T. J.; Bazylinski, D. A.; Prozorov, R.; Canfield, P. C. "Protein-Mediated Synthesis of Uniform Superparamagnetic Magnetite Nanocrystals", *Advanced Functional Materials 17*, 951 (2007).

[3] Prozorov, T.; Palo, P.; Wang, L.; Nilsen-Hamilton, M.; Jones, D.; Orr, D.; Mallapragada, S. K.; Narasimhan, B.; Canfield, P. C.; Prozorov, R. "Cobalt Ferrite Nanocrystals: Out-Performing Magnetotactic Bacteria", *ACS Nano 1*, 228 (2007).

[4] Wang, L.; Prozorov, T.; Palo, P.; Liu, X.; Vakhnin, D.; Prozorov, R.; Mallapragada, S. K.; Nilsen-Hamilton, M.; ″ Multimeric Structure and and Biphasic Iron-Binding Characteristics of Mms6, a Bacterial Protein That Promotes the Formation of Superparamagnetic Magnetite Nanoparticles of Uniform Size and Shape″, *Biomacromolecules 13*, 98 (2012).

[5] Prozorov, T.; Kashyap, S.; "Real-time studies of the nucleation and growth of protein-templated magnetic nanocrystals", Abstracts of Papers, 244th ACS National Meeting & Exposition, Philadelphia, PA, United States, August 19-23, 2012.

[6] Kashyap, S.; Liu, X.; Mallapragada, S. K.; Prozorov, T. "Direct Visualization of Iron-binding Proteinaceous Micelles", *in preparation for submission to ACS Nano*.

[7] Kashyap, S.; Perez-Gonzalez, T.; Faivre, D.; Rahn-Lee, L.; Komeili, A.; Prozorov, T. "Environmental Imaging of Magnetotactic Bacteria", *in preparation for submission to Nature Methods*.

[8] Preliminary results were obtained at the Center for Functional Nanomaterials, Brookhaven National Laboratory.

Active Assembly of Dynamic and Adaptable Materials: Artificial Microtubules

Task Lead: Erik D. Spoerke
Principal Investigator: George D. Bachand
Co-Investigators: Erik D. Spoerke, Mark Stevens, and Darryl Sasaki
Mailing Address: Electronic, Optical, and Nano Materials, Sandia National Laboratories, PO Box 5800, MS 1411, Albuquerque, NM 87185
Email: edspoer@sandia.gov

Program Scope

The *Active Assembly of Dynamic and Adaptable Materials* research program examines fundamental materials science issues at the intersection of biology, nanomaterials, and hybrid interfaces. The overall program goal is to understand nature's strategies for non-equilibrium materials assembly, and apply these principles in hybrid or composite materials whose assembly and organization can be programmed, and/or "self-directed." More specifically, we are exploring materials systems that exhibit adaptive behaviors based on the use of energy consuming proteins and/or synthetic analogs capable of removing the constraints imposed by diffusion and chemical equilibria. Research tasks are focused on (1) the active assembly of hybrid nanomaterials based on motor protein-driven transport and dynamic polymerization of cytoskeletal filaments, and (2) the design and exploration of "artificial microtubules" that can mimic the dynamic, non-equilibrium behaviors of the natural filaments in synthetic systems

Many of unique behaviors found in living systems (e.g., self-replication, adaptivity) are commonly associated with dynamic self-assembly processes.[1] The interactions responsible for such self-assembly depend strongly on the dissipating of energy, commonly through enzymatic reactions that alter biomolecular interactions. Our program has focused on the components involved in one of nature's active transport systems, specifically microtubules (MTs) and their associated motor proteins (Fig. 1). MTs are hollow filaments composed of αβ tubulin dimers whose energy-dissipative assembly is used to push, pull, or rearrange the cell's cytoskeleton. These filaments also serve as "train tracks" for the bidirectional transport of macromolecules and organelles by the motor proteins kinesin and dynein through the conversion of chemical energy into mechanical work. Living organisms use the concerted and dynamic interactions between kinesin and MTs for physiological processes ranging from chromosomal segregation at the cellular level to macroscopic color changing behaviors at the organismal level.[2] Thus, learning to exploit, mimic, and/or translate the role of active proteins in emergent biological behaviors represents an opportunity to dramatically advance nanomaterials assembly.

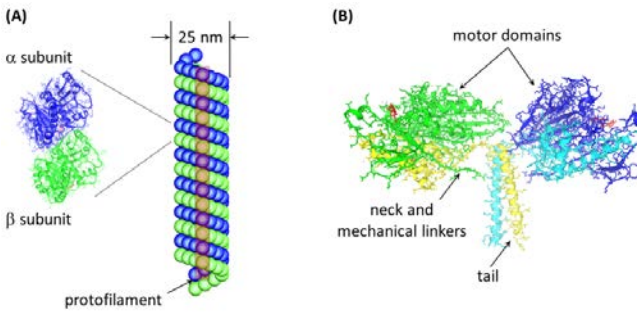

Fig. 1. (A) Crystal structures of tubulin and diagram showing an assembled microtubule (MT) filament. (B) Crystal structure of a kinesin motor protein.

Recent Progress

This abstract highlights efforts in the *Artificial Microtubules* subtask exploring synthetic systems aimed at mimicking elements of natural microtubule assembly and function. These efforts have involved complementary study of thermally reversible dendrimeric polymers, synthetic peptide assembly, and a modeling/simulation element that ties together fundamental aspects of both the synthetic and natural protein systems.

Thermally-Reversible Dendrimeric Polymers

The research focus in this area builds on our previous expertise, working with Professor Dominick McGrath at the University of Arizona, using thermally-reversible furan-maleimide Diels Alder (fmDA) chemistry to polymerize dendrimeric building blocks.[4, 5] In particular we have taken cues from the biological MT system, in which the mechanism for assembly is functionally different from the mechanism of disassembly; one process is not simply the reverse of the other. Fig. 2 shows a new monomer system utilizing two orthogonal "click" chemistries in an effort to incorporate this theme into a synthetic linear polymer structure. Rather than polymerizing through fmDA bonds as we have done in the past, a furan maleimide bond is "prebuilt" into the monomer. Polymerization then occurs through copper-catalyzed azide-alkyne click (CuAAC) reactions. Once polymerized, depolymerization can be induced through the thermally reversible decomposition of the "prebuilt" furan maleimide. By incorporating both the functionally orthogonal fmDA and CuAAC bonds into the polymer backbone, we introduce a much-simplified mechanism to mimic dynamic elements of MT assembly.

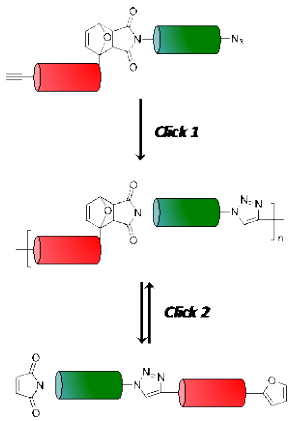

Fig. 2. Schematic polymer system containing orthogonal "click" chemistries for independent polymerization and depolymerization. Click 1 polymerizes to high molecular weight *via* CuAAC chemistry. Thermally reversible cleavage of furan-maleimide can lead to temperature-controlled depolymerization or repolymerization.

Theory and Modeling

We have continued our study of the self-assembly of artificial MTs[3] using wedge-shaped building blocks with binding sites on their surfaces. Our previous simulations showed that helical tubules are frequently formed even when the wedge monomers are achiral and designed for non-helical tubules. We have now determined that the occurrence of helical tubules is due to twist of the filaments, which brings the non-chiral monomer's interaction sites into alignment in chiral tubules. Consequently, the energy distributions for non-helical and helical tubules with pitch 1 overlap. In order to better control the chirality of the tubule, we have introduced chirality into the model monomer. (Fig. 3) Monomers with chirality m self-assemble into tubules with pitch $p = m$, $m\pm1$. The range in p is due the twist effect. For $|m-p|>1$, twist requires rotation about the monomer vertical axis that causes misalignment of the attractive sites and yields higher pair energies. Thus, a stronger vertical interaction that limits the vertical rotation would reduce the range of chirality in the tubules. In addition, a lock-and-key mechanism, analogous to binding sites on tubulin dimers, has been added to the model monomer along the vertical axis to make the $p \neq m$ unfavorable. (Fig. 3) We have successfully self-assembled well controlled chiral tubules

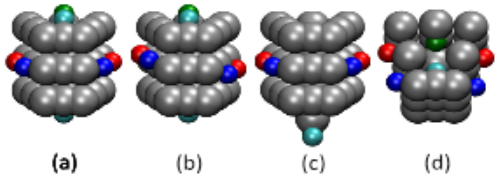

Fig. 3. a) An achiral wedge monomer for non-helical tubules (p=0). b) A chiral wedge monomer with chirality m=2 (for tubules with p = 2). c) An achiral wedge monomer with a lock-and-key configuration for the vertical binding site (sticking out the bottom surface). d) A chiral wedge monomer with m=2 and with a lock-and-key configuration for the vertical binding; top view shows vertical binding sites buried below the surface.

using the combined chiral and lock-and-key monomer, and in parallel to what is seen naturally, we have observed a range of structures (e.g. varying protofilament number). Not only do these models provide guiding insights for ongoing artificial MT synthetic studies, but they stand to provide valuable new perspective on the nature of tubulin self-assembly into MTs.

Synthetic Peptide Assembly

We are exploring self-assembling synthetic peptide systems designed to reproduce select aspects of MT assembly, structure, and function. In particular, we have developed a wedge-shaped peptide structure, inspired by our theory and modeling work, that allow us to study fundamental supramolecular processes key to mimicking MTs in simplified synthetic systems. As predicted by theory, we have observed that both structural and functional asymmetries in the molecular building blocks are key to driving the assembly of these peptides into one-dimensional nanostructures, such as nanofibers. (Fig. 4) Considering the structurally asymmetric peptide seen in Fig. 4a, assembly into nanofibers is strongly influenced by driving forces from amphiphilicity (hydrophilic asymmetry) and hydrogen bonding (vertical β-sheet formation along the nanofiber), and each of these forces is a necessary, but not independently sufficient, driver for the formation of supramolecular nanofibers. In addition, the balance and distribution of electrostatic charges within the peptide "branches" also strongly affects self-assembly. Imbalances in positive and negative charge prevent nanofiber assembly, while the asymmetric distribution of balanced charges within the branches is believed to influence peptide conformation and subsequent self-assembly into either nanofibers or lamellar structures. These studies inform the importance of these cooperating molecular interactions and the affects of molecular asymmetry on assembly and provide key insights needed for the development of more sophisticated MT-mimetic systems.

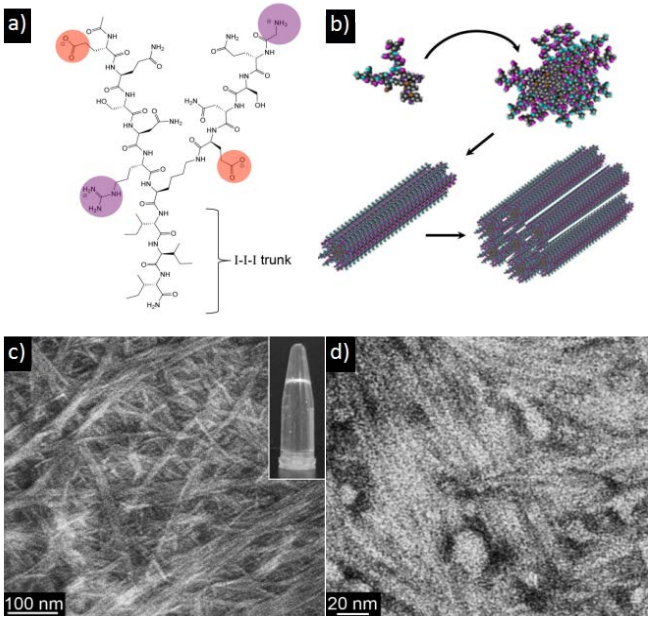

Fig. 4. a) Chemical structure of an amphiphilic wedge peptide with asymmetrically-distributed positive and negative charges. At neutral pH, these peptides assemble into bundled nanofibers (b), visible in SEM (c) and TEM (d) images.

Future Work

Guided by continued insights from theory and modeling work, we will continue to investigate new supramolecular systems capable of imitating elements of natural MT structure and function. In particular, we aim to create a multifunctional platform, integrating key elements of both the "click"-polymerized dendrimers and the asymmetric peptide structures into a modular molecular structure. The modular, multifunctional nature of this platform will allow us to investigate, both independently and within a larger molecular structure, new cooperative interactions between molecular elements such as thermally-controllable amphiphilicity, programmable dimerizing linkages, complex hydrogen bonding, and enzyme-responsive peptides. This versatile platform stands to enable significant progress towards creating fibers and tubules capable of simplified imitation of complex natural MT functions such as dynamic assembly, interactions with secondary materials or chemistries, and possibly even motility.

Acknowledgment

This research was supported by the U.S. Department of Energy, Office of Basic Energy Sciences, Division of Materials Sciences and Engineering, Project KC0203010. Sandia National Laboratories is a multi-program laboratory managed and operated by Sandia Corporation, a wholly owned subsidiary of Lockheed Martin Corporation, for the U.S. Department of Energy's National Nuclear Security Administration under contract DE-AC04-94AL85000.

Abstract References

1. Fialkowski, M., *et al*. *J. Phys. Chem. B* **2006,** 110, (6), 2482-2496.
2. Goldstein, L. S. B., *et al*. *Annu. Rev. Neurosci.* **2000,** 23, 39-71.
3. Cheng, S. F., *et al. Soft Matter* **2012,** 8, (20), 5666-5678.
4. Polaske, N. W., *et al. Macromolecules* **2010,** 43, (3), 1270-1276.
5. Polaske, N. W., *et al. Macromolecules* **2011,** 44, (9), 3203-3210.

DOE-Sponsored Publications (2011-2013)

- Gough, D.V., *et al*. "Supramolecular assembly of asymmetric self-neutralizing amphiphilic peptide wedges." *Soft Matter*, (2013).
- Spoerke, E.D., *et al*. "Biodynamic assembly of nanocrystals on artificial microtubule asters." *ACS Nano* **7**, 2012-2019 (2013).
- Bouxsein, N.F., *et al*., "A continuous network of lipid nanotubes fabricated from the gliding motility of kinesin powered microtubule filaments." *Langmuir* **29**, 2992-2999 (2013).
- Liu, H., *et al.*, "Effects of confinement on molecular motor-driven self-assembly of ring structures." *Cell. Mol. Bioeng.* **6**, 98-108 (2013).
- Cheng, S.F., *et al.*, "Self-assembly of artificial microtubules." *Soft Matter* **8**, 5666-5678 (2012).
- Bachand, M. and Bachand, G.D., "Effects of potential environmental interferents on kinesin-powered molecular shuttles." *Nanoscale* **4**, 3706-3710 (2012).
- Polaske, N.W., *et al.*, "Thermally reversible dendronized linear AB step-polymers via "click" chemistry." *Macromolecules* **44**, 3203 (2011).

UNIVERSITY GRANT PROJECTS

Program Title: Functional, Hierarchical Nanocomposites - Colloidal Liquid Crystal Gels and Liquid Crystal Elastomers

Principal Investigators: N.L. Abbott[1] and J.J. de Pablo[2,3]
Mailing Addresses:
[1].Department of Chemical and Biological Engineering, University of Wisconsin-Madison, 1415 Engineering Drive, Madison, WI 53706.[2].Argonne National Laboratory, Argonne, IL 60349. [3].Institute for Molecular Engineering, University of Chicago, Chicago, IL 60637
E-Mail: abbott@engr.wisc.edu and depablo@uchicago.edu

Program Scope

Liquid crystalline materials are widely encountered in biological systems as ordered yet mobile phases that can amplify molecular interactions through cooperative ordering transitions. They also respond to mechanical stresses to achieve spatial targeting of molecular and meso-scale species. Inspired by materials design principles encountered in biological systems, this project seeks to explore hierarchical designs of synthetic nanocomposite materials to achieve equilibrium and non-equilibrium properties not accessible in existing soft systems. For example, while recent studies have achieved notable success in exploiting surface-driven ordering transitions in synthetic liquid crystalline systems for amplification of molecular interactions into the optical scale, a potential limitation of past demonstrations has been the fluid nature of the liquid crystal (LC). Our proposed work seeks to overcome that limitation by designing, synthesizing, and characterizing solid-like LC elastomers and gels with tunable optical and mechanical properties.

Three parallel strategies are being pursued in our work. In the first, we consider the gelation of nematic LCs by addition of nano and micro-particles. In the second, we investigate LC micro- and nano-droplets and study LC-directed assembly of micro- and nano-particles at the interfaces of the droplets. In the third, we explore chemically cross-linked liquid crystalline elastomers. All three aspects of our work involve a concerted theoretical and experimental effort that lead to rational design of gels and elastomers, thereby allowing us to identify the origins of experimentally observed behaviors and to design or dial-in specific thermodynamic, mechanical, and optical responses by relying on advanced molecular models of the materials. The specific goals of the proposed work are to:

(i) Develop molecular models of colloid-in-LC gels capable of describing structure and properties at equilibrium and beyond equilibrium.
(ii) Develop hierarchical design principles that use defects and mechanical stresses in LC droplets to direct the interfacial organization of adsorbed particles.
(iii) Develop molecular models of LC elastomers that incorporate the kinetics of formation and that describe structure and properties both at and beyond equilibrium.

These goals are being pursued by adopting a cycle of model prediction, validation and experimentation that are allowing us to arrive at the proposed material platforms, while greatly expanding our fundamental understanding of a useful, emerging class of soft functional materials.

Recent Progress

*Colloid in Liquid Crystal Gels***:** In experiments performed over the past year, we have discovered that colloid-in-liquid crystal (CLC) gels can be formed via a two-step process that involves spinodal decomposition of a dispersion of colloidal particles in an isotropic phase of mesogens followed by nucleation of nematic domains within the colloidal network defined by the spinodal process (Figure 1). This pathway contrasts to previously reported routes leading to the formation of CLC gels, which have involved entanglement of defects or exclusion of particles from growing nematic domains. The new route provides the basis of simple design rules that enable control of the microstructure and dynamic mechanical properties of the gels.[1]

These experimental observations have been augmented by simulations based on coarse-grained mesogens that have been performed to provide fundamental insight into the origin of the interactions that underlie the formation of the gels.[2,3] Colloidal particles embedded within nematic LCs were found to exhibit strong anisotropic interactions arising from preferential orientation of nematogens near the particle surface. Such interactions are conducive to forming branched, gel-like aggregates. Anchoring effects also induced interactions between colloids dispersed in the isotropic liquid phase, through the interactions of the pre-nematic wetting layers. We observed that strong, nontrivial interactions can be induced between particles dispersed in mesogenic solvent, and explored how such interactions might be utilized to induce a gel state in the isotropic and nematic phases.

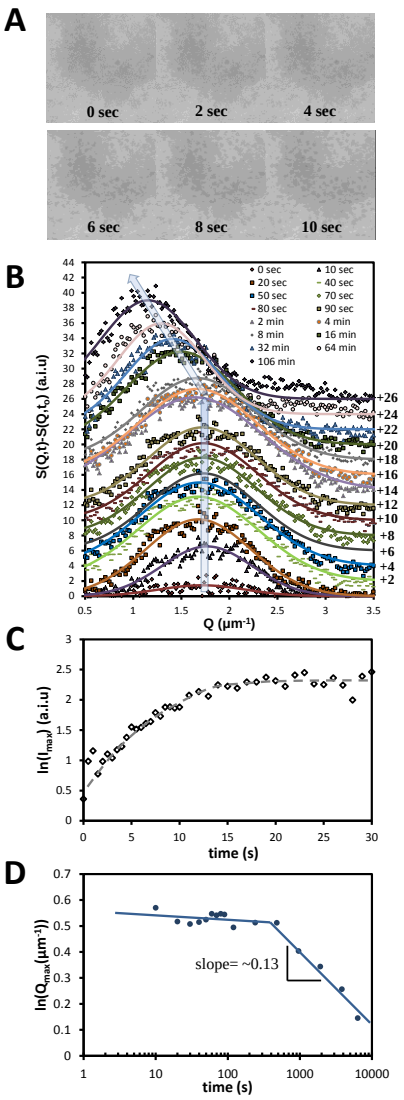

Figure 1. Analysis of a 13.3 wt% sulfate-PS/E7 gel quenched to 67°C from 71°C. (**A**) Time-series of bright field microscopy images. (**B**) Change in the structure factor, S(Q,t) with time plotted as a function of Q. (**C**) Change in structural peak height of S(Q,t) with respect to time during early stages of phase separation in CLC gel. (**D**) Change in structural peak position of S(Q,t) with respect to time.

*Colloids on LC Droplets***:** A second platform investigated over the past year for hierarchical design of soft materials involves LC droplets decorated with amphiphiles and particles. Specifically, through a series of simulations, we have demonstrated that LC can be used to impart order on the interfacial arrangement of a surfactant.[4 5,6] Recent experiments on macroscopic interfaces have hinted that an interfacial coupling between bulk LC and surfactant can lead to a two-dimensional phase separation of the surfactant at the interface, but have not had the resolution to measure the structure of the resulting phases. To enhance that coupling, we considered the limit of nanodroplets, the interfaces of which were decorated with surfactant molecules that promoted local perpendicular orientation of mesogens within the droplet. In the absence of surfactant, mesogens at the interface were all parallel to that interface. As the droplet was cooled, the mesogens underwent a transition from a disordered (isotropic) to an ordered (nematic or smectic) LC phase. As this happened, mesogens within the droplet caused a transition of the surfactant at the interface, which formed new

ordered nanophases with morphologies dependent on surfactant concentration. Such nanophases are reminiscent of those encountered in block copolymers, and include circular, striped and worm-like patterns (Figure 2).

Inspired by the above-described simulations, we have also pursued complementary experimental studies aimed at demonstrating that use of liquid crystalline droplets to direct the organization of interfacial adsorbates. Specifically, we have reported the use of liquid crystal (LC)-in-water emulsions for the synthesis of either spherical or non-spherical particles with chemically-distinct domains located at the poles of the particles.[7] The approach involved the localization of solid colloids at topological defects that form predictably at surfaces of water-dispersed LC droplets. By polymerizing the LC droplets displaying the colloids at their surface defects (Figure 3), we demonstrated formation of both spherical and, upon extraction of the mesogen, anisotropic composite particles with colloids located at either one or both of the poles. Because the colloids protruded from the surfaces of the particles, they also defined organized, chemical patches with functionality controlled by the colloid surface.

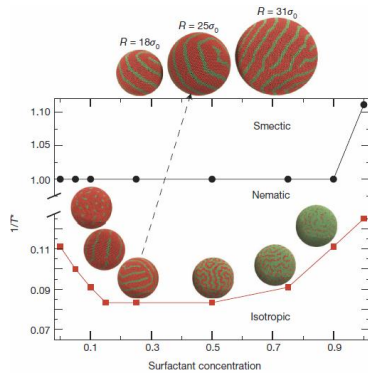

Figure 2: Phase diagram of adsorbates on LC nanodroplets.

LC Elastomers. The third materials platform that we have advanced over the past year involves liquid crystalline elastomers. In particular, via molecular simulations, we have studied the mechanism of the polydomain-monodomain transition in liquid crystalline elastomers at the molecular scale. A coarse-grained model has been developed in which mesogens are described as ellipsoidal particles. Molecular dynamics simulations were used to examine the transition from a polydomain state to a monodomain state in the presence of uniaxial strain. As shown in Figure 4, our model demonstrates soft elasticity, similar to that exhibited by side-chain elastomers in the literature. By analyzing the growth dynamics of nematic domains during uniaxial extension, we provide direct evidence that at a molecular level the polydomain-monodomain transition proceeds through cluster rotation and domain growth.[8 9]

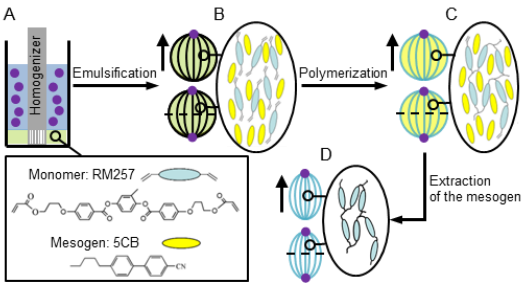

Figure 3. Schematic illustration of the liquid crystal-directed hierarchical synthesis of either spherical or non-spherical particles with chemically-distinct domains located at the poles of the particles

Future Directions

Our recent discovery of a new pathway leading to formation of colloid-in-LC gels suggests the basis of rationale designs of gels based manipulation of spinodal decomposition. Such designs shall be explored over the coming year. In addition, our experimental demonstration of hierarchical design of "patchy" particles provides the basis of a new class of "building blocks" for self-assembly on the meso-scale. Over the coming year, we will encode into the "patches" of the particles additional functionality, including catalytic functionality as the basis of active

materials. In addition, we will build on our recent accomplishments based on new models and simulation algorithms that are enabling unprecedented probing of the coupling between structure and thermodynamic properties of LCs and LC suspensions at the mesoscale. In particular, advanced metadynamics based sampling techniques will be used to determine the elastic coefficients of LCs from purely molecular considerations, thereby permitting high-precision prediction of such constants and paving the way for design of materials with specific mechanical, thermodynamic and optical responses. In a second example, theoretically informed mesoscale models will be used to predict the collective behavior of nanoparticles in arbitrary LC phases, thereby facilitating design of LC nanoparticle suspensions with controlled structures.

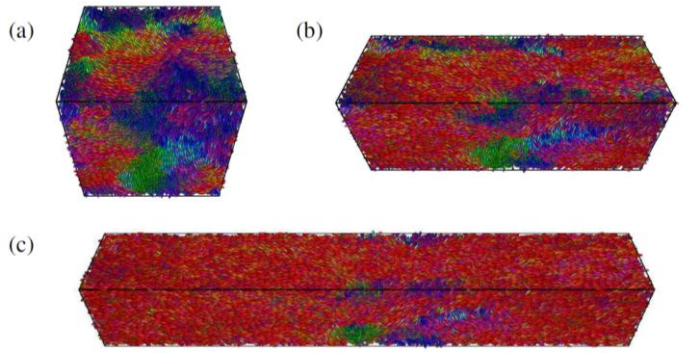

Figure 4. Representative configuration of LCEs with rigid crosslinkers at various points of a constant strain-rate simulation. Each particle is assigned an rgb value (x, y, z) equal to their orientation vector n. (a) Initial configuration, showing a clear polydomain structure. The average domain size is ≈ 150 particles, with 11 clusters having more than one thousand particles. (b) Under a strain of 1.0, domains begin to align and join. (c) At a strain of 2.5, only small misaligned clusters remain. The global order parameter for the latter system is S = 0.78.

References (which acknowledge DoE support)

1. Bukusoglu, E., Pal, S.K., Pablo, J.J.d. & Abbott, N.L. Colloid-in-Liquid Crystal Gels Formed via Spinodal Decomposition. *Soft Matter*, submitted(2013).
2. Whitmer, J.K., Joshi, A.A., Roberts, T.F. & de Pablo, J.J. Liquid-crystal mediated nanoparticle interactions and gel formation. *Journal of Chemical Physics* **138**(2013).
3. Tomar, V., Roberts, T.F., Abbott, N.L., Hernandez-Ortiz, J.P. & de Pablo, J.J. Liquid Crystal Mediated Interactions Between Nanoparticles in a Nematic Phase. *Langmuir* **28**, 6124-6131 (2012).
4. Tomar, V., Hernandez, S.I., Abbott, N.L., Hernandez-Ortiz, J.P. & de Pablo, J.J. Morphological transitions in liquid crystal nanodroplets. *Soft Matter* **8**, 8679-8689 (2012).
5. Moreno-Razo, J.A., Sambriski, E.J., Abbott, N.L., Hernandez-Ortiz, J.P. & de Pablo, J.J. Liquid-crystal-mediated self-assembly at nanodroplet interfaces. *Nature* **485**, 86-89 (2012).
6. Hernandez, S.I., Moreno-Razo, J.A., Ramirez-Hernandez, A., Diaz-Herrera, E., Hernandez-Ortiz, J.P. & de Pablo, J.J. Liquid crystal nanodroplets, and the balance between bulk and interfacial interactions. *Soft Matter* **8**, 1443-1450 (2012).
7. Frédéric Mondiot, Xiaoguang Wang, Juan J. de Pablo & Abbott, N.L. Liquid Crystal-Based Emulsions for Synthesis of Spherical and Non-Spherical Particles with Chemical Patches. *Journal of American Chemical Society* **135**, 9972-9975 (2013).
8. Shekhar, R., Whitmer, J.K., Malshe, R., Moreno-Razo, J.A., Roberts, T.F. & de Pablo, J.J. Isotropic-nematic phase transition in the Lebwohl-Lasher model from density of states simulations. *Journal of Chemical Physics* **136**(2012).
9. Whitmer, J.K., Roberts, T.F., Shekhar, R., Abbott, N.L. & de Pablo, J.J. Modeling the polydomain-monodomain transition of liquid crystal elastomers. *Physical Review E* **87**(2013).

Program Title: Actuation of Bioinspired, Adaptive "HAIRS" Powered by Responsive Hydrogels

Principle Investigator: Prof. Joanna Aizenberg[1]; Co-PI: Prof. Anna Balazs[2]
Mailing Address: [1]School of Engineering and Applied Science, Harvard University, Cambridge, MA 02138; [2]Chemical Engineering Department, University of Pittsburgh, Pittsburgh, PA 15261
E-mail: jaiz@seas.harvard.edu; balazs@pitt.edu

Program Scope

This program is motivated by a key, imminent challenge in materials science: the quest to "engineer" adaptiveness into the next-generation devices. Design of synthetic systems that sense and respond to environmental stimuli and chemical signals on both a microscopic and macroscopic level has been a longstanding scientific pursuit.[i] From a biological perspective, the interplay between signaling molecules and/or external stimuli and mechanical reconfiguration is commonplace, indeed fundamental, to nature's ability to self-regulate and adapt. The importance and versatility of naturally occurring chemo-mechanical systems serve as inspiration for the development of "smart" materials that are able to autonomously sense and adapt via self-regulated structural reconfiguration to trigger responsive changes in chemistry, wetting behavior, optical or thermal properties among others.[ii] The goals of this program is to understand and harness the power of combining chemically-induced mechanical responses with meaningful outcomes in terms of structure-function relationships, switchable surface properties, or directed chemical cascades.

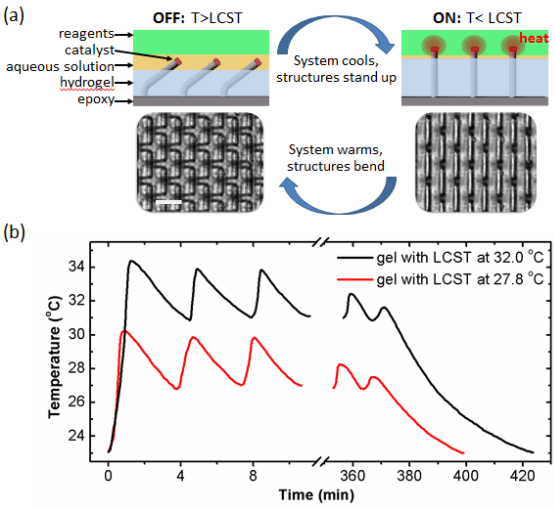

***Figure 1**. (a) Schematic demonstrating the feedback mechanism of a temperature-regulating SMARTS. The structure tips are coated with a catalyst which upon entering the reagent layer induces an exothermic reaction. This generated heat raises the surface temperature to above the LCST of the PNIPAAm hydrogel causing the gel to contract and the structures to bend over, removing the catalyst from the reagent layer and turning off the reaction. The surface cools to below the LCST and the structures stand up again, restarting the feedback cycle. Scale = 10 µm. (b) Surface temperature measurements for SMARTS with two PNIPAAm-based hydrogels with different LCSTs. As the LCST is changed, the temperature transition for actuation is similarly altered leading to fluctuations centered at tunable temperatures.*

The main strategy that we use to achieve our goals involves creating adaptive material systems by integrating high aspect-ratio nano/microstructures with responsive hydrogels, which are crosslinked polymer networks designed to swell or shrink in aqueous environments in response to various stimuli including temperature, pH, humidity, light, biomolecules, salt, magnetic and electric fields, redox state, etc.[iii] Hydrogels serving as an artificial "muscle", when combined with "skeletal" arrays of high-aspect-ratio (HAR) structures, is able to reversibly reconfigure and bend the embedded nano/microstructures, providing a means to switch surface properties and geometries in response to environmental cues.[2, 7-16] The interplay between controllable parameters provide for a highly tunable and customizable hydrogel-actuated integrated responsive structures (**HAIRS**). Based on platform, we have recently further explored these different modes of chemo-mechanical actuation, examining in detail how various chemical inputs as well as the physical combination of gel and HAR structure affect the mechanical response and in turn how we

can use this mechanical output for a variety of purposes, including 1) Self-regulating properties of system parameters as intelligent materials; 2) Catching and releasing biomolecules and cells of interest with potential application in point-of-care devices; 3) Multifunctional Actuation Systems Responding to Chemical Gradients.

The projects utilize the broad spectrum of expertise of Aizenberg group members in material chemistry and mechanics, polymer synthesis, biochemistry, fabrication of micro/nanomaterial systems, microscopy characterization techniques, in a joint effort of Balazs group on computational simulation.

Recent Progress

1) Adaptive chemo-mechano-chemical systems: towards artificial homeostasis We have designed a new materials platform that can mediate a variety of chemo-mechanochemical processes with a possibility to build in homeostatic feedback loops. The system reversibly transduces external or internal chemical inputs into user-defined chemical outputs via the "on/off" mechanical actuation of microstructures. High-aspect-ratio "skeletal" microstructures (epoxy microfins) decorated with a catalyst and partially embedded in a hydrogel "muscle" reversibly actuate as the gel swells/contracts in response to a chemical stimulus (C1). When this system is immersed in a bilayer liquid, this actuation (M) moves the catalyst or reagent affixed to the microstructure tips into and out of a top "nutrient" layer of reactants, such that a chemical reaction (C2) is turned on when the microstructures straighten and turned off when they bend, realizing a synchronized cascade of chemo-mechanical energy inter-conversions (C1→M→ C2), demonstrated by well-controlled switching of inorganic, organic and biochemical reactions.[3,5] By matching C2 with C1, we have created a complete, continuous feedback loop, C↔M, in the Self-regulated Mechano-chemical Adaptively Reconfigurable Tunable System, **SMARTS** (Fig. 1).[5] We demonstrated this unique capacity by creating multiple self-powered, self-regulated oscillating systems in which the mechanical action of a temperature-responsive gel, poly(N-isopropylacrylamide) PNIPAAm, was coupled to several exemplary exothermic catalytic reactions. Computational simulation results captured the key features of the chemo-mechanical self-regulating, oscillatory behavior seen in the experiments and assess the contributions of different variables.

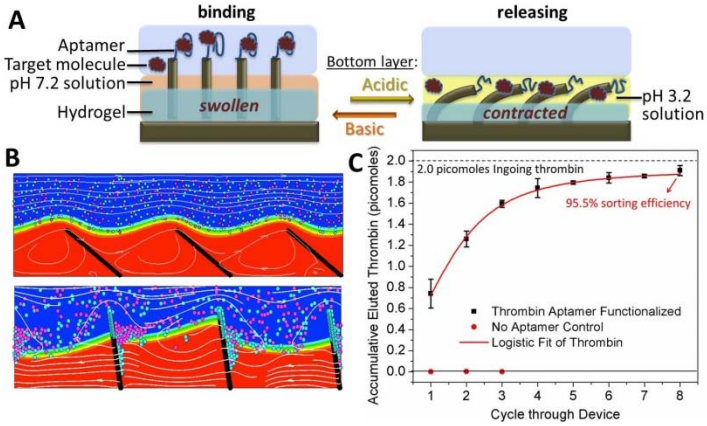

Fig. 2. *A. Schematic and design of the biomolecule catch and release device based on adaptively reconfigurable chemo-mechanical system. B. Sorting Capacity of Aptamer-functionalized Microdevice. C. Thrombin Collected from Recycling Ingoing Solution. Thrombin (2 picomoles) was pumped into the top layer of the device, showing elution of 95.5% of the ingoing thrombin in the bottom layer after 8 cycles of capture-and-release.*

2) Molecule Catch and Release by Aptamer-functionalized Adaptively Reconfigurable Systems We have applied the adaptively reconfigurable dynamic material system "SMARTS" to an efficient sorting device capable of reversible, dynamic capture and release of unmodified target molecules from solution. Specifically, we have integrated a pH-responsive hydrogel embedded in microstructures modified with pH-sensitive aptamers, which are known to strongly bind to the protein thrombin at physiological pH, and subsequently unfold at lower pH to release the biomolecule (Fig. 2A). We have done computational simulation to study the dynamic chemo-mechanically modulated target protein capture and release process (Fig. 2B) and also experimentally shown the microdevice is able to capture thrombin from a given solution in a constant flow and the sorting efficiencyachieved 95.5% by recycling the same solution through

multiple capture and release cycles (Fig. 2C). This clearly demonstrates the robustness of the microdevice towards repeated catch-and-release cycles and the capability of capturing and eluting quantities of thrombin significantly greater than the device's binding capacity.[1]

3) Multifunctional Actuation Systems Responding to Chemical Gradients We developed a multifunctional actuation system in which microstructures embedded in a pH-responsive gel can undergo multiple actuation scenarios: (i) highly localized, directional movement of embedded microstructures in response to pH *gradients*, but not to the change in the bulk pH, as in previously described pH-responsive systems, (ii) uniform large-area actuation upon hydration/dehydration.[6] We explored the fundamental mechanisms of such novel behavior including investigation of how the chemical gradient is translated to the physical structure of the hydrogel and in turn how the system provides the ability to control the direction of bending, location and area of bending, and degree of bending of embedded structures. We incorporated hybrid surfaces with pH-sensitive hydrogel, but not responsive to homogeneous pH, into microchannels. Aqueous solutions of pH = 2 and 10 were pumped into the channel creating a sharp pH gradient at the laminar flow interface (Fig. 3). We investigated the actuation of both microfins and posts and observed that structures always bent toward the direction of the acid within a "transition zone" of finite width across the interface while preserving an upright position farther from the interface both in the acidic and basic channels. We could reversibly control the bending direction of the structures and the position of the transition zone by changing the location, shape, and gradient direction.

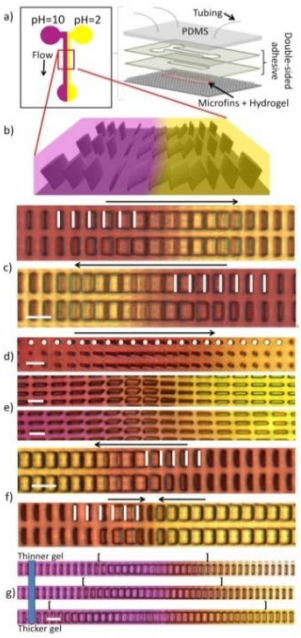

Fig. 3. *Patterned actuation of microstructures driven by a pH-responsive hydrogel induced by a pH gradient, which was created by flowing acid and base in a microfluidic channel.*

Future Plans

(1) Capture and Release with Aptamer-functionalized SMARTS We plan to expand on the different types of biomolecules that SMARTS can sort by moving from sorting proteins such as thrombin, to cells. Specifically we will be using the leukemia T-lymphoblast cells, CCL-119 cell line, to prove the versatility of our system. We plan to carry out experiments to characterize the capacity of the microdevice to capture the cells with optimized flow rate, as well its selectivity for CCL-119 cells over other cell types. We will measure the capture/release capacity, sorting efficiency through repeated actuation cycles, and selectivity of cell-sorting.

(2) Development of a Light-responsive Hydrogel for Local Actuation of a Hydrogel-embedded Microstructure Array In an attempt to expand the capabilities of our hydrogel-actuated integrated responsive system, we are working to increase the different types of responses the system can be sensitive to, from pH, temperature, humidity, to light. With the ability to actuate by light, we aim to introduce resolved, local actuation defined by the light beam width on the sample. In order to achieve this, we will add a light-responsive moiety, a benzospiropyran, and graft the molecule onto the backbone of the pH responsive hydrogel by free radical polymerization. We aim to achieve the light-induced actuation by a laser source, which irradiates in the visible range.

References

[i.] Stuart, M. A. C.; Huck, W. T. S.; Genzer, J.; Müller, M.; Ober, C.; Stamm, M.; SukhorukovI, G. B.; Szleifer, I.; Tsukruk, V. V.; Urban, M.; Winnik, F.; Zauscher, S.; Luzinov, I.; Minko, S., "Emerging applications of stimuli-responsive polymer materials." *Nature Materials 9*, 101-113, 2010.

[ii] Sidorenko, A.; Krupenkin, T.; Taylor, A.; Fratzl, P.; Aizenberg, J. "Reversible Switching of Hydrogel-Actuated Nanostructures into Complex Micropatterns." *Science 315*, 487-490, 2007.

[iii] Kim, P.; Zarzar, L. D.; Zhao, X.; Sidorenko, A.; Aizenberg, J. "Microbristle in gels: Toward all-polymer reconfigurable hybrid surfaces." *Soft Matter 6*, 750-755, 2010.

Publications (2-year list, supported by DoE BES)

1. He, Ximin; Shastri, Ankita; Lynn McGregor, Kuksenok, Olga; Balazs, Anna C.; Aizenberg, Joanna, "Chemo-mechanically Modulated Biomolecule Catch and Release by Aptamer-functionalized Adaptively Reconfigurable Systems", in preparation
2. A. Grinthal and J. Aizenberg, "Adaptive All the Way Down: Building Responsive Materials from Hierarchies of Chemomechanical Feedback,' Chem. Soc. Rev., (Invited Tutorial Review for special issue on Stimuli Responsive Materials), DOI: 10.1039/C3CS60045A.
3. X. He, R. S. Friedlander, L. D. Zarzar, J. Aizenberg, "Chemo-Mechanically Regulated Oscillation of an Enzymatic Reaction", Chem. Mat., 2013, 25(4), 521-523.
4. H. A. Burgoyne, P. Kim, M. Kolle, A. K. Epstein, J. Aizenberg, "Screening Conditions for Rationally Engineered Electrodeposition of Nanostructures (SCREEN): Electrodeposition and Applications of Polypyrrole Nanofibers using Microfluidic Gradients", Small, 2012, 8, 3502-3509.
5. X. He, M. Aizenberg, O. Kuksenok, L. D. Zarzar, A. Shastri, A. C. Balazs, J. Aizenberg, "Synthetic Homeostatic Materials with Chemo-mechano-chemical Self-regulation", Nature, 2012, 487, 214-218.
6. L.D. Zarzar, Q. Liu, X. He, Y. Hu, Z. Suo, J. Aizenberg. "Multifunctional actuation systems responding to chemical gradients." Soft Matter, 8, 8289-8293, 2012
7. M. A. Bucaro, Y. Vasquez, B. D. Hatton, J. Aizenberg, "Fine-tuning the Degree of Stem Cell Polarization and Alignment on Ordered Arrays of High-aspect-ratio Nanopillars", ACS Nano, 2012, 6, 6222-6230.
8. L. D. Zarzar, B. S. Swartzentruber, J. C. Harper, D. R. Dunphy, C. J. Brinker, J. Aizenberg, B. Kaehr, "Multiphoton Lithography of Nanocrystalline Platinum and Palladium for Site-Specific Catalysis in 3D Microenvironments", J. Am. Chem. Soc. 2012, 134, 4007-4010.
9. A. Grinthal, S. H. Kang, A. K Epstein, M. Aizenberg, M. Khan, J. Aizenberg, "Steering Nanofibers: An Integrative Approach to Bio-inspired Fiber Fabrication and Assembly", Nano Today, 2012, 7, 35-52.
10. P. Kim, A. K Epstein, M. Khan, L. D. Zarzar, D. J. Lipomi, G. M. Whitesides, J. Aizenberg, "Structural Transformation by Electrodeposition on Patterned Substrates (STEPS): A New Versatile Nanofabrication Method", Nano Lett., 2012, 12, 527-533.
11. P. Kim, W. E. Adorno-Martinez, M. Khan, J. Aizenberg, "Enriching Libraries of High-aspect-ratio Micro- or Nanostructures by Rapid, Low-cost, Bench-top Nanofabrication", Nature Protoc., 2012, 7, 311-327 [Invited].
12. P. Kim, L. D. Zarzar, M. Khan, M. Aizenberg, J. Aizenberg, "Environmentally responsive active optics based on hydrogel-actuated deformable mirror arrays", Proc. SPIE, 7927, 792705, 2011.
13. P. Kim, L. D. Zarzar, X. M. He, A. Grinthal, J. Aizenberg, "Hydrogel-Actuated Integrated Responsive Systems (HAIRS): Moving towards Adaptive Materials", Curr. Opin. Solid State Mater. Sci., 2011, 15, 236-245.
14. M. Matsunaga, M. Aizenberg, J. Aizenberg, "Controlling the Stability and Reversibility of Micropillar Assembly by Surface Chemistry", J. Am. Chem. Soc., 2011, 133, 5545–5553.
15. L. D. Zarzar, P. Kim, J. Aizenberg, "Bio-inspired Design of Submerged Hydrogel-Actuated Polymer Microstructures Operating in Response to pH", Adv. Mater., 2011, 23, 1442-1446.
16. L. D. Zarzar, P. Kim, M. Kolle, J. Brinker, J. Aizenberg, B. Kaehr, "Direct Writing and Actuation of Three-Dimensionally Patterned Hydrogel Pads on Micropillar Supports", Angew. Chem. Int. Ed., 2011, 50, 9356-9360.

Integrating modeling and experiments to design robust self-healing materials

Anna C. Balazs, PI (University of Pittsburgh)

Kris Matyjaszewski, Co-PI (Carnegie Mellon University)

Project Scope

Integrating expertise in computational modeling and chemical synthesis, our goal is to design and construct self-healing coatings, which are formed from cross-linked nanogel particles. The inter-particle cross-linking involves bonds that can undergo a rapid degenerative exchange, allowing new bonds to be formed as old bonds are broken. Due to this behavior, the network of nanogel particles exhibits unique attributes: in response to mechanical deformation, the particles can quickly rearrange and reshuffle so that the mechanical integrity of the coating is maintained. In effect, this dynamic behavior prevents the coating from undergoing catastrophic failure. Since the coating remains intact, it protects the underlying material from the mechanical strain and severe damage. Thus, the research will yield a new approach for extending the sustainability and durability of manufactured components and systems. While the need for designing more sustainable systems is clear, there are still few general approaches that can be readily adapted to address this need. Since the nanogel coatings can be applied to large variety of materials, these films could pave the way for transformative changes in manufacturing practices.

Recent Progress

The Balazs and Matyjaszewski groups collaborated to develop a hybrid computational model for the behavior of networks of cross-linked polymer-grafted nanoparticles (PGNs) [1-2]. The individual nanoparticles are composed of a rigid core and a corona of grafted polymers that encompass reactive end groups. With the overlap of the coronas on adjacent particles, the reactive end groups can form permanent or labile bonds, which lead to the formation of a "dual cross-linked" network. To capture these multi-scale interactions, our approach integrates the essential structural features of the polymer grafted nanoparticles, the interactions between the overlapping coronas, and the kinetics of bond formation and rupture between the reactive groups on the chain ends. Via this model, we determined the tensile properties of the dual cross-linked samples (see Fig.1). We found that the mechanical behavior of the network can be tailored by

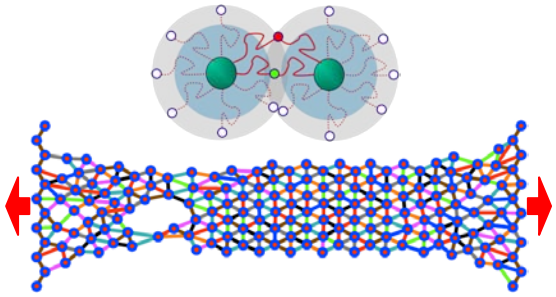

Fig 1. **Top image**: two polymer grafted nanoparticles (PGNs). The image shows the nanoparticle cores, the grafted chains, the coronas, the overlap areas and the reactive groups on the ends of the chains. **Bottom image:** structure of the dual cross-linked network under a tensile deformation. We found that the behavior of dual cross-linked PGNs is controlled by the bond energies of the labile bonds and the fraction of permanent bonds.

altering the bond energies of the labile bonds, the fraction of permanent bonds in the network and the thickness of the polymer corona. In particular, for a network with weaker labile bonds, an increase in fraction of permanent bonds and the contour length of the chain can yield a tough network that behaves like a polymeric material, which exhibits cold drawing/necking. On the other hand, similar changes to the network with stronger labile bonds lead to an increase in toughness, with the network characteristics being similar to that of a purely ductile material.

Variations in the ratio between the strain rate and the bond rupture rate were also found to affect the response of the networks. Our model provides a powerful approach for predicting how critical features of the system affect the performance of cross-linked polymer-grafted nanoparticles and yields design rules for creating self-healing nanocomposites. Notably, a graphic from this served as the back inside cover of *Soft Matter*.

In another recent study, we were inspired by molecular mechanisms that cells exploit to sense mechanical forces and convert them into biochemical signals. Our aim was to design biomimetic mechano-chemical switches that could be integrated into synthetic materials. Using the adhesion protein fibronectin, where essentially each of its multiple repeats (see Fig. 2) displays another molecular recognition motif, a computational model was derived [3] asking how minimalistic designs of repeats translate into mechanical characteristics of their fibrillar assemblies: the hierarchy of repeat-unfolding within fibrils is not just controlled by their relative mechanical stabilities, as found for single molecules, but also by the strength of cryptic interactions between adjacent molecules that become activated by stretching. The force-induced exposure of cryptic sites furthermore regulates the nonlinearity of stress-strain curves, the strain at which such fibers break, as well as the refolding kinetics and fraction of misfolded repeats. Gaining such computational insights at the mesoscale is significant since translating protein-based concepts into novel polymer designs has proven difficult. Importantly, the results reveal how such modular units can be utilized to inscribe seal-healing behavior into networks of coiled copolymers. We note that these studies build on our prior joint efforts [4]. The paper describing these new results appeared in *Biophysical Journal* and we obtained the cover of this issue. The graphic that is featured as part of this cover is shown in Fig. 2.

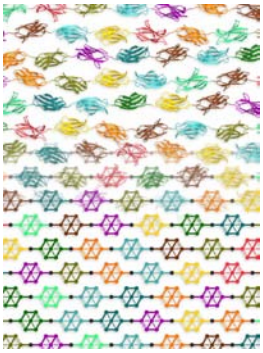

Fig. 2 Graphic that appears on the cover of the Nov. issue of *Biophysical Journal* highlighting our paper.

The experimental studies resulted in several papers [5-10] and presentations delivered by members of the research group. Matyjaszewski reported on a new method to control self-healing of covalently cross-linked polymers by reshuffling thiuram disulfide moieties in air under visible light, published in *Adv. Mater* [5]. He also described in ACS *Macro Letters* [6] how changes in network structure of chemical gels can be controlled by solvent quality through photoinduced radical reshuffling reactions of trithiocarbonate units. Matyjaszewski and Balazs also reported in *Macromolecules* [8] on new self-healing polymer films based on thiol-disulfide exchange reactions and self-healing kinetics measured using atomic force microscopy.

The PIs gave a number of invited talks on the findings that emerged from these studies. This September, Balazs delivered an invited seminar at the Self-healing Summer School held in Vlietland, Netherlands. Notably, Balazs was a plenary speaker at the Fourth International Conference on Self Healing Materials held in June 2013 in Ghent, Belgium and she described the findings from refs. [1] and [2] at that meeting. At national ACS meetings, Matyjaszewski reported on various self-healing of covalently cross-linked polymers via photoinduced radical transfer reactions and on AFM studies of self-healing polymer films based on thiol-disulfide exchange reactions.

In October 2013, Balazs was awarded the Mines Medal, which is a national award presented by the South Dakota School of Mines and Technology to honor engineers and

scientists who have demonstrated exceptional leadership and innovation. During the last year, Matyjaszewski have received several national and international awards, including Dannie-Heineman Prize from University of Goettingen, Germany, Maria Sklodowska-Curie Medal, Polish Chemical Society, Société Chimique de France Prize, Marie Sklodowska-Curie Science Medal, Pilsudski Institute of America. He also was elected as a Foreign Member of Russian Academy of Sciences and Honorary Fellow of the Chinese Chemical Society.

Future Plans

The above results indicate that our model provides a powerful approach for predicting how critical features of the system affect the performance of nanoparticle networks and yields significant insight into the microscopic phenomena contributing to the global behavior of the material. Hence, our recent studies form a strong foundation for the proposed research, where our goal is to isolate factors that can contribute to improving the reconfigurability, mechanical properties and self-healing of the dual cross-linked PGNs. The experimental component of the work will involve the synthesis and characterization of composite hybrid materials with self exchanging moieties and the subsequent testing of the predictions that emerge from the computational models. Below are some of the studies that we will jointly perform in the next year to establish design rules for creating new nanoparticle networks that are strong, tough and self-healing. The ideas for the studies listed below emerged from our joint group meetings, which are held on a regular basis and involve all the participants working on this project.

1. ***Apply a cycle of tensile and compressive forces*** In the studies in ref [1], we only considered the recovery after the relaxation of one application of the applied tensile force. We will now apply multiple cycles of tensile and compressive forces and determine the extent to which the properties of the material can be altered or degree of self-healing that can be accomplished through these cyclic deformations. Notably, the number of broken bonds could be effectively reformed and hence, a damaged material could be "resuscitated" by this cycle of applied forces

2. ***Randomize the distributions of permanent bonds*** In the above studies, at $P = 1$ or $P = 2$, each PGNs is connected by one or two permanent bonds, respectively. This skeleton of permanent bonds plays an important role in the strain recovery. In the proposed studies, we will maintain this fraction of permanent bonds, but allow them to be randomly distributed in the system. Hence, at $P = 1$ in this randomized scheme, some of the particles will not be connected by the permanent bonds and some will be connected by two or three of these bonds. This scenario more accurately reflects the experimental reality, i.e., it is difficult to synthesize systems where each particle is connected by exactly one permanent bond. We will then determine how this randomization affects the recovery behavior and self-healing properties.

3. ***Introduce different types of particles*** All the PGNs are identical in the samples considered above. We will consider binary mixtures of *A* and *B* particles so that the *A*-*A* and *B*-*B* binding interactions are stronger than the labile *A*-*B* interactions. In other words, $U^l_{AB} < U^l_{AA} = U^l_{BB}$. In this scenario, under weak deformation, the *A* and *B* species can readily slip past each other and the material would exhibit an elastic deformation. At a larger deformation, however, the *A*-*A* and *B*-*B* interactions would lock in a particular morphology. In effect, we are attempting to achieve a controlled plasticity. If the particles are initially localized in a particular arrangement, we could lock in a specific structure with a large scale deformation. In other

words, an applied weak force (one leading to elastic deformation) could produce one structure, but a larger force (i.e., producing the plastic deformation) would lead to another structure. The application of yet another large force could also lead to a structural reconfiguration. In all these cases, the distinct behavior is due to the fact that the *A-B* bonds allow for some reshuffling of bonds, but the stronger *A-A* and *B-B* bonds inhibit this reshuffling and thus, lock in structure. We will vary the fraction of *A* and *B* species, the initial location of these species in the sample and the strength of the applied force to determine how to optimally exploit this combination of parameters to achieve materials that exhibit controllable reconfiguration.

Publications

[1] Iyer, B.V.S., Salib, I.G., Yashin, V.V., Kowalewski, T., Matyjaszewski, K. and Balazs, A.C., "Modeling the response of dual cross-linked nanoparticle networks to mechanical deformation", *Soft Matter*, *Soft Matter* 9 (2013) 109-121.

[2] Iyer, B.V.S., Yashin, V.V., Kowalewski, T., Matyjaszewski, K. and Balazs, A.C., "Strain Recovery and Self-healing in Dual Cross-linked Nanoparticle Networks", *Polymer Chemistry*, 2013, DOI: 10.1039/C3PY00075C

[3] Peleg, O., Savin, T., Kolmakov, G.V., Salib, I. G., Balazs, A.C., Kroger, M., Vogel, V., "Fibers with Integrated Mechano-Chemical Switches: Minimalistic Design Principles Derived from Fibronectin", *Biophysical Journal*, 103 (2012) 1909-1918.

[4] Salib, I., Kolmakov, G.V., Bucior, B.J., Peleg, O., Kröger, M., Vogel,V., Matyjaszewski, K., and Balazs, A. C. "Using Mesoscopic Models to Design Strong and Tough Biomimetic Polymer Networks", *Langmuir*, 27 (2011)13796–13805.

[5] Amamoto Y, Otsuka H, Takahara A, Matyjaszewski K. Self-Healing of Covalently Cross-Linked Polymers by Reshuffling Thiuram Disulfide Moieties in Air under Visible Light. *Adv. Mater*. (Weinheim, Ger.) 2012; 24:3975-3980.

[6] Amamoto Y, Otsuka H, Takahara A, Matyjaszewski K. Changes in Network Structure of Chemical Gels Controlled by Solvent Quality through Photoinduced Radical Reshuffling Reactions of Trithiocarbonate Units. *ACS Macro Letters* 2012; 1:478−481.

[7] Matyjaszewski K. Atom Transfer Radical Polymerization: From Mechanisms to Applications. *Isr. J. Chem*. 2012;52:206-220.

[8] Yoon JA, Kamada J, Koynov K, Mohin J, Nicolay R, Zhang Y, Balazs AC, Kowalewski T, Matyjaszewski K. Self-Healing Polymer Films Based on Thiol-Disulfide Exchange Reactions and Self-Healing Kinetics Measured Using Atomic Force Microscopy. *Macromolecules* (Washington, DC, U. S.) 2012;45:142-149.

[9] Amamoto Y, Kamada J, Otsuka H, Takahara A, Matyjaszewski K. Self-Healing of Covalently Cross-linked Polymers Via Photoinduced Radical Transfer Reactions. *Polym. Prepr.* (Am. Chem. Soc., Div. Polym. Chem.) 2011; 52:657-658.

[10] Zhang Y, Yoon JA, Kamada J, Koynov K, Urban MW, Mohin J, Nicolay R, Balazs AC, Kowalewski T, Matyjaszewski K. AFM studies of self-healing polymer films based on thiol-disulfide exchange reactions. *Polym. Prepr.* (Am. Chem. Soc., Div. Polym. Chem.) 2011;52:620-621.

Inducing Artificial Morphogenesis in Soft Synthetic Materials

Anna C. Balazs, Chemical Engineering Dept. University of Pittsburgh, Pittsburgh, PA 15261

Program Scope

In biology, morphogenesis refers to the process that causes an organism to develop its shape. In the proposed studies, we will design synthetic systems that can exhibit a form of "artificial morphogenesis", where three-dimensional microscopic objects actively control their association into macroscopic structures. In effect, we will be devising a Lego set where the individual pieces autonomously come together to form a larger assembly and can dynamically rearrange to perfect their structure. Furthermore, in one of the proposed systems, the individual pieces of our Lego set are soft, deformable objects that can morph into different shapes. Hence, the collective migration and merger of these deformable units can lead to larger-scale objects that exhibit a tremendous variety of morphologies. In effect, we will be developing new methods for engineering the growth, shape and functionality of smart, biomimetic materials.

The fundamental issue we are attempting to address through these studies is: to what extent can we drive soft matter to organize or self-organize in a programmable manner? We focus on two distinct systems that offer unique attributes for addressing this question. Namely, "communicating" microcapsules can undergo autonomous motion and thus, could provide ideal candidates for self-organizing, programmable systems. Photo-responsive gels constitute another ideal system since their shape can be readily manipulated and our preliminary studies have revealed a novel means of using light to organize and combine the individual pieces (see below). By attempting to control the shape and growth of soft materials over a range of length scales, we will be addressing one of the stated grand challenges for DOE-related research. Furthermore, by controlling the structure of these systems, we could achieve unprecedented control over the functionality of the material.

Recent Progress

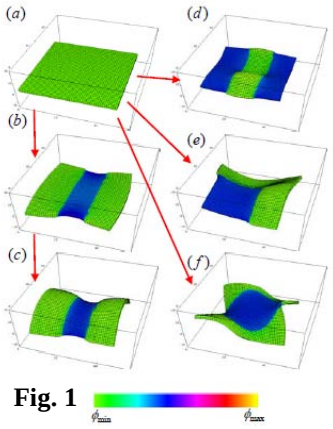

Fig. 1

The ability to dynamically change shape in response to variations in the environment is a distinctly biological trait. Through such shape-shifting, biological species achieve one of their vital functions: survival. The ability to undergo dynamic reconfiguration in response to external stimuli would prove particularly advantageous in the realm of functional materials. Namely, it would be highly desirable to create materials that could be molded via an external cue into a particular shape, which would permit a particular function. And then to use that same external cue to dynamically remold the given sample into another shape, which could enable a different function. Such processes would have a dramatic effect on manufacturing and sustainability since the same sample could be used and re-used for multiple applications, or multiple "lives". Inspired by the adaptability of shape-changing biological species, we used computational modeling to design a soft, responsive material that can be driven to undergo controlled variations in shape through the use of light.

Here, we focus on designing polymer gels whose shapes can be reconfigured "on demand" [1]. In addition, we show that by repeatedly sweeping a light source over the material, the sample can be driven to exhibit another distinctive biological behavior: directed, sustained motion [1]. To the best of our knowledge, this is the first example of a material that can undergo

both multiple shape reconfigurations and robust, directed motion. Both the shape-changing and the directionality of the sample's movement are prescribed dynamically via visual light and no pre-programming is required to achieve these behaviors. Removing the light source results in the complete recovery of the material's initial shape and arrests the sample's net motion.

To carry out these studies, we developed a computational model for photo-responsive polymer gels containing spirobenzopyran chromophores. Illumination with blue light causes isomerization of these chromophores into the closed ring conformation (into the spiro form, or *SP*), which is hydrophobic. The incorporation of these chromophores into gels formed from N-isopropylacrylamide (PNIPAAm) in aqueous solutions provides a means of harnessing light to control the gel's swelling or shrinking. We first validated our new model by determining the effects of uniform illumination on the temperature-induced volume phase transitions in these gels, and showed good agreement between our results and available experimental data. We then demonstrated that these gels can be patterned remotely and reversibly by illuminating the samples through photomasks and thus, "molded" into a variety of shapes with features sizes that are on the sub-*mm* length scale. For example, a certain shape can be achieved by illuminating the gels through a photomask with a specific opening. This shape can then be dynamically altered by shifting to a photomask with a different opening, as illustrated in **Figs. 1**. The sample remains flat in the absence of illumination (Fig. 1a), but can be "molded" into various shapes (Fig. 1b-f) as we change the openings in the mask and illuminate the sample. Multiple shapes can be written and rewritten into the same sample due to the complete reversibility of the process.

The anchored chromophores introduce another remarkable feature of this system: in the presence of spatially and temporally varying light, the photosensitive gel can undergo autonomous, directed motion, as illustrated in **Fig. 2**. Starting with an initially non-illuminated sample, we repeatedly move a light source from the left to the right, as marked by the yellow arrow in Fig. 2a. Specifically, the sample is illuminated through a relatively narrow rectangular opening in a photomask (with a width of *w=20*) and this opening is rastered over the sample so that its left edge, $l_1(t)$, is moved from A_1 to A_2 along the *x*-direction with a speed v_L. Similar to the examples above, when the opening is located directly over a specific area, the light causes that region to shrink. With a shift of the light to the right, the region that is now in the dark swells, and the newly illuminated region shrinks. The continual swelling/shrinking of contiguous regions results in the directed movement of the sample. As can be seen in Fig. 2b, after multiple passes (i.e., a total of *N* passes) of the stripe of light, the gel undergoes a net displacement to the left (as marked by the open arrow).

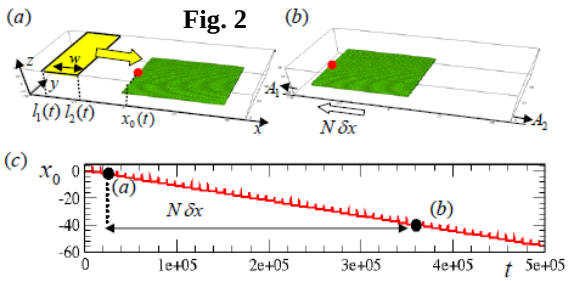

Fig. 2

To help visualize the sample's motion, the central node on the front face of the gel is marked by a red dot. The *x*-coordinate of this point, $x_0(t)$, is plotted as a function of time in Fig. 2c and clearly shows multiple small-scale oscillations. Notably, the gel moves due to the inter-diffusion of the solvent and polymer; hence, the motion of solvent in one direction causes movement of the polymer in the opposite direction. As the light is moved from left to right, the solvent is effectively "pushed" to the right; this net movement of solvent causes the polymer to move in the opposite direction, i.e., the polymer moves to the left.

We also observed that if a sample is placed in a temperature gradient, then rastering with light over portions of the sample experiencing different temperatures will result in their motion with effectively different speeds. To illustrate the consequences of this behavior, we now place a ring-shaped sample in a temperature gradient, with the highest temperature, T=30^0 C being on the top of the box shown in **Fig. 3** (at z=40) and with the lowest temperature, T=20^0 C, being on the bottom of this box (at z=20). The sample size is $180\times8\times3$ and the initial swelling of this sample corresponds to T=25^{0}C.

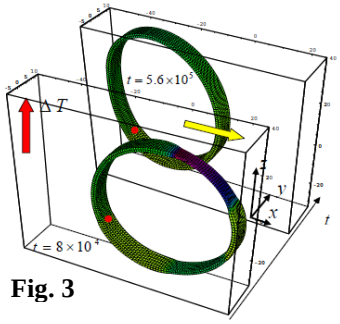

Fig. 3

Similar to the behavior shown in Fig. 2, repeated motion of the light source over the sample from the left to the right (indicated by the yellow arrow) induces the net motion of the sample to the left (Fig. 3). The imposed temperature gradient, however, significantly alters the shape and motion of this gel. In particular, the temperature gradient gives rise to a greater shrinking of the portion of the sample that is at the higher temperature. The additional, dramatic effects of the temperature gradient can be explained as follows. If the ring in Fig. 3 were held at a constant, uniform temperature, it would move uniformly to the left along the x-direction (due to the light), without any displacement in the vertical direction. The velocity of this motion, however, depends on temperature. Within the range of temperatures considered in Fig. 3, the velocity of the sample increases with the increase in T. Hence, when the sample is placed in a temperature gradient, the top portion of the sample moves to the left with a slightly higher velocity and thus, gives rise to a distorted shape where the upper portion of the ring effectively "leads" the movement. Hence, in subsequent swipes, the light now moves over a distorted, slightly elongated sample (rather than the initial ring-shaped object). The top of the elongated sample extends higher along the temperature gradient and again moves with a higher velocity, so that this top portion too appears to lead the movement. Further swipes of the light of over the sample continue to amplify this effect until ultimately, more and more of the sample is driven towards the higher temperatures. Hence, at late times, the sample exhibits a net displacement to the left and upwards. This net motion can clearly be seen by comparing the front and back images in Fig. 3 for the respective early and late time positions of the gel.

Fig. 4

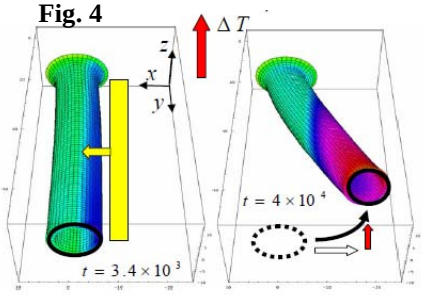

The distinctive features of the gel's light-induced motion within a temperature gradient are robust and are observed for a wide variety of sample shapes. Furthermore, the motion occurs in a similar manner even when one end of the sample is anchored to a wall. In particular, **Fig. 4** shows a tubular structure that is attached to the wall at one end. Repeated motion of illuminated region over the sample placed in a temperature gradient results in the superposition of the motion in the direction opposite to the motion of light and motion towards higher temperature (upwards). Additionally, the direction of the sample's motion can be controlled by specifying the directionality of the rastering light.

Our simulations show that the motion of a light source over gels containing spirobenzopyran chromophores induces a well-defined expansion and contraction along the sample and results in its directed motion. By repeatedly moving this light in a specific direction along the gel, we could drive samples of different shapes to undergo a net displacement in a

well-defined manner. The ability to remotely manipulate both the shape of the sample and its directed motion is critical for driving multiple samples to "recognize" each other and to ultimately "dock" to form soft, self-assembled structures with distinctive architectures. Importantly, this light-controlled shape-changing and guided motion opens new routes for fabricating a range of dynamically reconfigurable materials. In particular, this "molding" technique permits the assembled pieces to be re-shaped and hence, the same sample can be used or reused for a range of different functionalities. In effect, the technique ascribes the material with a remarkable adaptability: the ability to change shape (and function) with a change in environment.

Future Plans

In the next grant period, we plan to build on our collaborations with other members of the DOE Biomaterials Contractors group, including Igor Aronson [2] and Todd Emrick [4,6], as well as Dan Hammer and Joanna Aizenberg. In particular, we will continue our work on the SP-containing gels, determining how introducing variations and specific patterns in crosslink density affect the morphological changes and directed motion of the gel. The results will reveal how crosslink density variations can be exploited to tailor the functionality of the material.

We will also continue our work on communicating and responsive microcapsules. Our aim will be to coordinate our efforts with new experimental studies being performed by Aronson, Emrick and Hammer. Through iterative interaction with this group of researchers, we will attempt to validate our previous predictions and provide a springboard for new experimental studies.

Publications

1. Kuksenok, O. and Balazs, A.C., "Modeling the Photo-induced Reconfiguration and Directed Motion of Polymer Gels" *Adv. Func. Mater.*, in press.
2. Kolmakov, G., Schaefer, A., Aronson, I. and Balazs, A.C. "Designing Mechano- responsive Microcapsules that Undergo Self-propelled Motion", *Soft Matter* 8 (2012) 180-190.
3. Maresov, E., Kolmakov, G. V., Yashin, V.V., Van Vliet, K. and Balazs, A.C "Modeling the Making and Breaking of Bonds as an Elastic Microcapsule Moves over a Compliant Substrate", *Soft Matter* 8 (2012) 77-85.
4. Kratz, K., Narasimhan, A., Tangirala, R., Moon, S.C., Revanur, R., Kundu, S., Kim, H.S., Crosby, A.J. Russell, T.P., Emrick, T., Kolmakov, G. and Balazs, A.C. "Probing damaged substrates with 'repair-and-go' ", *Nature Nanotechnology* 7 (2012) 87-90.
5. Edington, C., Murata, H., Koepsel, R., Andersen, J., Eom, S., Kanade, T., Balazs, A.C., Kolmakov, G., Kline, C., McKeel, D., Liron, Z., and Russell, A.J., "Tailoring the Trajectory of Cell Rolling with Cytotactic Surfaces", *Langmuir* 27 (2011) 15345–15351.
6. Kolmakov, G. V., Emrick, T., Russell, T.P., Crosby A. J., and Balazs, A.C., "Design of a Repair-and-go System for Site-specific Healing at the Nanoscale", Self-Healing at the Nanoscale: Mechanisms and Key Concepts of Natural and Artificial Systems, V. Amendola, Ed., Taylor and Francis, Chapter 13, (2012) 313-332.
7. Kolmakov, G.V., Salib, I.G., and Balazs, A.C., "Modeling Self-healing Processes in Polymers: From Nanogels to Nanoparticle-filled Microcapsules", Self Healing Polymers, W. Binder, Ed., Wiley, Chapter 3 (2013) 91-111.
8. Salib, I., Yong, X., Crabb, E.J., Moellers, N. M., McFarlin, G., Kuksenok, O., and Balazs, A.C, "Harnessing Fluid-Driven Vesicles to Pick Up and Drop Off Janus Particles", *ACS Nano*, 7 (2013)1224–1238.

High Efficiency Biomimetic Organic Solar Cells

M.A. Baldo, ***Dept. of Electrical Engineering and Computer Science, MIT***
T. Van Voorhis, ***Dept. of Chemistry, MIT***

Program Scope

Organic photovoltaics (OPVs) are a promising, low cost, solar cell technology. But unlike conventional solar cells, OPVs generate localized excitons when they absorb light. The best model for organic solar cells is photosynthesis, since it shares much of the same physics. Consequently, this program seeks to exploit ideas from photosynthesis for OPVs. There are two focus areas: (i) the photosynthetic reaction center, where charge is efficiently separated, and (ii) the photosynthetic antenna, where light is captured and then directed in the form of an exciton.

We address two key questions:

1. How do we build devices that mimic the charge separation efficiency of photosynthesis?
2. Can we build an 'antenna' on top of a conventional solar cell to improve its efficiency?

Recent Progress

As is the case in photosynthesis, our current understanding is that some kind of multi-step interface is required to dissociate charge transfer states in organic PV. We have designed and built multi-layer devices to demonstrate this.[1] But these structures are complex and it is difficult to maintain the integrity of a multi-layer interface when the morphology is rough or a blend. Given the high efficiencies of many simple donor-acceptor organic PVs, it seems likely that some existing interfaces possess a fortuitous band bending or polarization shift that replicates the benefits of the more complex multi-layer interfaces.

Our goal is the *rational design* of such fortuitous interfaces. In the future, we hope that good donor-acceptor combinations can be engineered rather than simply chanced upon.

Experimental test of the effect of the dielectric constant and spin on recombination

We have been interested to identify a clean experimental test for our theoretical predictions of exciton dissociation at donor-acceptor interfaces. But this interfaces are difficult to change systematically without also causing significant impact to the materials or electronic states. To solve this experimental challenge, we have begun applying physical pressure to change the dielectric constant within organic solar cells. There is preliminary data from the Friend group in Cambridge that confirms that applied pressure red-shifts the CT state.[2] We have extended the technique to provide the first experimental probe of the spin dependence of recombination.

We performed measurements on a donor-acceptor blend of MTDATA and 3TPYMB; see Fig. 1. This forms a solar cell with quantum yield as high as 50%, and has the advantage of relatively

efficient luminescence from the donor-acceptor charge transfer state, allowing direct interogation of the CT states under pressure.

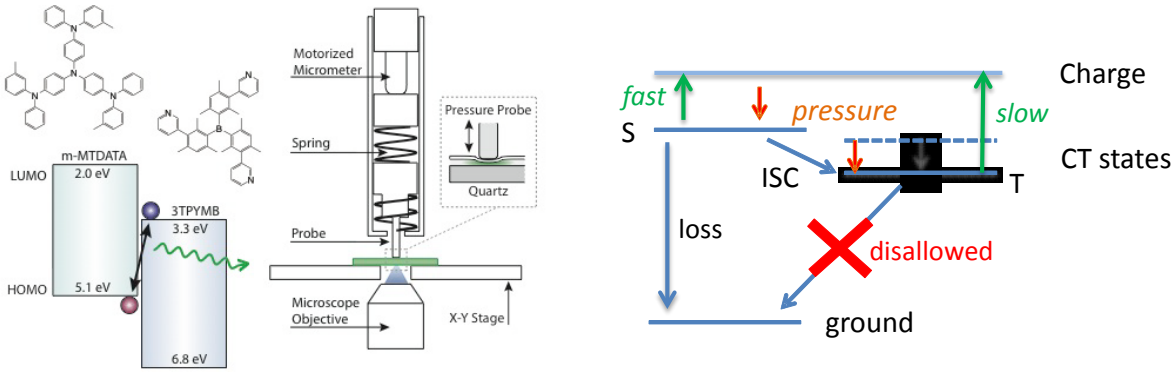

Fig. 1. A possible model for our preliminary data. Application of pressure reduces the e-h spacing, increasing the binding energy and exchange splitting in the CT state.

To date we have performed transient fluorescence, electric field, and magnetic field effect measurements on this system. For the first time, we have been able to vary the singlet-triplet spacing in situ and understand the impact of spin on organic solar cells.

To summarize our results:

(i) Application of pressure increases luminescence from the CT state because ISC slows down as the exchange splitting increases and CT dissociation into charge is reduced due to higher binding energy; see Fig. 2.

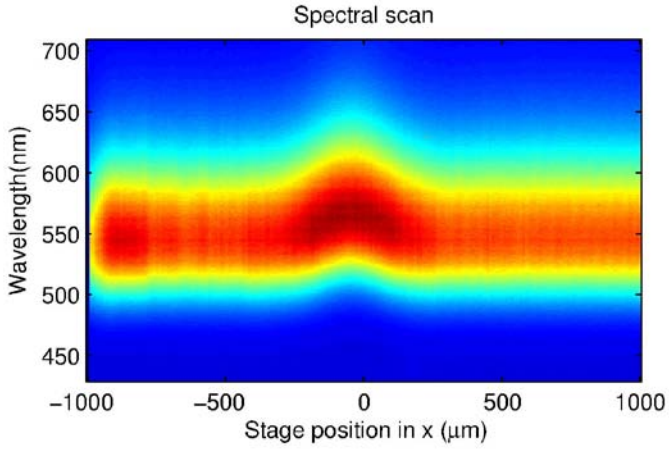

Fig. 2. Application of local (at $x = 0$) pressure to a film of MTDATA-3TPYMB red-shifts and increases the PL intensity of the CT states.

(ii) We find that the CT states exhibit prompt and delayed components in their fluorescence; see Fig. 3a. The delayed fluorescence must be predominantly due to reverse intersystem crossing from the triplet CT. If it was from charge formation followed by recombination, then delayed fluorescence would vanish under an applied electric field, which is not observed; see Fig. 3b.

(iii) The approximately 1000× difference in lifetime between prompt and delayed fluorescence suggests that the exchange splitting is ~ 0.16eV

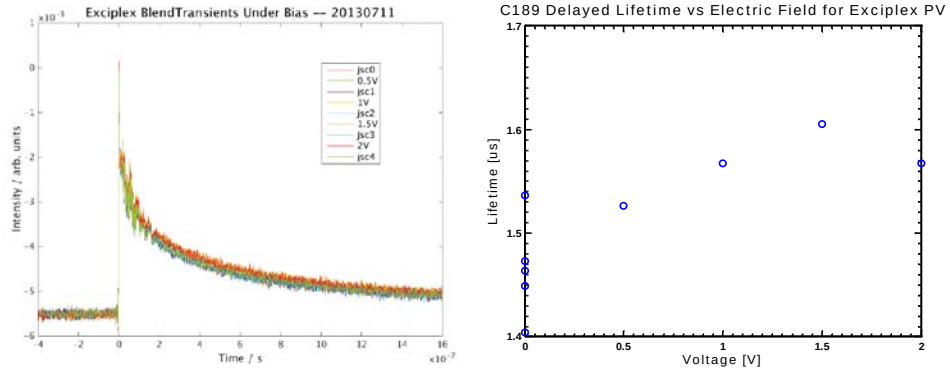

Fig. 3. The transient behavior of the CT state shows a prompt ~ns decay followed by delayed fluorescence. In a solar cell, the delayed fluorescence lifetime decreases at short circuit, where the internal electric field is largest. This indicates that triplet states are slowly dissociated by the electric field.

(iv) We find a magnetic field effect on luminescence and photocurrent; see Fig. 4. This originates in a reduction in intersystem crossing from S to T. The field effect shows that photocurrent generation is more efficient from the triplet (because there are fewer competing loss processes – radiation, no radiative decay to singlet ground state). The effect goes away under an electric field because then CT dissociation into charge dominates the radiative and non-radiative losses.

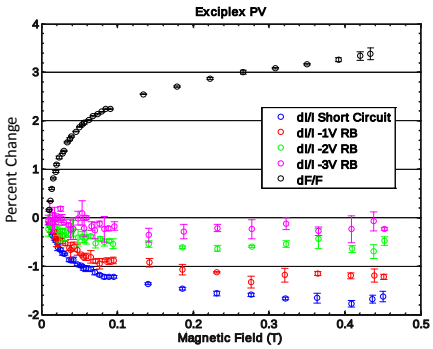

Fig. 4. Application of a magnetic field effect reduces the intersystem crossing rate. We find a corresponding increase in fluorescence and a decrease in photocurrent.

(v) Since delayed fluorescence originates in the triplet CT state, its modulation under pressure is due to a change in the exchange splitting; see Fig 5. We estimate that the splitting is modulated by approximately 4 meV under application of pressure. This result demonstrates a unique capability for this experiment.

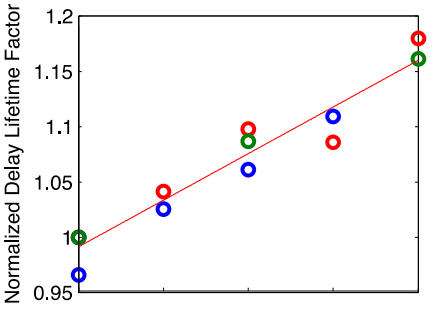

Fig. 5. A 16% change in the delayed fluorescence lifetime corresponds to a 4meV change in the exchange splitting.

Tentative conclusions:

The role of triplet CT states has attracted interest in organic PVs because their recombination is spin disallowed. Thus, spin control of CT states in organic PV could significantly improve device performance.

Here we have found that the triplet CT state offers weak protection against recombination by increasing the number of CT states to include three states without radiative or fast non-radiative losses. Recombination is not completely disallowed because the triplets also have much slower charge generation rates due to the exchange splitting. Our preliminary expectations are that

coupling between singlet and triplet CT states will lower the recombination rate by approximately a factor of four at best. The size of the exchange splitting doesn't matter much as long as the initial ISC rate out competes the singlet losses.

The CT states are the lowest energy states in our experimental system. On the other hand, if there is a triplet exciton underneath the CT states, then it is likely that we should desire large exchange splittings to slow down ISC. Consequently, we find that the exchange splitting is a significant design parameter in the limit that the initial ISC rate should be slow, which removes any triplet state effect. Of course, it may be difficult to achieve a large exchange splitting while keeping the binding energy low enough to promote charge generation.

Future plans

Utilization of triplet states can significantly reduce recombination losses in organic solar cells. But the main issue for PVs still appears to be the binding energy of the CT state. How can we reduce it? In the following year, we will focus increasingly on materials designed to exhibit very weak electron-hole overlap. Such materials have recently found application in organic light emitting devices that exhibit thermally-activated delayed fluorescence.[3]

References

1. Heidel, Hochbaum, Sussman, Singh, Bahlke, Hiromi, Lee, and Baldo, Journal of Applied Phyiscs, **109**, 104502, (2011)
2. Schmidtke, Friend and Silva, Physical Review Letters **100,** 157401 (2008)
3. Uoyama, H., Goushi, K., Shizu, K., Nomura, H. & Adachi, C. *Nature* **492**, 234-238 (2012)

Publications supported under this program

1. Heidel, Hochbaum, Sussman, Singh, Bahlke, Hiromi, Lee, and Baldo, "Reducing recombination losses in planar organic photovoltaic cells using multiple step charge separation" Journal of Applied Phyiscs, 109, 104502, (2011)
2. S. Difley and T. Van Voorhis, "Exciton/Charge-Transfer Electronic Couplings in Organic Semiconductors", *J. Chem. Theo. Comp.* **3**(7) 594-601 (2011).
3. S. R. Yost, L. P. Wang and T. Van Voorhis, ": Molecular Insight Into the Energy Levels at the Organic Donor/Acceptor Interface: A Quantum Mechanics/Molecular Mechanics Study", *J. Phys. Chem C* **115**(29) 14431-14436 (2011).
4. S. R. Yost and T. Van Voorhis, "Electrostatic effects at organic semiconductor interfaces: A mechanism for "cold" exciton breakup", *J. Phys. Chem C Submitted.*

Optimizing immobilized enzyme performance in cell-free environments to produce liquid fuels

Grant No. DE-SC0006520

Joseph J. Grimaldi, Cynthia H. Collins and Georges Belfort
Howard P Isermann Department of Chemical and Biological Engineering, and
Center of Biotechnology and Interdisciplinary Studies
Rensselaer Polytechnic Institute, Troy, NY 12180-3590
and

Mithun Radhakrishna, Sanat Kumar
Department of Chemical Engineering
Columbia, New York, NY 10027

Program Scope:

The increasing demand to find more carbon neutral energy sources has motivated the search for biologically-derived fuel products. The largest concern facing alcohol-based biofuels is the ability to develop an efficient high-yield scalable commercially available production process (1). With the recent discovery of abundant gas resources in the USA through "fracking" technology and recent and expected future drop in energy prices, the challenge for competitive alternate energy sources is more acute (2). Many options that until recently were considered viable, are clearly less so today (3). This quantum change in the US energy mix will force funding agencies such as DOE and energy companies to reevaluate their focus. Limitations on biofuel production using cell culture (*Escherichia coli*(4), *Clostridium(5)*, *Saccharomyces cerevisiae(6, 7)*, brown microalgae(8), blue-green algae(9) and others) include low product (alcohol) concentrations (2-5 vol%)(1) due to feed-back inhibition, instability of cells, low titers and difficulty in scale-up (1)-(10).

Fig 1. Two-step enzymatic reaction to produce i-butanol from ketoisovaleric acid

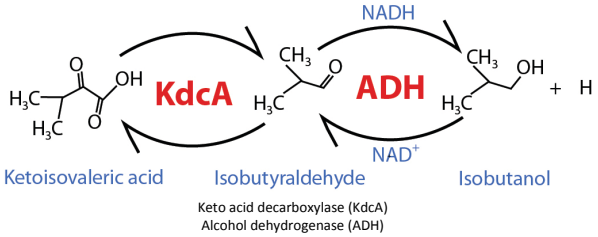

The research funded by this grant for the past two years focused on the bioconversion of acids to aldehydes to alcohol (butanol) using a two-enzyme system. While this enzymatic route offers great promise and excellent selectivity for the production of biofuels, enzymes exhibit slow kinetics, low volume capacity in solution and product feedback inhibition. These limitations have to be overcome so that biofuels can be produced economically. A novel approach is used here to address these limitations. Enzymes synthesized via recombinant DNA technology are immobilized on a solid substrate in order to stabilize them and allow the product to continuously be removed while retaining catalyst. This cell-free enzyme system will be coupled with a separation technique, possibly pervaporation, to constantly remove the desired butanol. Thus we address slow kinetics (genetic mutation, enzyme coupling and removal of inhibitory product), low volume capacity (immobilization and stabilization of enzymes) and product feedback inhibition (product removal) with our approach.

We offer an alternate simplified biofuel production approach to cell culture with the hope of overcoming all three limitations listed above, while speeding up the process considerably and possibly reducing the cost of fuel production. Our semi-*in vitro* partial cell-free scheme requires the following steps (**Fig. 1**):

1. *E. Coli cells:* Production/isolation of two critical enzymes (ketoacid decarboxilase, KdcA, and alcohol dehydrogenase, ADH) using standard fermentation.
2. *Starting Substrate: Streptomyces cinnamonensis* mutants overproduce 2-ketoisovaleric acid to titters of 2.4 g/L (11).

3. *Cell-free:* Simultaneous *in vitro* application of the two enzymes (KdcA and ADH) attached to solid substrates to convert acid (ketoisovaleric acid) to aldehyde (isobutyraldehyde) and then to alcohol (isobutanol, the fuel).
4. *Recovery:* Continuous removal and recovery of isobutanol in order to drive the reactions toward isobutanol (12).

This process is attractive because there are no cells that undergo product feed-back inhibition, enzymes are produced at high titer using standard fermentation *sans* feed-back limitations (step (i) above), protein engineering is used to stabilize the two enzymes to high product titer and high temperature (step (iii)), enzymes are stabilized through immobilization (step (iii)), and the reaction is driven toward product through its continual removal of alcohol (recovery) (step (iv)). We plan to publish three manuscripts where we first optimize the immobilization of two tetramer enzymes, β-galactosidase (control) and ADH, in the first manuscript (13). The other two manuscripts will report on KdcA stabilization using protein engineering (14) and a combination of the two enzymes (KdcA and ADH) into the complete scheme with product recovery.

Research Progress

Fig. 2. Normalized ADH kinetic activity in solution and immobilized passively (just adsorbed) or covalently on non-porous silica, porous SBA-15 and porous methacrylate (resin) particles. (A) ADH covalently attached on 200 (◆) and 100 (▲) nm acid functionalized silica nanoparticles, in solution (■), and nanoparticles with no immobilized ADH (●). (B) ADH passively immobilized on SBA-15 (◆), ADH passively immobilized on SBA-15 after multiple washes (▲), SBA-15 particles with no immobilized ADH (●), ADH free in solution (■). (C) ADH covalently attached to amino functionalized methacrylate resin as a function of bound ADH concentration: methacrylate resin no ADH (●), 3 µg ADH/mg resin (✖), 7 µg ADH/mg resin (▲), 15 µg ADH/mg resin (◆), 17 µg ADH/mg resin (O), equivalent ADH free in solution (■). All absorbance readings were normalized by their initial absorbance.

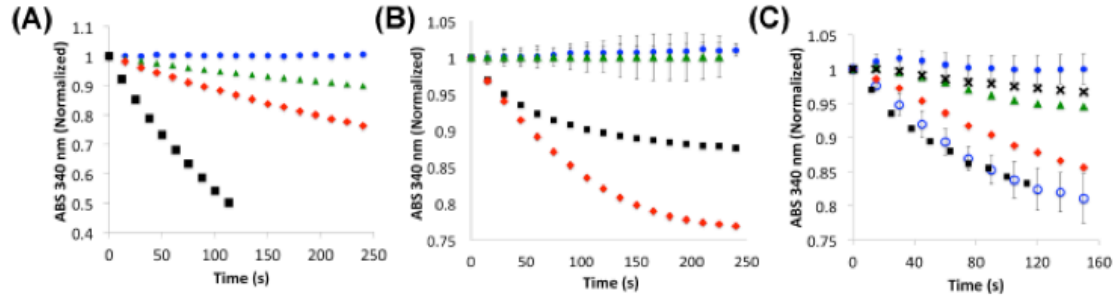

Last year, we demonstrated that the enzyme activity differs when immobilized on either 200 nm and 100 nm mean diameter silica particles. In addition, SBA-15, a mesoporous silica, provided a negative curvature surface in which confinement stabilized the protein and retained its activity. Further studies were performed to test the effect of surface coverage and particle loading. The particle system was tested with a model enzyme, ß-galactosidase, and our two critical enzymes for alcohol production, alcohol dehydrogenase (ADH) and keto-acid decarboxylase (KdcA). This past year, we developed a viable method for immobilizing enzymes with multiple domains on commercial methacrylate resin. When immobilized, the enzyme must exhibit high activity or retain a large fraction of its solution activity and be able to remain immobilized and active through multiple reactions without leaching from the support. Of the four steps listed above, this past year we have:

1. Tested the reaction of a model multi-domain enzyme, β -galactosidase (β -gal), with a simple colorimetric assay ─immobilized on various surfaces to identify the best surface and curvature (concave or convex).

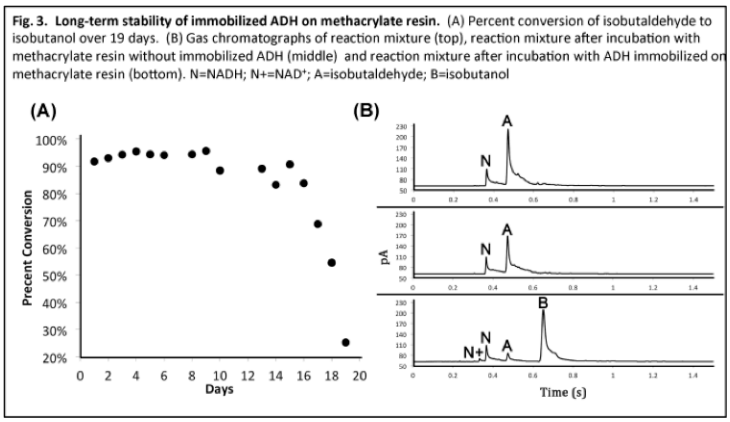

Fig. 3. Long-term stability of immobilized ADH on methacrylate resin. (A) Percent conversion of isobutaldehyde to isobutanol over 19 days. (B) Gas chromatographs of reaction mixture (top), reaction mixture after incubation with methacrylate resin without immobilized ADH (middle) and reaction mixture after incubation with ADH immobilized on methacrylate resin (bottom). N=NADH; N+=NAD+; A=isobutaldehyde; B=isobutanol

2. Immobilize ADH onto the optimal surface obtained from (1) and compared its conversion efficiency with that in free solution for aldehyde to alcohol (**Figs. 2 & 3**).

Production and optimization of keto-acid decarboxylase (KdcA)*:* One key component of the two-stage enzymatic reaction is the first enzyme of the reaction, KdcA, which is not commercially available. We have earlier cloned, overproduced and purified KdcA and successfully tested its activity alone and in combination with immobilized ADH and KdcA in free solution (**Fig. 4**). KdcA is unstable when immobilized and looses its activity.

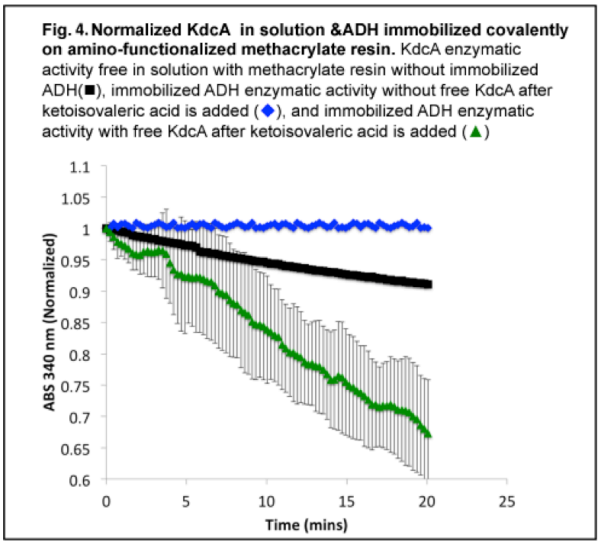

Fig. 4. Normalized KdcA in solution &ADH immobilized covalently on amino-functionalized methacrylate resin. KdcA enzymatic activity free in solution with methacrylate resin without immobilized ADH(■), immobilized ADH enzymatic activity without free KdcA after ketoisovaleric acid is added (◆), and immobilized ADH enzymatic activity with free KdcA after ketoisovaleric acid is added (▲)

Future Plans

Future work will use protein engineering to search for mutations that stabilize KdcA and focus on integrating the system into one process and then recovering i-butanol, the product.

Development of a recovery system for iso-butanol*:* A laboratory scale pervaporation/RO module system and a settling device will be built to study membrane and sedimentation separations of iso-butanol from water.

Simulations

Retention of enzymatic activity upon immobilization is a great challenge due to the structural changes the enzyme undergoes upon immobilization and subsequently losing its activity. It is therefore imperative to understand as to how enzymes interact with variety of surfaces (hydrophobic, neutral and hydrophilic) and different geometries (flat supports, curved surfaces). In the current work, we have tried to understand the physics of protein folding/unfolding and stability of these enzymes on different surfaces and geometries in the framework of the 'Hydrophobic-Polar' (H-P) lattice model through Monte Carlo simulations.

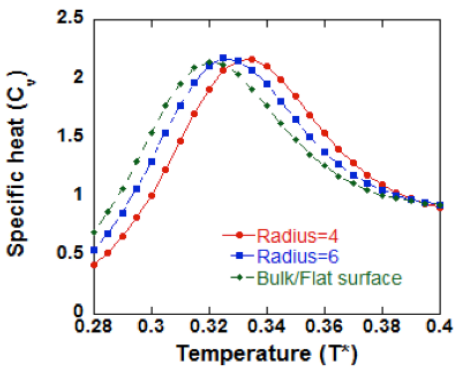

Figure 5: **Simulations:** Specific heat curve of the 64-mer HP protein at different degrees of athermal confinement, at both a flat surface and inside spherical cavities of radius 4 and 6.

Progress

Our results show that, a neutral confinement stabilizes the folded (native) state of the protein against reversible unfolding. Therefore, the folding temperature of the protein shifts to higher temperature for progressively smaller cavities (**Figure 5**). On hydrophobic surfaces, we observe a small stabilization of the protein on flat supports at weak surface hydrophobicity whereas denaturation happens for stronger hydrophobic surfaces due to preferential protein-surface interactions. A hydrophobic confinement always tends to destabilize the protein. Nevertheless, the protein can be still stabilized at weak surface hydrophobicities

relative to that in free solution, due to the entropic dominance of confinement inside such pores (**Figure 6**).

Our simulation results helps to qualitatively rationalize many previous experimental results and most importantly provides us a rationale to explain the experimental findings of our collaborators of increased enzymatic activity of ADH when it is immobilized inside hydrophilic SBA-15 pores and unaffected activity inside weakly hydrophobic PMMA pores. Inside hydrophilic SBA-15 pores, the protein has no energetic propensity to unfold. Further, it is also stabilized as a result of entropic effect due to confinement. In the case of immobilization inside pores, we believe the unaffected activity of ADH is as a result of mutual balance between the entropic and energetic contributions. We believe that the proper tailoring of energetic effects in spherical confinements can be employed to change the activity of the protein at will.

Figure 6: Simulations: Folding (melting) temperature (Tm) of the 64-mer HP protein as a function of surface hydrophobicity (λ) for different degrees of confinement

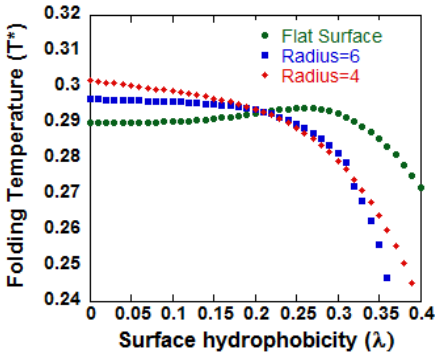

Future Work

We want to extend the above study for hydrophilic surfaces. Inter-protein interaction between the immobilized enzymes is believed to be one of the major causes for loss in enzymatic activity upon immobilization. We want to investigate mechanisms through which surface properties (hydrophobicity/hydrophilicity) can be modified for different geometries (flat support, inside pores, outside curved surfaces) so that we retain maximum retention of enzymatic activity.

Publications (acknowledging DOE support)

1. Radhakrishna, M.; Sharma, S.; Kumar, S. K., Enhanced Wang Landau sampling of adsorbed protein conformations. *J Chem Phys* **2012,** 136, (11), 114114-114114.
2. Sharma, S.; Berne, B. J.; Kumar, S. K., Thermal and Structural Stability of Adsorbed Proteins. *Biophysical Journal* **2010,** 99, (4), 1157-1165.
3. Radhakrishna, M.; Grimaldi, J.; Belfort, G.; Kumar, S. K., Stability of Proteins Inside a Hydrophobic Cavity. *Langmuir* **2013**.

References:

1. Fischer C, Kleinmarcuschamer D, Stephanopoulos G. 2008. *Metabolic Engineering* 10: 295-304
2. Yethiraj A, Striolo A. 2013. *The Journal of Physical Chemistry Letters* 4: 687-90
3. Tullo A, Johnson J. 2013. *C&EN* 91: 9-13
4. Inui M, Suda M, Kimura S, Yasuda K, Suzuki H, et al. 2007. *Applied Microbiology and Biotechnology* 77: 1305-16
5. Atsumi S, Hanai T, Liao JC. 2008. *Nature* 451: 86-9
6. Lee WH, Seo SO, Bae YH, Nan H, Jin YS, Seo JH. 2012. *Bioprocess and Biosystems Engineering*: 1-9
7. Steen EJ, Chan R, Prasad N, Myers S, Petzold CJ, et al. 2008. *Microbial Cell Factories* 7: 36
8. Wargacki AJ, Leonard E, Win MN, Regitsky DD, Santos CNS, et al. 2012. *Science* 335: 308-13
9. Zhou J, Li Y. 2010. *Protein & cell* 1: 207-10
10. Daugulis AJ, Axford DB, McLellan PJ. 2009. *The Canadian Journal of Chemical Engineering* 69: 488-97
11. Pospíšil S, Kopecký J, Přikrylová V, Spížek J. 2006. *FEMS microbiology letters* 172: 197-204
12. Strathmann H, Gudernatsch W. 1991. *Extractive Bioconversions*: 67-89
13. Grimaldi J CC, Belfort G. *(To be submitted by Aug 1st)*
14. Grimaldi J CC, Belfort G. *(In Prep)*

Self Assembling Biological Springs: Force Transducers on the Micron and Nanoscale

Ying Wang[a], *Angel Young*[b], *Aleksey Lomakin*[a], *and George B. Benedek*[a,b]

[a]Materials Processing Center, [b]Department of Physics,
Massachusetts Institute of Technology, 77 Massachusetts Avenue, Cambridge, MA 02139

PI: George B. Benedek

Program Scope:

We are developing a new tool for measuring forces within and between nanoscale biological molecules based on mesoscopic springs made of cholesterol helical ribbons. These ribbons self-assemble in a wide variety of complex fluids containing sterol, a mixture of surfactants and water [1]. The X-ray studies have shown that the cholesterol helical ribbons are single crystal strips wrapped into a helical form [2]. For such a crystal strip, i.e. a cholesterol helical ribbon, the spring constant can be calculated from its observable geometrical features: width w, contour length s, and radius R [3]. In a mixture solution of sterol and surfactants, the self-assembled helical ribbons have markedly diverse geometrical features and thus have spring constants in the range from 0.5 to 500 pN/nm [4]. A helical ribbon with a spring constant appropriate for a particular application can be readily selected from a polydisperse ensemble of ribbons formed in solution.

To utilize these springs experimentally they must be tethered to biologically active binding tips, and to stationary suspension posts (Fig.1). In this way it should be possible to create mesoscale force transducers whose spring constants are well suited to probe quantitatively the forces acting in a wide variety of biological systems such as biopolymers, membranes, motile cells, protein-ligand pairs, and protein motors. However, direct tethering of cholesterol ribbons is difficult because of its delicacy and absence of chemically active groups on its surface. Various means to modify the surface of the helical ribbons have been explored, and we have found that polydopamine surface coating provides the desired adhesion. In addition, this coating renders the helical ribbons more robust, and also enables further surface modifications such as metal plating.

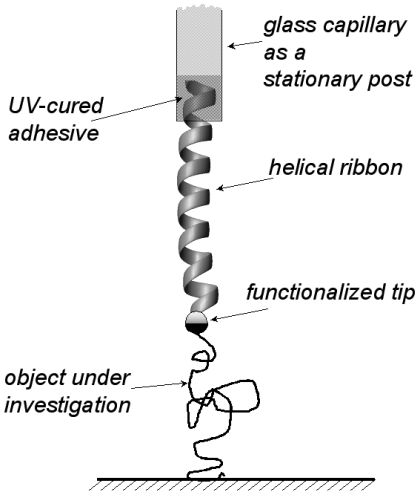

Figure 1. A schematic (not drawn to scale) showing the important components that would be associated with using the helical ribbons as force probes. The helix is attached at one end to a glass capillary that controls the extension by its connection to a micromanipulator, while the other end is attached to the biomolecule under investigation through the use of a functionalized latex sphere.

Our helical ribbons are soft and have the same pitch angle in their unstrained form independent of external solution conditions, but can change in response to a local strain. These properties suggest the use of helical ribbons as strain detectors and indicators to measure plastic and elastic deformation in hydro gels.

Recent progress

Our recent research has been focused on (1) designing of the force measurement device using cholesterol helical ribbons, and (2) demonstrating the utility of such device.

Design of the force measurement device based on cholesterol helical ribbons.

We have developed a practical force measurement device using cholesterol helical ribbons. The structure of this device is very simple and economic. It consists of a functionalized helical ribbon glued to the tip of a glass capillary (Fig. 2A), and a functionalized latex bead held by suction on another capillary (Fig. 2B). To prepare the functionalized helical ribbon, we have coated the cholesterol helical ribbons from commercial Chemically Defined Lipid Concentrate (CDLC) with polydopamine. The polydopamine coating can be further functionalized for particular applications. One example is to coat a layer of antibody on top of the polydopamine coating using glutaraldehyde as chemical cross-linker. The functionalized helical ribbons are then tethered to a capillary using 5-minute Epoxy glue. The other part of the force measurement device is a functionalized bead. For particular applications, the functionalized beads are either commercially available, such as the protein A coated beads which bind to IgGs, or they can be prepared in the lab using various techniques including polydopamine coating.

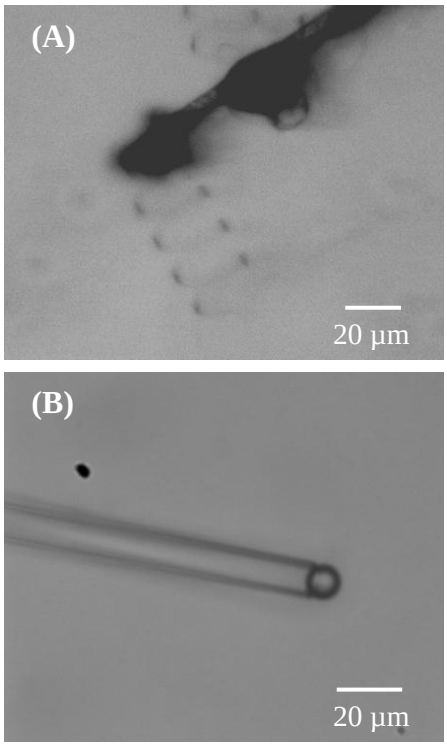

Figure 2. The force measurement device based on mesoscopic springs. (A) a polydopamine coated cholesterol helical ribbon tethered to a glass capillary using 5-minute Epoxy; (B) a polydopamine coated latex bead held on a capillary by suction.

Preparation of this device takes advantage of the combination of polydopamine coating and Epoxy glue. As compared to the other helical ribbon tethering methods, this tethering method is much easier and more reproducible. Indeed, a student without any experience with cholesterol helical ribbons can successfully tether a helical ribbon to the capillary using this method. Also, the polydopamine layers allow a variety of further functionalizations. Therefore, this device can be easily adapted for measuring force in different biological systems. Furthermore, the latex bead can be readily and precisely transferred using a micromanipulator. The interactions between the coating layers on the bead and the helical ribbon is through a very small area of contact between the bead and the ribbon. The minimal contact area is beneficial for the measurement of force between a single pair of molecules.

Measurement of the interaction between polydopamine coatings.

The polydopamine coating is a novel biomimetic approach to modify the surface properties of various materials [5]. It is of fundamental interest in material science to quantify

the interfacial interaction between polydopamine coatings. In the present period of study, we demonstrated the utility of our mesoscopic spring device by measuring the interaction between polydopamine coatings.

In this measurement, we brought a polydopamine coated latex bead in contact with a polydopamine coated cholesterol helical ribbon. Then, we use the micromanipulator to pull the bead until it was detached from the helical ribbon. The geometrical parameters of the helical

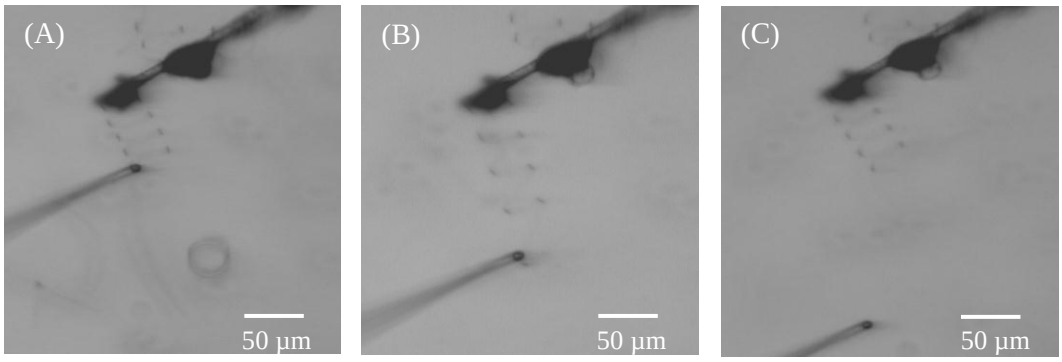

Figure 3. force measurement of the interaction between polydopamine coatings. (A) the polydopamine coated bead in contact with the polydopamine coated cholesterol helical ribbon; (B) the helical ribbon elongated when the bead was pulled away; (C) the helical ribbon relaxed to its initial length after detachment.

ribbons were determined under an optical microscope: width w = 8µm, contour length s = 328µm, radius R = 39µm, and pitch angle φ_0 = 20°.(Fig.3) In our previous theoretical and experimental studies [1-4], we have determined the relation between the external geometrical parameters of a helical ribbon and its spring constant viz: $K_{spring} = \kappa w/R^{1/2}s$, where κ is a proportionality coefficient equal to 1.37×10^{-6} N/m$^{1/2}$ for cholesterol helical ribbons [3]. Using this relation, the spring constant of this helical ribbon was calculated from its external geometry: K_{spring}=5.35 pN/µm. Under an optical microscope, we observed that the pitch angle of this helical ribbon increases from 11° to 20° before the bead detached from the helical ribbon.(Fig.3) Since the length of the helical ribbon follows $l = s\times\sin\varphi$, the elongation of helical ribbon upon detaching the bead is equal to $\Delta l = s(\sin\varphi - \sin\varphi_0)$=50 µm. Therefore, the force needed to detach the bead from helical ribbon is equal to $F = K_{spring}\,\Delta l$ = 265pN. This rupture force characterizes the interaction between the polydopamine coatings on the bead and on the helical ribbon. The polydopamine coatings interact with each other through hydrogen bonds. The magnitude of this rupture force is comparable to that of biotin-streptavidin interaction (250 pN) or the hydrogen bond between a pair of water molecules (300 pN) [6].

For this particular ribbon we have found that the pitch angle at which the detachment of the bead occurs varies from 20° up to 23°. Actually, 23° is a critical angle for cholesterol helical ribbons. We have previously demonstrated that, under sufficient pulling force, part of the ribbon starts to unravel into a straight phase in mechanical equilibrium with the helical phase having the critical pitch angle [4]. Indeed, we have observed this mechanical phase transition of helical ribbon a few times in this force measurement (Fig.4). In these cases, the

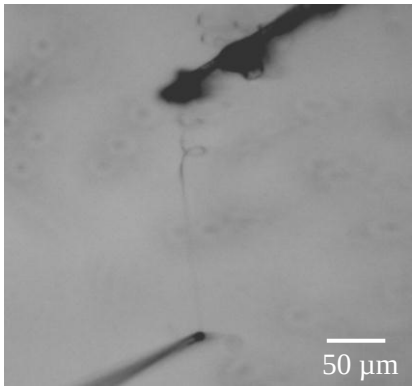

Figure 4. the cholesterol ribbon with a helical portion and a straight portion in mechanical equilibrium.

helical ribbon becomes a constant force transducer which applies constant rupture force of 351 pN. To measure the rupture force above 351pN, we can use a shorter helical ribbon with smaller radius or larger width. Therefore, the interaction between polydopamine coatings ranges from 265pN to higher than 351pN. The variation in rupture force reflects the stochastic nature of this biological interaction which depends on the shape of the contact between the ribbon and the bead.

Strains measurement using helical ribbon embedded gels.

In the present period of study, we have also investigated the application of helical ribbons as mesoscopic gauges for detecting local strains in hydrogels. We have developed a protocol to embed the helical ribbons in both polyacrylamide gel (hard gel) and collagen gel (soft gel). Using helical ribbons embedded in collagen gel (rat tail collagen from Sigma Aldrich), we have demonstrated the utility of the embedded helical ribbon for detecting highly localized strain in the gel induced by poking with a glass capillary (Fig.5). Since collagen gels are widely used in biotechnology and biomaterial science, this approach may find applications in monitoring the strain distributions in many biomechanical systems.

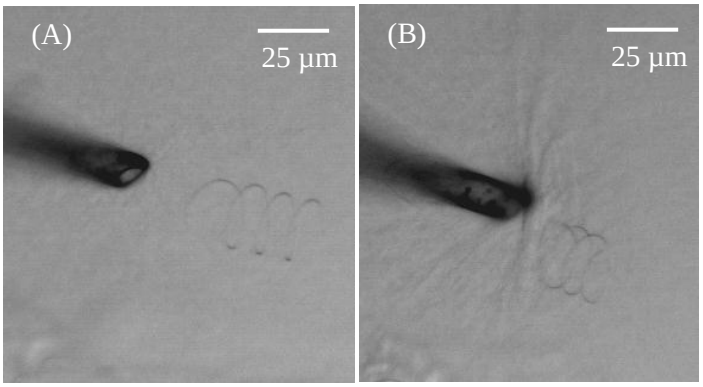

Figure 5. Local deformation in a helical ribbon embedded into collagen gel. (A) No local strain in the vicinity of the helical ribbon. (B), compression in the vicinity of the helical ribbon mechanically induced by a capillary.

Future plans:

The progresses summarized above demonstrate the utility of sterol helical ribbons as mesoscopic springs and rulers. We are currently setting up experiments to apply this device in two systems to measure the forces between: (1) the streptavidin-coated beads and the biotinylated helical ribbons; (2) the protein A-coated beads and the IgG antibody coated helical ribbons.

References:

[1] Zastavker YV, Asherie N, Lomakin A, Pande J, Donovan JM, Schnur JM, Benedek GB. Self-assembly of helical ribbons. P Natl Acad Sci USA. 1999;96(14):7883-7.
[2] Khaykovich, B., Hossain, C., McManus, J. J., Lomakin, A., Moncton, D. E., and Benedek, G. B., "Structure of cholesterol helical ribbons and self-assembling biological springs" Proc. Natl. Acad. Sci. USA (2007), 104, 9656-9660.
[3] Khaykovich B, Kozlova N, Choi W, Lomakin A, Hossain C, Sung Y, Dasari RR, Feld MS, Benedek GB. Thickness-radius relationship and spring constants of cholesterol helical ribbons. P Natl Acad Sci USA. 2009;106(37):15663-6.
[4] Smith B, Zastavker YV, Benedek GB. Tension-induced straightening transition of self-assembled helical ribbons. Phys Rev Lett. 2001;87(27) pp. 278101-278104.
[5] Lee H, Dellatore SM, Miller WM, Messersmith PB. Mussel-inspired surface chemistry for multifunctional coatings. Science. 2007;318(5849):426-30.
[6] Herman J.C. Berendsen, "Bio-Molecular Dynamics Comes of Age," Science 271(16 February 1996):954-955.

Program Title: Rigid Biopolymer Nanocrystal Systems for Controlling Multicomponent Nanoparticle Assembly and Orientation in Thin Film Solar Cells

Principle Investigator: Jennifer N. Cha
Email: Jennifer.Cha@colorado.edu

Program Scope

The focus of the proposed research is to **direct the assembly of single or binary nanoparticles into meso- or macroscale three-dimensional crystals of any desired configuration and crystallographic orientation without using prohibitively expensive lithographic processes.** The ability to control nanoparticle organization in both 2- and 3D can revolutionize technologies for energy to generate new types of solar cells that yield maximum conversion efficiencies. For example, it has been proposed that having a nanostructured bulk hetero-interface will enable efficient charge-carrier separations, similar to organic based heterojunction cells but with potential improvements, including thermal and long-term stability, tunability of energy levels, large adsorption coefficients and carrier multiplication. However, engineering such devices requires nanoscale control and ordering in both 2- and 3-dimensions over macroscopic areas and this has yet to be achieved.

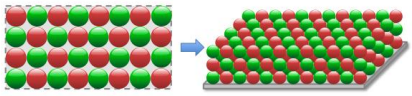

Figure 1. An ordered 2-D nanocrystal array can provide a seed layer for epitaxial growth in the z-direction.

In Nature, bulk organic and inorganic materials are arranged into precise and ordered programmed assemblies through the sequestration of raw materials into confined spaces and association through highly specific non-covalent interactions between biomolecules. Using similar strategies, the proposed research will focus on confining metal and semiconductor nanocrystals to pre-determined surface patterns and controlling their arrangement through tunable, orthogonal biomolecular binding (Fig. 1). The proposed research utilizes the ability of biomolecules to bind specific targets in a tunable, orthogonal, multivalent, and reversible manner. When conjugated to nanoparticles, these biomolecules can control particle arrangements on chemically defined surfaces. Through careful balance of the attractive and repulsive forces between the particles, the array, and the outside surface, it is envisioned that single or binary nanoparticles can be packed to adopt uniform crystal orientation in two and three dimensions from simple mixing and annealing of biomolecule-nanoparticle conjugates with biomolecule-stamped surfaces. To control the crystallographic alignment of each particle with its neighbors, the nanoparticles will be assembled using a mixture of DNA interactions. One technical challenge has been the creation of solar cells in which layers of donor and acceptor nanocrystals are not only oriented normal to the top and bottom electrodes but that every donor is surrounded by an acceptor. To create this type of structure, multicomponent nanocrystals (e.g. CdSe, CdTe) will be conjugated with biochemical linkers such that only interactions between the CdTe and CdSe will drive particle packing and assembly within the array. The use of DNA to assemble QDs on surfaces will also provide methods to fabricate QD thin films with control over thickness and roughness in just a few steps, with minimal material waster and use of completely benign processes. Furthermore, in recent years, because transient adsorption and electrical measurements have shown that electron and hole mobility is possible in double stranded DNA (dsDNA), it is possible that the DNA strands used for assembly may also provide modalities for charge transport.

Recent Progress

Scalable Assembly of 3D Excitonic Nanocrystal Assemblies by using DNA Interactions

Background

To translate the use of DNA to mediate particle packing and orientation in 3-D thin films directly from a substrate, we recently showed that highly ordered hexagonally close packed nanocrystal superlattices could be obtained on geometrically and chemically confined DNA patterns on a substrate by using DNA sequences that mediate interparticle hybridization as well as thermal annealing. This work underscored the proven ability of biomolecules, particularly DNA, to bind specific targets in a tunable, orthogonal, multivalent, and reversible manner. In follow-up work, we investigated the use substrate-adsorbed DNA for producing nanoparticle arrays that are organized in both 2- and 3D. For this, DNA sequences ("linker DNA") were designed to specifically hybridize to two different sets of DNA conjugated gold nanocrystals. By using two chemically distinct DNA conjugated gold nanoparticles and DNA linkers on the substrate that hybridize to both, 3D packing was thought to be favored because it maximizes the number of DNA hybridization events per particle, thereby resulting in nanoparticle arrays that are organized in both 2- and 3-dimensions. *All of the lessons gained with gold nanoparticles were applied in the research shown here toward assembling semiconductor nanocrystal thin films. In this work, we first report high-yielding chemical conjugation strategies to attach DNA strands directly to QDs that also retain stability up to 125mM $MgCl_2$. Furthermore, we show that these DNA conjugated QDs can be used to produce uniform thin films with controllable film thicknesses in just two steps. Finally, in order to study the effect of DNA on charge separation for solar applications, we fabricated test ITO/TiO_2/DNA-CdTe/Au devices to show that the incorporation of DNA in the QD thin films did not impede electron-hole separation and that photovoltaic effects could be observed.*

Discussion of Findings.

In this research, we have developed methods to conjugate DNA directly to semiconductor nanocrystals to produce quantum dots (QDs) with uniform coatings of DNA. These DNA-conjugated QDs are stable to oxidation and remain suspended in high ionic strength environments. Furthermore, we show that these DNA-conjugated nanocrystals can be used to produce QD thin films with control over thickness and roughness. The films were formed in only a few steps with minimal material waste and use of benign solvents, as opposed to processes such as spin coating or dip-coating which also require multiple layer-by-layer deposition steps. Using these techniques, DNA-conjugated CdTe nanocrystals were assembled onto TiO_2 films to fabricate ITO/TiO_2/DNA-CdTe/Au thin film test devices. From current-voltage measurements, these DNA conjugated QD devices showed photovoltaic characteristics comparable to those obtained with ligand-exchanged semiconducting nanocrystal films and close-packed arrays showed significantly improved performance over disordered arrays. Charge separation at the DNA-QD interface has never been shown before and these studies demonstrate the potential of using a single ligand such as DNA to minimize processing steps, organize nanocrystals in thin film devices, drive carriers under illumination to mediate charge separation, and engineer functional solar cells.

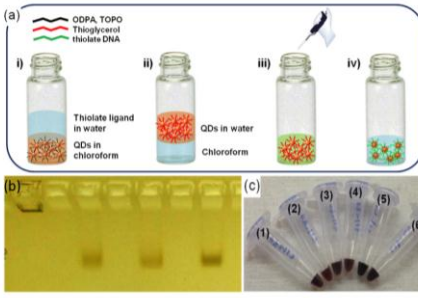

Figure 2. Methods used for DNA conjugation. (b) gel electrophoresis of DNA-conjugated QDs. (c) Optical image if DNA-conjugated CdTe Qds.

The strategy used for producing stable DNA conjugated CdTe quantum dots (DNA-CdTe) is depicted in Figure 2. First, a buffered thioglycerol (TG) solution was directly added to the as-synthesized CdTe QDs in chloroform to form a biphasic mixture. Once the TG conjugated QDs completely transferred to the aqueous phase, thiolated DNA was added at basic pH. By using an intermediate ligand exchange method, we were easily able to conjugate high yields of DNA to each QD without excessive use of DNA as well as impart stability to the DNA-QDs in buffer and salts.

UV-Vis adsorption measurements also showed that the excitonic peaks of the QDs after DNA conjugation were preserved with less than 5 nm blue shifts observed which correlated to less than 0.22nm decrease. In terms of the uniformity of DNA coating on the CdTe QDs, gel electrophoresis showed very sharp bands of the T_{10}-CdTe QDs indicating that all the nanocrystals have roughly the same coverage of DNA.

In order to produce close packed nanoparticle thin films using DNA interactions, we previously found that the use of salt such as $MgCl_2$ was needed as it helped to both screen the negative charges of DNA as well as increase the melting temperature of DNA.[37] However, while we found that the TG-DNA-CdTe QDs could be stable in Mg^{2+} concentrations as high as 125mM $MgCl_2$, because salts could have a negative influence on charge transport, we decided to use the minimum amount of Mg^{2+} needed to facilitate DNA-DNA hybridization which we determined to be 10mM $MgCl_2$. To study the use of DNA-QDs for photovoltaic devices, solar cells consisting of ITO/TiO_2/DNA-CdTe/Au were fabricated. TiO_2 films were first deposited on ITO by spin-coating commercial TiO_2 nanoparticle solutions followed by sintering. Next, equimolar solutions of 5'-SH-DNA-CdTe, 3'SH-DNA-CdTe were mixed with DNA which simultaneously hybridizes with both the 5' and 3' DNA-QDs ("linker DNA"). Next, the solutions were adsorbed to the TiO_2 surfaces followed by drying in vacuum for 5 minutes. Comparison studies with no linker DNA were run simultaneously. Immediately, the difference between using linker DNA and no linker DNA was clearly discernable by eye as the films produced with the A_n linker DNA to promote interparticle hybridization[31] produced highly uniform QD films whereas with no linker DNA, the films were visibly rough with clear differences in thickness across the entire area. After adsorption and vacuum drying, the DNA-CdTe films with or without linker DNA underwent humid annealing at 60^{o}C to further promote DNA interactions followed by vacuum annealing. Finally, a gold electrode was deposited on top of the DNA-CdTe layer.

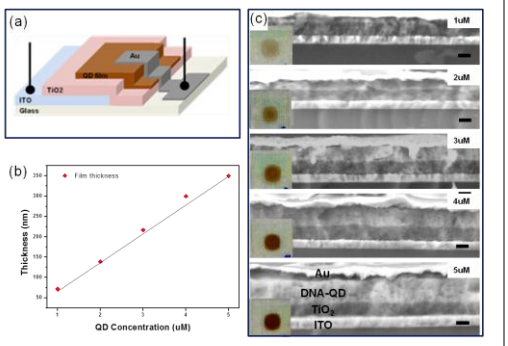

Figure 3. Schematic and film thickness measurements as DNA-QD solutions (b and c)

While typical procedures for making thin films either use multi-step spin coating which wastes valuable material or dip-coating which is highly labor intensive and not scalable, the use of DNA enabled film generation in just a couple steps and under completely benign processing conditions. Furthermore, because the method only requires adsorption of a single solution followed by drying and thermal annealing, it was very simple to produce films of variable thicknesses by tuning the initial DNA-CdTe concentrations (Figure 3). As shown in Figure 3, as we increased the QD concentrations, there was a clear gradation in color that corresponded to increases in film thicknesses. Cross-sectional SEM images of the DNA-CdTe films on TiO_2 showed not only a clear correlation between film thickness and QD concentration but that the films remained relatively smooth and that the QD-DNA layers were intact throughout the film.

Next, to study the use of DNA-QDs for photovoltaic devices, solar cells consisting of ITO/TiO_2/DNA-CdTe/Au were fabricated and tested. Based on the relative energy levels of the assembled ITO/TiO_2/DNA-CdTe/Au devices, the DNA-CdTe and TiO_2 would act as a hole and electron transport layer respectively (Figure 4). To test this, DNA-CdTe QD films composed of different sized nanocrystals were prepared and devices were tested as a function of linker DNA, QD size and film thickness. First as a measure of comparison, films made with no linker DNA showed absolutely little to no consistency in current-voltage characteristics as a function of QD size (Figure 4b). It is hypothesized that the random formation of QD organization within the no DNA linker films could only result in irreproducible and overall poor device performance. In direct contrast, devices with linker DNA showed consistent current-voltage characteristics where in all of the three sets of

devices with different QD sizes, the V_{oc} values were set around 400mV and the short circuit current (J_{sc}) showed an increase as a function of a size of the CdTe QDs (Figure 4c). Overall, the J_{sc} values measured from the films with linker DNA were comparable to a previously reported use of pyridine coated CdTe/CdSe nanocrystals where ligand exchange was run but the nanocrystals were not sintered.[43]

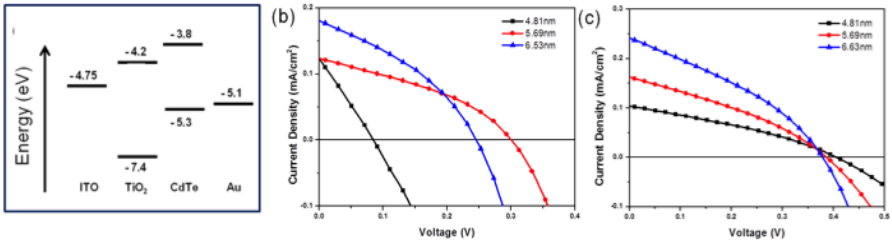

Figure 4. Energy levels andIV curves from (b) no linker DNA (b) and (c) with linker DNA.

Effective separation of electron-hole pairs is critical to achieve a photovoltaic effect. In the case of nanocrystals, the electronic coupling between particles decreases exponentially as a function of interparticle distance. For example, when the ligands on the QDs are the hydrocarbons used for their synthesis, the coupling energy diminishes an order of magnitude every ~2Å increase in interparticle distance. In previous work with small area (3-5 micron) DNA-gold nanoparticle superlattices, we determined that the interparticle distance is primarily driven by the lengths of the dsDNA used. If this is roughly maintained with these large area (over 3 x 3mm^2) DNA-QD films, the spacing (surface to surface distance) between the CdTe nanocrystals is theoretically calculated to be ~3nm. Should this be the case, the distance between neighboring CdTe QDs is potentially too long to assume easy carrier hopping from one particle to the next which lends to the possibility that the DNA itself plays a role in enabling carrier migration. Because electron mobility through double stranded DNA has been demonstrated, it is not implausible that an electron generated in a QD could move through the surrounding DNA to the next QD.

Future Studies:

Future studies on QD-DNA clusters and films will further elucidate the mobility characteristics of the carriers within the DNA strands in between the QDs. In addition, methods to generate higher order from the DNA-QD assemblies will be studied by starting with well-organized QD superlattices on DNA printed domains. Currently, while we believe the DNA-QDs in the films to be close-packed, the extremely large areas of the devices has made it challenging to create well-ordered arrays that show crystallographic orientation. Characterization of the films with grazing incidence angle XRD will be done in collaboration with the Materials Research Lab (MRL) at UCSB. In addition to film characterization and optimizing nanoparticle ordering, blended organic-inorganic devices will be studied as well as multicomponent QD films (e.g. CdSe/CdTe). Since the ability to merge DNA with conducting polymers has already been shown, the use of DNA to create ordered QD arrays as well as generate highly blended polymer-QD systems will be studied and tested.

List of publications (with DOE support: Financial support from July 2011-June 2012 only due to move from UCSD to Univ. of CO, Boulder. FY12 –present funds to arrive Aug/Sept 2013.)

1. P.F. Xu, H. Noh, J.H. Lee, D.W. Domaille, M. Nakatsuka, A.P. Goodwin*, J.N. Cha*, "The Role and Potential of DNA for Next-Generation Materials", *Materials Today, in press* (2013)

2. H. Noh, P. Nagpal, J.N. Cha*, "Scalable Assembly of 3D Excitonic Nanocrystal Assemblies by using DNA Interactions and DNA Mediated Charge Transport", *submitted* (2013)

Self-Assembly and Self-Replication of Novel Materials from Particles with Specific Recognition

Principle Investigator: P. Chaikin*, Co-PIs: N. Seeman†, M. Weck†, D. Pine*
***Dept. of Physics, †Dept. of Chemistry, New York University, New York, NY 10003**

Program Scope

The goals of our program are to understand, discover, design and control the basic interactions between nanoscopic and microscopic units so that complex self-assembly processes and architectures are enabled. We are particularly interested in specific interactions between particles which potentially allow the design of functional structures involving many different components precisely arranged. To this end we have been using DNA with its specific hybridization only between complementary sequences to make both reversible and irreversible bonds. The reversibility results from the strong temperature dependence of the hybridization so that bonds form on cooling through a designed temperature and melt on heating. One of our major accomplishments is to bind some of the hybridized pairs both selectively and permanently, using cinnamate functionalization and UV light. We take as a major challenge for demonstrating complex self-assembly the development of a process whereby a designed information-containing structure can be self-replicated and grow exponentially. This would accomplish something that has previously only been observed in living systems and in the beautiful ribozyme experiments of Lincoln and Joyce[Ref. 1]. It will also have a great impact on nanotechnology since large scale production of nanogenerators, machines, electronics, reactors, sensors etc. could be performed with exponential growth, faster (in the limit infinitely faster) than any conventional process. Moreover with exponential growth comes the possibility of evolving nanodevices with higher efficiency than they can be designed. In this work we report our first realization of exponential growth.

Recent Progress

Polygamous particles [Pub. 1] In order to perform complex self and directed assembly using colloidal particles it is necessary to have particles that specifically recognize and bind to specific partners. Each particle must have multiple functionalities. While DNA hybridization between complementary single strands provides such a specific link, it was not known to what extent one particle could address many other particles using this interaction. We studied both theoretically and experimentally the limits to which one particle could specifically address many others. For a conventionally prepared 1 micron colloidal particle as many as 20,000 DNA single strands can be attached. However as the number of different kinds of strands, “flavors”, increases, the number associated with each flavor decreases reducing the binding energy and melting temperature and increasing the association or aggregation time. Our study shows that for reasonable times and temperatures a one micron particle can specifically address ~ 40 other particles. The number of flavors is also limited to a similar number by the sequences that are available without inter-strand crosstalk.

Photolithography with Cinnamate-Bearing DNA [Pub. 5] To enable complex self-assembly as well as self replication it is useful to have both reversible and permanent links between particles. We have shown that incorporation of a Cinnamate group, substituted for complementary bases in a DNA structure, provides a highly specific bond that can subsequently be cross-linked by exposure to UV light.

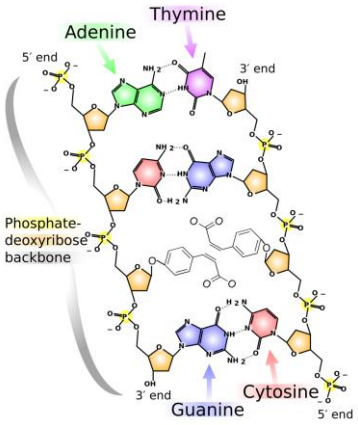

Fig. 1 Schematic of complementary complementary DNA strands with a substitute pairs of cinnamate groups. On exposure to UV light the adjacent double bonds open and form two covalent bonds between the cinnamate groups permanently linking the strands, hence linking the particles or surfaces to which the strands are attached.

We further showed that this modified DNA chemistry enables a new technology, DNA based photolithography, that is capable of patterning a surface with micron-submicron resolution with different types of DNA and anything that can be bound to DNA. Thus we can pattern a surface so that colloids and nanoparticles stick in a particular area either reversibly or permanently or we can make DNA chips, or we can functionalize a surface chemically, e.g. hydrophobic and hydrophilic regions.

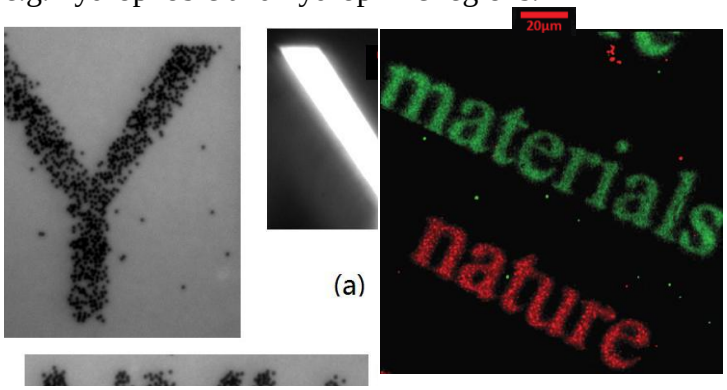

Fig. 2 Bottom left shows UV exposure pattern. Upper left are 1 micron DNA covered colloids hybridized to the patterned surface. On the right we have exposed a pattern to which we attach complementary DNA with fluorescein and another pattern to which we attached biotin and then rhodamine dyed streptavidin.

DNA patchy particles [Pub. 4] Self-assembly can also be facilitated by having particles with only one area or patch functionalized. We developed a simple way to put a DNA patch on colloidal particles by sedimenting them on a substrate. The particles as purchased have a coating of streptavidin which binds to biotin. It is also easy to prepare or purchase DNA strands with a biotin attached to their ends. We prepare a surface with complementary DNA and bind to it the biotinylated DNA with the biotin standing up from the surface. A sedimented particle which touches the

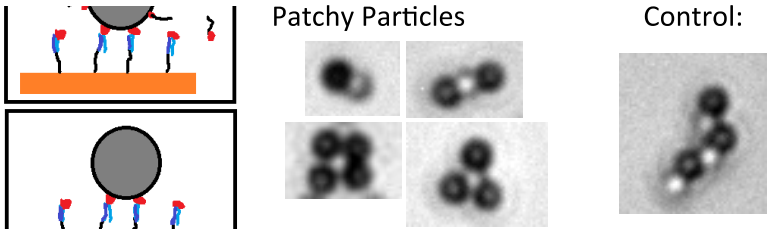

Fig. 3 Cartoon at left shows sedimented particle with attached "blue" DNA. The "black" DNA strands are inactive polyT strands. The four middle figures show dark patchy particles which only stick to one complementary particle because their functionality is only in a small patch. The control experiment has completely coated particles which bind to several other particles.

surface permanently binds the biotinylated strand on the patch where it contacts the surface. We then cover the rest of the particle surface with neutral DNA (a sequence like TTTTT..) which is inactive. On heating, the particle, along with its patch, dehybridizes from the surface and is collected. Further complexation with complementary particles demonstrates that only the patch is functional. Two or more patches may be available using two surfaces or by using magnetic particles and orienting them before sedimentation.

Self-Replication and Exponential Growth. Shortly after our initial proposal we published an article in Nature (478, 227, (2011)) reporting that we had used DNA tiles to perform the first self-replication experiments on an artificial system of arbitrarily arranged tiles. In that study we showed that seeds could be replicated to produce daughters and granddaughters. However the system was rather "clunky" in that crosslinkers had to be added for each cycle and the system had to be washed. To improve the independence of the system and its potential for exponential growth we developed the Cinnamate photocrosslinker and another UV crosslinker made from CNV. We (particularly a brilliant graduate student Xioajin He) also changed the basic tile structure from a triple duplex DNA system to a more versatile DNA origami system.

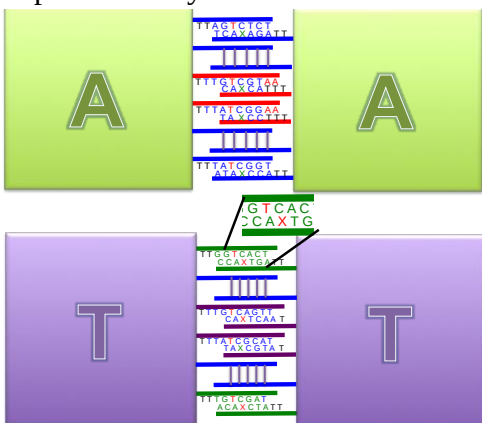

Fig. 4 Cartoon of DNA origami tiles, designed squares formed from long viral DNA and short DNA staple strands. The seeds are A-A tiles. There are DNA sticky ends on each A tile which hybridize to and align the T tiles directly on top of each A tile. Seeds are placed in a soup of separate T's and A's. Temperature is lowered and the T's assemble on the A-A seeds. UV then permanently links the red X-T in the blowup. Heating the sample allows the T-T daughters to dissociate from the A-A seeds doubling the number of offspring each generation.

This system works exceedingly well. We now load the system with a seed (pairs of origami tiles) and simply cycle temperature and light. Our first successful run showed almost perfect replication for 9 cycles - that is the number of offspring doubled each time for a total yield of ~500 for each seed. This was limited by the amount of DNA origami introduced at the start. We now grow for 4 cycles and use 1/16 of the offspring to seed the next four cycle growth. We have succeeded in exponential growth for **24 generations, an amplification of over 7 million.** We are presently using a two-origami seed and will soon shift to a four-origami seed. We then expect to force evolutionary changes by putting in variants of the DNA origami tiles and providing different environments.

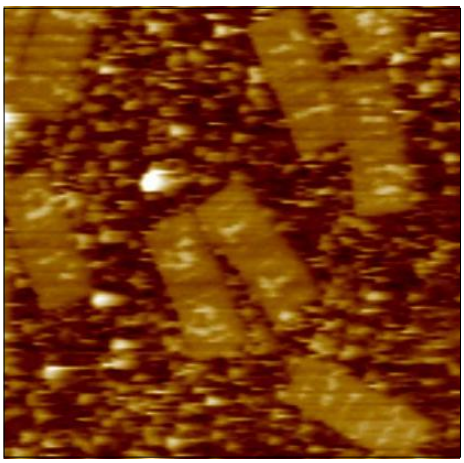

Fig. 5. AFM image of AA and TT dimers. Each origami tile labeled with T or A in DNA hairpins.

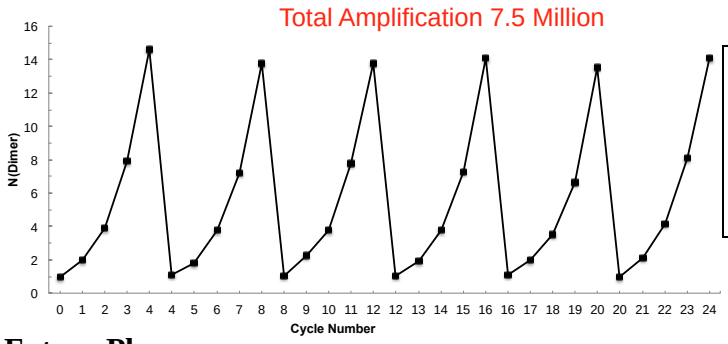

Fig. 6 Replication by transfer experiment (Xiaojin He). After four generations, a fraction of dimer offspring are transferred to fresh monomer tiles. Exponential growth over 24 generations is observed.

Future Plans

Replication of DNA Origami: We plan to continue the self replication with more complexity in number and diversity of tiles in the initial seed. We will test fidelity of the replication process and begin some elementary evolution experiments.
DNA Emulsions: DNA coated colloids stick where they attach. We would like to have particles that can rearrange after binding so that they can find their designed configurations. In collaboration with the group of Jasna Brujic at NYU we have functionalized oil emulsions with DNA and have demonstrated not only that they bind specifically, but that the effective valency of the droplets is controllable by the amount of DNA on their surfaces. When droplets come together, the mobile DNA on their surface migrates to an adhesion patch. The adhesion patch contains a certain number of DNA strands. If we coat the droplets with that amount or less we have one patch – valency one. If we have enough for two patches – valency two, etc. We can also make materials using DNA to link fluid droplets and solid particles.

References

1. Self-Sustained Replication of an RNA Enzyme, T. A. Lincoln and G. F. Joyce, Science **323**, 1229-1232, (2009).

Publications (Supported by DOE since initiation of grant, 1 year ago)

1. Polygamous Particles, Kun-Ta Wu, Lang Feng, Ruojie Sha, Rémi Dreyfus, Alexander Y. Grosberg, Nadrian C. Seeman, and Paul M. Chaikin, PNAS 109, 18371 (2012)
2. Self-Assembled DNA Crystals: The Impact on Resolution of 5′- Phosphates and the DNA Source, Ruojie Sha, Jens J. Birktoft, Nam Nguyen, Arun Richard Chandrasekaran, Jianping Zheng, Xinshuai Zhao, Chengde Mao and Nadrian C. Seeman, *Nano Lett.*, *13*, 793–797, (2013)
3. Site-specific inter-strand cross-links of DNA duplexes, Miao Ye, Johan Guillaume, Yu Liu, Ruojie Sha, Risheng Wang, Nadrian C. Seeman, and James W. Canary, Chem. Sci., **4**, 1319 (2013)
4. DNA patchy particles, Lang Feng, Remi Dreyfus, Ruojie Sha, Nadrian Seeman, Paul Chaikin, Advanced Materials, 25, 2779-2783, (2013)
5. Cinnamate-based DNA photolithography, Lang Feng, Joy Romulus, Minfeng Li, Ruojie Sha, John Royer, Kun-Ta Wu, Qin Xu, Nadrian Seeman, Marcus Weck, Paul Chaikin, Nature Materials, doi:10.1038/nmat3645 (20130
6. Kinetics of DNA-Coated Sticky Particles, Kun-Ta Wu, Lang Feng, Ruojie Sha Remi Dreyfus, Alexander Y. Grosberg, Nadrian C. Seeman, and Paul M. Chaikin (Accepted Physical Review E)

Program Title: Multicomponent Protein Cage Architectures for Photocatalytsis

Principle Investigator: Trevor Douglas; Co-PI: Bern Kohler
Mailing Address: Department of Chemistry and Biochemistry, Montana State University, Bozeman, MT 59717
tdouglas@chemistry.montana.edu

Program Scope

Virus capsids and other protein cage architectures exhibit a remarkable variety of sizes and can be produced in large quantities. Selective deposition of organic or inorganic materials, by design, at precise, symmetry-defined, locations on the protein cage affords a high degree of control over the size, spacing, and assembly of nanomaterials, resulting in uniform and reproducible nano-architectures. A simple approach is to genetically modify the protein subunits for the specific function of directing the growth of desired nanoparticles and polymers that can serve as basic building blocks for functional materials. This multidisciplinary effort was aimed towards the development of a biomimetic approach to materials synthesis that utilizes protein-based templates to couple light harvesting and catalytic sites in designer nanoparticles.

Recent Progress

The central focus of this work is the development of protein architectures for the templated synthesis of catalytic nanoparticles. These include the directed encapsulation of highly active enzymes, small molecule catalysts, and polymers that incorporate light harvesting and catalytic sites. Using this bio-inspired approach, we have utilized the capsid derived from the bacteriophage P22 to direct the encapsulation of a range of enzymes important for energy utilization together with small molecule catalysts as well as synthetic approaches for polymer bound co-catalysts in close proximity.

1) Directed co-assembly and encapsulation using the P22 protein cage. The bacteriophage P22 assembles with the assistance of a scaffold protein (SP) into a 60 nm icosahedral shell with a 50 nm central cavity, comprising 420 copies of the coat protein. Only the C terminal region of the SP (~65 residues) is necessary for capsid assembly while the N-terminus can be truncated or fused to other proteins or polypeptides, with little to no effect on capsid assembly. We have demonstrated the fusion of a wide range of proteins and polypeptides to the SP and demonstrated assembly of the P22 and encapsulation of the fusion products.

- The fusion of green fluorescent protein (GFP) and/or red fluorescent protein (mCherry) to the SP results in assembly of the P22 capsid with the GFP or RFP encapsulated on the inside in high copy number. Catenation and co-confinement of GFP and mCherry fluorescent protein co-encapsulated inside P22 results in efficient energy transfer between this donor and acceptor pair, independent of the linker length between the GFP and mCherry [1]. Un-encapsulated controls of this pair showed the expected distance dependence. These results strongly suggest that co-encapsulation(at high density) of interacting macromolecules within the P22 results in enforced communication between the active cargo molecules.
- Co-encapsulation of a glucosidase enzyme (CelB), which cleaves lactose into glucose and galactose, together with a glucokinase (GluK) and a galactokinase (GalK) has been investigated (**Fig 1**) through catenation of the three enzymes together as a fusion to the SP [2]. This coupled series of reactions represents a portion of a synthetic metabolic pathway for disaccharide utilization. This highlights the potential of this approach for directed synthesis of

designed synthetic metabolic reactions for energy applications. The materials synthesis is performed here at the level of molecular biology and these unique P22 nanoreactors self assemble in *E. coli* in highly reproducible manner.

- A similar approach using the SP fusion to direct the enzyme encapsulation has been successfully applied to the co-encapsulation of the two subunits of the *E. coli* [NiFe] hydrogenase (hyda and hydB). The resulting P22 nanoreactors self assemble in *E. coli*, package up to 200 copies of the heterodimeric enzyme in each P22 capsid, are air stable, and exhibit increased thermal tolerance (**Fig 2**). The enzyme very efficiently catalyzes the formation of H_2 (measured by gas chromatography) using reduced methyl viologen.

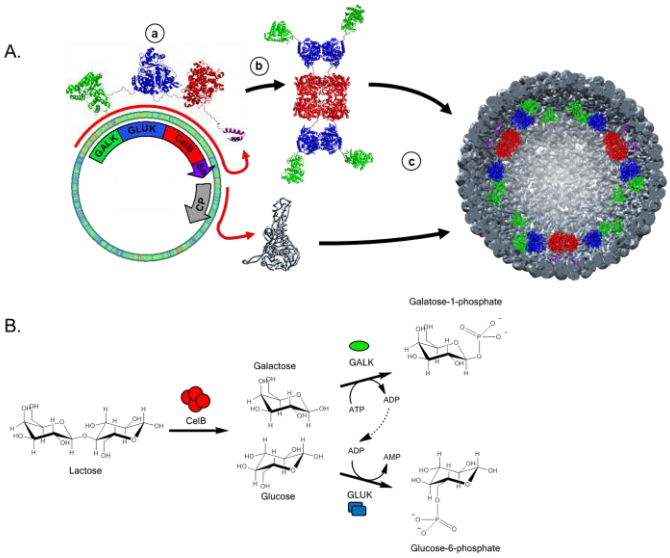

Fig 1. Three enzyme encapsulation A.a) expression of CP and the multi-enzyme fusion with SP, b) association of the multi-enzyme fusion c) capsid formation. Enzymes and domains are colored as follows: CP (Gray), SP (Purple), CelB (Red), GLUK (Blue), GALK (Green). (PDB: 2GP8, 1UA4, 1S4E, 3APG, 2XYY). B) Coupling the activities of CelB, GALK, and GLUK to create a synthetic metabolon. CelB catalyzes the hydrolysis of lactose to galactose and glucose, which are utilized by GALK and GLUK, respectively.

- By combining both enzymatic and small molecule catalysts togetherin the P22 architecture, new hybrid biological-synthetic catalytic materials have been produced incorporating the best of biological and synthetic systems. We have encapsulated the enzyme alcohol dehydrogenase (AdhD) inside the P22 capsid, by fusing the protein to the truncated SP as described above. We introduced a reactive cysteine at the C-terminal end of the encapsulated AdhD which allowed us to conjugate a small organometallic co-catalyst, $Cp^*Rh(phen)Cl^+$, in close proximity to the enzyme (**Fig 3**). The $Cp^*Rh(phen)Cl^+$ catalyst converts NAD+ to NADH using formate as a reductant, while the AdhD enzyme reduces 2-hydroxybutanone to 2,3-butandiol using NADH. The reaction kinetics of this coupled co-catalyst system can be tuned to so that NADH production and consumption are balanced.

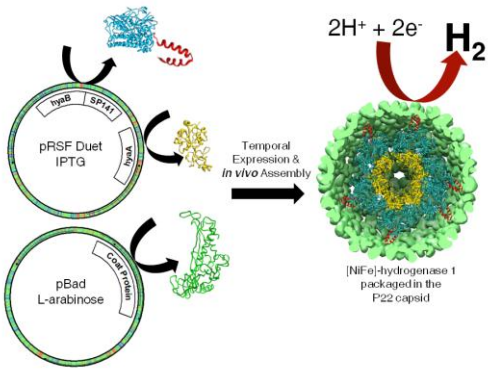

Fig. 2. Co-expression of the subunits hyaA and hyaB as SP fusion proteins, together with CP results in encapsulation of [NiFe] hydrogenase, which is active for H_2 production.

2) Templated Synthesis of Polymers within Protein Cage Architectures

We have demonstrated growth of a series of crosslinked polymers within the P22 capsid using metal coordination [3] and atom transfer radical polymerization (ATRP) [4,5], initiated in a site

selective manner on the interior protein cage surface (**Fig 4**). We can control the growth of the polymer, the degree of crosslinking and importantly the functionality of the monomeric unit.

- Modification of the interior P22 capsid with small molecule initiators can be used to synthesize functional polymers constrained within the capsid architecture. This is a promising strategy to take full advantage of the interior volume. A cysteine mutant S39C was used to anchor the initiator for atom transfer radical polymerization (ATRP) and this approach has been used to incorporate monomers of $Ru(phen)_3^{2+}$ in which each phen carries a acrylamide functionality and is thus can act as a crosslinking agent between polymer strands. The incorporated $Ru(phen)_3^{2+}$-AEMA polymer is photoactive and, under visible illumination, the P22-AEMA-Ruphen composite efficiently catalyzes the reduction of methyl viologen using ethanol as a sacrificial reductant.
  Incorporation of $Co(dmg)_2(py)Cl$ into the AEMA polymer was achieved using a isothiocyanite modified pyridine and reaction of the of the AEMA amines. Coincorporation of the photocatalyst and the proton reduction catalyst results in efficient formation of H_2 and NADH (from NAD+).

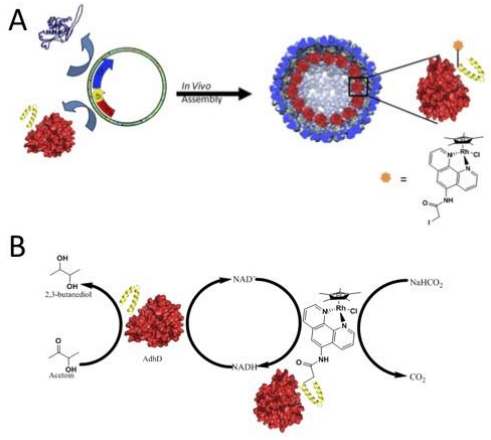

Fig. 3. A. Self-assembly of the P22-AdhD nanoreactor and attachment of the Cp*Rh(phen)Cl. B. The reaction catalyzed by AdhD oxidizes NADH and converts acetoin into 2,3-butandiol. The reaction catalyzed by the CP*Rh reduces NAD+ using formate as the

3) Modification of the Exterior Surface of P22 Protein Cages and Hierachical Assembly

We have demonstrated the controlled assembly of protein cages using modifications to the capsid exterior. The C-terminus of the CP extends to the exterior of the assembled capsid and can be readily modified. Individual P22 capsids fused with coiled-coil peptides (either E-coil or K-coil) assemble to form higher order structures only when the complementary capsids are mixed together. Structural analysis of these hierarchically assembled materials is underway in collaboration with Dr. Masafumi Fukuto and Dr. Lin Yang at Brookhaven National Laboratory by small angle X-ray scattering. Data collection on the assembled structures using the SAXS facility at beamline X9 at NSLS indicates close-packing of the P22 but no significant long-range order in the assembly.

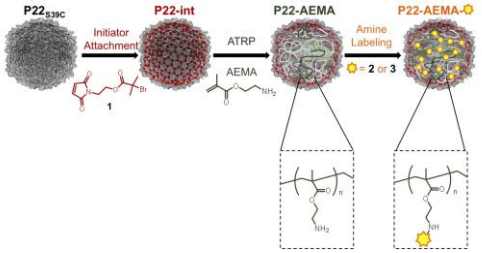

Fig 4. Assembly of the internal polymer P22 VLP. $P22_{S39C}$ modified with a cysteine reactive ATRP initiator (**1**) is used as macroinitiator and a size constrained reaction vessel for ATRP growth of poly(AEMA) strands inside the virus like particle. This introduced polymer scaffold can subsequently modified with primary amine reactive agents.

Future Plans:

- Encapsulation of enzymes that constitute fragments of a metabolic pathway for the production of butanol are underway. We are packaging 2 adjacent enzymes in the pathway in each P22 capsid using the very robust methodology previously developed and using the coiled-coil interactions between

capsids to assemble materials capable of catalyzing the formation of high-energy fuel from readily available feed-stocks.

- We are coupling the packaged Hyd-1 inside the P22 capsid with small molecule photocatalysts to drive the production of H_2 from simple sacrificial reductants and light.
- The coupled photosensitisor/proton reduction catalyst systems are being studied by femtosecond transient absorption and emission spectroscopy in the Kohler Lab, which has expertise in the ultrafast photophysics of photoactive species. When paired with transient absorption signals, emission lifetime measurements provide unambiguous assignment of rates of forward and back electron transfer between catalyst and photosensitizer.

References (which acknowledge DOE support)

1) Alison O'Neil, Peter E. Prevelige, Gautam Basu, Trevor Douglas, "Co-Confinement of Fluorescent Proteins: Spatially Enforced Interactions of GFP and mCherry Encapsulated Within the P22 Capsid" *Biomacomolecules* (2012) 13, 3902-3907.
2) Dustin P. Patterson, Benjamin Schwarz, Ryan S. Waters, Tomas Gedeon, Trevor Douglas "Advanced Biomimetic Nanocatalysts: Encapsulation of an Enzyme Cascade within the Bacteriophage P22 Virus-Like Particle" *Angewandte Chemie (2013) submitted – in review.*
3) Masaki Uchida, David S. Morris, Sebyung Kang, Craig C. Jolley, Janice Lucon, Lars O. Liepold, Ben LaFrance, Peter, E. Prevelige, Jr. and Trevor Douglas, "Site directed coordination chemistry with P22 virus-like particles", *Langmuir* (2012) 28, 1998-2006.
4) Janice Lucon, Shefah Qazi, Masaki Uchida, Greg Bledwell, Ben LaFrance, Peter Prevelige, and Trevor Douglas "Use of the interior cavity of the P22 capsid for site-specific initiation of atom-transfer radical polymerization with high-density cargo loading" *Nature Chemistry* (2012) 4, 781-788.
5) Janice Lucon, Ethan Edwards, Shefah Qasi, Masaki Uchida, Trevor Douglas "Atom Transfer Radical Polymerization on The Interior of the P22 Capsid and Incorporation of Photocatalytic Monomer Crosslinks" *Eur. Polymer Journal* (2013) *DOI:* 10.1016/j.eurpolymj.2013.06.010
6) Oleg A. Zadvornyy, Janice E. Lucon, Robin Gerlach, Nikolay A. Zorin, Trevor Douglas, Timothy E. Elgren, and John W. Peters "Photoinduced H_2 production by stable [Ni-Fe]-hydrogenases from *T. roseopersicina* covalently linked to a Ru(II) photosensitizer" *Journal of Inorganic Biochemistry* (2012) 106, 151-155.

Program Title: Modular Designed Proteins Constructions for Solar Generated H2 from Water

Principle Investigator: P. Leslie Dutton

Mailing Address: Department of Biochemistry and Biophysics, Johnson Research Foundation, University of Pennsylvania, Philadelphia, PA 19104

E-mail: Dutton@mail.med.upenn.edu

Program Scope

Development of efficient manmade constructs for promoting efficient solar light capture, primary charge separation, long-range electron-transfer relays to terminal sites for multi-electron oxidative and reductive catalysis will be important to fulfill human energy needs. In this program we focus on design and engineering of protein maquettes capable of. Our strategy is to design and construct novel proteins that can support light activation and catalysis by integrating two sets of design principles. The first is the assembly of a stable and adaptable elementary protein framework drawn from first-principle studies on the folding of repeating amino acid heptads of 4-α-helical bundles. The second is to secure cofactors within this framework according to the 5 to 25 Å scale functional electron-transfer engineering of natural oxidoreductases, without resorting to atomic level mimicry.

Recent progress

Work to date on homotetrameric and homodimeric-α-helical protein designs to support oxidoreductase functions has yielded a set of proof-of-principle demonstrations of cofactor assembly strategies and functions representative of the key sub-classes of the oxidoreductase family. This includes light- and redox-active cofactors supporting oxidation-reduction, proton coupling, ligand exchange including the generation of a stable oxyferrous heme state familiar in oxygen transport by globins. However, the at least two-fold symmetry and sequence duplication of earlier homotetrameric and homodimeric structures hinders diverse, multiple cofactor assembly. The symmetry problem was solved with the support of DOE funding by threading symmetric structures into a single-chain 4-α-helical protein. In depth analysis of this monomeric 4-α-helical protein reveals several independent domains for functional engineering that targets diverse natural activities, including dioxygen binding and superoxide/peroxide generation, interprotein electron-transfer to natural cytochrome *c*, and light-activated intraprotein energy-transfer and charge-separation approximating the core reactions of photosynthesis, cryptochrome and photolyase.

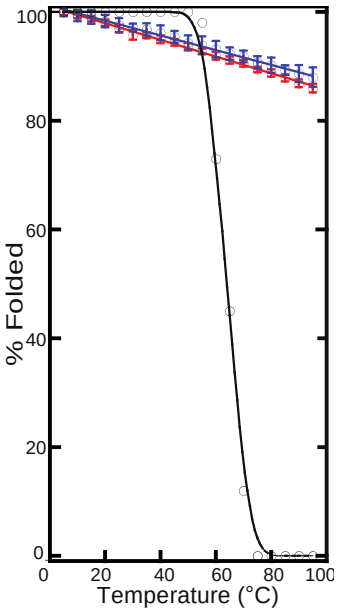

Figure 1: Single chain heme binding maquettes withstand temperatures of 60C or higher without unfolding.

Thermal stability: We demonstrated that an artificial protein can achieve hyperthermal stability while maintaining dynamic adaptability necessary for cofactor binding and function, presumably because the minimalist structural and sequential design avoids overly complex interlocking and interhelical interactions in the bundle interior. This four-helix-bundle heme-binding protein maintains its secondary structure is both the apo and holo forms past 95°C (Figure 1), maintains heme ligation for days, stably binds oxygen, and is highly expressible in *E. coli*. This protein has the potential to support variety of applications both *in vitro* (photo-activatable charge separation, electron transport) and, in view of its demonstrated ability to interface with natural proteins, *in vivo*.

Cofactor ligation kinetics: We have uncovered the physical chemistry that control the assembly rate between porphyrins and protein. Mixing a series of maquette variants with heme B at multiple temperatures allowed for a direct examination of the transition state barriers underlying this process. The protein structure can be changed to lower both the entropy of assembly (lowering the oligomeric state) and the enthalpy (molten globular apo state). The malleable interior of the maquette is capable of binding a variety of porphyrins, revealing a direct correlation between the partition coefficient (log-P values) of the porphyrin and the assembly rate. Figure 2 summarizes the process of assembly. Using a combination of Log-P values and temperature plots each kinetic barrier can be observed and manipulated.

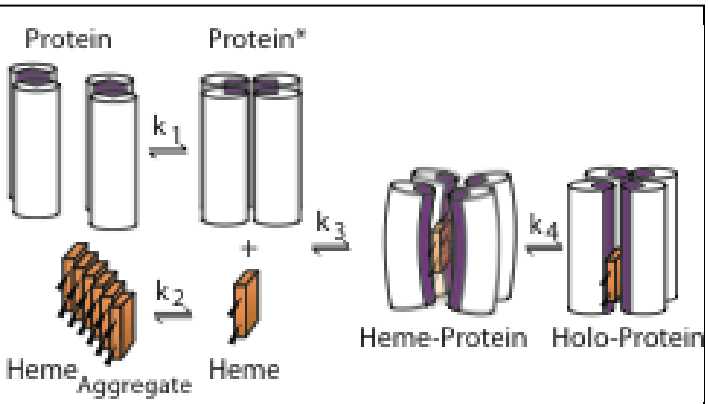

Figure 2: Kinetic scheme of cofactor assembly: site preparation (k_1), cofactor dispersion (k_2), cofactor/maquette partitioning (k_3) cofactor anchoring (k_4).

Inter-protein and intra-protein electron transfer: We exploited charge patterning to create short interprotein electron-transfer chains. Electrostatic coupling of a negative charge patterned maquette exterior to the positively charged lysine patch of the natural protein cytochrome *c* or coupling of two maquettes with complementary charges and diverse cofactors, leads to rapid interprotein electron transfer. Using the cofactor diversity enabled by the single chain design, we have shown light- activated intra-protein charge separation in several different dyad systems: heme/Zn-chlorin; heme/ Zn- porphyrin; flavin/heme; and chorin / naphthoquinone amino acid. Our theoretical analyses of cofactor number for efficient light

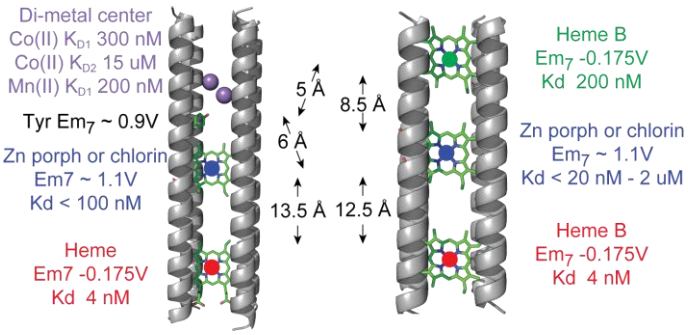

Figure 3: Light activated, multi-cofactor maquette designs with binding affinities, redox midpoint potentials and electron-transfer distances.

energy conversion to a stable redox potential free energy difference show that cofactor triad and tetrad designs are a great improvement over dyads. Figure 3 shows two designs that are partly characterized. They prove monomer maquettes can be lengthened from approximately 4 nm to 6 nm in order to include 3 or 4 cofactors at appropriate electron transfer distances.

Different ligations: Design of single chain monomer allowed us explore alternative ligations to previously established bis-his ligation to heme. We have successfully designed, expressed his-cys, single cys ligated heme containing maquettes. In natural proteins cofactor spectral and redox properties are suitably tuned towards catalysis by ligating aminoacids. Fig 4 shows dramatically different spectra of different heme ligations achieved in the monomeric maquette. The redox midpoint potential of heme B is tuned from -290 mV to -150 mV from changing bis-his ligation to cys ligation. These alternative ligations provides a basis for designing multi cofactor maquettes with site specific ligations with desired redox and spectral properties.

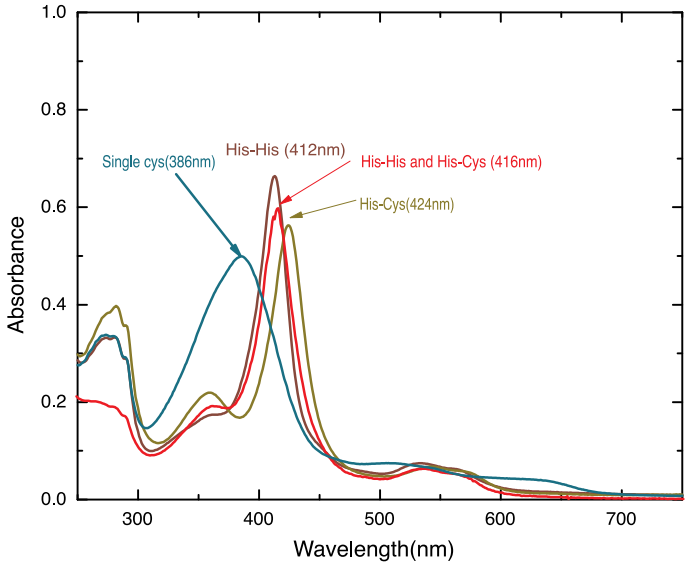

Figure 4: Control over tetrapyrrole cofactor ligation as shown by UV-Vis spectra of oxidized heme B.

Flavoproteins: Flavoproteins are a ubiquitous class of redox enzymes that participate in a host of biological processes whose diverse utility stems from the flavin cofactor's ability to accept one or two electrons and/or facilitate hydride transfer with redox potentials spanning ~600mV. These properties are modulated by specific interactions between the flavin and its protein matrix. Our results demonstrate successful coupling of two flavin analogues to four different maquette topologies with midpoint potentials from -272mV to -70mV. We have utilized maquettes to construct an enzyme capable of the oxidation of nicotinamide analogues and photochemical oxidation of tryptophan. These results not only help us understand the natural oxidoreductases but also bring us closer to realizing fully synthetic flavin enzymes for novel catalysis.

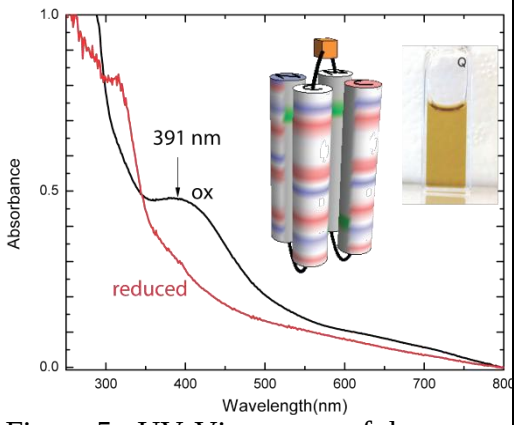

Figure 5: UV-Vis spectra of the redox states of a maquette placing a FeS cluster at one extreme--the second loop.

Low potential designs (collaboration with Golbeck): We have begun collaboration with Prof. John Golbeck at Penn State University aimed at generating low potential catalysts. We aim to couple these to H_2 production

drawing on his expertise with photosystem I (PSI) and natural hydrogenases. So far, we have expressed a ferredoxin maquette to act as a shuttle for electrons between the low potential source and the $2H+/H_2$ catalyst. We have succeeded in using this 4Fe4S cluster to transfer electrons from gold as a stand in for PSI at this stage. These tests are currently being pushed forward at PSU.

FeMoCo and Nitrogenase Activities: The effective incorporation of flavins, iron sulfur clusters, and porphyrins necessary for light harvesting and electron transfer reactions suggest that maquettes can serve as scaffolds for other cofactors and metalloclusters of importance for the construction of a peptide capable of hydrogen production. FeMoco, the catalytic metallocluster of nitrogenase, and the FeGP cofactor, the active cofactor of the iron only hydrogenase, are two cofactors that can be readily extracted from their respective enzymes and potentially bound to our maquettes through cys ligation. The design of proteins capable of incorporating these low potential cofactors *in vitro* will enable future designs that can harness the ability of the FeMoco and/or the FeGP cofactor to generate hydrogen. We have recently demonstrated that a consensus sequence inserted into the maquette is recognized by the cell's biosynthetic machinery and allowed for the covalent attachment of heme *c* into our protein designs *in vivo*. Based on this success, we will insert into our protein designs consensus sequences recognized by the iron-iron hydrogenase biosynthetic machinery in hopes of using the cell to incorporate the highly active H-cluster into our maquettes *in vivo*.

Future plans: We intend to exploit the variety of combinations of diverse cofactors made possible by the single chain design to enable electron transfer between cofactors in both the high and low potential domains, using electrodes and light-activated cofactors as the source of reductants and oxidants. A principle interest is the accumulation of multiple oxidants or multiple oxidants in clusters on one or the other or both ends of the maquette designs, so that multi-electron oxidative and reductive catalysis can be initiated and optimized.

References

1. Farid, T.A., Kodali, G., Solomon, L.A., Lichtenstein, B.R., Sheehan, M., Fry, B., Bialas, C., Ennist, N., Siedlecki, J., Zhao, Z., Stetz, M., Valentine, K., Anderson, J.L.R., Discher, B., Wand, A. J., Moser, C. C. and Dutton, P.L. "Open-ended design of a four α-helical protein for diverse oxidoreductase functions". Accepted for review **Nature Chemical Biology**, 03/14/13.

Manuscript in preparation:

2. Sheehan, M.M. Moser C.C and Dutton, P.L. "A novel, highly stable protein platform for the design of functional proteins". **Journal of the American Chemical Society**.
3. Solomon, L.A., Kodali, G., Moser, C.C., and Dutton, P.L. "Engineering Proteins for Self-assembly with Cofactors. **Journal of the American Chemical Society**.
4. Solomon, L.A., Fry B.A., Kodali, G., Moser, C.C., and Dutton, P.L. "Electron transfer reactions in a series of designed 4-å-helix bundle proteins" **J. Phys. Chem. Letters**
5. Fry B.A., Solomon L.A., Discher B.M., Moser C.C., and Dutton P.L. **"**Rapid electron transfer between a maquette protein and the natural protein cytochrome-c" **Biochemistry**
6. Kodali G., Solomon L.A., Siedlecki, J., Nakamaru-Ogiso E., Moser, C. C., and Dutton, P.L. "Design and characterization of hemoprotein maquettes with diverse ligations" **Journal of the American Chemical Society**.

Project Title
Experimental Realization of 'Repair-and-Go' Using Microencapsulation of Nanomaterials

Principle Investigator: Todd Emrick
Mailing address: Department of Polymer Science and Engineering
University of Massachusetts Amherst, MA 01003
E-mail: tsemrick@mail.pse.umass.edu

Program scope. The objective of this project is to validate and implement the concept of localized delivery of objects, materials, and/or reagents to damaged regions of substrates by a mechanism termed '*repair-and-go'.* Repair-and-go is a bio-inspired encapsulation/delivery technique, mimicking the action of leukocytes in the body, that was previously confined to a theoretical challenge and that we are working to realize experimentally.[1,2] Our experimental efforts seek innovative experimental utilization and characterization of the fundamental repair-and-go concept, and evolution of the concept to new experimental realizations, including: 1) optimizing experimental conditions of *repair-and-go*; 2) characterizing the repair of damaged substrates following deposition of nanoparticles, sub-micron particles, and/or monomers, pre-polymers, or polymers; 3) preparing novel polymers for microencapsulation and sensing of surface particulates or contaminants; and 4) using polymer capsules both for repair by nanoparticle deposition, and for picking up nanoparticles, and potentially for transporting nanoparticles along the substrate from point A to point B in a 'pickup and drop off' mechanism of action.

Recent Progress. Our initial implementation of repair-and-go involved the transport of hydrophobic quantum dots over a damaged substrate, where the quantum dots are held within polymer-stabilized oil-in-water emulsion droplets (capsules). The damaged substrate was ultraviolet ozone (UVO)-treated poly(dimethylsiloxane) (PDMS), which affords a hydrophilic and, after stretching or swelling, produces the damaged regions (cracks) that expose hydrophobic (unoxidized) PDMS. This differential wetting character enables deposition of hydrophobic nanoparticles (*i.e.*, alkyl-functionalized CdSe quantum dots) specifically into the cracked regions, rather than across the entirety of the substrate, thus conserving the filler material into well-defined regions. In the initial stage of this project, we have optimized the *repair-and-go* process over our initial published findings by 1) increasing the number of flow cycles (from 1 to 3 cycles, each cycle representing 50 passes of the capsules over the substrate) and 2) increasing the intermittent rest time (from 5 to 15 seconds) of the capsules over the substrate. Tuning these parameters significantly improved nanoparticle deposition into the hydrophobic cracks. **Figure 1** shows representative fluorescence microscopy images that illustrate this point. The fluorescence intensity and the number of filled cracks increased with rest time and number of cycles.

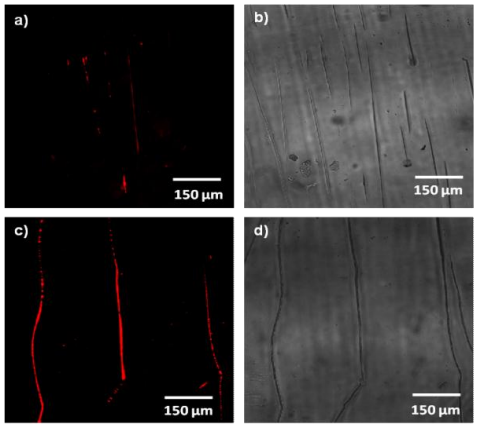

Figure 1: Fluorescence confocal microscope images of UVO-treated and cracked PDMS substrate post repair. Greater fluorescence intensity and more deposition within the cracks are seen when flow cycles and rest time are increased from 1 cycle and 5 seconds rest time (top) to 3 cycles and 15 seconds rest time (bottom).

A project objective is to expand the range of nanoparticles that can be delivered to damaged regions of substrates, both in terms of nanoparticle composition and size. Success in this area would establish a generality to repair-and-go methodology, and allow for insertion of desired NP compositions into any of a variety of damaged substrates. We began this part of the project with silica (SiO_2) NPs of a significantly larger diameter (~50 nm) than the QDs (~ 5 nm), in part because deposition of larger NPs would, in principle, contribute to a greater filling of the cracks, potentially improving the opportunity to observe mechanical repair. Silica NPs offer a versatile platform with respect to controlling particle size and surface functionality, with functional versions (amine and epoxy) allowing curing mechanisms to be introduced following NP deposition. Unlike QDs, silica nanoparticles are not fluorescent, thus to identify NP location post-deposition, FITC-doped silica nanoparticles were synthesized and used in repair-and-go experiments. These fluorescent nanoparticles were surface-functionalized (methylated) with hexamethyldisilazane (HMDS) to impart hydrophobic character and promote deposition into the hydrophobic cracks. **Figure 2** shows results of initial experiments, providing convincing evidence for successful deposition of fluorescent silica nanoparticles into the cracks. Going forward, we will characterize the interfacial activity of the NPs to gauge their relative affinity for the oil-water interface that impacts their utility in repair-and-go experiments. We are currently using additional examples of SiO_2 nanoparticles with varying surface functionality, while adjusting NP and polymer concentration to ensure efficient NP encapsulation during flow, and promote release of NPs into the cracked regions of surfaces.

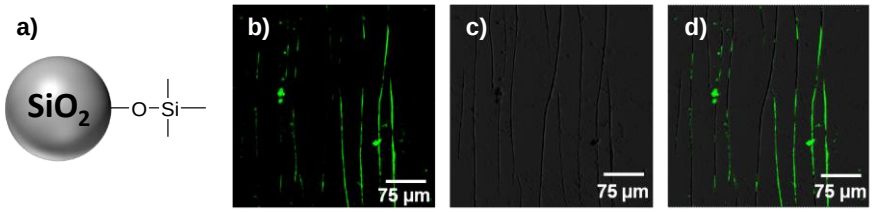

Figure 2: a) HMDS functionalized silica nanoparticles b) Fluorescent c) optical d) overlayed images of repaired substrate with FITC- doped HMDS functionalized SiO_2 NPs .

We are studying the fundamental capabilities of amphiphilic polymers as capsules, and their ability to perform a variety of functions in conjunction with nanoparticles, including recognition of nanoparticle-decorated surfaces and the removal of nanoparticles from surfaces. Balazs and coworkers recently utilized dissipative particle dynamics (DPD) simulations to model interactions between fluid-driven nanoscopic lipid vesicles and Janus nanoparticles on a hydrophilic substrate.[3] This study demonstrated the ability of Janus nanoparticles to be lifted from a substrate by vesicles, and transported along the plane of the surface. As described below, we have initiated experiments that address this topic, using emulsion droplets rather than lipid vesicles, which would provide experimental verification of the theory. While the nanoparticles we use are not Janus in nature, we show that the concept applies more generally to conventional hydrophobic and hydrophilic nanoparticles, and is sensitive, to some degree, to the chemical structure of the polymer present in the capsule wall.

Our initial experiments utilized novel amphiphilic graft copolymer capsules that combine the interfacial characteristics needed to form stable capsules with the functionality needed to detect and pickup nanoparticles. **Figure 3** (top) shows the example of a poly(cyclooctene-graft-phosphorylcholine) surfactant containing pentafluorophenyl ester (PFPE) pendent groups. This polymer was used to form capsules (oil-in-water emulsion droplets), and these capsules were seen to pick up silica nanoparticles having amines on the surface. The concept here is covalent-bond-driven-pickup, in which amide formation between the amines on the nanoparticle surface

and the pendent ester groups on the polymer lead to fixation of the nanoparticles to the capsule periphery. The experiments were conducted on UVO-treated PDMS substrates that were covered with nanoparticles by drop-casting a nanoparticle solution onto the substrate. A solution

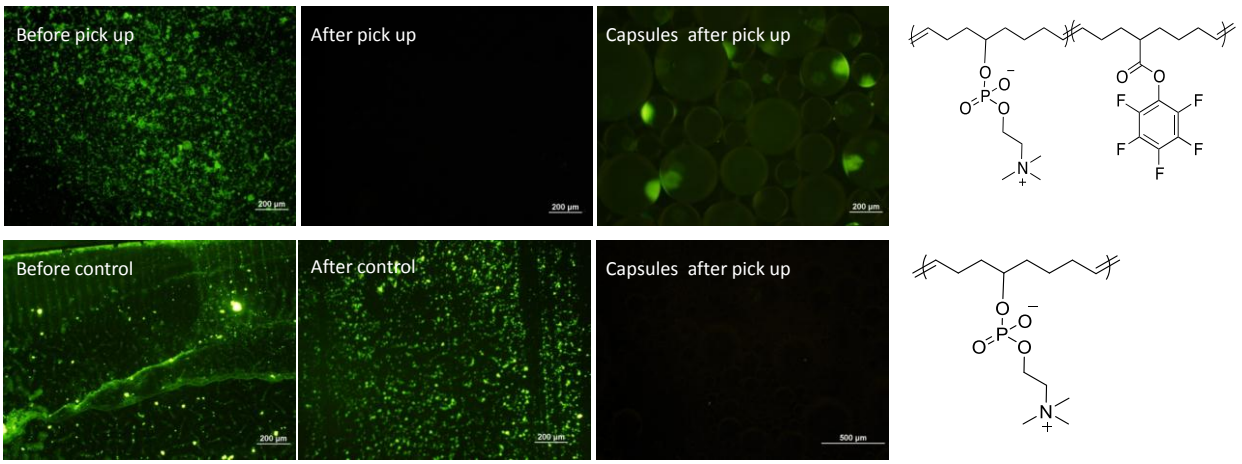

Figure 3. Substrates and capsules before and after pick-up, and the structure of polymers used for each experiment.

of polymer capsules was then passed along the substrate in pulsed intervals (5 seconds flow; 15 seconds rest). Fluorescence microscopy of the substrate and capsules before and after the experiment revealed the ability of the capsules to pickup the NPs (**Figure 3**). The fluorescence intensity from the substrate decreased substantially when capsules with PFPE functionality were used relative to control experiments with PC-COE in which much less, if any, nanoparticle pick up was seen. Additionally, microscopic characterization of the capsules after pickup shows a significant fluorescence, confirming successful pick up of nanoparticles. Moreover, increasing the extent of PFPE functionality in the copolymer used to prepare the capsules leads to greater pickup efficiency (judging qualitatively from the fluorescence spectra). We suggest that this nanoparticle pickup hinges on the formation of amide bonds between the amines on the silica nanoparticles and activated carbonyl of the PFPE groups. In a control experiment using PC-polycyclooctene as the polymer capsule (*i.e.*, having no reactive groups), little fluorescence was seen in the capsules following attempted pickup, and the substrate showed little-to-no reduction in fluorescence. We are currently exploring the effect of rest time, extent of amine functionality on the surface of silica nanoparticles, and solution pH to better understand structure-property relationships between the polymer capsule wall and objects to be removed from the surface.

The range of useful functionality on polymer capsules for performing pick up, or drop off, o nanoparticles is open question. To begin to probe this question, a system was studied involving a copolymer of PC-COE and dopamine-grafted cyclooctene. The dopamine-functionalized polymer was used with HMDS-coated silica nanoparticles. The fluorescence image in **Figure 4** suggests that these catechol-functionalized structures successfully pickup the NPs. However, in a bit of a surprise, control experiments with PC-grafted homopolymer also showed signs of nanoparticle engulfment. This result is exciting, as it suggests that hydrophobic-hydrophobic interactions between nanoparticles on a substrate and the encapsulted polymer solution might be sufficient to enable engulfment of nanoparticles into the emulsion droplet oil phase even, in this case, without the benefit of (or need for) tailored functionality.

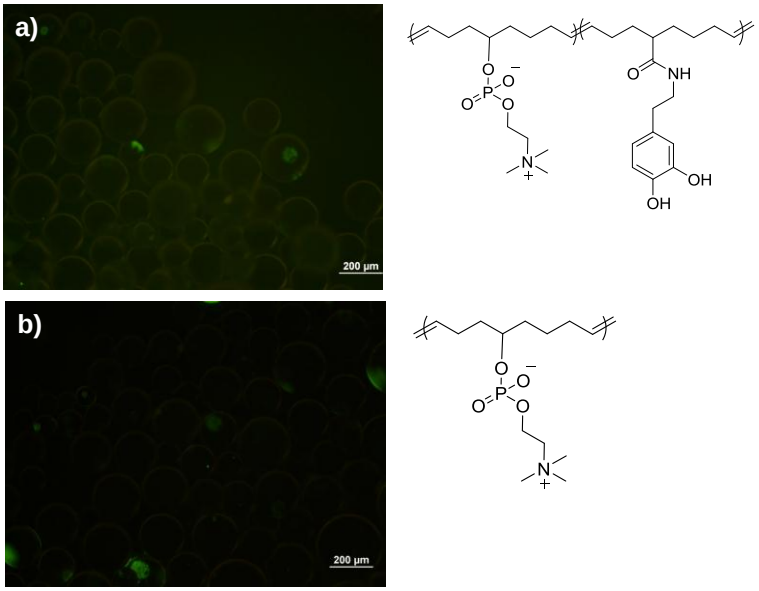

Figure 4. Capsules after pickup experiments with a) dopamine functionalized polymer and b) PC-polyolefin homopolymer.

Future Plans. We have not yet achieved complete filling of the cracks, and will continue to work towards determining the extent of crack filling by AFM and profilometry measurements. To determine the extent of mechanical repair on nanoparticle-filled substrates, microindentation experiments will be conducted. We are particularly enthusiastic about the prospect of studying nanoparticle pick up using various functional capsules, nanoparticle compositions, and tailored wetting and chemical interactions associated with the process.

References which acknowledge DOE support (none as of yet).

Other references

1. Verberg, R.; Dale, A.T.; Kumar, P.; Alexeev, A.; Balazs, A.C. 'Healing substrates with mobile, particle-filled microcapsules: designing a 'repair and go' system', Journal of the Royal Society Interface 2007, 4, 349-357.

2. Kratz, K., Narasimhan, A., Tangirala, R., Moon, S., Revanur, R., Kundu, S., Kim, H. S.; Crosby, A.J.; Russell, T.P.; Emrick, T.; Kolmakov, G.; Balazs, A.C. 'Probing and repairing damaged surfaces with nanoparticle-containing microcapsules', *Nature Nanotechnology*, 2012, *7*, 87–90.

3. Salib, I., Yong, X., Crabb, E. J., Moellers, N. M., McFarlin, G. T., Kuksenok, O., & Balazs, A. C. 'Harnessing Fluid-Driven Vesicles to Pick Up and Drop Off Janus Particles' *ACS Nano*, 2013, *7*, 1224-1238.

Program Title: Directed assembly of hybrid nanostructures using optically resonant nanotweezers

Principle Investigator: David Erickson
Mailing Address: Sibley School of Mechanical Engineering, Cornell University, Ithaca, NY, 14853
E-mail: de54@cornell.edu

Program Scope

In this research I propose to perform a comprehensive theoretical and experimental investigation into the assembly of hybrid nanomaterials and nanostructures using nanophotonically directed optical forces. Recently [1, 2] we have demonstrated how the electromagnetic fields in nanophotonic devices are sufficiently strong that they can be used to physically manipulate biological (nucleic acids & proteins) and non-biological (nanoparticles) materials as small as a few nanometers in size. Some of the first work performed under this effort ***[DOE Ref #1]*** beat our previous record for size manipulation published in Nature [1].

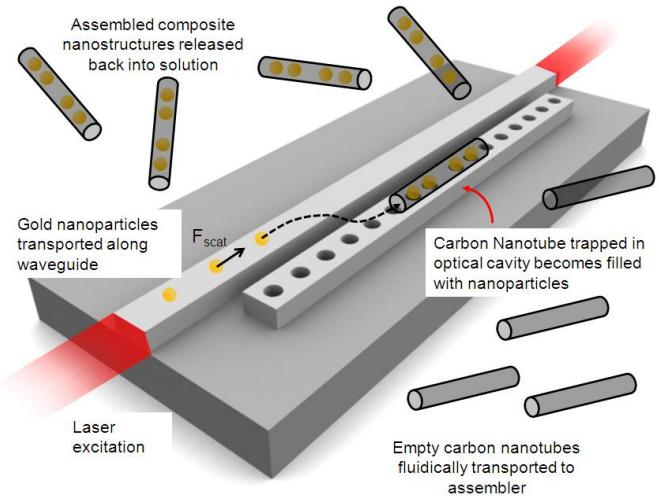

Figure 1: Envisioned Optically Driven Nano-Factories. The ultimate goal of this proposal is to demonstrate the assembly of hybrid nanostructures. Image shows envisioned technique for assembling gold nanoparticles inside a carbon nanotube in an optically resonant trap.

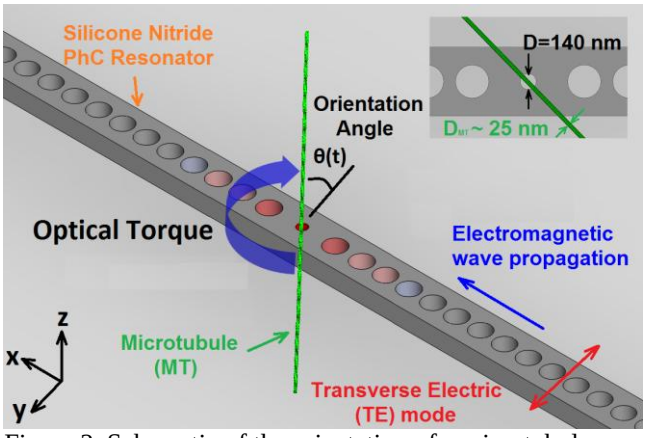

Figure 2. Schematic of the orientation of a microtubule on a photonic crystal resonator.

The overarching goal of this work will be to extend this technique to enable the directed assembly of hybrid nanostructures which cannot be manufactured by other means (*e.g.* self-assembly or chemical synthesis). Although we focus our work here on understanding some of the fundamental physics behind this new approach, we envision the ultimate implementation of the technique to look something like the optical nanofactory shown in Figure 1. The image shows how we would eventually use an optically resonant nanotweezer [3] to thread gold nanoparticles inside a single carbon nanotube**.** We envision that structures created with this technique could yield unique high efficiency photo-electric or photo-thermal energy conversion devices and enable more precise studies of the fundamental structure of nanomaterials.

Recent Progress

The main scientific accomplishments in the last two years have been the demonstration of angular orientation and rotational control of both biological and non-biological nanoscale rods using the photonic crystal nanotweezer technology ***[DOE Ref #2]*** and the development of a better understanding of the optothermal conditions surrounding the resonator that can prevent/enhance directed assembly ***[DOE Ref #3]***. In the first section below, we demonstrate the dynamics of the orientation of microtubuals (MTs) in the cavity of a photonic crystal resonator will be examined at different trapping laser powers and compared with an analytical model. In the second section, dynamic control over the orientation of carbon nanotubes via hydrodynamic flow is also demonstrated. Figure 2 displays a schematic view of the photonic crystal with a microtubule. The final section we provide an update regarding the company that is commercializing the technology.

Demonstration of Orientation Dynamics. Figure 3 illustrates how a single microtubule is oriented by the optical torque in the evanescent field of a silicon nitride photonic crystal resonator. The microtubule is initially oriented at 70 degrees to the field polarization. It is then moved as close as possible to the resonator using a slow flow rate (u = 1 μL/hr) from left to right. When it moves onto the resonator and starts to interact with the electric field, it is polarized by the electric field and experiences the optical torque. As a result it is aligned with the field. The time constant of the orientation, τ, was determined by measuring the orientation angle as a function of time.

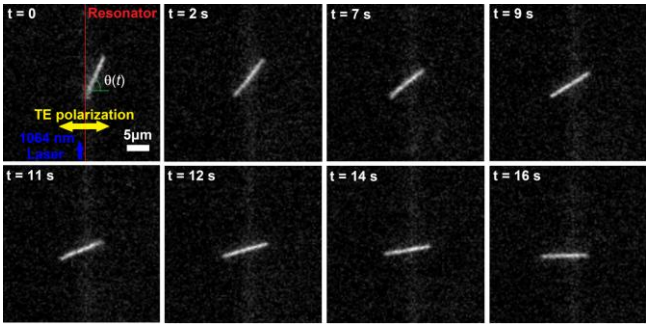

Figure 3. Sequential images of the orientation of a microtubule observed by epifluorescent microscopy using the fluorescent-labeled microtubule (bright line).

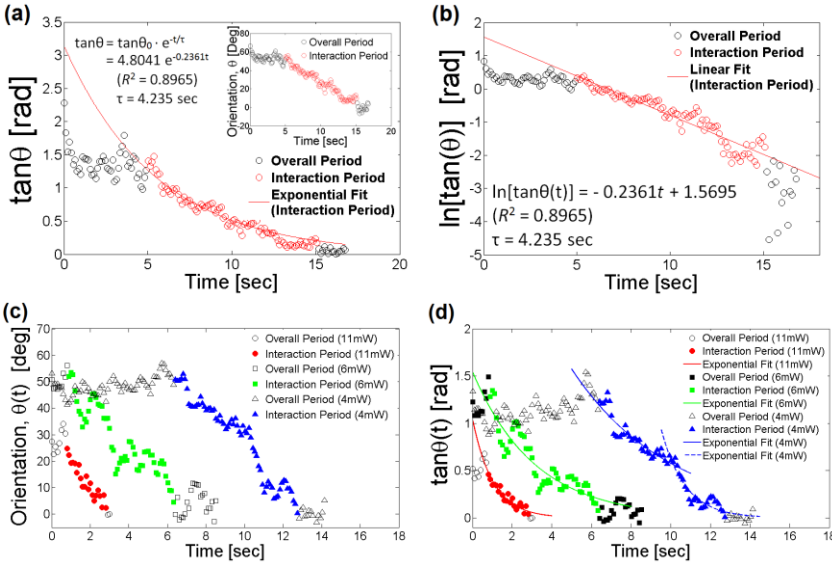

Figure 4. Quantitative analysis of the orientation of the microtubule interacting with the cavity of a photonic crystal resonator.

Figure 4(a) and (b) show the measured orientation angle with respect to time for the data set shown in Figure 2 (the estimated power coupled into the resonator is 16 mW). The quantitative orientation measurements were performed in ImageJ with the plugin OrientationJ. The plot of ln(tanθ(t)) was verified to be linear with respect to time (R^2 = 0.89). The slope of the linear fit of ln(tanθ(t)) is 1/τ where τ was determined to be 4.235 s from these experiments. The good linear fit indicates

that the orientation of the microtubule in this experiment is not the result of random thermal fluctuations but the effect of the electric field acting on it. In Figure 4, the highlighted markers correspond to the portion of the curves where the microtubule interacts with the field. Deviations of the measured curve to the fitted approximation is attributed to errors in the angle measurement, and to fluctuations in the electric field acting on the MT as it moves along the resonator and as its height fluctuates.

Figure 4 (c) and (d) display the orientation process for different input power. The time constants were determined to τ = 4.975 s (4mW), τ = 3.125 s (6mW), τ = 1.041 s (11mW). In the highlighted interaction period, the analytical model and the experimental curve are in good agreement (R^2 = 0.86 (4mW), R^2 = 0.7699 (6mW), R^2 = 0.8155 (11mW)). These data sets illustrate the power dependence of τ showing larger powers lead to smaller orientation times. However, because small variations in the initial position of the microtubule in the experiment led to large changes in the electric field it experiences, a quantitative verification of the relation could not be performed. For the lowest coupled power, 4 mW, the exponential fit was observed to break down in the middle. Two distinct interaction periods are noticeable, the earliest is labeled with a continuous line (—) and the latest with dotted line (---). The transition (— → ---) was observed during the interaction period and might be the result of the microtubule being pushed from one optical hotspot to another. The time constant in the earlier region was τ = 4.975 s (—) whereas it was τ = 1.203 sec (R^2 = 0.6111) after the transition (---) signifying that the interaction with the later hotspot was stronger.

Hydrodynamic Torque on Carbon Nanotubes to Enable Orientation. The previous experiments were performed with little to no fluid flow in the microfluidic channel. Fluid flows, however, can balance the optical torque and offer another way to dynamically control the orientation of trapped nanorods. We describe here in qualitative terms the influence of the hydrodynamic torque on their orientation. In these experiments, hydrodynamic forces affect the CNTs initially as they are propelled upwards by the radiation pressure along the resonator as seen in Figure 5(a). This radiation pressure transport along waveguides affect has been documented previously in our other works. When moving along the resonator, the hydrodynamic forces tend to orient the nanotubes along their direction of motion (90 degrees in our convention from Figure 2) until they come to the trap where they are quickly reoriented back to the orthogonal position. It is also observed that the resonator can only support two carbon nanotubes at a time.

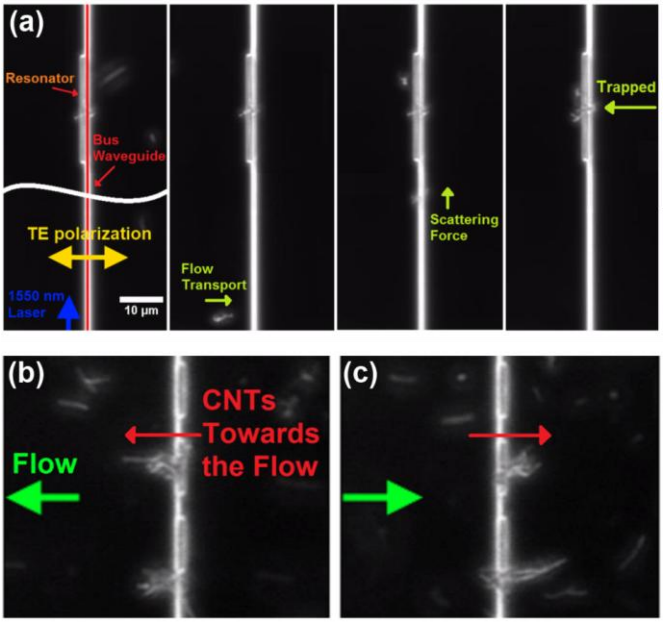

Figure 5. (a) Sequential image of trapping and orientation of a carbon nanotube observed under dark field microscopy. In the first image, a carbon nanotube is already trapped on the silicon PC resonator, another one is transported along the bus waveguide to the resonator where it remains trapped. Time lapse between the first and last frame is 10 s.

Hydrodynamic forces can also be used to actively orient the trapped carbon nanotubes. The carbon nanotubes were observed to be preferentially trapped close to their extremities. Taking advantage of the flow, which was orthogonal to the resonator, the carbon nanotubes were oriented left or right as shown in Figure 5(b). The flow was applied with a mechanical syringe pump set at 30 μL/hour. At the surface of the substrate, the flow speed is lower because of the parabolic flow profile in a microchannel. With this method the flow speed at the surface was measured to be 7.12 ± 1 μm/s. With more microfluidic ports, the orientation of the trapped nanotubes could have been chosen to cover nearly 2π spread with the microfluidic assembly line.

Update on start-up company commercializing the technology. In January 2011 we formed a start-up company called Optofluidics, Inc. whose focus is to exploit the nanotweezer technology advanced by this grant. The company currently employs ~10 people (including 4 full time Ph.D.'s) in the Philadelphia, PA area. In 2012 they attracted private investment in order to launch their first project which will be a scientific instrument based around the NanoTweezer technology (Figure 6). Further information is available at http://www.optofluidicscorp.com.

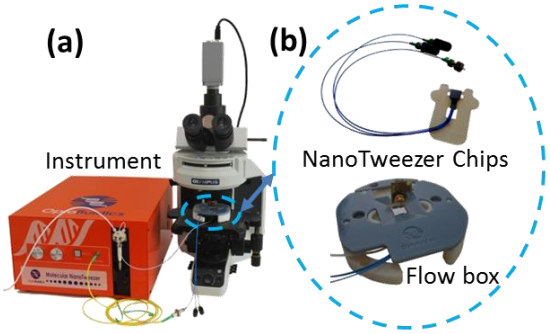

Figure 6: The Molecular NanoTweezer. (a) Configuration of Molecular NanoTweezer System (b) Inset shows Optofluidics flowbox and pre-optically coupled NanoTweezer chips

Future Plans

Over the course of the next couple of years we will focus what we refer to as "OptoMechanical Chemistry" or the use of these optical resonators to drive chemical reactions and hybrid assemblies that would otherwise not occur. We have already completed the first draft of our work in this area **[DOE Ref #4].**

References (which acknowledge DOE support 2012-2013)

DOE #1 – Chen Y.-F., Serey, X., Sarkar, R., Chen, P., Erickson, D., "Controlled photonic manipulation of proteins and other nanomaterials" Nano Letters 12 (3), 1633-1637 (2012).

DOE #2 – Serey, X., Mandal, S., Chen, Y.-F., Erickson, D., "DNA Delivery and Transport in Thermal gradients near optofluidic resonators" Physical Review Letters 108, 048102 (2012).

DOE #3 - Kang, P., Serey, X., Chen, Y.-F., Erickson, D., "Angular Orientation of Nanorods using Nanophotonic Tweezers" Nano Letters 12, 6400-6407 (2012).

DOE #4 – Serey, X., O'Dell, D., Erickson, D., "Optomechanical Chemistry" Submitted (2013)

Other References

1. Yang, A.H.J., et al., *Optical manipulation of nanoparticles and biomolecules in sub-wavelength slot waveguides.* Nature, 2009. **457**(7225): p. 71-75.
2. Yang, A.H.J., T. Lerdsuchatawanich, and D. Erickson, *Forces and Transport Velocities for a Particle in a Slot Waveguide.* Nano Letters, 2009. **9**(3): p. 1182-1188.
3. Mandal, S. and D. Erickson, *Nanoscale optofluidic sensor arrays.* Optics Express, 2008. **16**(3): p. 1623-1631.

Material Lessons from Biology: Single Crystal Synthesis and Polymorph Selection

John Spencer Evans, New York University

Program Scope

The nacre layer of the mollusk shell is a high-performance composite consisting of the calcium carbonate polymorph, aragonite, and a three-dimensional network of proteins that surround and inhabit each single crystal nacre tablet. Three protein classes (framework, intracrystalline, pearl) are associated with nacre and not only contribute to its material properties but are also responsible for it synthesis. From the BES energy-related materials viewpoint, the nacre layer offers a molecular "code" for three important processes: synthesis of high performance single crystals; mesocrystal assembly and polymorph stabilization. But to tap into this code, we need to understand what role(s) nacre proteins play in these crystal building schemes.

Recent studies now point the way to a plausible protein-based scenario for crystal building and assembly: the non-classical pre-nucleation cluster (PNC) pathway. Small PNCs form from supersaturated solutions and subsequently assemble to form larger clusters of amorphous minerals that are liquid-like in nature.[1-3] These amorphous clusters are stable up to a certain size, then become transformable into single crystals or into mesocrystal assemblies.[1-3] What is so attractive about the PNC pathway is that there are several stages, such as PNC formation, cluster assembly, and transformation, that are amenable to protein control. The question is, which stage(s) are controlled by which nacre proteins, and how is this control exerted?

Surprisingly, the answer to the latter question comes from synthetic systems known as polymer-induced liquid precursors (PILP).[4] PILPs are comprised of disordered polymers that can assemble PNCs, stabilize amorphous inorganic clusters, and permit transformation events.[4] With the recent discovery by our laboratory that some nacre proteins behave like disordered polymers,[5-8] we believe that the mollusk uses mechanisms similar to the PILP concept to create nacre biocomposites. Now, the challenge is to deduce which protein assemblies control what stages of aragonite nucleation, to determine if nacre protein assemblies are indeed "PILP-like" in character, and establish the molecular forces that drive nacre protein behavior.

Our BES program will achieve the following: (1) Establish framework, pearl, and intracrystalline nacre protein participation within the PNC pathway to aragonite; (2) Determine the structure and dynamics of defined nacre protein assemblies; (3) Evaluate the impact of defined protein ensembles on where and when inorganic nucleation precursors form. The benefits of this program to the BES mission statement will be as follows: (1) Our proposed studies will elucidate complex protein – inorganic nucleation systems and harness the potential of macromolecular control over PNCs for energy-related materials; (2) Our studies of intrinsic disorder, aggregation-prone sequences, and fluid-like protein assemblies will expand the use and design of proteins in the field of macromolecular assembly, thereby broadening the impact of our work beyond biomineralization.

Recent Progress

PFMG1, an "on-demand" nucleation protein. The formation of the nacre pearl in marine invertebrates represents an on-demand production of mineralization in response to an irritant or parasite threat to the mantle organ. In the Japanese pearl oyster (Pinctada fucata), this process is mediated by a 12-member protein family known as PFMG (Pinctada Fucata Mantle Gene). One of these proteins, PFGM1, has been implicated in modulating calcium carbonate crystal growth and has been reported to possess a EF-hand – like domain. In this report, we establish that the recombinant PFMG1 (rPFMG1) is an intrinsically disordered "imitator" EF-hand protein that increases the number of calcium carbonate mineral crystals that form relative to control scenarios and does not induce aragonite formation (Figure 1). This protein possesses a modified pseudo-EF hand sequence at the C-terminal end which exhibits low homology (30-40%) to the pseudo-EF hand mitochondrial SCaMCs buffering/solute transport proteins. This low sequence homology is the result of the inclusion of disorder-promoting amino acids and short amyloid-like aggregation-prone cross-beta strand sequences within the putative PFMG1 pseudo-EF hand sequence region (Figure 2). Similar to other nacre proteins, rPFMG1 oligomerizes to form amorphous, heterogeneously-sized protein oligomers and films in vitro, and this process is enhanced by Ca^{2+}, which promotes the formation of aggregation-prone extended beta strand structure within rPFMG1. From these results, we conclude that PFMG1 forms supramolecular assemblies that play an important role in amplifying the nucleation process that is crucial for coating or neutralizing the threat to the

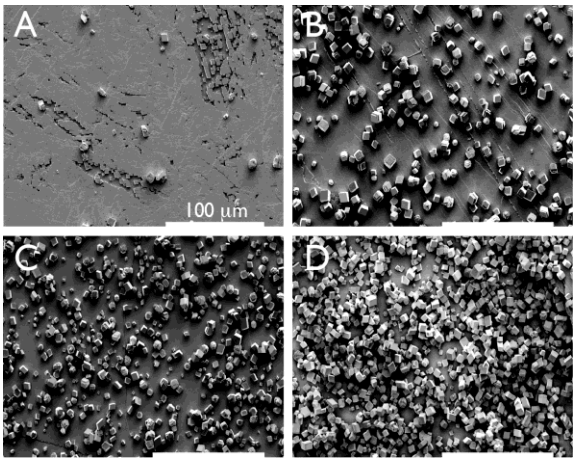

Figure 1: Scanning electron micrograph of mineral deposits captured by geologic calcite fragments in ammonium carbonate vapor diffusion mineralization assays. (A) Protein-free assay (negative control). (B,C,D) 1.8, 3.7, and 7.3 µM rPFMG1 assays, respectively. Note that as rPFMG1 concentrations increase, the number of calcite crystal increases. Scalebars = 100 microns.

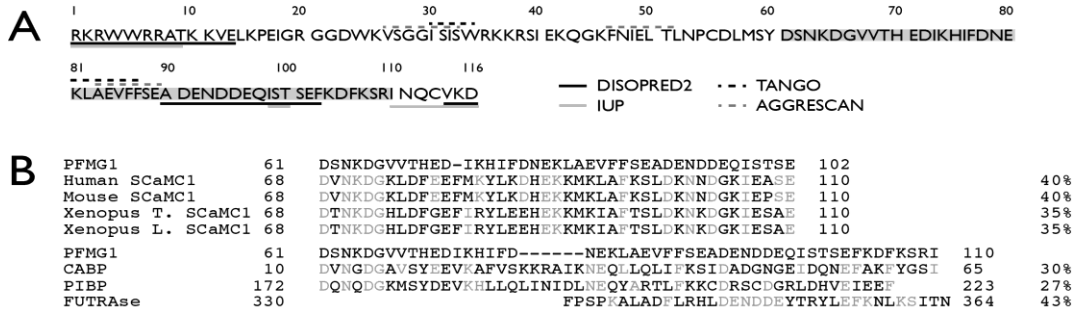

Figure 2: (A) Bioinformatics analysis of the PFMG1 primary sequence. Disordered sequence regions (solid lines) were identified using IUP_PRED and DISOPRED2 prediction algorithms, and cross-beta strand sequence regions (dashed lines) which exhibit association propensities were identified using TANGO and AGGRESCAN. The gray highlighted region represents the putative EF-hand domain. (B) BLAST sequence alignment of PFMG1 with other EF-hand protein sequences. Gray residues denote homologies with PFMG1. The SCaMC1 proteins are members of the pseudo-EF hand family.

mantle organ. This type of protein could serve as a "molecular kickstarter" to create biocomposite coatings in collaboration with other polymers or proteins.

Protein-directed crystal engineering: nacre proteins assemble nanoparticles into defined orientations. How do biological organisms engineer structurally important mineral crystals? It appears that this process initiates from an amorphous precursor which then transforms into a crystalline solid. Although the comprehensive mechanism for amorphous-to-crystalline transformation is not known, it has been proposed that proteins play important roles in the formation of crystalline solids from an amorphous phase.[1-8] As an example, AP7 and n16.3 are proteins found in the nacre (aragonite polymorph) layer of different mollusks and both proteins can participate in aragonite formation (i.e., polymorph selection) in vitro.[5-8] However, recent studies in our lab suggest that both proteins possess another unique function: *mineral assembly*.

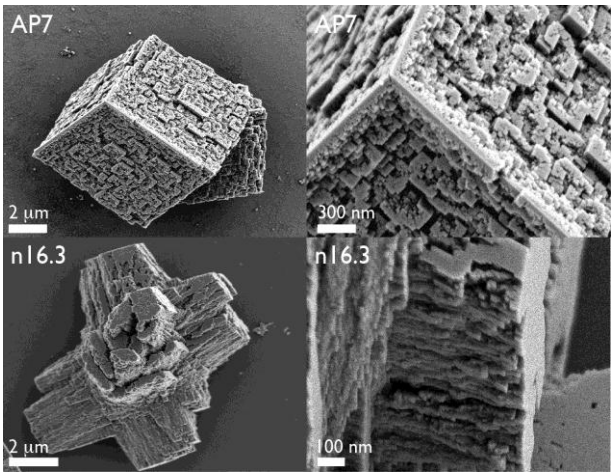

Figure 3: SEM images of in vitro AP7 and n16.3 mesocrystal Calcite assemblies, with accompanying high magnification images.

Using the *in vitro* ammonium carbonate diffusion method, AP7 and n16.3 supramolecular assemblies induce the formation of aragonite at low efficiencies (< 10%) over many hours. However, under different assay conditions ("burst" mineralization), we observe the formation of highly complex mesocrystal *calcite* assemblies at higher efficiencies (30-50%) *within 1 minute* (Figure 3). And, for each protein the resultant mesocrystal assemblies are distinctly different in architecture and symmetry. Two conclusions can be drawn. First, environmental "tuning" has a greater effect on the polymorph selection process than proteins do. Second, irregardless of environmental conditions, nacre proteins such as AP7 and n16.3 retain a core functionality that we term directed crystal assembly. We believe that this core functionality and its application will have a tremendous impact on the development of energy-related materials, particularly with regard to single crystal formation and mesocrystal assemblies at the nanoscale.

Future Plans

Our recent successes in detecting mesocrystal formation in the lab are now propelling our research into a new direction away from polymorph selection and stabilization. We are now in the process of exploring how proteins assemble nanoparticles in solution (e.g., PNCs, amorphous clusters) and how this process can be manipulated. Further, we are testing combinations of nacre layer proteins within *in vitro* assays to determine if any particular protein combinations yield results that significantly depart from those obtained for the individual proteins. For example, do certain protein pairs facilitate polymorph selection or not? Do given protein combinations influence nanoparticle assembly, and if so, how? Ultimately, our goal is to develop a recipe for

matrix construction that gives rise to inorganic solids and composites with desired mechanical and chemical properties for energy-based materials research and engineering.

References

1. Gebauer, D., Volkel, A., Coelfen, H. (2008) Stable prenucleation of calcium carbonate clusters. *Science* **322**, 1819-1822.
2. Gebauer, D., Coelfen, H. (2011) Prenucleation clusters and non-classical nucleation. *Nano Today* **6**, 564-584.
3. Gebauer, D., Coelfen, H., Verch, A., Antonietti,M. (2009) The multiple roles of additives in CaCO3 crystallization: A quantitative case study. *Advanced Materials* **21**, 435 – 439.
4. Wolf, E., Leiterer, J., Pipich, V., Barrea, R., Emmerling, F., Tremel, W. (2011) Strong stabilization of amorphous calcium carbonate emulsion by ovalbumin: Gaining insight into the mechanism of 'polymer-induced liquid precursor' processes. *J. Am. Chem. Soc.* **133**, 12642-12649.
5. Evans, J.S. (2012) Identification of intrinsically disordered and aggregation - promoting sequences within the aragonite-associated nacre proteome. *Bioinformatics* **28**, 3182-3185.
6. Ponce, C.B., Evans, J.S. (2011) Polymorph crystal selection by n16, an intrinsically disordered nacre framework protein. *Crystal Growth and Design* **11**, 4690-4696.
7. Amos, F.F., Evans, J.S. (2009) AP7, a partially disordered pseudo C-RING protein, is capable of forming stabilized aragonite in vitro, *Biochemistry* **48**, 1332-1339.
8. Amos, F.F., Ndao, M., Ponce, C.B., Evans, J.S. (2011) A C-RING-like domain participates in protein self-assembly and mineral nucleation. *Biochemistry* **50**, 8880-8887.

Publications

Perovic, I., Mandal, T., and Evans, J.S. (2013) A pseudo EF-hand pearl protein self-assembles to form protein complexes that amplify the mineral nucleation process. *Biochemistry*, submitted.
Seto, J., Picker, A., Evans, J.S., Colfen, H. (2013) A nacre protein sequence organizes the mineralization space for polymorph formation. *Crystal Growth and Design*, submitted.
Chandrababu, K.B., Lokappa, S.B., Dutta, K., Ndao, M., Evans, J.S., Moradian-Oldak, J. (2013) Biophysical studies on the structural adaptation of amelogenin in the presence of SDS micelles. *Biophys. J.*, in press.
Evans, J.S. (2013) "Liquid-like" biomineralization protein assemblies: A key to the regulation of non-classical nucleation. *Crystal Engineering Communciations*, in press.
Ndao, M., Ponce, C.B., Evans, J.S. (2012) Oligomer formation, metalation, and the existence of aggregation-prone and mobile sequences within the intracrystalline protein family, Asprich. *Faraday Discussions* **159**, 449-462.
Kim, I.W, Collino, S., Evans, J.S. (2012) Cooperative modulation of mineral growth by prismatic-associated Asprich sequences and Mg(II). *Int. J. Mol. Sci.* **13**, 3949-3958.
Evans, J.S. (2012) Identification of intrinsically disordered and aggregation - promoting sequences within the aragonite-associated nacre proteome. *Bioinformatics* **28**, 3182-3185.

Program Title: Long Range van der Waals-London Dispersion Interactions for Biomolecular and Inorganic Nanoscale Assembly

Principal Investigator: R. H. French*, N. F. Steinmetz**

Mailing Address: *Materials Science & Engineering, **Biomedical Engineering, Case Western Reserve University
Cleveland Ohio, 44106,
E-mail: roger.french@case.edu

Program Scope

The goal of this joint program is to gain an understanding of the electronic structure and long-range interactions (LRI) in a variety of organic and inorganic molecules and nanoscale systems. A thorough understanding of the polar, electrostatic, and van der Waals-London dispersion (vdW-Ld) forces between realistic geometries and morphologies will guide the development of nano- and meso-scale design. Vacuum ultraviolet (VUV) spectroscopic techniques are used to determine the optical properties, and Hamaker coefficients are derived from Lifshitz theory. Optical spectra are then compared to those calculated using *ab initio* methods (UMKC). Static light scattering (SLS) is used to measure the second virial coefficient A_2, the net interaction strength between biomolecules, and A_2 is correlated to osmotic stress experiments (UMass). Systems of interest include collagen and BSA, DNA oligonucleotides, triplex DNA and quadruplex DNA; and biologically relevant inorganic materials, including SiO_2 and $AlPO_4$. Parameters are then varied in order to gauge the dependence of the LRIs on these variables: protein A_2 values are considered as a function of buffer salt type and concentration, and solution pH. UV molar absorptivity measurements for DNA show how counter-ion type, base pair composition, and stacking sequence affect fine features in the UV spectrum. VUV spectra are analyzed for insights into the electronic structure and interband optical properties of the materials, which govern the vdW-Ld forces within these systems. These results provide a deeper understanding of the parameter space that controls LRIs in biomolecules, an important step in the control of mesoscale design and self-assembly. In order to advance this goal and more widely distribute these results, the Gecko Hamaker open-source software (http://geckoproj.sourceforge.net/) provides a platform for the distribution of London dispersion spectra and the calculation of Hamaker coefficients for layered systems.

The scope of this project necessitates a broad range of expertise in both theoretical and experimental methods, and as a result benefits greatly from our extensive collaboration with our partner institutions.

Recent Progress

1. Gecko Hamaker (CWRU, UMass) Gecko Hamaker is an open-source software platform for the calculation of fully retarded Hamaker coefficients through quantum electrodynamic Lifshitz theory (UMass), as well as the distribution of the VUV optical properties which feed into these calculations. The open-source distribution facilitates broader applicability of the work, and encourages collaboration. We have recently released Gecko Hamaker 2.0, which includes a more user-friendly interface and more options for the attachment of analytical wings at the low- and high-energy cutoffs of spectra. Work in progress includes the implementation of new configuration geometries, including spheres and anisotropic cylinders, and the creation of a web database and service for the distribution of spectra.

2. Interband Optical Properties of $AlPO_4$ (CWRU, UMKC, UMass) (paper #1) Berlinite $AlPO_4$ was studied using VUV spectrometry and ellipsometry. The complex interband optical properties were determined over a range of 0.5 to 45 eV (Figure 1), and features were indexed with respect to the underlying electronic structure. The vdW-Ld spectrum was determined for $AlPO_4$, and Hamaker coefficients were calculated for systems involving $AlPO_4$. The electronic structure and interband optical properties are comparable to those of both quartz and amorphous SiO_2, suggesting that the PO_4 tetrahedra--similar in structure to SiO_2 tetrahedra--are responsible for the electronic structure and interband optical properties. The results were consistent with previous *ab initio* calculations by Ching

(UMKC), work which was also funded by the Department of Energy. The dominance of PO_4 on the interband optical properties and vdW-Ld behavior of $AlPO_4$ indicate that the phosphate complex ion may play a central role in the electronic structure and intermolecular interactions of phosphate-containing materials ubiquitous in biological systems, including apatites, DNA, and phospholipids.

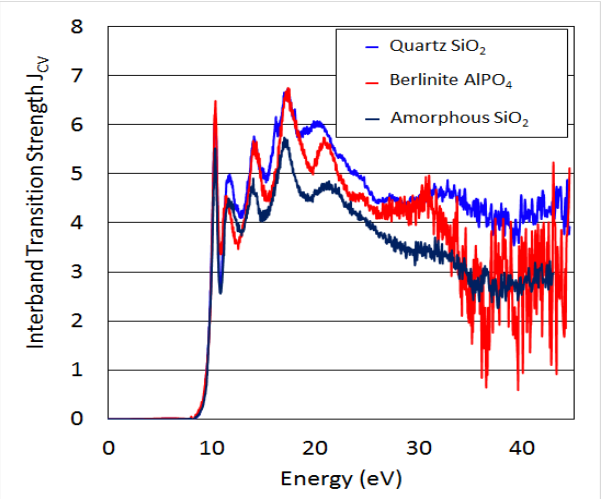

Figure 1 Re(J_{cv}) for berlinite $AlPO_4$, quartz SiO_2, and amorphous SiO_2

3. Role of Single Interatomic Bond Transitions in Long Range Interactions and Excitons in SiO_2 (UMass, CWRU, UMKC) (paper #2) The presence of narrow excitonic peaks in the optical spectra of SWCNTs motivated the study of their effect on the Hamaker coefficient for vdW-Ld interactions. UMass have formulated a theoretical approach that shows how a change in the dielectric response over a narrow frequency interval has complicated consequences on the vdW-Ld interactions. Optical properties of amorphous SiO_2 (a-SiO_2) glass were calculated (UMKC) and compared with experimentally determined spectra (CWRU), which contain an excitonic peak (See Figure 2). The effect of the excitonic peak on the vdW-Ld interactions was then studied. The results show that the effect depends crucially on the position and intensity of the peak, and that the peak position affects all the terms in the Matsubara frequency summation in a non-monotonic fashion. Contrary to the common wisdom, the presence of an additional optical peak has affects the Hamaker Coefficient across all Matsubara frequencies, not just those at energies near the optical peak.

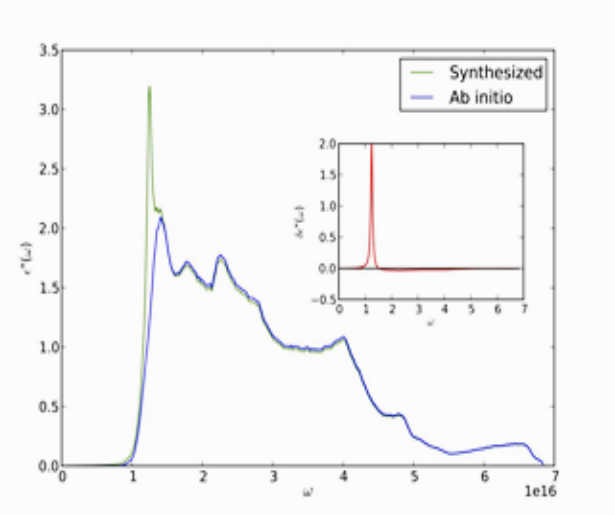

Figure 2 *Ab initio* ε" spectra for amorphous SiO2, with and without a synthesized "exciton" peak. Inset: synthesized "exciton peak" without background spectrum.

4. Molar Absorption Coefficient of DNA Oligonucleotides in the UV Range The concentration of DNA oligonucleotides in solution is commonly estimated (roughly) from UV absorbance measurements at 260 nm. Careful analysis of the UV range between 200 and 300 nm reveals a large number of fine features surrounding the broad 260 nm peak, which may provide insights into the electronic structure of the DNA oligonucleotides. We have determined the decadic molar absorptivity of a variety of DNA oligonucleotides in the UV range between 200 and 300 nm. The fine features vary for differing oligonucleotides, indicating dependence on composition, stacking sequence, purity, or other solution parameters. Work is in progress to correlate these features with DNA electronic structure, composition, stacking sequence, and solution parameters. These results will be linked to the Hamaker coefficients and A_2 values for various compositions of DNA, elucidating the link between optical properties, electronic structure, and intermolecular forces.

5. Second Virial Coefficient of BSA using Static Light Scattering (CWRU, UMass, UMKC) The dependence of the coefficient A_2 on pH for BSA has been examined using SLS. Buffer solutions were created at a range of pH values, resulting in A_2 values ranging from 2.8e-5 to 8.39e-5 mol·mL·g^{-2} (Figure 3), which are in good agreement with literature values. The positive A_2 indicates repulsive net interaction between the BSA molecules. The minimum A_2 is obtained at pH 4.6, the isoelectric point at which the molecules carry no net surface charges and vdW-Ld interaction is the dominating force.

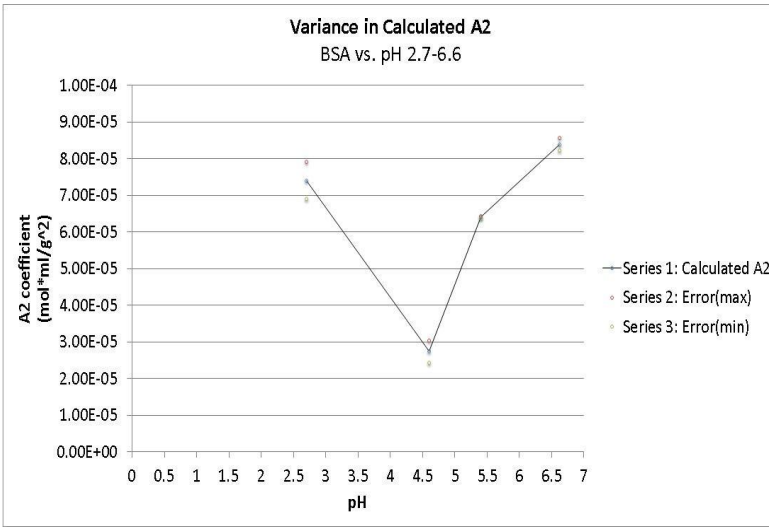

Figure 3 Dependence of A2 on buffer pH for BSA, measured by SLS

6. Long Range Interactions in Assembly of VNPs Review paper (CWRU) (paper #3) Viruses have a propensity to self-assemble into meso-scale structures and furthermore are nanocontainers that carry a cargo, their genome. From a materials science perspective, viruses are core-shell hierarchical structures that spontaneously self-assemble through LRIs. Physical virology seeks to define the principles of physics underlying viral infections, traditionally focusing on the fundamental processes governing virus assembly, maturation and disassembly. A detailed understanding of virus structure and assembly has facilitated the development and analysis of virus-based materials for medical applications as well as energy applications. Per invitation from the journal of Physical Biology, we prepared a review article, discussing how LRIs play a role in nanotechnology and its branch interfacing medical research and application. Although the article is focused on medicine, the underlying physics applies to a broad spectrum of disciplines.

Work in Progress and Future Plans

1. Bulk sample preparation and VUV spectroscopy (CWRU, UMass) In order to take VUV spectra, we are creating bulk samples via die and arbor press. We will refine our method and apply it to BSA, collagen and amino acids. These samples will be used for VUV spectrometry measurements, and their electronic structure (see figure 4 for collagen) and vdW-Ld forces will be studied. In addition, highly ordered samples of concentrated DNA have been prepared (UMass) and will be studied. The samples were prepared by the standard Rupprecht method of wet spinning, extensively described in A. Rupprecht, *Acta Chem. Scand.* **20** 494 (1966).

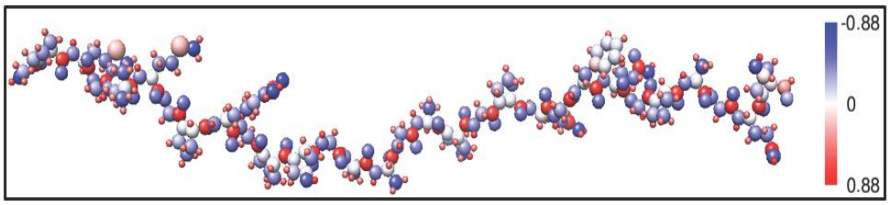

Figure 4 Surface charges for collagen from *ab initio* electronic structure calculations

2. Second virial coefficient of BSA, DNAs and virus capsids (CWRU, UMass, UMKC Previous research about BSA focused on osmotic pressure, viscosity, turbidity, but neglected the effect of pH, ionic strength or ion types of the bathing solution on A_2. Since A_2 is closely related with the LRIs between biomolecules, we will perform a systematic study on the A_2 of BSA, DNA oligonucleotides and virus

capsids at various buffer conditions. Studies are underway on the dependence of A_2 of BSA on sodium ions concentrations at constant pH 4.6.

3. Triplex DNA, Quadruplex DNA Preparations (CWRU, UMass, UMKC) Long range vdW-Ld interactions between duplex DNA *versus* triplex and quadruplex DNA molecules are fundamentally different, the latter being larger than in the duplex case. This may lead to quadruplex DNA aggregation even in monovalent salt solutions at physiological conditions, so a comprehensive study of quadruplex DNA will enhance the scientific conclusions of the overall program. Quadruplex DNA will be prepared by the following protocol: oligonucleotides of the sequence d[AG3(T2AG3)3] (d=4-12) will be obtained from IDT (Integrated DNA Technologies), oligonucleotides will be dissolved and stored in sodium or potassium phosphate buffers at pH 6.5-7.0 with and without 0.1-0.5 mM EDTA. Oligonucleotides will be denatured at 95 °C for 5 min, and then annealed by cooling down to room temperature. Triplex will be prepared and measured as a comparison of duplex and quadruplex DNA.

Postdocs, Grad Students, Undergrads

At CWRU, Ph.D. students: D. Dryden (100%) and Yingfang Ma (100 %), Undergrad students: Lijia Liu, Matt DelBrocco (Senior), Ian Kidd (Senior), Diana Acosta (Sophomore) and Jacob Schimelman (Sophomore).

Publications and Presentations

1. Daniel M. Dryden, Guolong L. Tan, Roger H. French, "Optical Properties and van der Waals-London Dispersion Interactions in Crystalline $AlPO_4$ determined by Vacuum Ultraviolet Spectroscopy", In Preparation.
2. Jaime E. Hopkins, Daniel M. Dryden, Wai-Yim Ching, Roger, H. French, V. Adrian Parsegian, and Rudolf Podgornik, "Dielectric response variation and the strength of long range van der Waals interaction", in preparation (2013)
3. Amy M. Wen, Pooja H. Rambhia, Roger H. French, Nicole F. Steinmetz, "Design rules for nanomedical engineering: from physical virology to the applications of virus-based materials in medicine", Journal of Biological Physics, 39 (2): 301-325, 2013. Published
4. R. Rajter, R. H. French, W. Ching, R. Podgornik, V. A. Parsegian, "Chirality-Dependent Properties of Carbon Nanotubes: Electronic Structure, Optical Dispersion Properties, Hamaker Coefficients and van der Waals – London dispersion interactions", RSC Advances, 3 (3), 823 (2013). Published.
5. Roger H. French, Nicole F. Steinmetz, Rudolf Podgornik, Wai-Yim Ching, V. Adrian Parsegian, "Nanoscale Assembly by Manipulation of Long Range Interactions", Sosman Award Symposium, MS&T 2012, Pittsburgh PA, Oct. 7-11, 2012.
6. Yingfang Ma, Daniel M. Dryden, Diana M. Acosta, Lijia Liu, Lin DeNoyer, Wai-Yim Ching, Nicole F. Steinmetz, Rudolf Podgornik, Roger H. French, V. Adrian Parsegian, "Optical Properties and van der Waals-London Dispersion Interactions in Inorganic and Biomolecular Assemblies", MRS 2013 Fall, Boston MA. Submitted.
7. Jaime C. Hopkins, Daniel M. Dryden, Wai-Yim Ching, Roger H. French, V. Adrian Parsegian, Rudolf Podgornik, "Dielectric Response Variation and van der Waals London Dispersion Interaction", MRS 2013 Fall, Boston MA. Submitted.

Program Title: Simulations of Self-Assembly of Nanoparticle Shape Amphiphiles

Principle Investigator: Sharon C. Glotzer
Mailing Address: Department of Chemical Engineering / BioInterfaces Institute, University of Michigan, North Campus Research Complex, 2800 Plymouth Rd, Ann Arbor, MI 48109-2800
Email: sglotzer@umich.edu

Program Scope

Self-assembly of nanoparticle building blocks including nanospheres, nanorods, nanocubes, nanoplates, nanoprisms, and nanopolyhedra hold great promise for achieving organized structures in 1D, 2D and 3D for functional and useful materials. "Patchy particles"[1,2] – nanocolloids of arbitrary shape functionalized with organic ligands, biomolecules, gold or other materials in patterns to create specific or nonspecific directional interactions – have received enormous attention as candidate building blocks in this regard. Under this grant, we first conceptualized the idea of patchy particles [1] and proposed a unifying framework [2] for designing and exploring them for self-assembly. Previously, we fleshed out details of key anisotropy dimensions (Fig. 1 (left)) and their role in assembly.[2] In doing so, we have motivated and provided interpretation for experimental instantiations by many research groups.

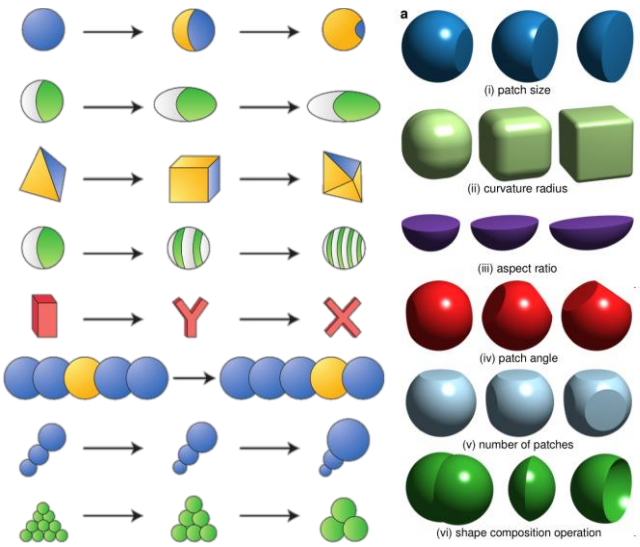

Figure 1. (Left) Anisotropy dimensions for patchy particles [1]. (Right) Anisotropy dimensions for entropically patchy particles. [5]

We have made significant progress in understanding the general principles underlying self-assembly of patchy, anisometric particles. We developed needed computational tools for the study of self-assembly of these particles and applied those tools to the design and reverse engineering of new building blocks capable of self-assembling into novel structures with desired functionalities. Research on patchy particles by the community has led to the discovery of many new unexpected nanoscale structured phases and our theoretical work has revealed over-arching design rules for patchy particles. Our simulations are providing foundational understanding of the science of assembly of these complex nanoscale systems.

Recent Progress

Science. In the past several years, we explored many aspects of the design and assembly of patchy particles. In particular, we demonstrated the importance of entropy as a stabilizing factor in many instances. Examples include (1) We investigated the role of size polydispersity in successfully assembling various anisometric nanoparticle systems, showing that small but experimentally feasible amounts of polydispersity (between 3% and 10%) and other imperfections can be tolerated by entropic assemblies as complex as gyroid and quasicrystal phases [7,8]. For micellar systems of patchy nanoparticles, we showed that polydispersity is a

necessary requisite for a dodecagonal quasicrystal (DQC) phase (Fig. 2), and provided a theoretical explanation for all previously observed entropically stabilized micellar DQCs [12 and references therein]. (2) We predicted that molecular ligands adsorbed onto the surface of facetted nanoparticles (Fig. 3) would preferentially localize on high curvature features such as corners and edges due to entropy [11]. To accomplish this, we investigated how simple approximate models can be developed and used to quickly determine the configurations into which ligands will self assemble in nanoscale systems, derived criteria that determine when these models are expected to be accurate, and proposed a generalized two-body approximation that can be used as a toy model for the self-assembly of tethers in systems of arbitrary geometry and applied this to the self-assembly of self-assembled monolayers on a planar surface. (3) We modeled the self-assembly of patchy spheres into colloidal clusters as mesoscale building blocks, and predicted their equilibrium structures in terms of spherical code solutions [9], again demonstrating the role of entropy in stabilizing certain unexpected structures. (4) Most recently, we proposed the idea of "entropically patchy particles"[4,5] in parallel with our original concept of enthalpically patchy particles [1,2], and proposed shape-based anisotropy dimensions for entropically patchy particles [5] (Fig. 1 (right)). We developed a generalized framework for describing and quantifying emergent, effective, attractive entropic "patches" that drive assembly of nanoparticle shapes even in the absence of traditional sticky patches [4], providing a new, rational approach for designing particles for self assembly.

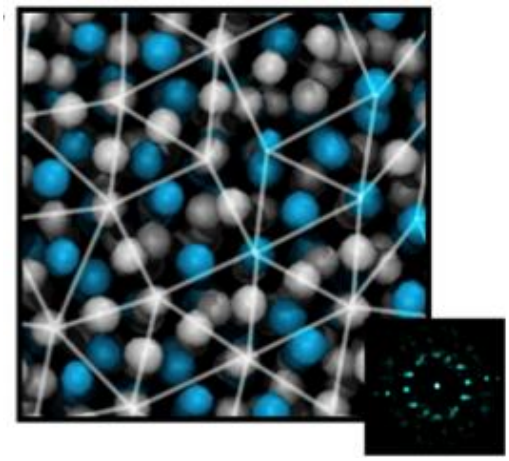

Figure 2. Self assembled dodecagonal quasicrystal from micelles formed from patchy nanoparticles. Each bead in the image corresponds to a micelle comprised of dozens of nanoparticles.[PNAS]

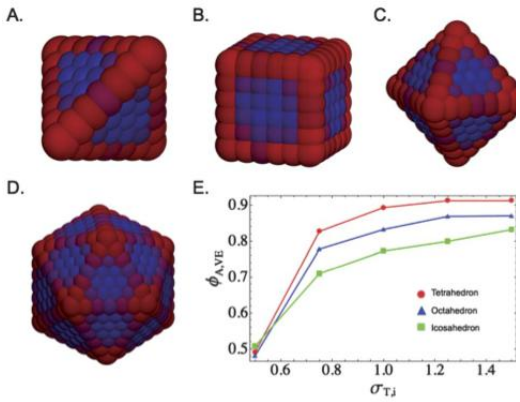

Figure 3. Occupancy for sites on the surface of various polyhedra, red for highest occupancy, blue for lowest. In E) the average fraction of vertex/edge sites vs. bead radius of the ligand.

Tools. To carry out simulations of nanoparticle self assembly, we developed new computational algorithms and tools that allow fast and highly efficient use of graphics processors in order to simulate larger systems over longer time scales. Our contributions include (1) We developed new methods for (i) expediting random number generation on GPUs [14] and (ii) simulating rigid bodies [13], both necessary for nanoparticle simulation. For the former, we developed a new method in which a micro-stream of pseudorandom numbers is generated in each thread and kernel call. These high quality, statistically robust micro-streams require no global memory for state storage, are more computationally efficient than other schemes in memory-bound

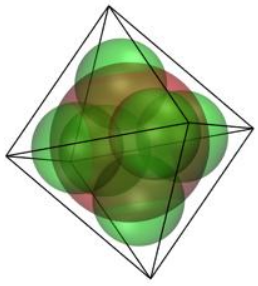

Figure 4. Filling solution for an octahedrally shaped nanocolloid.

kernels, and uniquely enable the DPD simulation method without requiring communication between threads. The scheme is 2-7 times faster than previous schemes for the DPD thermostat. For the latter, we extended the basic MD-based methods in HOOMD-Blue *with rigid body constraints* to enable composite particles with complex shapes such as anisotropic nanoparticles (using our filling solution; see below), grains, molecules, and rigid proteins to be modeled. Simulations with rigid bodies may now be run with larger systems and for longer time scales on a single workstation than was previously possible on large clusters. (2) We developed a new algorithm, termed "filling" to represent an arbitrary particle shape by overlapping spheres in such a way as to minimize the number of spheres needed for a given level of approximation of the shape [10]. Spatial partitioning problems are well known in mathematics and physics, and are critically important for a wide range of applications, including cybersecurity and packaging. They typically address the *packing* of hard shapes in a confined space, or the *covering* of a space by overlapping shapes. Filling provides a new way of subdividing space that has applications ranging from energy distribution networks to wireless sensor coverage. It is similar to both packing and covering but different from both. We derived a heuristic solution capable of quickly solving the problem in 2D, with applications to the optimal placement of, e.g., laser beams, sensors, transmitters, and explosives. We employed numerical nonlinear optimization techniques and developed computer codes that find an approximate optimal filling given any simple polygon and any *N*. Extensive classification of the behavior of the solutions leads us to several conjectures about the behavior of the solution space. These conjectures enable smart heuristics to be programmed into the codes that decrease the time spent searching for optimal solutions while at the same time increasing their accuracy and precision. Achieving maximal coverage of an interior space without exceeding the boundaries is critically important for a wide range of applications from modeling interactions between nanoparticles to manufacturing microelectronics to medical treatments.

Future Plans

Building on our prior work, we plan to (1) develop a design framework in which enthalpic and entropic patches are judiciously combined (Fig. 4) through predictive design and inverse engineering to self-assemble nanoparticles into targeted structures. Examples of target structures include complex, open structures such as clathrates for CO_2/methane capture and storage that heretofore have been inaccessible to nanoparticle assemblies; and (2) Explore the implications of directional entropic forces / entropic patchiness in biomolecular and colloidal crowding.

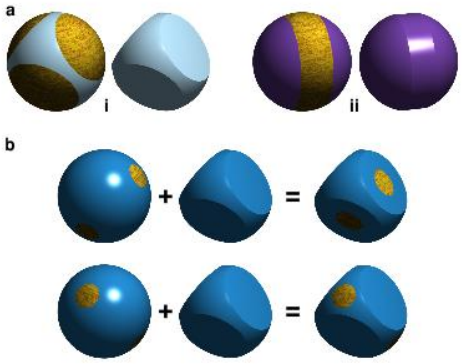

Fig. 4. (Top) Two examples of enthalpically and entropically patchy particle analogues. (Bottom) Combinations of enthalpic and entropic patches for self assembly.

References

1. Z.L. Zhang and S.C. Glotzer, "*Self-assembly of patchy particles*," Nano Lett. **4**(8), 1407-1413 (2004). Web Release Date: 24-Jul-2004, DOI: 10.1021/nl0493500.
2. S.C. Glotzer and M.J. Solomon, "*Anisotropy of building blocks and their assembly into complex structures*," Nature Materials, **6**, 557-562 (2007). Progress article. Selected for top 20 landmark articles in Nature Materials, 2002-2012.

Recent publications acknowledging DOE support (last two years)

3. Xingchen Ye, Jaime A. Millan, Michael Engel, Jun Chen, Benjamin T. Diroll, Sharon C. Glotzer, Christopher B. Murray, "Binary assemblies of nanorods and spherical nanocrystals," preprint (2013).
4. G. van Anders, et al., "General framework for directional entropic forces in colloids," preprint (2013).
5. G. van Anders, et al., "Entropically patchy particles," preprint (2013)
6. R. Marson, C.L. Phillips, J. Anderson and S.C. Glotzer, "Self-assembly of nanoparticle telechelics into complex supercrystals," preprint (2013).
7. P. Damasceno, et al., "Self-assembly of imperfect tetrahedra," preprint (2013).
8. C.L. Phillips and S.C. Glotzer, "*Effect of nanoparticle polydispersity on the self-assembly of polymer tethered nanospheres*," J. Chem. Phys., **137** (10) 104901 (2012). DOI: 10.1063/1.4748817
9. C.L. Phillips, E. Jankowski, M. Marval and S.C. Glotzer, *"Self-assembled clusters of spheres related to spherical codes,"* Phys. Rev. E, **86** (4) 1124 (2012). DOI: 10.1103/PhysRevE.86.041124 [41]. Highlighted in Video gallery for American Physical Society March Meeting 2012.
10. C.L. Phillips, J.A. Anderson, G. Huber and S.C. Glotzer, "*Optimal Filling of Shapes,"* Phys. Rev. Lett, **108**, 198304 (2012). DOI: 10.1103/PhysRevLett.108.198304 [32]. News highlights include:
    - APS Spotlighting Exceptional Research – Synopsis: Thinking Inside the Box, May 10, 2012.
    - Science Daily 5/10/2012: New Twist On Ancient Math Problem Could Improve Medicine, Microelectronics
    - Featured on AoNano.com: Nanotechnology Researchers Find New Problem
11. A. Santos, J.A. Millan and S.C. Glotzer, *"Faceted patchy particles through entropy-driven patterning of mixed ligand SAMS*," Nanoscale, **4** (8), 2640-2650, (2012). online 24 Feb 2012 (2012). **DOI:** 10.1039/C2NR11737A [31]
12. C.R. Iacovella, A.S. Keys and S.C. Glotzer, "*Self assembly of soft matter quasicrystals and their approximants,"* Proc. Natl. Acad. Sci., **108** (52) 20935-20940 (2011). [29]
13. TD Nguyen, CL Phillips, JA Anderson, SC Glotzer, *"Rigid body constraints realized in massively-parallel molecular dynamics on graphics processing units,"* Computer Physics Communications **182**(11), 2307-2313 (2011). [36]
14. CL Phillips, JA Anderson, SC Glotzer, "*Pseudo-random number generation for Brownian Dynamics and Dissipative Particle Dynamics simulations on GPU devices,"* J. Comp. Physics **230**(19), 7191-7201 (2011). [35]

BOOKS

15. C.R. Iacovella and S.C. Glotzer, "*Assemblies of Polymer-Based Nanoscopic Objects*," Comprehensive Polymer Science, 2nd Edition. Editors-in-chief: Kris Matyjaszewski and Martin Möller. Volume on Polymer Nanostructures, edited by E. Kumacheva and T. Russell (Elsevier, 2012).
16. S.C. Glotzer, A.S. Keys and E.R. Jankowski, "Challenges to Structure Prediction and Structure Characterization at the Nanoscale," Characterization of Materials, 2nd Edition. Editor-in-chief: E Kaufmann. (published online Oct 2012). DOI: 10.1002/0471266965.com114

A Hybrid Biological/Organic Photochemical Half-Cell for Generating Dihydrogen

Principal Investigator: John H. Golbeck; Co-PI: Donald A. Bryant
Mailing Address: Department of Biochemistry and Molecular Biology, The Pennsylvania State University, University Park, PA 16802
E-mail: jhg5@psu.edu, dab14@psu.edu

Program Scope

The goal of this program is to develop a hybrid biological/organic photo-electrochemical half-cell that couples a photochemical module, Photosystem I (PSI), which captures and stores energy derived from sunlight, with a catalytic module, hydrogenase (H_2ase), which catalyzes H_2 evolution with an input of two electrons and two protons. The challenge is to deliver electrons from PSI to the H_2ase rapidly and at high quantum yield, thereby overcoming diffusion-based limits on electron transfer. The strategy to achieve this goal is to employ a technology based on directly connecting surface-located redox centers in the two proteins with a molecular wire, which serves to tether the photochemical module to the catalytic module at a fixed distance so that an electron can quantum mechanically tunnel between the F_B cluster of PSI and the distal [4Fe-4S] cluster of a H_2ase enzyme at a rate faster than the competing charge recombination between P_{700}^+ and F_B^-. To link the photochemical and catalytic modules of our half-cell, a short aliphatic or aromatic dithiol molecule forms a coordination bond with an exposed Fe of the F_B cluster of a PSI variant and with an exposed Fe of the distal [4Fe-4S] cluster of a H_2ase variant. This is practically achieved by changing a ligating Cys residue of the [4Fe-4S] cluster of each protein to a Gly, thereby exposing the Fe atom for chemical rescue by the added dithiolate-containing molecular wire (**Figure 1**). We previously reported that, when ascorbate is the sacrificial donor, the PSI—wire—[FeFe]-H_2ase construct evolves H_2 at a rate of 2850 µmoles mg Chl^{-1} h^{-1}, which is equivalent to an electron transfer throughput of 5700 µmoles e^- mg Chl^{-1} h^{-1}, or 142 µmoles e^- PSI^{-1} s^{-1}. Putting this into perspective, cyanobacteria evolve O_2 at a rate of ~400 µmoles mg Chl^{-1} h^{-1}, which is equivalent to an electron transfer throughput of 1600 µmoles e^- mg Chl^{-1} h^{-1}, or 49 e^- PSI^{-1} s^{-1}, assuming a PSI to PSII ratio of 1.8 as occurs in the cyanobacterium *Synechococcus* sp. PCC 7002. The significantly greater electron throughput realized by our hybrid biological/organic nanoconstruct over *in vivo* oxygenic photosynthesis validates the concept of tethering proteins through their physiologically relevant redox cofactors to overcome diffusion-based rate limitations on electron transfer.

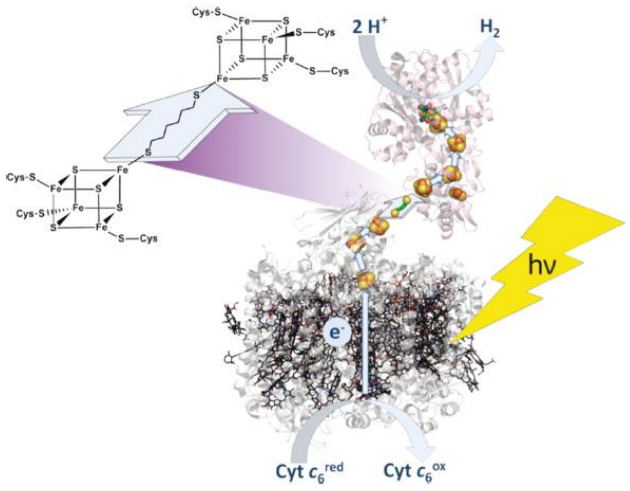

Figure 1. Schematic of the PSI—molecular wire—[FeFe]H_2ase construct. The connecting wire is 1,6-hexanedithiol. Soluble electron donors include Cyt c_6, ascorbate, and PMS. Arrows indicate electron transfer through the system, including reduction of protons to H_2.

Recent Progress

During the past year, we measured the quantum yield of light-induced dihydrogen (H_2), *i.e.* number of moles of H_2 produced per mole photons absorbed, for the cytochrome c_6 (cyt c_6) cross-linked PSI_{C13G}–1,8-octanedithiol–[FeFe]-H_2ase_{C97G} nanoconstruct. Consistent with prior experiments, the nanoconstruct was self-assembled under anoxic conditions during a dark incubation of 24 hours. The sample was illuminated with a restricted two-dimensional area of 4.15 cm^2 and assayed for H_2 production by gas chromatography at defined times. Interference filters were used to select 20 nm wavelength bands across the visible spectrum (400 to 700 nm) from a 100 W xenon arc white light source. The intensity of the light incident on the sample was measured with a Bio-spherical Instruments QSL-100 light meter. The absorbance of the sample was measured in a conventional spectrometer. As shown in **Table I**, the quantum yield for the cyt c_6 crosslinked PSI_{C13}–1,8-octanedithiol–[FeFe]-H_2ase_{C97G} nanoconstruct ranged between 0.06 and 0.30 molecules of H_2 per absorbed photon depending on the incident wavelength. The quantum yields for samples illuminated with longer wavelength light were consistent, as expected, and ranged between 0.06 and 0.13 molecules of H_2 per absorbed photon. With shorter wavelength light, which is absorbed more by the sample, the quantum yields were more variable and ranged between 0.05 and 0.30 molecules of H_2 per absorbed photon. The low and somewhat variable quantum yield for H_2 production could result from the presence of unproductive species in the sample such as a PSI_{C13G}–1,8-octanedithiol–PSI_{C13G} dimer or a [FeFe]-H_2ase_{C97G}–1,8-octanedithiol–[FeFe]-H_2ase_{C97G} dimer, neither of which would contribute to H_2 production. Given these results, experiments are planned to determine the concentration of nonproductive dimers and whether they can be minimized by new coupling strategies.

λ	Molecules H_2 (photon abs)$^{-1}$	SD
700	0.12	0.10
680	0.06	0.02
660	0.06	0.01
640	0.08	0.01
620	0.10	0.02
590	0.13	0.06
570	0.09	0.04
550	0.06	0.03
530	0.30	0.06
500	0.07	0.02
488	0.06	0.02
460	0.05	0.03
440	0.24	0.09
420	0.16	0.06
400	0.11	0.01

Table 1. Quantum yield measurements for the cytc_6 cross-linked PSI_{C13G}–1,8-octanedithiol–[FeFe]-H_2ase_{C97G} nanoconstruct in 50 mM NaP_i buffer (pH 6.5). SD refers to the standard deviation.

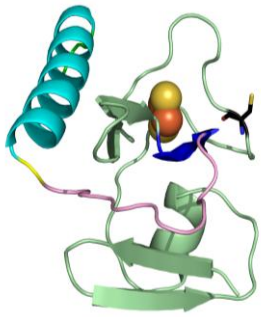

Figure 2. Structure of the N-terminal domain of CpI, including two α-helices made up of residues 61-63 (shown in blue) and 77-93 (shown in cyan). The hydrophilic loop that connects them is shown in pink and ends with Ser76 (shown in yellow). The solvent exposed Cys39 (shown by the red arrow) is represented as a stick model. The [2Fe-2S] cluster is shown in space-filling format with Fe and S atoms shown in orange and yellow, respectively.

We used the N-terminal domain fragment of *Ca*HydA to determine whether an attachment method other than wiring two [4Fe-4S] clusters together by a homo-bifunctional molecular wire might be possible. The N-terminal domain of the HydA hydrogenase of *Clostridium acetobutylicum* (denoted CaHydA-N75) comprises 75 amino acids with a predicted mass of 9.6 kDa. This domain is predicted to ligate a [2Fe-2S] cluster via cysteines 34, 45, 48, and 61 (**Figure 2**). The CaHydA-N75 recombinant polypeptide was expressed in *Escherichia coli*, and the [2Fe-2S] cluster was reconstituted using inorganic reagents. The EPR and UV-Vis spectra agree well with those obtained in a previous study of the N-terminal

76-amino acid fragment and the [2Fe-2S] cluster from *C. pasteurianum* HydA (CpI-N76). Because there are no other Cys residues in CaHydA-N75 other than those ligating the [2Fe-2S] cluster and surface exposed Cys 39 (see **Figure 2**), this domain could be a useful reporter for testing the ability of bifunctional crosslinkers to connect other redox proteins to the photochemical module. Two crosslinking agents, *N,N-bis*-(α-iodoacetyl)-2,2'-dithiobis(ethylamine) (BIDBE) and dithiobismaleimidoethane (DTME), were selected for testing. SDS-PAGE and mass spectrometry showed that the crosslinking reagents produced dimers and larger oligomers of CaHydA-N75 when the ratio of crosslinker to CaHydA-N75 was higher than 1:1. The qualitative assessment from SDS-PAGE agrees well with results from mass spectrometry. These control experiments showed that the optimal ratio of crosslinker to protein was 1:1. The crosslinker-treated CaHydA-N75 was reduced with DTT to expose the sulfhydryl group in the crosslinker for ligand exchange with the rebuilt F_B cluster of PsaC on the photochemical module. Ultrafiltration followed by SDS-PAGE showed that both BIDBE and DTME could link CaHydA-N75 to reconstituted PSI complexes, but BIDBE was more effective than DTME. Flash-induced absorption spectroscopy monitored at 820 nm showed that the BIDBE-assembled nanoconstructs had a very long-lived charge-separated state that was substantially longer than PSI alone. This result implies that electron transfer from the F_B cluster of the $PsaC_{C13G}$ variant to the [2Fe-2S] cluster associated with CaHydA-N75 occurs. Preliminary EPR studies also suggest that the electron has been transferred to the [2Fe-2S] cluster on CaHydA-N75. Based upon preliminary control experiments, it should be possible to determine if the electron is indeed on the [2Fe-2S] cluster by measuring the EPR spectrum at 40 K after photoaccumulation. If successful, we will attempt to wire the native CaHydA protein to PSI using Cys39 and the [2Fe-2S] cluster as the entry port for electrons and assay for light induced H_2 generation.

We also studied light-driven H_2 production in a diffusion-mediated system containing photosynthetic reaction centers isolated from *Heliobacterium modesticaldum* and a fusion protein of the 2[4Fe-4S] cluster-containing ferredoxin from *C. acetobutylicum* with the [FeFe]-H_2ase from *Chlamydomonas reinhardtii* (CaFd–Cr[FeFe]-H_2ase) (**Figure 4).** This fusion protein was developed in the lab of Thomas Happe (Ruhr-Universität Bochum). Heliobacteria contain a membrane bound homodimeric Type I photosynthetic reaction center that binds 22 bacteriochlorophyll *g* (BChl *g*) molecules and a single bound [4Fe-4S] cluster, F_X. In this simplified reaction center, electrons are donated to soluble 2[4Fe-4S] ferredoxins such as PshBI, and PshBII, which then can interact with other redox proteins in the cell. Recent work in this laboratory has shown that F_X can donate electrons to a number of soluble acceptor proteins, including flavodoxin. To test for light-driven H_2 production, the heliobacterial reaction centers (HbRC) were incubated separately with two H_2ase enzymes: the variant [FeFe]-H_2ase_{C97G} from *C. acetobutylicum*, and the fusion protein complex CaFd–Cr[FeFe]-H_2ase. Samples were assembled under anoxic conditions with 1:1, 1:2, and 2:1 molar ratios of HbRC and [FeFe]-H_2ase_{C97G}, and 1:1 molar ratio of HbRC and CaFd–

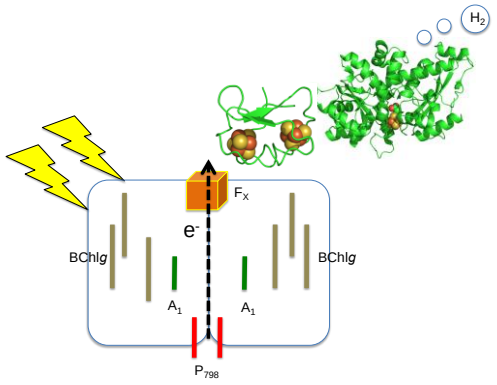

Figure 4. Representation of the Heliobacterial reaction center with Ca ferredoxin–Cr[FeFe]-H_2ase fusion complex.
PDB files: 3XL4, 1CLF

Cr[FeFe]-H_2ase (**Table 2**). Sodium ascorbate (100 mM) and phenazine methosulfate (30 mM) were added as soluble electron donors to HbRC. Moderate rates of light induced H_2 production were achieved with both of the H_2ase enzymes discussed here. Owing to the diffusional nature of the electron transfer between the HbRC and either H_2ase enzyme, there is a large dependency on the ionic strength of the buffer. Future experiments are being designed to take this dependency into consideration. Additionally, the native HbRC acceptor proteins, PshBI and PshBII, are being fused with the *C. reinhardtii* [FeFe]-H_2ase in place of the ferredoxin from *C. acetobutylicum*. These new fusion proteins should afford a higher degree of electron transfer between the HbRC and the [FeFe]-H_2ase, thus increasing hydrogen production.

Table 2. Rates of light-induced H_2 evolution using the variant [FeFe]-H_2ase_{C97G} from *C. acetobutylicum*, and the fusion protein complex CaFd–Cr[FeFe]-H_2ase with the Heliobacterial reaction center (HbRC).

Ratio and Sample used	μmol H_2 (mg BChl*g*)$^{-1}$ h^{-1}	e^- (HbRC)$^{-1}$ s^{-1}
1:1 HbRC : [FeFe]-H_2ase_{C97G}	240 ± 100	2.4 ± 1.0
1:2 HbRC : [FeFe]-H_2ase_{C97G}	100 ± 60	1.0 ± 0.6
2:1 HbRC : [FeFe]-H_2ase_{C97G}	30	0.3
1:1 HbRC : CaFd–Cr[FeFe]-H_2**ase**	130 ± 60	1.3 ± 0.6

Future Plans

Now that the goal of reproducibly generating high rates of light-driven H_2 has been realized in the PSI–wire–[FeFe]-H_2ase bioconjugate, we are poised to address a number of issues: (1) Analytical ultracentrifugation experiments are planned to show whether during the self-assembly process PSI_{C13G}–molecular wire–PSI_{C13G} dimers as well as [FeFe]-H_2ase_{C97G}–molecular wire–[FeFe]-H_2ase_{C97G} dimers in addition to the expected PSI_{C13G}–molecular wire–[FeFe]-H_2ase_{C97G} nanoconstruct are formed. (2) Extraction of the electron from the A1A and A1B sites is planned using a molecular wire consisting of 1-[15-(3-methyl-1,4-naphthoquinone-2-yl)]pentadecyl disulfide. (3) More complicated PSI–wire–Maquette nanoconstructs are being generated and tested with the maquette containing the FeMo cofactor of nitrogenase (in collaboration with L. Dutton). (4) Efforts to produce photochemical modules with modified PsaC subunits *in vivo* are continuing, and genetic tools for regulated expression of modified genes are also ongoing.

References

Lubner, C., Heinnickel, M., Bryant, D. A., and Golbeck, J. H. (2011) Wiring Photosystem I for Electron Transfer to a Tethered Redox Dye, *Energy Environ. Science 4*, 2428-2434.

Lubner, C., Applegate, A., Knörzer, P., Happe, T., Bryant, D. A., and Golbeck, J. H. (2011) A Solar Hydrogen-Producing Bio-Nanodevice that Outperforms Natural Photosynthesis, *Proc. Natl. Acad. Sci. U.S.A. 108,* 20988-20891.

Lubner, C., Bryant, D. A., and Golbeck, J. H. (2012) 'Wired Reaction Centers', In *Molecular Solar Fuels* (Hillier, W., and Wydrzynski, T., Eds.), Royal Society of Chemistry, London, pp. 464-505.

Project Title: Optical and electro-optic modulation of biomimetically-functionalized nanotubes.

PI's and Affiliations: Padma Gopalan (Materials Science and Engineering and The Department of Chemistry, University of Wisconsin-Madison), Mark Eriksson (Department of Physics, University of Wisconsin-Madison); Collaborators: Francois Leonard, Bryan Wong (Sandia National Lab).

Program Scope: Light triggered changes in biological molecules which enable various functions such as vision, photosynthesis[1] and heliotropism have long inspired materials chemists to mimmic these phenomenon to create new functional materials and devices. The ability to detect and translate the conformational changes in the small molecule retinal into the macroscopic effect of vision exemplifies a very powerful and elegant approach to the design of new functional materials[2]. Carbon nanotubes[3], with their exceptional electrical conductivity, robustness and small size, have attracted much interest as possible nanoscale replacements for inorganic semiconductors. Our goal is to *combine the best of these two worlds, to design a nanotube/chromophore hybrid material.* Here the nanotubes function as a probe of molecular transformation and also as a medium to translate the optical modulation of elecro-optic properties into useful devices. Our research is inspired by the biological process of vision and focusses on using a range of dipolar chromophores based on azo-benzene structure which undergo reversible wavelength dependent cis-trans isomerization[4]. These chromopores are photochemically stable, can be reversibly switched 10^5 to 10^6 cycles before fatigue and can be chemically tuned. We aim to answer key questions, such as whether the binding of the chromophore to the nanotube modifies the chemical response, is the chromophore optical absorption modified by the nanotube, and can we detect a single molecular transformation event by monitoring the nanotube conductance? One can reasonably envision a future functionalized-nanotube-based electro-optics with strong electro-optic coupling (due to well-engineered chemical functionalization), uniform response (due to single chirality), and high-speed (due to the intrinsic, and by now well demonstrated, high mobility of carbon nanotubes).

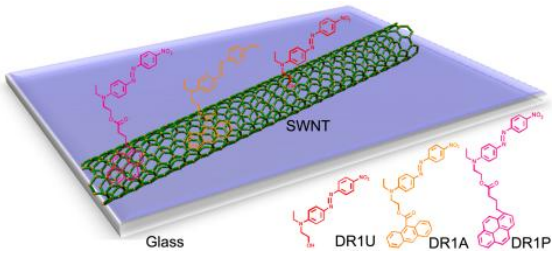

Figure 1 Structure of unmodified DR1 (DR1U), DR1 with anthracene (DR1A), DR1 with pyrene (DR1P) tethers and their SWNT hybrids.

Recent Progress: In the last funding cycle, we have 1) completed the synthesis of a series of azobenzene based dyes (Figure 1), 2) optimized the stability of these hybrids by designing the right tether for the chromophores, 3) developed a fundamental understanding for the electronic characteristics of these interfaces by a combination of theory and experiments, 4) developed a parallel effort on graphene, and 5) developed second harmonic generation tools to probe the molecular orientation on carbon based materials. Some of these achievements are elaborated below.

Probing molecular orientation by Second Harmonic Generation: Comparison of previous experimental measurements[5,6] and computational results for transport through chromophore-functionalized SWNTs suggested a model in which, the change in the chromophore dipole moment following isomerization alters the local electrostatic environment, resulting in a threshold voltage shift for hybrid SWNT-chromophore FETs[5]. However, the transport studies through FET-type devices could not probe the chromophore orientation, which is essential for understanding a photoisomerization. We showed through optical second harmonic generation (SHG) measurements that there is a partial radial orientation of the chromophores on the nanotubes. Periodic UV illumination of a DR1/SWNT hybrid caused a modulation of the SHG signal, which was attributed to reduction in the molecular hyperpolarizability of the chromophore following *trans-cis* isomerization (Figure 2). *Our studies were the first to demonstrate the use of SHG to probe the dynamic chromophore orientation in chromophore/SWNT interfaces subject to both time-dependent external illumination and applied electric field.* We measured the photoisomerization kinetics and extracted the time scales for both forward (*trans-cis*) and backward (*cis-trans*) isomerization. The dynamics of both processes are found to be biexponential, with a fast (of order seconds) and a slow (of order one minute) time scale. The fast component is similar to previous measurements extracted from FET conductivity. The direct experimental measurement of this order supports existing device simulation models in which dipole moment changes upon chromophore isomerization perturb the local electrostatic environment of the nanotube, resulting in a threshold voltage shift in the SWNT FET device. This is possible only if at least some of the chromophores are oriented perpendicular to the nanotubes. With coverage of about 3 chromophores per 100 carbon atoms in SWNTs, the *p*-polarized SHG signal was sufficiently above the noise to measure the SHG angular dependence for *s* and *p* polarized fundamental, and to determine the *average chromophore tilt angle of 40 ± 3 degrees*. Periodic illumination with unpolarized 495 nm light followed by dark storage resulted in reversible switching of the SHG signal via *trans-cis* photoisomerization of the chromophore. *During this study, we asked the question if these dipolar molecules can be poled by an external field to enhance molecular orientation similar to that used in electro-optic polymers (guest-host) system? In fact our experiments show that chromophore orientation is enhanced by an applied*

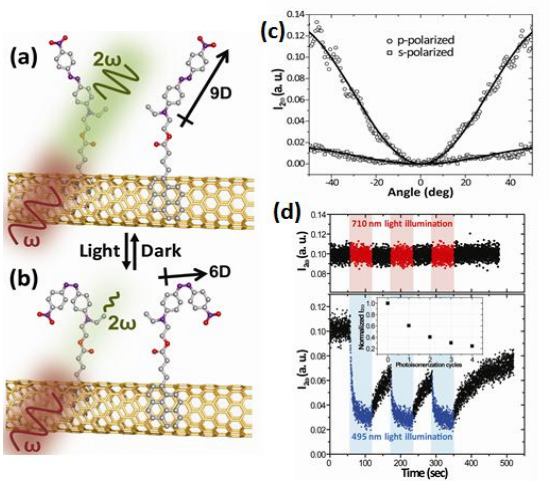

Figure 2. A depiction of SHG by (a) *trans*- and (b) *cis*-DR1-P on SWNT. The orientation of DR1-P on SWNT is for illustrative purposes only. (c) Transmitted 532 nm (*p*-polarized) SHG vs. angle of incidence for DR1-P/SWNT using *p*-polarized (circles) and *s*-polarized (squares) incident fundamental. Solid lines are theoretical fits. And (d) Plot of transmitted 532 nm (*p*-polarized) second harmonic intensity vs. time for DR1-P/SWNT under periodic 495 nm (blue trace) and 710 nm (red trace) illuminations. Inset shows normalized SHG signal level following removal of 495 nm LED in an identical experiment, except that LED on-time is increased to 5 minutes.

external electric field, and the cis-trans back-isomerization kinetics can be effectively controlled by this field. This observation is particularly significant as it suggests that the gate field in hybrid transistors can act akin to a poling field, controlling both the chromophore orientation and the switching dynamics.

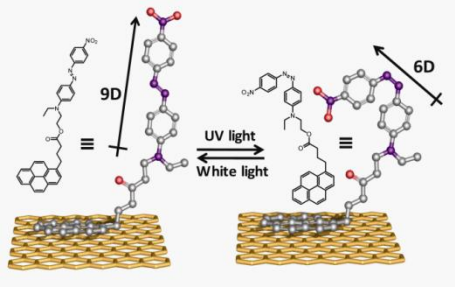

Figure 3. Illustration of photoisomerization of DR1P on graphene. DR1P is tethered to the surface of graphene via π-π interactions between

From Nanotubes to Graphene Hybrids: Graphene shares many of the same excellent electronic properties as carbon nanotubes; however, unlike nanotubes, graphene can be grown over large areas and does not have the sample heterogeneity issues. The planar nature of this 2D material makes the interpretation of molecular interactions and direct experimental observation by XPS and Raman spectroscopy appealing. Based on our earlier studies the pyrene containing chromophore (DR1P) should give the best attachment to graphene to create a stable hybrid, hence we used primarily DR1P for these studies (Figure 3). Raman spectroscopy measurements were done with 633 nm excitation laser, which is outside the wavelength range where DR1P absorbs. To induce photoisomerization of DR1P between *trans* and *cis* forms, 500 μW/cm^2 hand-held UV lamp with 365 nm wavelength and 150 W tungsten lamp were used as UV and white light sources, respectively. Figure 4a shows representative

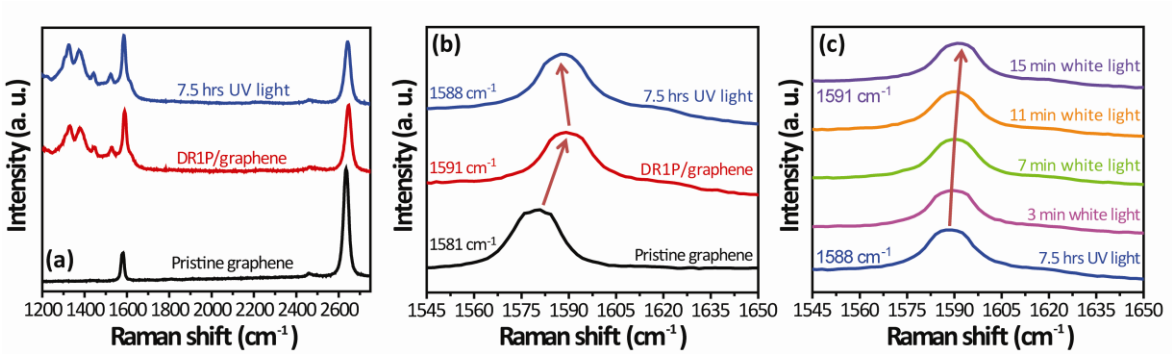

Figure 4: Raman spectra (a) of pristine graphene, DR1P/graphene, and UV illuminated DR1P/graphene, (b) of pristine graphene, DR1P/graphene, and UV illuminated DR1P/graphene showing the changes in the G band position, (c) of UV illuminated DR1P/graphene samples showing changes in G band upon white light illumination

Raman spectra of DR1P/graphene as prepared, and after UV illumination as well as the pristine graphene for comparison. The G band is upshifted by 10.0 cm^{-1} after deposition of DR1P on graphene, indicating that graphene is potentially doped by DR1P. UV illumination of DR1P/graphene induced a clear downshift (~2.7 cm^{-1}) in G band. This shift in G band was reversed upon white light illumination (Figure 4c). UV illumination induces isomerization of DR1 from *trans* to *cis* form, leading to decrease in the dipole moment. The decrease in dipole moment can alter the extent of doping in graphene, i.e., change the charge carrier concentration in graphene, which is reflected in the shifts in G band. Subsequent illumination with white light isomerizes the *cis* back to *trans* form. Quantitative estimates of the charge carrier concentration can be obtained from both G band and Dirac point shifts. The extent of doping by functionalization of one DR1P molecule per 100 carbon atoms in graphene is comparable to

substitutional p-doping of graphene by 2.5 wt% of boron. *More importantly, the photo-switchable dipolar molecules offer the unique advantage of light induced modulation of doping by 18% without need for further synthesis. The sensitivity of the readout by graphene in the given transistor architecture is striking, as a relatively small change in electrostatic potential of 0.14V results in a 40 times voltage amplification. This is exciting as now it is possible to envision synthetic analogues with a potential to have single photon detection capabilities with further improvements in this system.* In addition to stability of the devices, doping graphene using non-covalently latched organic molecules is to preserve the mobility of graphene.

Future Plans: Our focus for future work is specifically on the development and understanding of these hybrid interfaces through a combination of new functionalization chemistry, characterizing the interface through spectroscopic and surface characterization tools, as well as modeling. Specific tasks involve synthesis of new chromophores to tune the flexibility of linker in the dipolar molecule, and expand the absorption window of the chromophore to near-IR range for dual wavelength detection; Second harmonic generation (SHG) and photoinduced birefringence measurements to create *spatially addressable, reversible modulation of the DR1P-SWNT linear optical properties*, and implementation of Near Edge X-ray Absorption Fine Structure (NEXAFS) characterization of hybrids**.**

Publications Supported by BES in the last two years: 1) Molecular Orientation and Photoswitching Kinetics on Single-Walled Carbon Nanotubes by Optical Second Harmonic Generation. McGee, D. J.; Huang, C.; Kim, M.; Choi, J., Eriksson, M. A.; Gopalan, P. *Appl. Phys. Lett.* **2012**, *101*, 264101.**; 2)** Light-Driven Reversible Modulation of Doping in Graphene. Kim, M.; Safron, N. S.; Huang, C.; Arnold, M. S.; Gopalan, P. *Nano Letters* **2012**. *12*, 182–187. 3) Spectroscopic Properties of Nanotube-Chromophore Hybrids. Huang, C.; Wang, R.; Wong, B.; McGee, D.; Leonard, F.; Kim, Y. -J.; Johnson, K.; Arnold, M. S.; Eriksson, M.; Gopalan, P. *ACS Nano* **2011**. *5*, 7767-7774; 4) Functionalization of Single-Wall Carbon Nanotubes with Chromophores of Opposite Internal Dipole Orientation" Zhao, Yuanchun; Huang, Changshui; Kim, Myungwoong; Wong, Bryan; Leonard, Francois; Gopalan, Padma; Eriksson, Mark (in review).

References:

(1)Andersson, M.; Malmerberg, E.; Westenhoff, S.; Katona, G.; Cammarata, M.; Wohri, A. B.; Johansson, L. C.; Ewald, F.; Eklund, M.; Wulff, M.; Davidsson, J.; Neutze, R. *Structure* **2009**, *17*, 1265.
(2)Komarov, V. M.; Kayushin, L. P. *Studia Biophysica* **1975**, *52*, 107.
(3)Balasubramanian, K.; Burghard, M.; Kern, K.; Scolari, M.; Mews, A. *Nano Lett* **2005**, *5*, 507.
(4)Rau, H. *Photoisomerization of Azobenzenes*; CRC press, Boca Raton FL, 1990.
(5)Simmons, J. M.; In, I.; Campbell, V. E.; Mark, T. J.; Leonard, F.; Gopalan, P.; Eriksson, M. A. *Physical Review Letters* **2007**, *98*.
(6)Zhou, X. J.; Zifer, T.; Wong, B. M.; Krafcik, K. L.; Leonard, F.; Vance, A. L. *Nano Lett* **2009**, *9*, 1028.

Phospholipid Vesicles in Materials Science

Steve Granick

University of Illinois
Department of Materials Science and Engineering
1304 West Green St.
Urbana, IL 61801
sgranick@uiuc.edu

Program Scope: This proposal has the objective to develop the science basis needed to deploy phospholipid bilayers as functional materials in energy contexts, specifically to: (1) Develop an integrated molecular-level understanding of what determines their environmental shape and contour responsiveness, and (2) Develop understanding of their active transport in nature.

Recent Progress: **Lévy Walks Emerge Bottom-Up.** A fundamental problem of living matter is active transport of mass and signal. Understanding to date has mainly focused on the molecular level: motor proteins drag cargos along microtubule tracks with deterministic nanometer steps. Regarding the link to long-range transport, too little is known, except that molecular fluctuations should in principle produce randomness that may converge to Brownian-like diffusion.

Fig. 1. Endosomes are transported on microtubules in straight paths, but also make turns. **a**, Illustration that cargos are transported through microtubule networks by motors. In the "bidirectional transport" scenario, dragged by opposing motors that step in nanometers (box 1), cargo pauses, dissociates, rebinds, and reverses direction (box 2). Adding complexity is that microtubules run in multiple directions and cross paths forming networks (box 3).

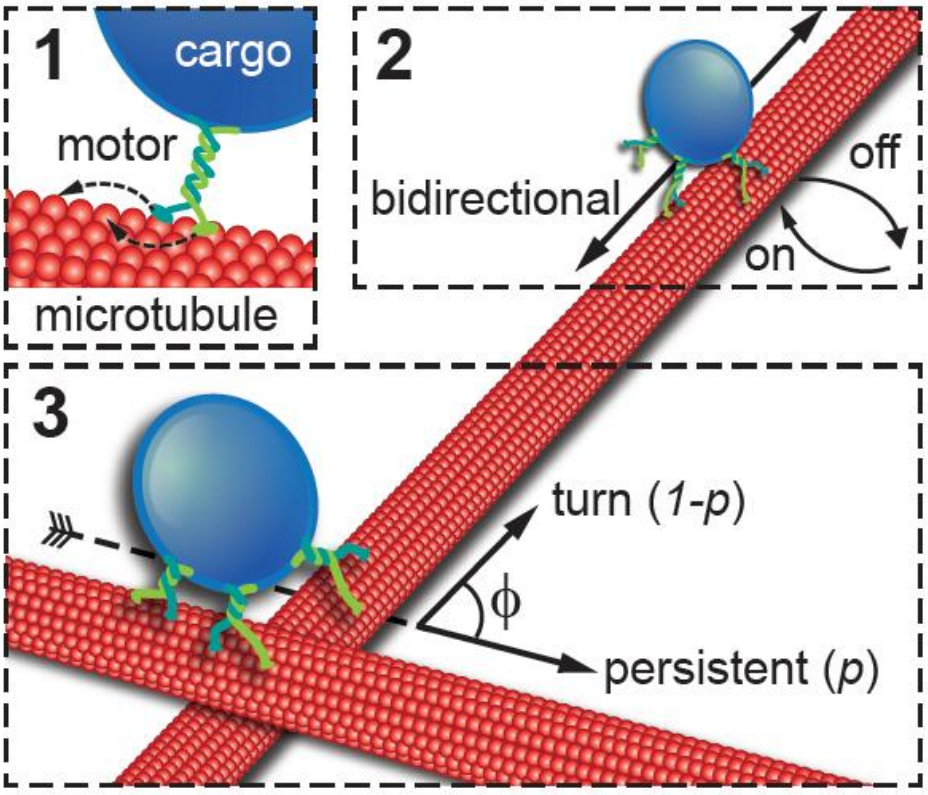

This year, voluminous datasets, acquired using optical sheet microscopy to track populations of endosomes (intracellular vesicles) that diverge in biological pathways, have demonstrated that intracellular transport likely in general follows an unexpected pattern: the probability of continuing in a given direction increases with the distance already traveled persistently in that direction. We showed, combining experiments and numerical modeling, that this non-stationary directional memory robustly generates Lévy walks, a class of stochastic processes that explore space more rapidly than Brownian random walks. The dynamics reverts to Brownian when cytoskeleton is perturbed, as the model predicts. This analysis extends to a molecular system the Lévy statistics known to optimize macroscopic-sized random searches. Our results demonstrate how this efficient search arises bottom-up from the active motion of individual motor proteins. This suggests a new mechanism that improves transport efficiency in cells. We have in mind that it could generalize in other media of active materials where search efficiency is important to generate using design rules.

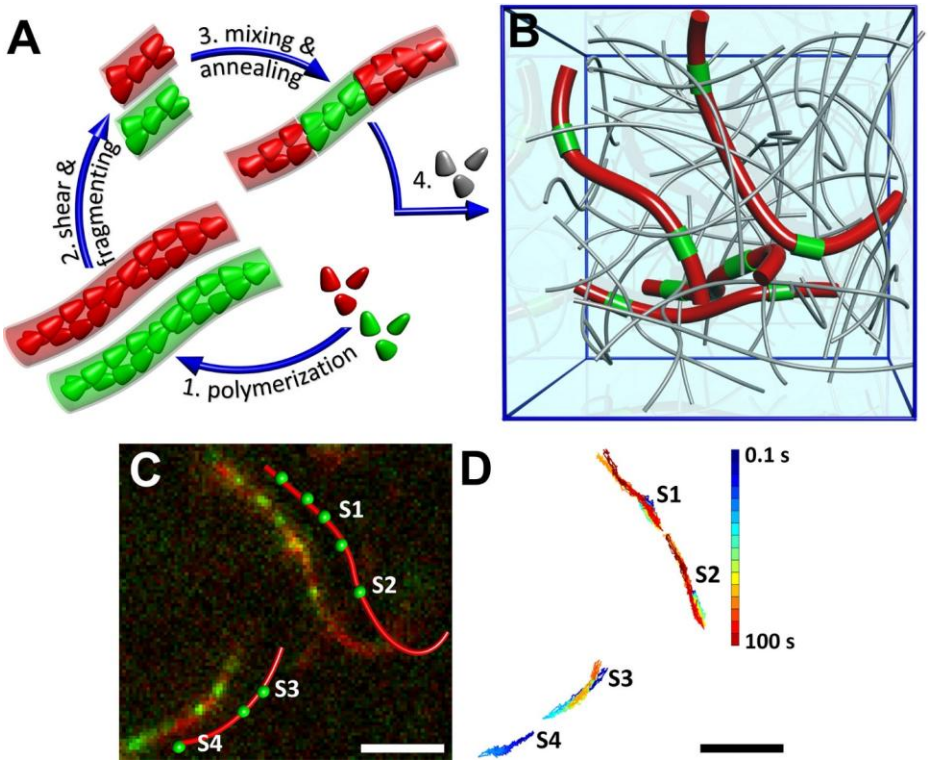

Fig. 2. Between discrete and continuum in microrheology. A spinoff of these optical imaging methods has involved two-point microrheology in a surprisingly productive fashion. The context is that the space-time dependence of viscosity plays a fundamental, crucial role in a number of natural and industrial processes, where the time dependence has been extensively studied by conventional methods, yet its spatial counterpart has not been directly determined. Our experiments have shown an imaging based method to measure the space-time dependent cooperative viscosity and have confirmed its validity in a biopolymer, F-actin solution. A space dependent master curve of cooperative viscosity has been identified with an exponential growth at short distance (correlation length ~ 8 times of mesh size) and a plateau at long distance (surprisingly large crossover distance ~ 18 times of mesh size), therefore visualizing the discrete-to-continuum transition of viscosity in real space

Modular stitching to image single-molecule DNA transport. All previous single-molecule imaging studies of polymer transport involve fluorescence labeling uniformly along the chain, which suffers from limited resolution due to the diffraction limit. We have demonstrated the

concept of submolecular single-molecule imaging with DNA chains assembled from DNA fragments such that a chain is labeled at designated spots with covalently-attached fluorescent dyes and the chain backbone with dyes of different color. High density of dyes ensures good signal-to-noise ratio to localize the designated spots in real time with nanometer precision and prevents significant photobleaching for long-time tracking purposes. To demonstrate usefulness of this approach, we imagedelectrophoretic transport of λ-DNA through agarose gels. The unexpected pattern was observed that one end of each molecule tends to stretch out in the electric field while the other end remains quiescent for some time before it snaps forward and the stretch-recoil cycle repeats. These features are neither predicted by prevailing theories of electrophoresis mechanism nor detectable by conventional whole-chain labeling methods. Even more recent experiments extend the concept to diffusion of DNA at rest, through entangled gel networks.

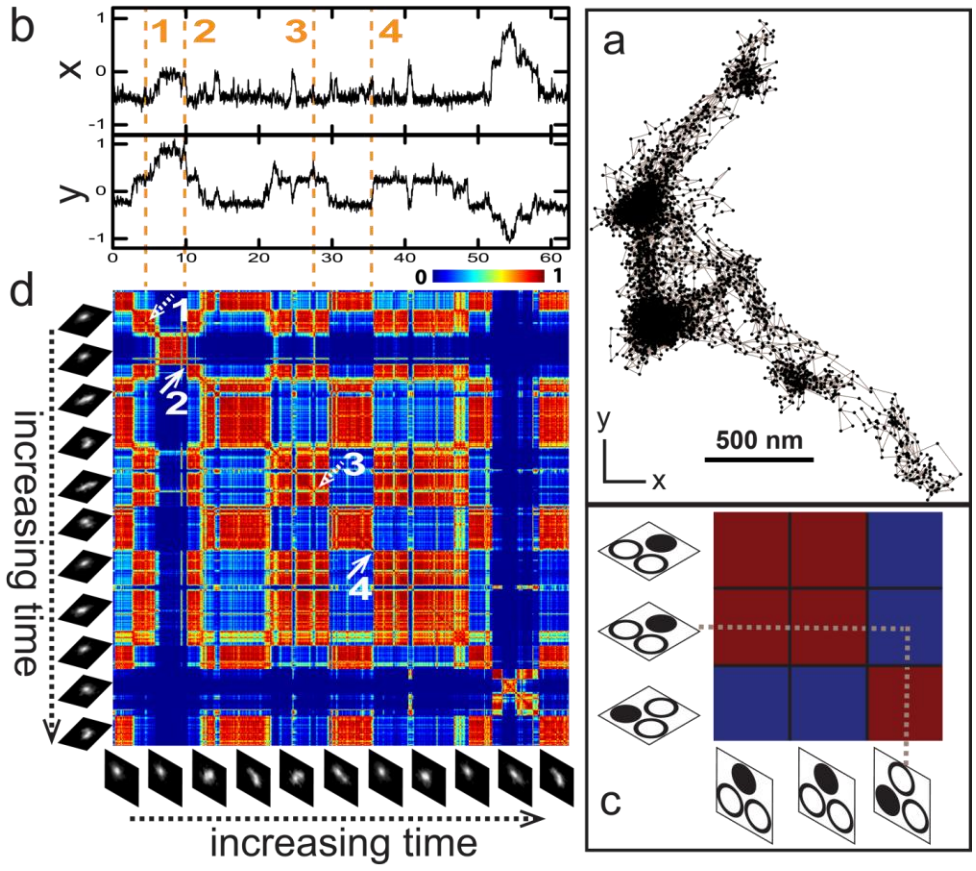

Fig. 3. a) A representative trajectory showing the center-of-mass of a λ-DNA tracked for 62 s in agarose gel in the absence of electric field. Presence of "cages" inside the network is evident. b) x and y center-of-mass position (μm) versus time (seconds) for the same molecule as in figure 2a. c) We define "similarity matrix" such that each element denotes the Pearson correlation coefficient between two images in a series of images. d) Similarity matrix calculated between any pair of two images recorded for the chain in Fig 2b. Both x and y axis of the matrix represents time in seconds, same as in Fig 2b. Red blocks indicate high similarity between two images whereas blue blocks indicate low similarity. A color bar is shown for comparison. Patterns on the similarity matrix correspond well with center-of-mass dynamics. For example, arrow 2 and 4 pointing at the intersection between diagonal red blocks correspond to two successful "jumps" that result in position changes around 10 s and 35 s in Fig 2b; arrow 1 and 3 pointing to stripes within a block correspond to two futile jump attempts where the molecule returns to the original position.

Future Plans: These exciting new developments will be pursued. In the area of phospholipid membrane fluctuations, one problem of intense interest will be to continue our ongoing study of what determines shape transformations in the presence of gradients of osmotic pressure and temperature, part of our intense interest in understanding how local mechanical properties link to large-scale deformations and shape. Chemical communication between vesicles is also under investigation. In the area of biomolecular models of mobility, single-molecule tracking will be further combined with computer simulation to separate system-specific from generic aspects of the surprising phenomenological behavior revealed in our preliminary studies of reptation at rest, where (tentatively) it seems that the elementary steps are an intermittent in nature, following distributions captured by a continuous time random walk. The findings regarding the molecular origins of target-seeking efficacy in active transport will be further extended and generalized.

Publications 2011 to date:

1. "How Liposomes Diffuse in Concentrated Liposome Suspension," Yan Yu, Stephen Anthony, Sung Chul Bae, and Steve Granick, ***J. Phys. Chem. B*** 115, 2748 (2011).

2. "Automated Single Molecule Tracking of DNA Shape," Juan Guan, Bo Wang, and Steve Granick, ***Langmuir*** 27, 6149 (2011)**.**

3. "When Brownian Diffusion is not Gaussian," Bo Wang, Sung Chul Bae, and Steve Granick, ***Nature Materials*** 11, 481 (2012)**.**

4. "Modular Stitching to Image Single-Molecule DNA Transport," Juan Guan, Bo Wang, Sung Chul Bae, and Steve Granick, ***J. Am. Chem. Soc.*** 135, 6006 (2013).

5. "Diagnosing Heterogeneous Dynamics in Single Molecule/Particle Trajectories with Multiscale Wavelets," Kejia Chen, Bo Wang, Juan Guan, Steve Granick, **arXiv**:1306.0505, 2013.

6. "Bursts of Active Transport in Living Cells," Bo Wang, James Kuo, Steve Granick, **arXiv**:1307.1898, 2013

7. "Lévy Walks Emerge Bottom-Up from Molecular Steps in Intracellular Trafficking," submitted.

8. "Visualizing the Spatial Dependence of Viscosity," Lingxiang Jiang, Boyce Tsang, Steve Granick, submitted.

Program Title: Bioinspired Hydrogen Bonding-Mediated Assembly of Nano-objects toward Adaptive and Dynamic Materials

Principle Investigator: Zhibin Guan, Ph.D.
Mailing Address: 1102 Natural Sciences II, Irvine, CA 92697
Email: zguan@uci.edu

Program Scope

The goal of this project is to develop strong polymeric materials having adaptive and dynamic properties for energy relevant applications. Inspired by natural dynamic and adaptive materials, both supramolecular interactions (hydrogen bonding) and dynamic covalent interactions are employed to introduce adaptive, autonomically responsive, and self-healing properties to the materials. Compared to other molecular mediators, well-defined hydrogen bonds are stronger and easier to control than other dynamic interactions (e.g., van der Waal, dipole-dipole, ionic, π–π stacking, etc) while much less expensive to prepare and can be easily scaled up compared to DNAs. Following the design and synthesis of the proposed nanomaterials, we plan to investigate the dynamic assembly of the H-bonding nano-objects. Finally, the adaptive and dynamic mechanical properties of the nano-assembled materials will be investigated in solution, and solid state.

Our basic investigation of dynamic materials has recently resulted in a major breakthrough for the development of dynamic, adaptive, and self-healing polymers using both noncovalent and dynamic covalent interactions. For dynamic noncovalent mechanism, we developed multiphase supramolecular thermoplastic elastomers that combine high modulus and toughness with spontaneous healing capability without any trigger. For using dynamic covalent interactions, my laboratory has recently demonstrated Ru-catalyzed olefin metathesis as a simple, effective method for healing polymers via dynamic exchange of strong carbon-carbon bonds. The main strategy we use to achieve our goals is *biomimicry*: copying nature's "bottom-up" approach to *multifunctional* and *mechanically robust* materials synthesis. Nature relies heavily on *dynamic non-covalent* and *covalent* interactions to organize structures over multiple length scales, imbuing natural materials with remarkable toughness, multifunctionality, and self-healing capability. Recent advance in material synthetic techniques dramatically enhances our ability to translate specific bio-inspired molecular designs into functional polymers and nano-objects. In earlier work we successfully combined the biomimetic design principles of modularity and programmed non-covalent interactions to obtain advanced multifunctional self-assembling polymers and materials.[1-5]

The projects involve the custom synthesis of novel dynamically-interacting oligomeric, polymeric, and polymer-grafted-particle nano-objects. The molecular constituents will be tuned to achieve controlled assembly of ordered, multiphase materials with specific emergent bulk properties. The project utilizes the broad spectrum of expertise of the group members in molecular and macromolecular synthesis and characterization, static and dynamic mechanical studies, biomimetic self-assembly, X-ray scattering, scanning probe, electron, and optical microscopy characterization techniques.

Recent Progress

Self-Healing Polymers via Supramolecular and Dynamic Covalent Interactions

BACKGROUND
The development of polymers that can spontaneously repair themselves after mechanical damage would significantly improve the safety, lifetime, energy efficiency, and environmental impact of manmade

materials. Most approaches to self-healing materials require the input of external energy in the form of either heat or light. For the few spontaneous self-healing polymers, some need healing agents (monomer and catalysts) and others are soft materials that require substantial solvation (hydrogels) or plasticization (rubber). Despite intense research in this area, the synthesis of a stiff material with intrinsic self-healing ability remains a key challenge. Building upon our previous biomimetic polymer design,[6] we recently successfully developed two strategies for achieving self-healing polymers using both noncovalent (hydrogen bonding)[7-9] and dynamic covalent (Ru-catalyzed olefin metathesis) interactions.[10, 11]

Discussion of Findings: In exploring supramolecular interactions for self-healing polymer design, we successfully developed a new multiphase design concept for thermoplastic elastomers that combine high modulus and toughness with spontaneous healing capability. In our first design, H-bonding brush polymers (HBPs) self-assemble into hard-soft microphase-separated system, combining the enhanced stiffness and toughness of hybrid polymers with the self-healing capacity of dynamic supramolecular assemblies.[7] In contrast to previous self-healing polymers, our systems spontaneously self-heals as a single-component solid material at ambient conditions without the need of any external stimulus, healing agent, plasticizer, or solvent. This work was highlighted by *C&EN News* (*http://cen.acs.org/articles/90/i14/Polymer-Heal-Thyself.html*) and *Angewandte Chemie (DOI: 10.1002/anie.201205226)*. In another design, supramolecular ABA triblock copolymers formed by dimerization of 2-ureido-4-pyromidone (UPy) end-functionalized polystyrene-*b*-poly(n-butylacrylate) (PS-b-PBA) AB diblock copolymers are synthesized, resulting in a self-healing material that combines the advantageous mechanical properties of thermoplastic elastomers and the dynamic self-healing features of supramolecular materials.[8] Most recently, we have also developed a core-shell nanoparticle system that can effectively self-heal at ambient conditions.[9]

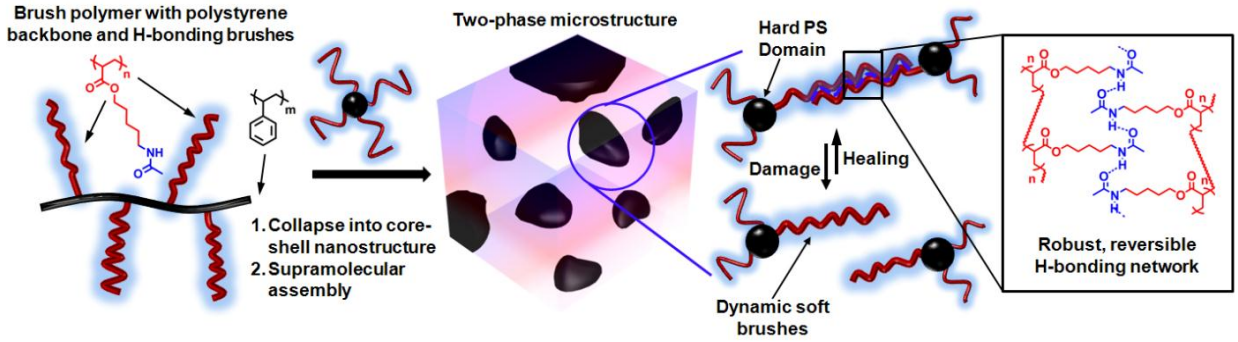

Figure 1. Design concept of H-bonding brush polymers (HBPs) as autonomous self-healing thermoplastic elastomers (TPEs).

In addition to employing *dynamic non-covalent* interactions (such as H-bonding) for self-healing materials, recently, we have had a breakthrough development of malleable/self healing network polymers employing *dynamic covalent* bonding. Specifically, we demonstrated for the first time that olefin metathesis induces very efficient exchange reactions between double bonds and produce materials that are both insoluble and malleable at room temperature (Fig. 2A).[10] By introducing a very low level of the Grubbs' second-generation Ru metathesis catalyst, a chemically cross-linked polybutadiene (PBD) network becomes malleable at room temperature while retaining its insolubility. The stress relaxation capability increases with increasing level of catalyst loading. In sharp contrast, catalyst-free control samples with identical network topology and cross-linking density do not show any adaptive properties. This chemistry should offer a possibility to combine the dimensional stability and solvent resistance of cross-linked polymers and the processability/ adaptibility of thermoplastics.

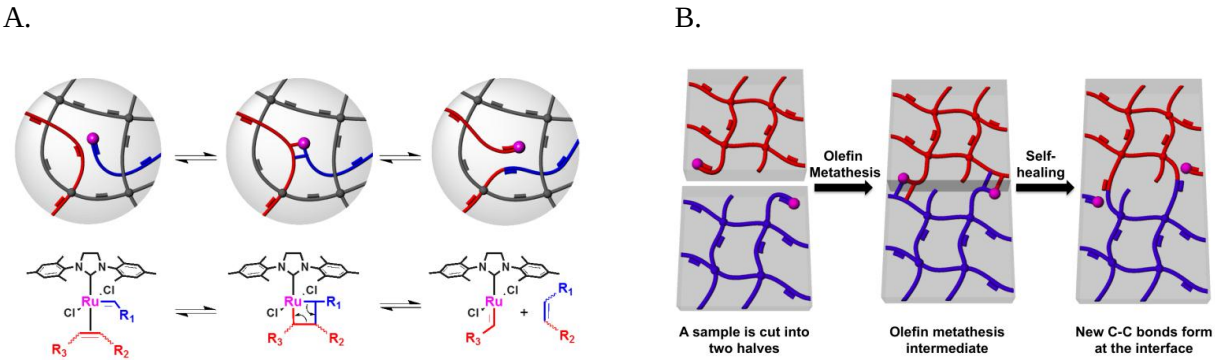

Figure 2. Malleable and self-healing polymer network via Ru-catalyzed olefin metathesis. (A) Internal olefin exchange affords malleability for the network; (B) Olefin exchange between fractured interfaces results in self-healing.

We further demonstrated that olefin metathesis provides an efficient mechanism for self-healing through dynamic covalent bond formation. By introducing Grubbs' second-generation Ru metathesis catalyst into cross-linked PBD network, the material self-heals effectively at various conditions under moderate pressures (Fig. 2B).[11] In sharp contrast, catalyst-free control samples with identical network topology and cross-linking density show minimal healing. The healing efficiency of the materials was carefully investigated under different concentrations of the Ru catalyst, compression pressure and temperature. It was demonstrated for the first time that a bulk polymer could effectively heal via dynamic covalent bond formation at sub-ambient temperature. The Ru-loaded PBD samples not only heal well with themselves but also with control samples without any catalyst. In addition, the materials could even heal by simply applying a small amount of Ru catalyst at the fracture surface. The simplicity and effectiveness of this self-healing approach make it potentially applicable to a wide range of olefin-containing polymers. The strength of covalent C-C double bonds may also offer the potential for developing really strong and autonomously self-healing materials. This work was highlighted by *C&EN News* (*http://cen.acs.org/articles/90/i33/Polymer-Healing-Olefin-Metathesis.html*).

Importance of findings both from experimental and theoretical perspectives: While several groups have reported self-healing systems through the incorporation of encapsulated monomers, reversible or irreversible covalent bonds, and dynamic non-covalent bonding into polymers, these systems either require solvents/plasticizers, healing reagents, or external stimuli, such as heat or light. Our initial biomimetic design success is the first example of a material that has the ability to combine excellent self-healing with the desirable and tunable mechanical properties found in commercial thermoplastic elastomers into a multifunctional single-component system which will self-heal spontaneously without the need of any plasticizer, solvent, healing agents, or external stimuli, validating our multiphase dynamic self-assembly approach to advanced energy-relevant materials. Our successful demonstration of using strong while dynamic covalent interactions (olefin metathesis) to achieve very efficient self-healing bode well for future development of strong self-healing materials in bulk solids.

Future Plans

(1) Two-tier Self-healing Design: Supramolecular and Dynamic Covalent Interactions
Building upon our success in self-healing polymer design using both noncovalent (H-bonding) and dynamic covalent (olefin metathesis) interactions, we propose to design a two-tier self-healing system incorporating both supramolecular and dynamic covalent interactions for optimal healing efficiency. Our hypothesis is as follows: the supramolecular interactions will provide quick healing immediately after

damage, which will bring the interfaces into molecular contact and allow permanent healing via dynamic covalent bond formation.

(2) Further Multiphase Self-healing Polymer Designs
Our multiphase self-healing concept is generally applicable for self-healing polymeric material design. We will continue exploration in this direction by varying a number of parameters including the composition for the hard phase and soft matrix, macromolecular architecture, and dynamic interaction motifs. This study will obtain the structure/property understanding required to tailor these new materials to specific energy-materials applications.

(3) Functional Self-assembled Nanocomposites for Dynamic, Strong Self-Healing Properties
We will synthesize various functional nanoparticles functionalized with supramolecular or dynamic covalent motifs. Furthermore, we will self-assemble them into bulk nanocomposites and investigate both their self-healing and emerging functional properties.

Publications in year 2009-2010 (which acknowledge DOE support):

1. Guzman Dora L, Randall A, Baldi P, Guan Z. Computational and single-molecule force studies of a macro domain protein reveal a key molecular determinant for mechanical stability. *Proc. Natl. Acad. Sci. U. S. A.* **2010**;107(5):1989-94.
2. Kushner AM, Vossler JD, Williams GA, Guan Z. A Biomimetic Modular Polymer with Tough and Adaptive Properties. *J. Am. Chem. Soc.* **2009**;131(25):8766-68.
3. Yu T-B, Bai JZ, Guan Z. Cycloaddition-promoted self-assembly of a polymer into well-defined beta sheets and hierarchical nanofibrils. *Angew. Chem., Int. Ed.* **2009**;48(6):1097-101.
4. Chen Y, Guan Z. Bioinspired modular synthesis of elastin-mimic polymers to probe the mechanism of elastin elasticity. *J. Am. Chem. Soc.* **2010**;132(13):4577-9.
5. Lu Y-X, Shi Z-M, Li Z-T, Guan Z. Helical polymers based on intramolecularly hydrogen-bonded aromatic polyamides. *Chem. Commun.* **2010**;46(47):9019-21.

Publications in year 2011-2013 (which acknowledge DOE support):

6. Kushner AM, Guan Z. Modular Design in Natural and Biomimetic Soft Materials. *Angew. Chem., Int. Ed.* **2011**;50(39):9026-57.
7. Chen Y, Kushner AM, Williams GA, Guan Z. Multiphase design of autonomic self-healing thermoplastic elastomers. *Nature Chem.* **2012**;4(6):467-72.
8. Hentschel J, Kushner AM, Ziller J, Guan Z. Self-Healing Supramolecular Block Copolymers. *Angew. Chem., Int. Ed.* **2012**;51(42):10561-65.
9. Chen Y, Guan Z. Self-assembly of core–shell nanoparticles for self-healing materials. *Polym. Chem.* **2013**;Advance Article.
10. Lu Y-X, Tournilhac F, Leibler L, Guan Z. Making Insoluble Polymer Networks Malleable via Olefin Metathesis. *J. Am. Chem. Soc.* **2012**;134(20):8424-27.
11. Lu Y-X, Guan Z. Olefin Metathesis for Effective Polymer Healing via Dynamic Exchange of Strong Carbon-Carbon Double Bonds. *J. Am. Chem. Soc.* **2012**;134(34):14226-31.

Multicomponent Protein Cage Architectures for Photocatalysis

Arunava Gupta[(a)] and Peter E. Prevelige[(b)]

[(a)] University of Alabama, Tuscaloosa, AL 35487
[(b)] University of Alabama, Birmingham, AL 35294
agupta@mint.ua.edu, prevelig@uab.edu

Program Scope: This is a collaborative project between Drs. A. Gupta (University of Alabama), P. Prevelige (Univesity of Alabama, Birmingham), T. Douglas (Montana State University), and B. Kohler (Montana State University) The primary goal of the project is to develop protein-templated approaches for the synthesis and directed assembly of semiconductor nanomaterials and dyes that are efficient for visible light absorption and hydrogen production. In general, visible-light-driven photocatalysis reactions exhibit low quantum efficiency for solar energy conversion primarily because of materials-related issues and limitations, such as the control of the band gap, band structure, photochemical stability, and available reactive surface area of the photocatalyst. Synthesis of multicomponent hierarchical nano-architectures, consisting of semiconductor nanoparticles (NPs) and coordination polymers with desired optical properties fabricated to maximize spatial proximity for optimum electron and energy transfer represents an attractive route for addressing the problem.

Virus capsids are highly symmetrical, self-assembling protein cage nanoparticles that exist in a range of sizes and symmetries. Selective deposition of inorganic or organic materials, by design, at specific locations on virus capsids affords precise control over the size, spacing, and assembly of nanomaterials, resulting in uniform and reproducible nano-architectures. We utilize the self-assembling capabilities of the 420 subunit, 60 nm icosahedral, P22 virus capsid to direct the nucleation, growth, and proximity of a range of component materials. Controlled fabrication on the exterior of the temperature stable shell is achieved by genetically encoding specific binding peptides into an externally exposed loop which is displayed on each of the 420 coat protein subunits. Localization of complimentary materials to the interior of the particle is achieved through the use "scaffolding-fusion proteins. The scaffolding domain drives coat protein polymerization resulting in a coat protein shell surrounding a core of approximately 300 scaffolding/fusion molecules. The fusion domain comprises a peptide which specifically binds the semi-conductor material of interest.

Recent Progress: In this funding period we have built on our previous success in nucleating the formation of CdS and ZnS nanocrystals on the exterior of P22 to demonstrate the feasibility of employing scaffolding-fusion proteins to nucleate internal nano-crystal formation of TiO_2 and CdS. Fusion scaffolding proteins were designed based on the observation that an N-terminally deleted version of the 303 amino acid scaffolding protein spanning residues 141-303 was capable of promoting assembly both *in vivo* and *in vitro*. Using standard molecular biology techniques, coding sequences encoding short peptides reported to bind TiO_2 (amino acid sequence: CHKKPSKSC) or CdS (amino acid sequence: SLTPLTTSHLRS) were introduced at the N-terminus of the coding sequence of the 141-303 scaffolding protein deletion. We have also generated a construct carrying the sequence RKLPDAPGMHTW which has been reported to nucleate the formation of anatase TiO_2 (Schoen et al. *Template engineering through epitope recognition: a modular, biomimetic strategy for inorganic nanomaterial synthesis.* J. Am. Chem. Soc, 2011, 133 18202-7).

Internal TiO_2 Mineralization of P22

- Peptides for internal mineralization: The peptide sequence CHKKPSKSC was fused to the N-terminus of the central and C-terminal region (residues 141-303) of P22 scaffolding protein (designated T141-303). This peptide was chosen because it had been reported to nucleate the

formation of TiO_2 from TiBALDH precursor. An additional construct carrying the sequence RKLPDAPGMHTW, which has been reported to nucleate the formation of anatase TiO_2 (designated S141-303), was also synthesized. A robust strategy for controlling the amount of fusion protein inside the protein cages by re-entry has been developed and employed insuring high occupancy.

• Characterization of TiO_2 nanoparticles: TiO_2 nanoparticles were formed by incubation of P22 shells loaded with scaffolding fusion proteins T141-303 and S141-303 with TiBALDH under room temperature conditions. Unstained transmission electron microscopy (TEM) and dark field STEM suggested the formation of electron dense clusters contained within the particles. Dynamic light scattering (DLS) and analytical ultracentrifugation (AU) demonstrated that the outer diameter of the protein cage was unchanged following treatment. High resolution TEM (HRTEM) was employed to ascertain whether the electron dense clusters were crystalline TiO_2 (Fig. 1). For both the T141-303 construct and the S141-303 construct distinct lattice fringes were observed. The measured *d*-spacing in the T141-303 particles was 3.2±0.16 Å, which corresponds to the 110 planes of rutile TiO_2 (3.19 Å), while the *d*-spacing in the S141-303 particle was 3.51±0.16 Å, which corresponded to the 101 planes of anatase TiO_2 (3.51 Å). The size of the particles within the protein cage was estimated by dissociation of the protein shell followed by sedimentation velocity AU of the TiO_2 particles (Fig. 2). The particles sediment with a narrow distribution of s-values, which can be used to estimate the diameter of the particles as ~ 4 nm. This diameter is roughly 10% of the internal diameter of the protein cage and suggests that multiple nucleation events are occurring within a given protein cage.

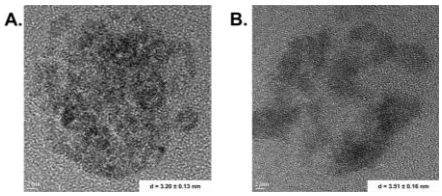

Fig. 1: HRTEM images of P22 stuffed shells containing either the T141303 scaffolding construct (A), or the S141303 scaffolding construct (B). The particles were incubated with TiBALDH for 24 h before imaging. The observed d-spacing in (A) corresponds nicely to the 110 planes of rutile and the *d*-spacing in (B) corresponds nicely to the anatase 101 planes.

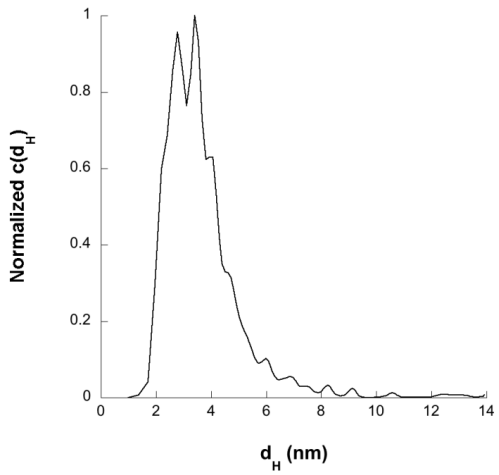

Fig. 2: Particle size distribution of the synthesized TiO_2 inside of P22. These data were obtained by performing a sedimentation velocity experiment with mineralized particles in 6 M GuHCl at 20˚C and 40,000 rpm. These data show that the weight-average TiO_2 particle diameter is ~4 nm. This suggests that nucleation likely occurs at multiple, discrete locations within the PLPs.

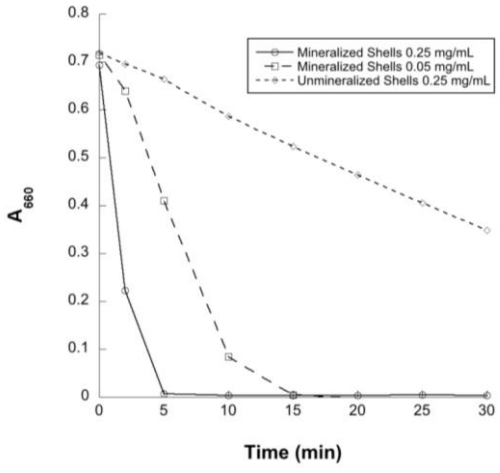

Fig. 3: Plot of A_{660} vs. time measuring the photoreduction of methylene blue in the presence of 0.25 mg/mL mineralized shells (solid line), 0.05 mg/mL mineralized shells (dashed line), or 0.25 mg/mL unmineralized stuffed shells (dotted line). The $t_{0.5}$ values for each of these samples is approximately 2.5 min, 6 min, and 30 min, respectively.

• Photoactivity of TiO_2 containing particles: The photoactivity of the TiO_2 containing particles was evaluated by measuring the photo-reduction of methylene blue (MB) upon illumination with a Xe arc lamp (Fig. 3). Photoreduction of MB results in a decrease in absorbance at 660 nm. Unmineralized shells have a $t_{1/2}$ of photoreduction of approximately 30 min, whereas the $t_{1/2}$ for photoreduction when the same quantity of mineralized shells is included drops to 2.5 min. As expected, smaller quantities of mineralized particles result in intermediate half-times.

Formation Mechanism of CdS Nanocrystals Confined Inside Engineered Virus Procapsid

We have carried out site-specific nucleation and growth of semiconducting cadmium sulfide (CdS) nanocrystals confined inside bacteriophage P22 VLP. To generate CdS binding VLPs the peptide sequence SLTPLTTSHLRS, confirmed to have binding specificity to CdS, was genetically fused onto the scaffolding proteins (SP). Confined synthesis of nanocrystals inside P22 VLP was achieved by incubating $CdCl_2$ with P22 VLP solution, followed by hydrolysis of thioacetamide (TA).

• Characterization of CdS nanoparticles: The Scanning Transmission Electron Microscopy image in Fig. 4 clearly indicates the presence of core/shell structures, confirming the confined growth of CdS inside the P22 procapsids. The average diameter of the shells and cores is determined to be 67.1 nm and 40.6 nm, respectively. Dynamic light scattering measurements indicate that the hydrodynamic size before and after growth remain essentially unchanged (68 nm), further confirming that the growth of CdS occurs inside the P22 VLP. Time-dependence TEM observations and a size-dependence simulation of the growth of CdS indicated that the synthesis of CdS involves initial uniform nucleation on the genetically engineered sites to form nanocrystals with size ~2.5 nm, and then randomly grow into nanoparticles with average size more than 5 nm.

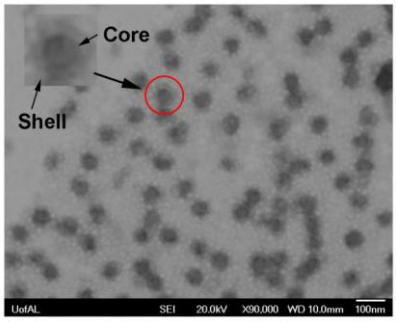

Fig. 4: STEM image of the growth of CdS constrained inside genetically engineered P22 procapsids.

• In-situ monitoring of CdS growth: We have monitored the growth of CdS in-situ by UV-VIS Spectroscopy. The absorbance at 260 nm, attributed to the absorption of thioacetamide, decreases with time, while the absorbance in the range 400 - 500 nm from CdS nanocrystals increases, as shown as Fig. 5. A broad absorption feature with a cut-off at longer wavelength is observed for the absorption of CdS. The absorption shoulder systematically shifts to longer wavelengths with increasing duration of TA hydrolysis. This shift is consistent with the increase in the average size of the nanostructures as observed from TEM. As expected, the integrated absorption intensity increases with reaction time, indicating an increase in the CdS concentration. We have used the spectroscopic data to analyze the TA hydrolysis kinetics under different reaction conditions. Without Cd ions, there is no consumption of HS^- and the TA concentration remains essentially unchanged in engineered P22 VLP solution. In the presence of Cd ions, HS^- is consumed to form CdS, thus favoring further dissociation of TA. Interestingly, as compared to the biotemplated synthesis of CdS, a much faster decrease in the TA concentration is observed in pure aqueous solution of Cd^{2+}. For all the different reactions the experimentally observed decrease in the TA concentration with time is exponential, indicating first order reaction kinetics. As compared to the case without biotemplates or wild-type coat proteins, the

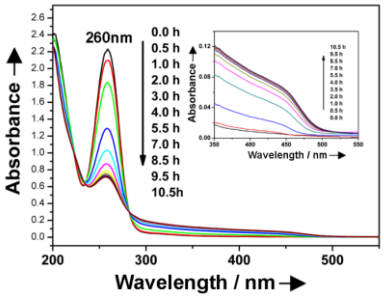

Fig. 5: In-situ observation of the growth kinetics of CdS by UV-Vis spectroscopy from monitoring changes in the absorbance of TA and CdS. The inset shows a magnified plot of the absorbance variation in the range of 550 - 350 nm due to changes in CdS concentration.

final concentration of TA in the engineered procapsid solution is statistically higher, and the rate constant is significantly smaller. In the absence of an engineered biotemplate, Cd ions in solution can combine freely with the sulfur ions released from hydrolysis of TA. However, in the presence of an engineered biotemplate, most of the Cd ions are likely to be bound around the genetically engineered scaffolding sites, which slow down the combination of Cd and S, thus retarding the hydrolysis of TA, and thereby influencing the final hydrolysis equilibrium.

Future Plans:

- Having demonstrated the ability to mineralize the interior and exterior of the particles in a controlled manner we will next generate hybrid particles with external CdS and internal TiO_2 and also hybrids with external gold particles and internal CdS. We will take advantage of two paths towards exterior mineralization with CdS (nucleation and binding preformed CdS particles) and the two paths towards interior TiO_2 mineralization (TiO_2-scaffolding fusion and sillifan-scaffolding fusion). Hybrid particles produced by these different approaches will be analyzed for integrity, stability, and the amount of each component bound. Hybrid structures will also be produced by chemical attachment of gold nanoparticles to the external surface of VLP containing internally mineralized CdS nanoparticles.
- We will focus on characterizing and stabilizing intermediates during the assembly of P22 protein cages. Stabilized assembly intermediates represent platform technology that can be used to pattern different functionalities on the interior and exterior surfaces of the protein cages, as for example in making Janus particles.
- Photoelectrochemical measurements on the TiO_2, along with CdS/TiO_2 and Au/CdS hybrid particles will be performed using an electrochemical analyzer in a standard three-electrode configuration with a platinum counter electrode, a saturated Ag/AgCl reference electrode, and semiconductor working electrode. A heterogeneous photocatalytic reaction apparatus has also been set up to quantitatively measure gas evolution by gas chromatography.

Publications 2012-2013:

1. J. Lucon, S. Qazi, M. Uchida, G. J. Bedwell, B. LaFrance, P.E. Prevelige, Jr., and T. Douglas, "Use of the interior cavity of the P22 capsid for site-specific initiation of atom-transfer radical polymerization with high-density cargo loading", Nature Chemistry 2012, **4**, 781-788.
2. Alison O'Neil, Peter E. Prevelige, Gautam Basu, and Trevor Douglas, "Co-Confinement of Fluorescent Proteins: Spatially Enforced Interactions of GFP and mCherry Encapsulated Within the P22 Capsid" Biomacomolecules 2012, **13**, 3902-3907.
3. X. Zhang, N. Z. Bao, K. Ramasamy, Y-H. A. Wang, Y. Wang, B. Lin, and A. Gupta, "Crystal phase-controlled synthesis of Cu_2FeSnS_4 nanocrystals with band gap around 1.5 eV", Chem. Commun. 2012, **48**, 4956-4958.
4. Kale, Y. Bao, Z. Zhou, P. E. Prevelige, A. Gupta, "Directed self-assembly of CdS quantum dots on bacteriophage P22 coat protein templates", Nanotechnology 2013, **24**, 045603.
5. X. Zhang, N. Z. Bao, B. Lin, and A. Gupta, "Synthesis of wurtzite Cu_2CoSnS_4 nanocrystals and the photoresponse of spray-deposited thin films", Nanotechnology 2013, **24**, 105706.
6. Ziyou Zhou, Gregory J. Bedwell, Rui Li, Peter E. Prevelige, Jr. and Arunava Gupta, "Formation mechanism of inorganic nanocrystals confined inside genetically engineered viruslike particles", in preparation.
7. Gregory J. Bedwell, Ziyou Zhou, Masaki Uchida, Trevor Douglas, Arunava Gupta, and Peter E. Prevelige, Jr., "Biotemplated synthesis and characterization of photoactive TiO_2 nanoparticles inside a P22-derived Protein Cage nanoarchitecture", in preparation.

Designing Smart, Responsive Communicating Microcapsules from Polymersomes

Daniel A. Hammer (PI) and Daeyeon Lee (co-investigator)
Department of Chemical and Biological Engineering
University of Pennsylvania
Philadelphia, PA 19104

Program Scope

The overall goal of this work is to make systems of communicating micro-sized particles, inspired by the theoretical work of Balazs [1-3]. The general principal of these systems is that capsules can move in a coordinated way when source capsules release attractors or repellers that induce the motion of neighboring capsules. The hydrodynamic coupling between capsules can induce coordinated motion from capsules that are positioned in ordered arrays.

We propose to test the principles of coordinated motion using polymersomes and other engineered capsules. Polymersomes are vesicles whose membranes are assembled from di-block co-polymers [5]. Polymersomes can be widely engineered through changes in polymer chemistry and solutes and particles can be packaged within vesicles in controlled ways using microfluidics. Using microcontact printing and stamping, we can print adhesive ligands in precise arrays on surfaces, and position adhesive vesicles in patterns. We have also developed ways of controlling the release of contents from vesicles and other capsules in response to light or pH. The goal is to assemble these components spatially and precisely and then elicit collective motion of capsules. The specific goals of this project are to:

1. To make well-defined capsules with encapsulated nanoparticles and solutes. We will use a double emulsion injection method to make uniform populations of polymersomes with nanoparticles encapsulated within the aqueous lumen or hydrophobic shell. Furthermore, we will broaden the palette of molecules that can be assembled into vesicles that possess the requisite elements that will also us to make responsive vesicles.

2. To demonstrate release from capsules, either driven by light or pH. To make light sensitive vesicles, we will incorporate porphyrins or gold particles in the hydrophobic shell. For optically sensitive polymersomes, we will measure the rate of release of nanoparticles as a function of the intensity and duration of light illumination. For pH sensitive polymersomes, we will measure the release of nanoparticles as a function of pH and polymer composition.

3. To use specific adhesion and micro-contact printing to make specific spatial arrays of polymersomes and microparticles. We will primarily employ carbohydrate-lectin and biotin-avidin binding for particle immobilization. We will place adhesive ligands in specific patterns using microcontact printing, and adhere both polymersomes and polystyrene microparticles to printed arrays. Patterns will be motivated by published theoretical predictions of inter-particle spacing that give rise to collective motion.

4. Demonstration of collective motion of micron-sized particles in response to light and pH. We will adhere particles weakly on printed arrays. We will combine photoresponsive or pH sensitive polymersomes or protein vesicles, equipped with nanoparticles, as signaling particles, and vary the density and spacing of target receiving particles. Collective motions will be catalogued as a function of interparticle spacing, nanoparticle density, and particle size. A long-term goal of the project is to compare haptokinesis (in which signaling particles emit nanoparticles that adsorb to substrates, thus pinning the gradient) to chemokinesis (in which

soluble molecules adsorb to the surface of the surface of the target particles) as a means of driving the directed motion of particles.

Recent Progress

1. Making polymer vesicles by double emulsion methods. We have established double emulsion-templating microfluidics to make large populations of giant polymer vesicles of uniform size. Illustrated in Figure 1, we can precisely control the number of 400 nm aminated-polystyrene nanoparticles we entrap inside the vesicle. We used micropipette aspiration to both track and

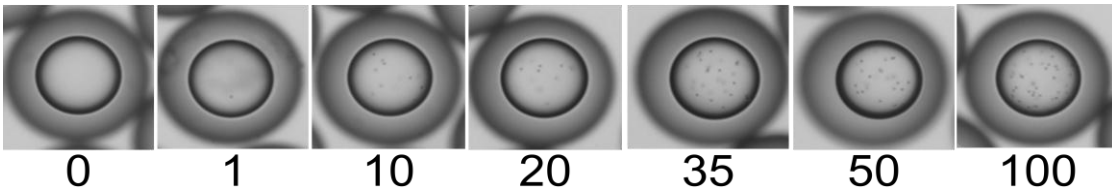

Figure 1. Incorporation of different numbers of 400 nm amine-PS nanoparticles, ranging from 0 to 100, within PEO-PBD block-co-polymer vesicles by double emulsion templating microfluidics.

verify solvent removal from double emulsion-templated polymersomes. This paper has now been published (publication Kamat et al., (2011)).

2. Making responsive polymer shells using microfluidics. Another way of inducing temporal hydrolysis of microcapsules is using poly lactic-glycolic acid (PLGA), which is pH sensitive. PLGA mediates long time-scale release, and will be useful when sustained release is needed. Furthermore, we will need particles of different chemistry on our arrays to induce communication, since we need sensors and responders. The stability and size of PLGA-containing double emulsions and microcapsules are controlled by varying the composition of water-in-oil-in-water (W/O/W) double emulsions. The size of PLGA-containing double emulsions and the resulting microcapsules can be readily tuned by osmotic annealing, which depends on the concentration ratio of a solute in the inner and outer phases of double emulsions. The osmotic annealing method can also be used to concentrate the encapsulated species such as colloidal suspensions and biomacromolecules within the PLGA shells. We have been able to assemble PLGA microparticles of controlled size (publication Tu & Lee, 2012).

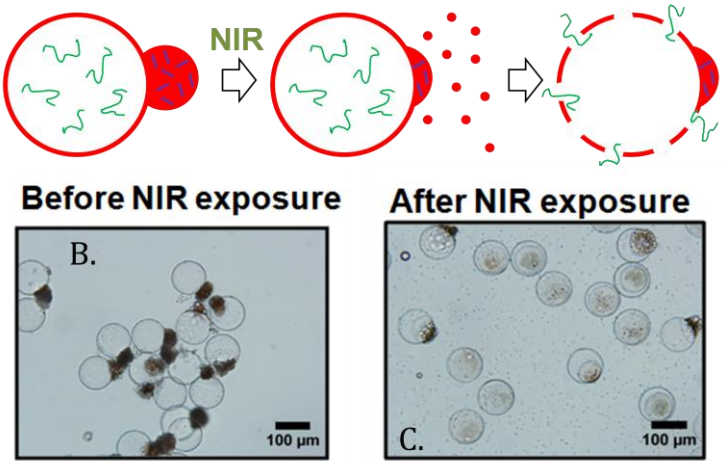

Figure 2. Gold nanorods entrapped in the shell of a PLGA capsule enable the release of entrapped nanoparticles in response light [4].

Furthermore, one of us (Lee) has illustrated the release of fluorophores and nanoparticles from PLGA with embedded gold nanorods by near IR illumination. PLGA particles were made by microfluidics with gold nanorods entrapped in the membrane. Illumination leads to the release

of entrapped nanoparticles (shown, Figure 2) or fluorophores (not shown) [4]. These particles provide an attractive alternative for our materials to engineer nanoparticle release.

3. Vesicles from recombinant proteins. We have assembled vesicles and other defined nanostructures from recombinant proteins. The molecules are naturally biocompatible, are of a single molecular weight as specified by recombinant methods, and hold the promise of designer biofunctionality, including adhesion moieties, protease cleavable domains, and catalytic domains, that could easily be incorporated within the surfactant by changing the gene that codes for the protein.

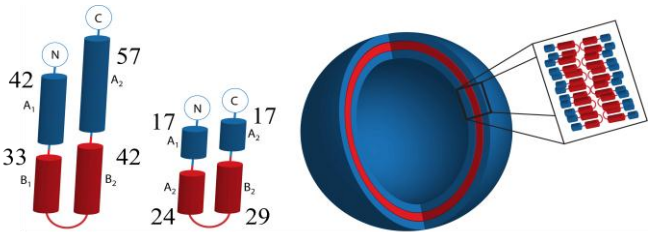

Figure 3. WT oleosin (left) and a shrunken version of oleosin (M1) center make protein vesicles. Oleo-M1 has a pH switch that allows conversion between vesicles and micelles.

We have made vesicles from recombinant proteins for the first time from the naturally occurring sunflower protein oleosin (publication Vargo et al., 2012). We used cryo-TEM to confirm self-assembled structures and studied the phase behavior of protein self-assembly as a function of solution ionic strength and protein hydrophilic fraction, observing nanometric fibers, sheets, and vesicles. Within the goals of the current DOE-funded project, we are constructing two types of responsive olesoin vesicles. One is an oleosin that includes a *pH switch*. By truncating the hydrophobic core of wild-type oleosin to 65 residues, we made a variant of oleosin called oleo-M1 (Figure 3) with a pK of 7.4. At more acidic pH's, the head groups are more protonated, which induces a curvature into the headgroups, and forces the structures out of the vesicles and into worm micelles and fibers. At pH's higher than 7.4, the chains can be tightly packed, and vesicles form. Therefore, the pK of the hydrophilic chains represents a pH switch that can be engineered to induce changes in structure from vesicles to worms, thus releasing entrapped contents. The other responsive elements are protease cleavable domains. Proteases are highly specific enzymes that attack defined peptide sequences in the backbones of proteins. With the tools of molecular biology, we can insert protease cleavable domains of defined sequence into any parts of the oleosin molecule we wish. We hypothesize that proteases can induce dynamic interconversion of structures, as well as coordinated release of materials from oleosin vesicles. We inserted the enterokinase cleavable domain (DDDDK/) at different locations of an oleosin, 11, 22, and 32 residues from the end of the protein, and treatment with protease yielded fragments as expected. We are now in the process of making vesicles from these materials to test release in response to protease activity.

4. Patterning vesicles in spatial arrays. We have micropattering adhesion molecules onto PDMS arrays by microstamping avidin, and then positioning vesicles made by microfluidic technologies by specific adhesive interactions. Stamps of defined geometry were made and used to ink surfaces with Neutravidin. Circles of 10 and 50 microns in diameter were made with a rhodamine fluorescent avidin, and the interspot spacing was varied over a wide range (see Figure 4). FITC and biotinylated-vesicles made by double emulsion methods containing 5% biotinylated PEO-PBD polymer. These vesicles were specifically bound to arrays with up to 75% coverage of the surface. The ability to make patterned arrays of defined geometry with adjustable numbers of uniform polymersomes is central to our goal of making communicating arrays. A paper on making polymersome arrays has appeared (publication Kamat, et al. (2013)).

5. Vesicle motility. We have made a significant step generating vesicles that can display random motility on weakly adherent surfaces. Glass slides were blocked with heat denatured BSA at 2%, and giant vesicles from PEO-PBD were made by microfluidics and imaged by interference reflection microscopy. Thermal fluctuations induced vesicle motion and translocation as the vesicle made and broke contacts.

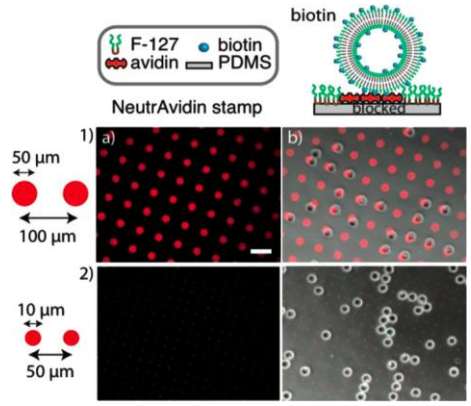

Figure 4. Biotinylated vesicles can be positioned on micro-contact printed avidin arrays with high spatial fidelity. Both 50 and 10 micron spots were made. Nonspecific adhesion was prevented by F127 pluronic.

Future Plans

We will encapsulate nanoparticles within microfluidically generated capsules (polymer vesicles that hydrolyze in response to pH, PLGA microshells that are activated by light, and protein vesicles that release in response to pH or proteases) and measure the release of nano-particles. We will then induce directed motion on weakly adherent particles by imposing a gradient of functionalized nanoparticles, deliver by a pipette. Also, we will measure the motility of weakly adherent polymer vesicles on microcontact printed surfaces with weak adhesion chemistries, including low affinity avidins and carbohydrate/selectin interactions. Finally, we will build arrays and measure displacement of adherent particles by competitive nanoparticles.

References

1. Bhattacharya, A., … and A.C. Balazs, *Self-Sustained Motion of a Train of Haptotactic Microcapsules.* Langmuir, 2009. 25(17): p. 9644-9647.

2. Kolmakov, G.V…. and A.C. Balazs, *Designing communicating colonies of biomimetic microcapsules.* PNAS USA, 2010. 107(28): p. 12417-12422.

3. Usta, O.B., A. Alexeev, G. Zhu, and A.C. Balazs, *Modeling microcapsules that communicate through nanoparticles to undergo self-propelled motion.* Acs Nano, 2008. 2:471-476.

4. Lee, M.H., … J.A. Burdick, and D. Lee, *Harnessing Interfacial Phenomena to Program the Release Properties of Hollow Microcapsules.* Adv. Func. Materials, 2012. 22, 131-138.

5. Discher, B.M. … F.S. Bates, D.E. Discher, and D.A. Hammer, *Polymersomes: tough, giant vesicles made from diblock copolymers.* Science, 1999. 284:1143-1146.

Publications

1. N.P. Kamat, S. J. Henry, D. Lee, and D. A. Hammer (2013). "Single vesicle patterning of uniform, giant polymersomes into microarrays," in press, Small, published online: 6 MAR 2013.

2. Neha P. Kamat, Myung Han Lee, Daeyeon Lee, and Daniel A. Hammer, (2011), "Micropipette aspiration of double emulsion generated, unilamellar polymersomes", Soft Matter 7:9863-9866, doi: 10.1039/C1SM06282D.

3. K. B. Vargo, R. Parthasarathy and D. A. Hammer, (2012). "Tunable Protein Suprastructures from Recombinant Oleosin", Proc. National Academy of Sciences USA 109 (29) 11657-11662.

4. J. S. Katz, K. A. Eisenbrown, E. D. Johnston, N. P. Kamat, J.A. Burdick and D. A. Hammer, (2012). "Soft Biodegradable Polymersomes from Caprolactone-Derived Polymers," Soft Matter 8, 10853 – 10862.

5. F. Tu, D. Lee "Controlling the Stability and Size of Double Emulsion-Templated Poly(lactic-co-glycolic)acid Microcapsules", Langmuir, 2012, 28, 9944-9952.

6. Hammer, D.A. and N.P. Kamat. (2012). "Towards an artificial cell," FEBS Letters 586 (18):2882-2890.

Surface Mechanical Properties of Bio-Inspired Architectures

Anand Jagota* (anj6@lehigh.edu) and Chung-Yuen Hui[&] (ch45@cornell.edu)

* D331 Iacocca Hall, Chemical Engineering, Lehigh University, Bethlehem PA 18015;
[&] Sibley School of Mechanical and Aerospace Engineering, Cornell University, Ithaca.

1. ***Program Scope:*** Our aims are to fabricate, study, and model bio-inspired architectures for controlled surface mechanical properties. The current focus of our work is on

- *Selectivity of Adhesion by Shape Complementarity*. We are studying how, by patterning a surface by an array of features such as ridges and channels, one can endow it with highly selective and enhanced adhesion.
- *Role of Solid Capillarity in Soft Biomaterials*. Forces due to solid capillarity that are usually negligible for conventional materials can play an important role in soft solids such as biomaterials. We are studying the role of solid capillarity in two different situations: flattening of a structured surface and deformation of thin films due to liquid drops.

2. ***Recent Progress:*** Our main recent accomplishments are

Selectivity of Adhesion by Shape Complementarity A common motif in nature is that of selective adhesion by shape complementarity. We have been investigating if and how simple patterning of an elastomeric material surface can endow it with selectivity of adhesion. Previously, in collaboration with Prof. Shu Yang of the University of Pennsylvania, we showed that highly selective adhesion can be achieved by using rippled surfaces. Recently, we have studied how patterning a surface with ridges and channels enhances its adhesion against a shape-complementary surface while at the same time attenuating its adhesion against other surfaces [1,2]. Figure 1 (a) (inset) shows scanning electron micrographs of two complementary patterned surfaces. For such shape-complementary surfaces, Figure 1 (a) shows that adhesion (characterized by energy release rate) can be enhanced by up to a factor of 40 compared to a flat, unstructured, control. The main surprising result is not so much that inter-penetrating ridge-channel structures result in strong adhesion but that, after being separated once, such shape-complementary surfaces can be made to adhere to each other in the presence of inevitable misalignment. Low-magnification optical micrographs of surfaces pushed into contact (Figure 1 b) are marked by striations. Upon examination at higher resolution (Figure 1b), we find that these striations are dislocations (usually screw in nature) that accommodate relative misorientation between the two patterned surfaces. Whereas dislocations permit adhesion of the two misaligned patterns in the first place, they also carry elastic strain energy, the release of which aids interfacial separation and is directly responsible for the reduction in interfacial adhesion with increasing interchannel spacing. We have modeled the structure and energetics of screw dislocations and are able to explain quantitatively several experimental observations, e.g., (i) dislocation density depends on relative misorientation; (ii) the structure of each dislocation is independent of global misorientation and depends only on material properties and the Burgers vector, (iii) The size of the dislocation core can be predicted by an energy balance argument, and (iv) the reduction in overall adhesion with increasing interchannel spacing can be related to elastic energy released by dislocations.

Figure 1(c) shows that strong selectivity of adhesion can be achieved by such structures. While this complementary pair of surfaces enhances adhesion by about a factor of 10, non-complementary surfaces (with a few special exceptions), show much reduced adhesion.

Role of Solid Capillarity in Soft Biomaterials

The surface tension of solids usually causes negligible deformation because in conventional materials the surface tension is a weak force compared to the resistance due to elasticity. For compliant materials, such as hydrogel-like biomaterials, surface tension can play a dominant role in many phenomena, but has been little studied until recently.

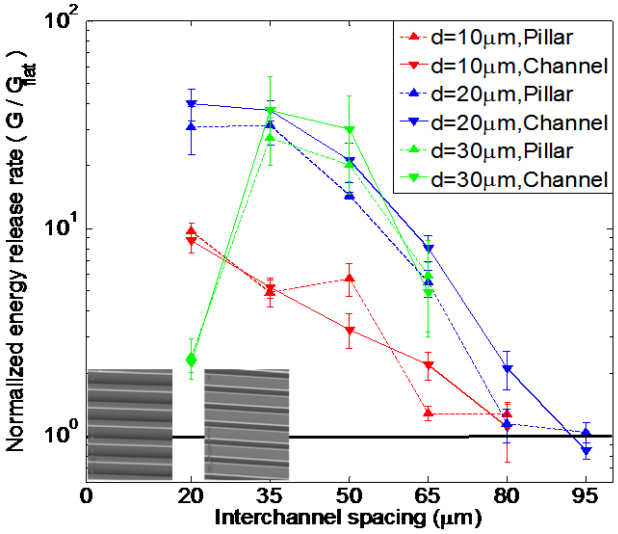

(a)

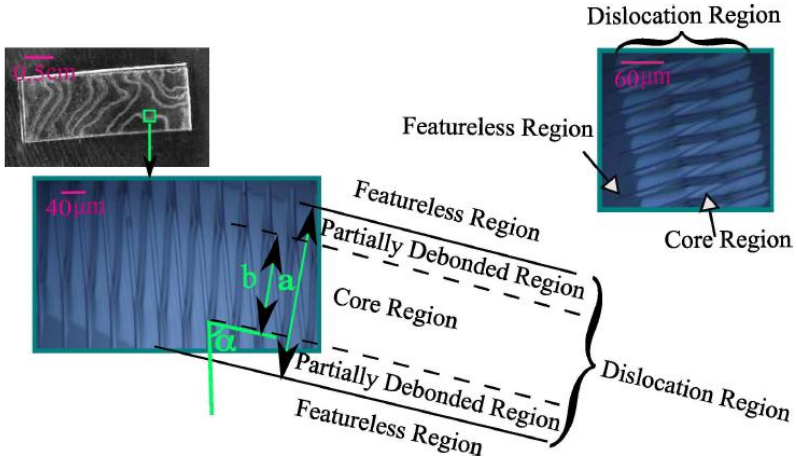

(b)

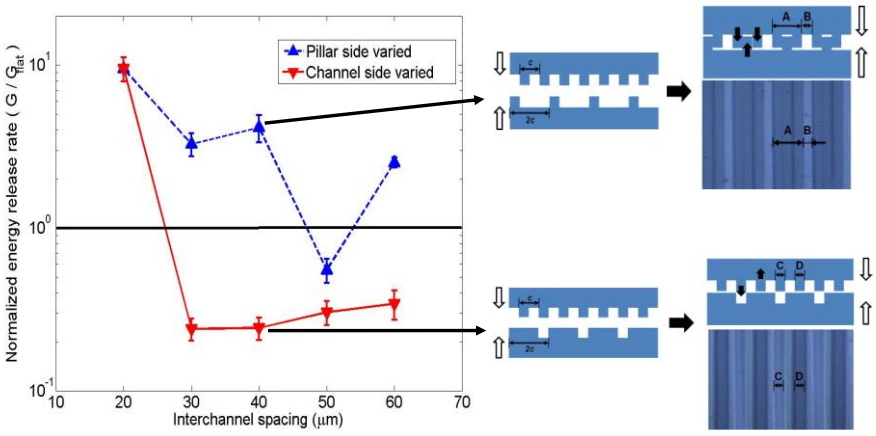

(c)

Figure 1 (a) Inset: Scanning electron micrograph of two complementary surfaces. Adhesion can be enhanced by up to a factor of 40 compared to a flat control. (b) A low-magnification optical micrograph shows the presence of striations. Higher magnification micrographs reveal that these striations are dislocations which accommodate relative misorientation between the two patterned surfaces. Release of the elastic energy stored in these dislocations weakens the interface and the decrease in adhesion with increasing inter-channel spacing is directly related to the increase in dislocation elastic energy. (c) Whereas complementary shapes enhance adhesion, mismatched shapes give much reduced adhesion, thereby demonstrating selectivity by shape recognition.

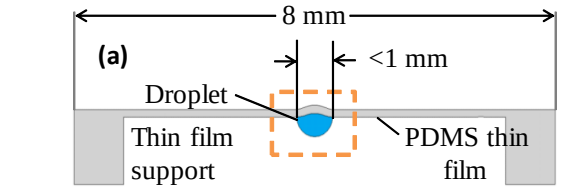

(a)

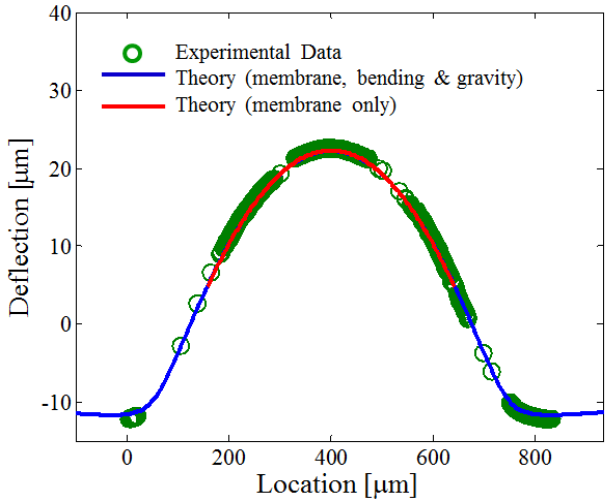

(b)

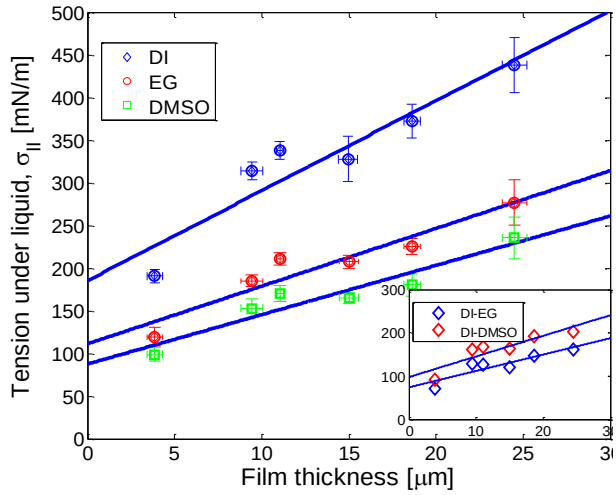

(c)

Figure 2 (a) Schematic drawing of a film suspended across a cylindrical hole with a water drop on its lower surface. (b) The Laplace pressure in the drop causes it to bulge by tens of microns (c) Analysis of the deformation yields tension in the solid film which, extrapolated to zero thickness, provides an estimate of solid surface tension.

In our work, we have investigated surface tension of soft solids. In one approach, we have shown that the amplitude of surface structures patterned on a hydrogel is attenuated due to the action of surface tension [3]. We demonstrated that surface tension of a material with modulus in the tens of kPa can reduce the amplitude of surface undulations by more than 60%. This process can be modeled quantitatively and measured amplitude reduction can be used to extract a value of solid surface tension.

We have also studied liquid surface-tension induced deformation of several-micrometer-thickness films spanning relatively large cylindrical holes [4] (Fig 2a). The interplay of liquid-vapor surface tension and tensions in the solid film results in a bulged membrane (Fig 2b). Its equilibrium shape can be analyzed by force balance, a version of Neumann's triangle, providing a novel method for estimating the film tension by measurement of bulge deformation. In the limit of vanishing membrane thickness, film tension may be interpreted as solid-fluid surface tension (Fig. 2c). Because deflections are quite significant, it permits the use of PDMS, a relatively stiff material in this area of research, but one that provides many conveniences. By using this technique, one can measure the surface tension of thin films in contact with both a liquid and air. Furthermore, this simple technique can potentially be used for measurements on a greater variety of materials by using an elastomeric thin film as a support substrate for stiffer and thinner (say, a few nanometers thick) materials.

3. Future Plans

Selectivity of Adhesion by Shape Complementarity. We have found that the key factor controlling the adhesion of shape-complementary interfaces is the type and mechanics of interfacial defects (e.g., dislocations) that are needed to accommodate imperfection and misorientation. We will address the following issues for 1D and 2D structures:

(a) How do the interfacial properties depend on geometrical parameters of the structure?
(b) What is the nature of interface dislocations that accommodate relative misorientation, stretch, and shear? How do they affect the energetics of interfacial separation?

Role of Solid Capillarity in Soft Biomaterials. We will continue to study experimentally and theoretically two aspects of capillarity in soft solids:
(a) Deformation and shape change driven by surface tension,
(b) Using elastic capillarity *directly* to measure surface tension of solids or to "close Young's equation" in a single experiment.

4. References and Publications which acknowledge DOE support (August 2011- August 2013)

1. Arun K. Singh, Ying Bai, Nichole Nadermann, Anand Jagota, Chung-Yuen Hui, "Adhesion of Micro-Channel Based Complementary Surfaces," *Langmuir*, **28** (9) 4213-4222 (2012).
2. Congrui Jin, Anand Jagota, Chung-Yuen Hui, "Structure and Energetics of Dislocations at a Micro-Structured Complementary Interface Govern Adhesion," *Advanced Functional Materials* DOI: 10.1002/adfm.201203337 (2013).
3. Anand Jagota, Dadhichi Paretkar, Animangsu Ghatak, "Surface-tension-induced flattening of a nearly plane elastic solid," *Physical Review E* **85**, 051602 (2012).
4. Nichole Nadermann, Chung-Yuen Hui, Anand Jagota, "Solid Surface Tension Measured by a Liquid Drop Under a Solid Film," *Proceedings of the National Academy of Sciences*, DOI 10.1073, (2013).
5. Ying Bai, Congrui Jin, Anand Jagota, C-Y. Hui, "Adhesion Selectivity by Electrostatic Complementarity: Part I, One-dimensional stripes of charge," *Journal of Applied Physics*, **110** (5) 054902 (2011).
6. Congrui Jin, Ying Bai, Anand Jagota, and Chung-Yuen Hui, "Adhesion Selectivity by Electrostatic Complementarity: Part II, Two dimensional Analysis," *Journal of Applied Physics*, **110** (5) 054903 (2011).
7. Anand Jagota and C-Y. Hui, "Adhesion, Friction, and Compliance of Bio-mimetic and Bio-inspired Structured Interfaces," *Materials Science and Engineering – Reviews*, **72** 253–292 (2011).
8. C. Jin, A. Jagota, C-Y. Hui, "An easy-to-implement numerical simulation on adhesive contact problems involving complex geometries," *J. Phys. D: Appl. Phys*. **44** (2011) 405303.
9. Congrui Jin, K. Khare, S. Vajpayee, S. Yang, A. Jagota, C-Y. Hui, "Adhesive Contact Between a Rippled Elastic Surface and a Rigid Spherical Indenter: From Partial to Full Contact," *Soft Matter* **7** (22), 10728 - 10736 (2011).
10. C.Y. Hui and R. Long, " Direct extraction of work of adhesion from contact experiments: Generalization of JKR Theory to Flexible Structures and Large Deformation." *Journal of Adhesion*, **88**,70-85, (2012).
11. Katrin Brörmann, Karin Burger, Anand Jagota, Roland Bennewitz, "Discharge during detachment of micro-structured PDMS sheds light on the role of electrostatics in adhesion," *Journal of Adhesion*, **88** [7] 589-607 (2012).
12. Hall, M. S.; Long, R.; Hui, C. Y.; Wu, M., Mapping 3D stress and strain fields with a soft hydrogel using a Fluorescence Microscope. *Biophyiscal Journal* **102** (10), 2241-2250, (2012).
13. C.Y. Hui, Xinzeng Feng and A. Jagota, "In-situ measurement of the viscoelastic modulus of gels using pure twist – Theory", *Soft Matter* **9**, 913–920 (2013).
14. X. Xu, A. Jagota, S. Peng, D. Luo, M. Wu, C.Y. Hui, "Gravity and Surface Tension Effects on Shape Change of Soft Materials", accepted for publication by *Langmuir*, July 1, (2013).

Program Title: Enzyme-Controlled Mineralization in Biomimetic Microenvironments Formed by Aqueous Phase Separation and Giant Vesicles

Principle Investigator: C. D. Keating
Department of Chemistry, Pennsylvania State University, University Park, PA 16802.
E-mail: keating@chem.psu.edu

Program Scope

The goal of the program is to develop a fundamental understanding of the mechanisms by which biological organisms control the structure and properties of materials during synthesis. Living cells perform mineralization at ambient temperature and pressure, in specially controlled microenvironments often smaller than a single cell. This crucial aspect of how living organisms control the process and outcome of reactions has received little emphasis in the biomimetic mineralization literature, perhaps because experimental systems for generating microcompartments were lacking. The program will perform studies of mineralization in biomimetic microcompartments. Such studies will provide new insight into how organisms control materials growth on the microscale, ultimately leading to nonbiogenic materials synthesis strategies with extraordinary structural and compositional control, for potential applications ranging from low-power electronics to solar cells.

A particular focus of the program is materials synthesis in macromolecularly crowded microcompartments provided by aqueous phase – separated systems and bounded by lipid vesicles. Aqueous two-phase systems (ATPS) form when two or more polymers are present in water at several weight percent [2]. They provide a spatially heterogeneous and biocompatible solvent system that models the macromolecular crowding observed in vivo, in which local concentrations, partitioning, and diffusion-limited reaction fronts can be controlled and symmetry-breaking can be achieved [3]. Molecular partitioning of solutes between the two phases of an ATPS provides a means of control over local concentrations of enzyme catalysts, metal cations, and other molecules that participate in the reactions [4]. By encapsulating aqueous phase systems within semipermeable microscale reaction vessels, artificial mineralizing vesicles will be produced to perform materials synthesis. It is anticipated that the approach should be quite general and will be applicable to many materials systems including but not limited to those traditionally formed by living systems. The program initially focuses on the well-characterized biogenic material $CaCO_3$ to determine what advantages synthesis in aqueous phase systems and mineralizing vesicles can offer over existing methods. The goal is to both understand and emulate the exquisite control that living systems routinely exert over mineral deposition.

Recent Progress

Background. When living cells perform biomineralization, they do so in crowded environments filled with many macromolecules, only some of which are thought to be actively involved in the mineralization process. The process typically occurs within specialized subcellular organelles called mineralizing vesicles. These structures fulfill several key requirements for intracellular mineral precipitation. Perhaps most critically, they compartmentalize the reaction so that the rest of the organism is protected from the mineralizing conditions, e.g. high Ca^{2+}, high pH, solid mineral formation. Additionally, these mineralizing compartments provide favorable conditions for nucleation and growth of specific morphologies, crystal forms, and compositions of material.

Discussion of findings. *(1) Localized mineralization in ATPS.* Mineralization in the presence of high concentrations of background macromolecules was shown to produce similar final products as in the absence of these molecules, as determined by powder x-ray diffraction and scanning electron microscopy analysis. Addition of a morphology-directing additive also yielded essentially the same results in the presence and absence of the polymers. We further demonstrated that enzyme partitioning into one of two coexisting aqueous phases could be used to restrict $CaCO_3$ formation to only this phase, based on local availability of carbonate [1].

Significance. This is important because it indicates that mineralization in ATPS is a viable means of compartmentalization, and that this system will not necessitate "reinventing the wheel" with regards to existing knowledge of molecules that have been found to modify $CaCO_3$ mineralization in polymer-free solutions.

(2) Development of artificial mineralizing vesicles. A very simple experimental model for biomineralizing vesicles has been developed based on ATPS emulsion droplets that are stabilized by a corona of lipid vesicles. These structures are simple to prepare, capture several key properties of their biological counterparts, and offer additional benefits for biomimetic mineralization research. The droplets are not themselves lipid vesicles –which are difficult to produce in uniform, high-yield populations under conditions conducive to mineralization, such as 20 mM Ca^{2+}, and which require modification with transporter peptides or proteins to permit entry/egress of ions and molecules. Rather, they are a new form of stabilized emulsion droplets, in which both phases are aqueous polymer solutions. As such, they are related to the well-known Pickering emulsions [5], in which microparticle assembly at oil/water interfaces stabilizes the oil/water or water/oil emulsion.

Our water-in-water emulsions consist of a dextran-rich and a PEG-rich phase. At the boundary between the phases are many ca. 200 nm ("large") diameter unilamellar lipid vesicles, or LUVs. Figure 2 shows dextran-rich phase droplets dispersed in a continuous, PEG-rich phase. The red fluorescence arises from rhodamine-labeled lipids at the interface: these lipids exist in many, individual LUVs rather than as a single continuous bilayer. This has been demonstrated by a combination of fluorescence recovery after photobleaching, transport, and LUV release studies. Because the LUVs do not fuse, even relatively large solutes can diffuse into the stabilized droplets (i.e. artificial mineralizing vesicles) across the LUV corona.

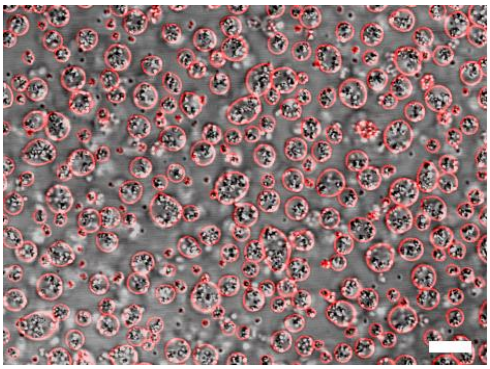

Figure 2. Urease-catalyzed, localized $CaCO_3$ precipitation in a chelator-stabilized LUV emulsion. Precipitation is occurring uniformly across the population of droplets. Overlaid transmitted (DIC) and fluorescence (labeled lipid) channels. Scale = 10 μm.

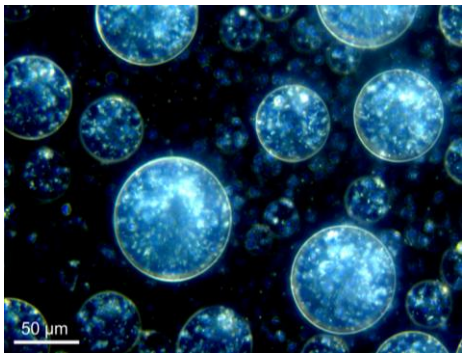

Figure 3. Dark field optical microscope image of $CaCO_3$-containing stabilized dextran-rich droplets in a continuous PEG-rich aqueous phase. Mineralization is localized within the dextran-rich phase microcompartments due to the higher concentration of urease inside.

Figure 2 shows enzymatically-produced $CaCO_3$ mineral formed within this experimental system; the reaction was initiated by adding the substrate, urea, to the artificial mineralizing vesicles. After $CaCO_3$(s) production, the droplets remain intact and the vast majority of the mineral appears to be located within them. In this image, the fluorescence channel (red) that shows LUV location is confocal, i.e. it's image depth in the vertical direction is quite small, while the transmitted differential interference contrast (DIC) image views a much thicker "slab" of the sample. Figure 3 illustrates more clearly that the mineral is inside the droplets. This darkfield image highlights scattering from the mineral itself, and, to a lesser extent also from the droplet boundaries. For this lipid composition, we do not see preferential nucleation on the LUV corona; future experiments will alter the lipid composition to influence nucleation site.

Experiments are underway in which mineralization-directing additives are being added to the model mineralizing vesicle system. We have begun this work with polyaspartic acid (PAA) because this molecule had previously been implicated in formation of polymer-induced liquid precursors (PILPs)[6]. This liquid precursor is likely a coacervate phase formed when Ca^{2+} binding renders the polymer less well solvated. Such a phase is attractive both because something similar is likely to occur in mineralizing organisms and because it promises a pathway to forming and stabilizing the amorphous calcium carbonate phase (ACC) long enough to control the overall shape and dimensions of its crystallization, allowing it to adopt the shape of its container. When PAA is added to the PEG/dextran ATPS, it partitions somewhat into the dextran-rich phase. In the presence of Ca^{2+}, it forms a third, PAA-rich phase that presumably also contains most of the Ca^{2+}. Mineralization releases PAA back into the dextran-rich phase, eventually resulting in mineral formation throughout it. Work is ongoing to better characterize this system both in terms of its assembly, its mineralization reaction, and the physical properties of the resulting mineral phase, which we expect is ACC and will verify by vibrational spectroscopy.

Significance. The artificial mineralizing vesicles developed here are of interest both practically and from a fundamental perspective. They solve key challenges in experimentally producing robust, high-yield biomimetic microscale mineralizing compartments for use in further studies. From a more fundamental standpoint, these vesicle-stabilized droplets are a new type of biomimetic Pickering-style emulsion system in which the particulates are noncovalent assemblies, and both the dispersed and continuous phases are crowded aqueous solutions, compatible with, and able to localize, enzymatic activity.

Future Plans

(1) Characterization of materials formed in model mineralizing vesicles. Work will continue on performing mineralization within these compartments, and we will move towards more thorough characterization of where the Ca^{2+} ions are as a function of time (which phase, free vs. bound, etc) and on collecting post-mineralization samples for further analysis by XRD, SEM, SIMS, and vibrational spectroscopy. Additional known mineralization-directing additives will be tested. We hope to see a clearer control over the mineral shape from the shape of the reaction container and/or site of nucleation within the containers. We anticipate that by control over container morphology and organization (e.g., many PAA/Ca^{2+} droplets vs. one, lipid headgroup chemistry, etc.), it should be possible to control morphology and to generate hierarchical structures.

(2) Mechanistic studies of aqueous-aqueous Pickering emulsions. These LUV-stabilized water-in-water emulsions are an interesting new type of structure, so in addition to using them as

mineralization compartments, we are also working to understand their physical properties and mechanism of formation. They differ from traditional Pickering emulsions in several ways: (i) In all-aqueous phase systems the interfacial tension is orders of magnitude lower than for oil/water, and consequently provides less of a driving force for particle assembly at the interface. (ii) Because both phases are aqueous, electrostatic effects work differently in ATPS emulsions as compared to oil/water. Finally, (iii) polymeric volume excluders are present in both phases of our ATPS emulsions. Experiments will be performed to understand the mechanism by which stabilization occurs in these systems. This will provide insight into how versatile these structures are, and how they can be used in materials synthesis.

(3) Mineralization in nonequilibrium structures. Efforts will be undertaken to control and understand what dictates the site of mineralization within the complex droplet morphologies when multiple subcompartments are present within droplets and/or giant vesicles, and what controls wettability at the interior/exterior interface during this process. This understanding will lead to better control over the shape of mineral that is deposited. In addition, although we have a working system for mineralizing vesicles now with the LUV-decorated droplets, it is of interest to go back now and use what we have learned in stabilizing these droplets to see if we can now produce decent yields of ATPS-containing giant unilamellar lipid vesicles[3] in an analogous way.

References

1. Biocatalyzed mineralization in an aqueous two-phase system: Effect of background polymers and enzyme partitioning. Cacace, D. N.; Keating, C. D., *J. Mater. Chem. B* **2013**, *1*, 1794-1803.
2. Albertsson, P. *Partition of Cell Particles and Macromolecules* John Wiley & Sons, New York, 2nd edn, 1960.
3. Aqueous phase separation as a possible route to compartmentalization of biological molecules. Keating, C. D. *Accounts of Chemical Research* **2012**, *45*, 2114-2124.
4. RNA catalysis through compartmentalization. Strulson, C. A.; Molden, R. C.; Keating, C. D.; Bevilacqua, P. C. *Nature Chem*. **2012**, *4*, 941-946.
5. Zeng, C.; Bissig, H.; Dinsmore, A. D. Particles on droplets: From fundamental physics to novel materials. *Solid State Commun*. **2006**, 547-556.
6. Gower, L. B. Biomimetic model systems for investigating the amorphous precursor pathway and its role in biomineralization. *Chem. Rev*. **2008**, 108, 4551-4627.

DOE-Supported Publications

1. Biocatalyzed mineralization in an aqueous two-phase system: Effect of background polymers and enzyme partitioning. Cacace, D. N.; Keating, C. D., *J. Mater. Chem. B* **2013**, *1*, 1794-1803. (front cover).
2. Inorganic protocells: Gated access to microreactors. Keating, C. D., *Nature Chem. (News & Views)* **2013**, *5*, 449-451.

Program Title: DNA-Grafted Building Blocks Designed to Self-Assemble into Desired Nanostructures

Principle Investigator: S. Kumar
Co-PIs: V. Venkatasubramanian, M. Collins and O. Gang (BNL)
PI Address: Department of Chemical Engineering, Columbia University
Mailing Address: 500 W. 120th St. Mudd 510, New York, NY 10027
E-mail: sk2794@columbia.edu

Program Scope

Conventional experiments and modeling of DNA-grafted nanoparticle building blocks (DNA-NPs) follow the traditional Edisonian model of trial and error (Fig. 1 "Forward Problem"). While this approach has led to the development of new theories and interesting simulation results[1-4], it does not allow for specific design of the nanoparticles such that they will self-assemble into a desired structure. In order to address this issue, we seek to define a new inverse procedure (Fig. 1 "Reverse Problem"). Essentially this involves determining the parameters with which to design the building blocks so that they will spontaneously self-assemble into a pre-determined desired structure. The new approach demands for the development of a novel model that can accurately and quickly converge to a solution despite the presence of non-linear relationships of DNA-NPs modeling and the large space of possible crystal structures. Previous studies performed by Venkatasubramanian[5-7] indicate that genetic algorithms (GA) are particularly suited for these optimization requirements. As a result, the main goal of the project will be to develop combine a forward modeling approach with the genetic algorithm to create a hybrid GA model that allows for the bottom-up design of DNA-NPs self-assembly.

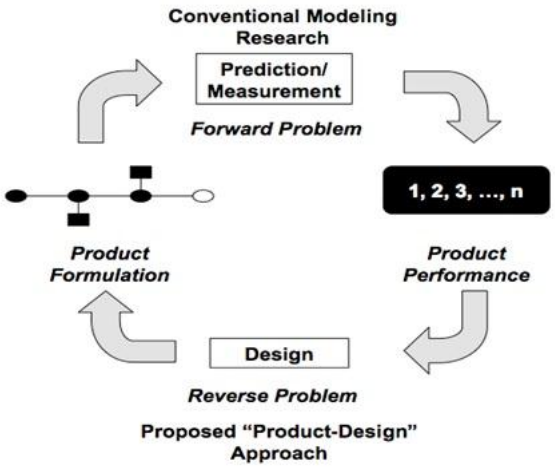

Figure 1. Traditional and Reverse Modeling Approaches

Recent Progress

We choose the Complementary Contact Model[1] (CCM) developed by Mirkin to serve as the forward modeling component of our hybrid GA.

Genetic Algorithm: Genetic algorithm utilizes the traditional Darwinian idea of "survival of the fittest" as the foundation. Within a population, there will be individuals that are naturally better fitted to survive. These individuals are considered to be better adapted to the environment and thus tend to survive longer and have an increased likelihood of propagating their genetic

materials to the next generation. Building upon this idea, we developed a specialized GA framework as shown in Figure 2. There are four major steps to this protocol: 1). Initialization of the test population (range: DNA-NP size ratio from 0 to 1 and DNA linker ratio from 0 to 3). 2). Structure prediction of each individual within the population using the forward CCM. 3). Fitness evaluation of each individual with respect to the desired structure. 4). Reproduction and adaption between the individuals within the current population to create the offspring for the next generation. This cycle is then repeated until no further increase in fitness is observed within successive generations.

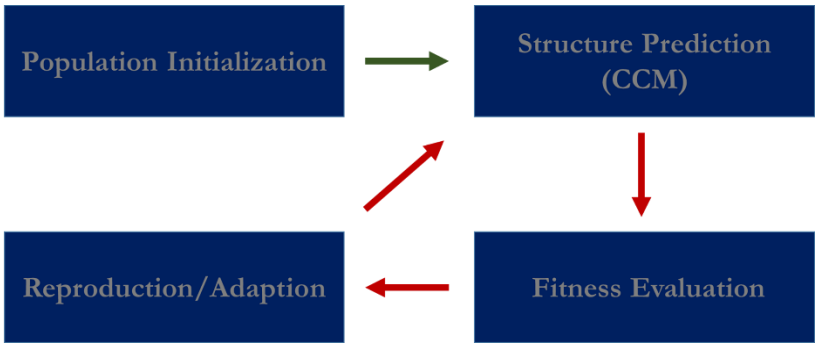

Figure 2. Genetic Algorithm Framework

Our results indicate the ability of the GA to accurately reproduce the original phase diagram proposed by Mirkin[1] as well as elucidate the formation of four new phases – AgI, Cu_5Zn_8, Pt_3O_4, and Pd_5Th_3 – not previously observed within the same phase space, as shown in Figure 3.

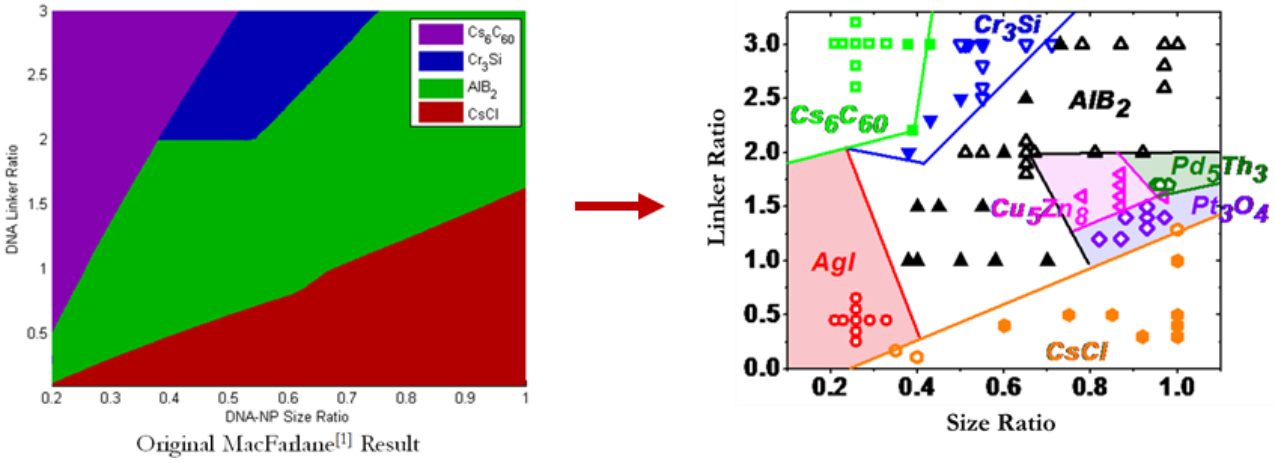

Figure 3. Genetic Algorithm Search

A study of the population growth towards 3 different desired structure – Cr_3Si, Cs_6C_{60}, and Pt_3O_4 – reveals that the developed GA framework is not only a rapidly converging algorithm but also highly selective in that is produces consistent yields of greater than 80%, indicating that most of the population have been driven towards the desired lattice and thus the parameters derived from the final population should allow for self-assembly into our desired structure.

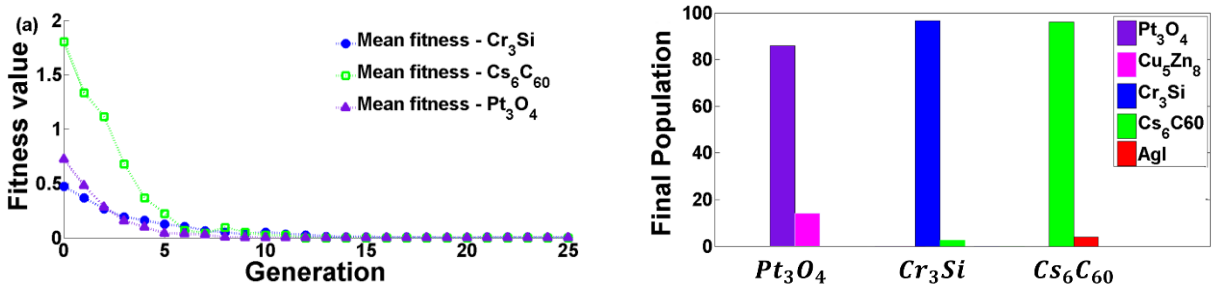

Figure 4. Population Growth Towards Desired Structure

Forward Modeling: The success of the GA framework greatly depends on the accuracy of the forward CCM model in its structure predictions. Recent findings from Gang have indicate both the formation of clusters rather than distinct structure as well as regions of discrepancy with the Mirkin phase diagram and an observed transition from CsCl to CuAu structure with surface reorganization. Additionally, as shown in Table 1, there exists degeneracies in inputs to the CCM causes it to not be able to differentiate between a variety of different structures.

Table 1.

Original CCM						
Lattice	NN^{*}_{AA}	NN_{AB}	NN_{BA}	NN_{BB}	NP^{**}_{A}	NP_B
CsCl	0	8	8	0	1	1
CuAu	0	8	8	0	1	1
Cr_3Si	0	4	12	0	3	1
FCC	0	4	12	0	3	1
Actual NN Parameters						
Lattice	NN_{AA}	NN_{AB}	NN_{BA}	NN_{BB}	NP_A	NP_B
CsCl	0	8	8	0	1	1
CuAu	4	8	8	4	1	1
Cr_3Si	0	4	12	0	3	1
FCC	8	4	12	0	3	1

$^{*}NN_{ij}$ nearest neighbor to particle i of type j
$^{**}NP_i$ number of particle of type i in unit cell (normalized)

In order to resolve these issues, we have incorporated the following effects into the CCM

- Symmetry analysis for cluster prediction
- Nearest neighbor interactions with all particles in 1st nearest neighbor shell
- Multiple linker grafting per particle
- Repulsion effect between non-complementary DNA linkers
- Energy based phase prediction

These new modifications enabled the CCM to not only predict the CsCl to CuAu phase transition but also differentiate between cluster and crystal lattice formation (Figure 5).

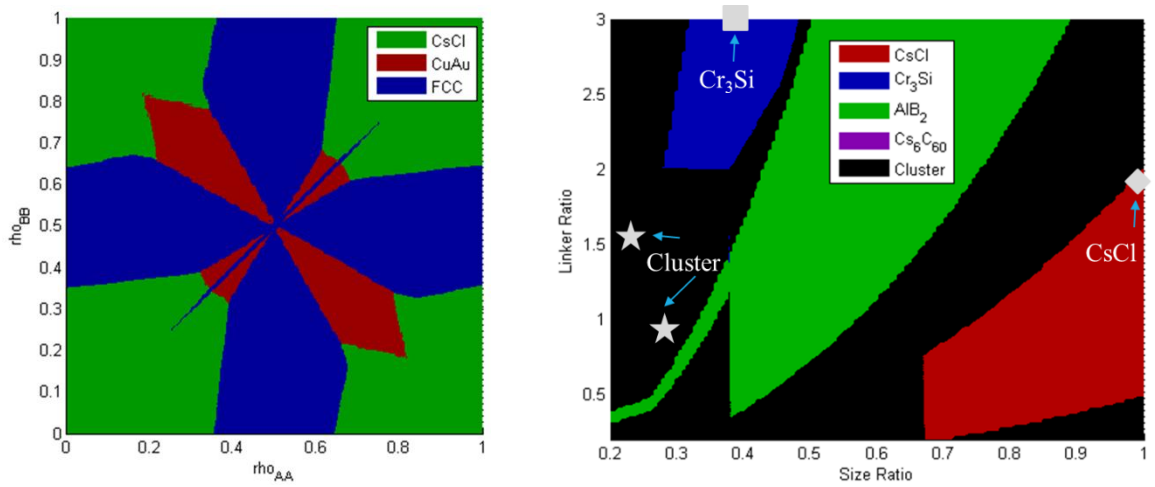

Figure 5. (Left) CsCl→CuAu Transition. (Right) Phase Diagram with Cluster Prediction.

Future Plans

The major expansions have enabled a great increase in the design capabilities of the CCM. Preliminary analysis have revealed that the grafting of multiple linkers on the same nanoparticle lead to the formation of new crystal structure previously unobserved for the single linker grafting case. We plan to expand the GA to consider these newer DNA-NPs parameters so that we can find the optimal parameters with which to produce the newer crystal structures. Additionally, we plan to perform simulations to better understand the mechanism governing the cluster formation and phase transition processes so that both the CCM and GA framework can be modified to better optimize the final design parameters.

Publications (with acknowledgement of DOE support)

[1]."Designing DNA-grafted particles that self-assemble into desired crystalline structures using the genetic algorithm." Srinivasan B, Zhang Y, Gang O, Kumar S, Venkatasubramanian V. (under review)

References

[1]. R. J. Macfarlane, B. Lee, M. R. Jones, N. Harris, G. C. Schatz, and C. A. Mirkin, Science **334**, 204 (2011).
[2]. W. B. Rogers and J. C. Crocker, Proceedings of the National Academy of Sciences **108**, (2011).
[3]. M. E. Leunissen and D. Frenkel, Journal of Chemical Physics **134** (2011).
[4]. T.I.N.G. Li, R. Sknepnek, R. J. Macfarlane, C. A. Mirkin, and M. O. de la Cruz, Nano Letters **12**, 2059 (2012).
[5]. A. Sundaram, P. Ghosh, J. Caruthers, and V. Venkatasubramanian, AIChE **47** (2001).
[6]. A. Sundaram and V. Venkatasubramanian, J. Chem. Info. and Comp. Sci. **38** (1998).
[7]. S. Katare, V. Venkatasubramanian, J. Caruthers, and W. Delgass, Computers and Chemical Engineering **28** (2004).

Programmed nanomaterial assemblies in large-scale 3D structures: Applications of genetically-engineered peptides to bridge nano-assemblies and macro-assemblies

PI: Hiroshi Matsui

Department of Chemistry and Biochemistry, City University of New York, Hunter College, 695 Park Avenue, New York, NY 10065, e-mail: hmatsui@hunter.cuny.edu

i) Program Scope

The main goal is to establish a new peptide-assisted material assembling technology for the generation of 3D macroscale multi-component materials that still retain superior nanoscale properties. To achieve this goal, our strategy is to develop novel biomimetic material fabrication technology that can program directed assemblies of multi-nanomaterials, nanoparticles (NPs) and peptides, in the tailored shape and superstructure in large volumes (μm^3 - mm^3). The projects involve robust assemblies of genetically-engineered peptides forming large-scale 3D frameworks by co-assembling NPs as joints and the generation of the 3D hybrid superlattices in precise NP arrangement with remarkable long-range order. In the course of this work, reconfiguration of 3D superstructure was observed with time in the pH range the peptide undergoes the conformation change,[1] and this reconfiguration was applied to tune energy transfer by changing interparticle distance in the 3D NP-peptide superstructures. The reconfiguration energy of peptide on porous templates of metal-organic-frameworks (MOFs) was also used to power autonomous motors,[2] and the course of swimming motion could be directed with pH gradient at air-liquid interface. To grow semiconductor materials in the peptide frameworks at ambient temperature for the proposed solar cell application, a new catalytic peptide discovery process was developed by using a modified phage display library approach,[3] and by coupling it with hydrogelation process, we could discover catalytic peptides that behave like enzyme, protease, to condensate or hydrolyze amide and ester bonds. These minimal catalytic peptides may support one of various original pathways in the evolution of the more active, more specialized enzymes and the discovery of such precursors to enzymes may hold important information to our understanding of the origins of life.

ii) Recent Progress

(a) Large-scale & reconfigurable 3D structures of precise nanoparticle (NP) assemblies in self-assembled collagen peptide grids and energy transfer of NPs in the 3D superstructures

In this work, nanoscale peptides and ligand-functionalized nanoparticle joints were self-assembled into micron scale 3D cube-shaped crystals, creating a physical framework for the proposed biomimetic assembly strategy [1]. In this approach we took advantage of the naturally robust assembly of collagen-like triple helix peptides and used them as nanowire building blocks for the 3D crystal generation. Using streptavidin-functionalized Au nanoparticles and the α1 chain of type I wild type collagen specifically modified with a biotin moiety *in vivo* [Figure 1(a)], we created micro-sized 3D superlattice cubes with peptide nanowires as grids and Au NPs as joints (Figures 1(b), left). SAXS spectra indicate that Au NPs are arranged in b.c.c structure in the collagen peptide frameworks. The reconfiguration of the 3D directed assembly was observed as the salt bridge was incorporated in the collagen peptide sequence. Due to this salt bridge insertion, the conformation change of peptide building blocks can be induced by lowering pH (<4.0) and this dynamic conformational transformation triggers the disassembly of the hybrid NP-peptide cube, following the reassembly of reconfigured peptides into different shapes such as rod and rhombus after several days [Figure 1(c)]. The conformation change of peptide could also be induced by changing the size of Au NPs, resulting in the transformation of superlattice

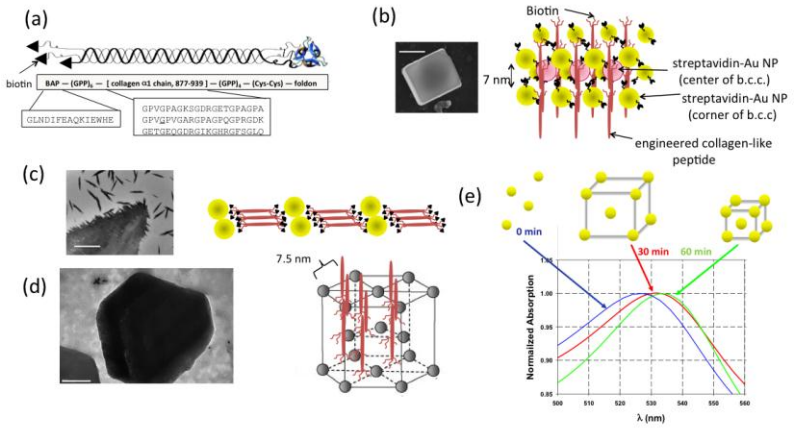

Figure 1. (a) Illustrated structure and sequence of the genetically-engineered triple helix peptide. Biotin is displayed at N-terminus to bind streptavidin-functionalized NP joints. (b) The 3D superlattice structure of the biotinylated triple helix peptides and streptavidin-functionalized Au NPs (ϕ = 10 nm) co-assembled by the streptavidin-biotin interaction and lateral peptide-peptide association through the collagen motif. The interparticle distance is 7 nm (edge-to-edge). (left) SEM image of the 3D superlattice. Scale bar = 2 μm. (c) Reconfiguration of (b) as the conformation change of peptide is triggered by pH change (pH = 4). Scale bar = 2 μm. (d) Reconfiguration of (b) as the conformation change of peptide is triggered by NP size change (ϕ = 30 nm). Scale bar = 600 nm. (e) Reconfiguration of NP alignment in (b) with assembling time monitored by UV/Vis spectra. The interparticle distance of Au NPs agrees with simulated peak positions of Au NPs.

structure to close-packed hexagonal poles [Figure 1(d)]. The evolution for dynamic reconfigurability was also observed with absorption spectrum shifts and the spectral simulation. Based on the red shift of absorption spectrum in Figure 1(e), the aggregation of Au NPs in the peptide frameworks starts at 30 minutes and the inter-particle distance is shortened with time. The assembling time of 1 hour yields the interparticle distance of 11 nm (edge-to-edge distance), and at 2 hours of assembly time the interparticle distance becomes shortest of 7 nm (edge-to-edge distance). When Au NPs and QDs were assembled in the ordered 3D superstructure with the peptide framework, fluorescence (FL) lifetime is quenched significantly as compared to the random aggregation of QDs and Au NPs (4.7 ns -> 2.7 ns). This comparison indicates that the energy transfer from CdSe QD (donor) to Au NP (acceptor) becomes very efficient as they are assembled into 3D superlattices. The interparticle distance becomes shorter as the assembly time becomes longer (Figure 1-e), and thus it is consistent that the FL lifetime becomes shortest (2.0 ns) as the assembly time is extended to 60 min. This observation supports the hypothesis that the peptide superlattice is applicable as a framework to assemble multiple QDs in precise configuration within the distance of electronic coupling, and thus this assembly methodology serves as a powerful toolbox for the future photovoltaic device fabrication.

(b) Catalytic Peptides Discovered by New Hydrogel-Based Combinatorial Phage Display Approach and Their Enzyme-Mimicking 3D Assembly

Recently, we developed a new methodology that enables the selection of catalytic oligopeptides from sequence libraries based on their catalytic turnover. [2] By this modified phage display method, four protease-mimicking peptides were discovered. While these selected catalytic peptides are very specific to the amide condensation reaction, the catalytic activity is 100 times lower as compared to enzymes, probably due to the lack of structured catalytic pocket. To increase the activity, we added a short amyloid peptide sequence to the catalytic peptide (SMESLSKTHHYR) to form artificial β-sheet catalytic pockets resembling enzymes. As the protease-like peptide was conjugated with amyloid sequence of FFKLVFF, the modified peptides were assembled into anti-parallel β-sheet and remarkably the catalytic activity of the peptide assembly is increased 100 % for the ester hydrolysis as compared to the one in the monomeric form. The molecular dynamic simulation shows that the triads are folded into the catalytic configuration within a few hundred nanoseconds, and subsequently stayed locked in this highly active configuration – consistent with the experimental studies.

(c) New Autonomous Motors of Bio-Metal-Organic Framework (bio-MOF) Powered by Reorganization of Self-Assembled Peptides at interfaces

Recently, we developed a new bioinspired autonomous motor system, bio-metal-organic framework (bio-MOF) encapsulating diphenylalanine (DPA) peptides in its MOF pores [Figure 2(a)3] In this system, release of the stored peptides from the MOF and their subsequent reconfiguration into hydrophobic assemblies at the interface creates a non-equilibrium condition by generating a large surface tension gradient, driving force for the motion. MOF is a perfect peptide storage for the motor because of its capability to assemble molecules in the highly ordered pore array of the coordination framework and release guest molecules in a isotropic

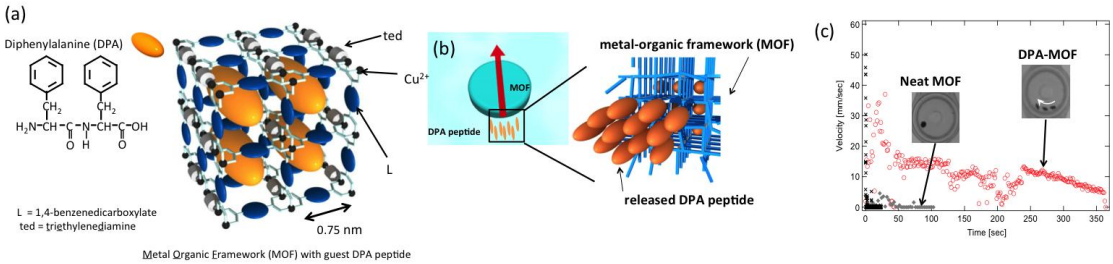

Figure 2. (a) Chemical structures of DPA peptide and MOFs. (b) Mechanism of DPA-MOF motion: after releasing DPA peptides from the MOF, the re- assembly of DPA peptides creates a hydrophobic domain at the end of the MOF particle. Because this domain lowers the surface tension of the MOF on the released side, the MOF particle moves in the direction of the red arrow as a result of the surface tension gradient with no energy input. (c) While the MOF does not move in aqueous solution (grey), when the DPA peptides are incorporated in the MOF it can sustain the swimming motion for longer than 6 min as the released peptides are re-assembled at the interface (red).

direction *via* bond-breaking of the framework. The release of peptides triggered by partial destruction of the outer MOF surface quickly induces reorganization of peptides at the MOF-liquid interface [Figure 2(b)]. The chemical energy generated by this process propels the MOF to swim like bacteria towards the higher surface tension side of the gradient. The windmill motion of the peptide-MOF superlattice was also demonstrated by limiting the peptide release at the ends of bar-shaped superlattice in the opposite direction *via* masking the MOF in between.

iii) Future Plans

Various collagen-like peptides will be assembled with CdSe QDs (ϕ = 10 nm) to generate 3D superlattices. The reconfiguration of QD geometry in the 3D superlattices will be studied with assembling time in various conditions inducing the peptide conformation change, and then physical property and dynamic assembly mechanism of 3D superstructures will be investigated by experiments and molecular modeling. Once we establish the correlation between the QD packing configuration and the assembling time in each reconfiguration condition, the peptide-QD superlattice with a specific inter-particle distance is extracted from solution and assembled between electrodes for electrical measurements and photocurrent spectral response, targeting the application in solar cells. For the application of catalysis, catalytic peptide moieties for protease activity will be displayed at C-terminus of the collagen-like peptide and these catalytic peptides will be assembled into 3D catalytic superlattices. Structural transformation of the 3D superlattices with time *via* reconfiguration will be correlated with the change in catalytic activity by amide-hydrolysis assay, and the optimized activity will be compared with the one for natural enzymes. For autonomous motor application, the 3D peptide-MOF superlattices will be designed to swim, sense, and collect heavy metals in solution by incorporating heavy metal-binding peptide moieties as receptors in the bio-MOFs. (i.e., environmental micro-bots). Micro-windmills powered by a propeller of peptide-MOF assembly will also be used for the generation

of electric power *via* electromagnetic induction between rotating magnets on the propeller and coils. All peptides will be evolved more systematically *via* molecular modeling for their assemblies in diverse 3D superstructures with more controlled reconfigurability, and the discovery of new functionality, reconfigurability, and physical property of the resulting 3D hybrid peptide superlattices will be accomplished through feedback loop between peptide design, assembly, and structural analysis among Matsui's group and collaborators.

iv) References

1. Kaur, P.; Maeda, Y.; Mutter, A.C.; Matsunaga, Y.; Xu, Y.; Matsui, H.: 3D Self-Assembly of Peptide Nanowires into Micron-Sized Crystalline Cubes with Nanoparticle Joints. *Angew. Chem. Intl. Ed.*, **49**, 8375-78 (2010).
2. "Catalytic Peptides for Inorganic Nanocrystal Synthesis Discovered by New Combinatorial Phage Display Approach", Z. Wei, Y. Maeda, H. Matsui, *Angew. Chem. Intl. Ed*., **50**, 10585-88, (2011). (selected as a hot paper in 2011)
3. "Autonomous motors of a metal–organic framework powered by reorganization of self-assembled peptides at interfaces", Y. Ikezoe, G. Washino, T. Uemura, S. Kitagawa, H. Matsui, *Nature Mater.*, **11**,1081-85 (2012). (featured news in RSC Chemistry World)

v) Publications resulting from work supported by the DOE project over the last two years.

1. "Negative differential resistance in ZnO coated peptide nanotube", D. Joung, L. Anjia, H,.Matsui, S.I. Khondaker, *Appl. Phys. A*, **339**, in print (2013).
2. "Biomimetic assembly of proteins into microcapsules on oil-in-water droplets with structural reinforcement via biomolecular recognition-based cross-linking of surface peptides", Y. Maeda, Z. Wei, H. Matsui, *Small*, **8**, 1341-1344 (2012).
3. "Genetically engineered protein nanowires: Unique features in site-specific functionalization and multi-dimensional self-assembly", Y. Maeda, H. Matsui, *Soft Matter*, **8**, 7533-44 (2012).
4. "One-Pot Crystalline ZnO Nanorod Growth in Mineralizing Peptide Gels", L. Anjia, Z. Wei, H. Matsui, *RSC Adv*, **1**, 5516-19 (2012).
5. "Biomimetic Fabrication of Strong Freestanding Genetically-Engineered Collagen Peptide Films Reinforced by Quantum Dot Joints", Z. Wei, Y. Maeda, H. Matsui, *Soft Matter*, **8**, 6871-6875 (2012).
6. "Effects of Divalent Metals on Nanoscopic Fiber Formation and Small Molecule Recognition of Helical Proteins", S.K. Gunasekar, L. Anjia, H. Matsui, J.K. Montclare, *Adv. Func. Mater.* **22**, 2154-59 (2012).
7. "Direct Enzyme Patterning with Microcontact Printing and the Growth of ZnO Nanoparticles on the Catalytic Templates at Room Temperature", K.I. Fabijanic, R. Perez-Castillejos , H. Matsui, *J. Mater. Chem*., **21**, 16877-79, (2011).
8. "Interfacial templating of inorganic nanostructures using a growth directing and reducing peptide", L. Leon, W. Su, H. Matsui and R. Tu, *Small*, **7**, 10285-90, (2011).
9. "Assemblies of functional peptides and their applications in building blocks for biosensors", R. de la Rica, C. Pejoux, H. Matsui, *Adv. Func. Mater*. **21**, 1018-24 (2011).
10. "Electrical transport properties of peptide nanotubes coated with gold nanoparticles via peptide-induced biomineralization", S. Shekhar, L. Anjia, H. Matsui, S.I. Khondaker, *Nanotechnology*, **22,** 095202 (2011).

Biological and Biomimetic Low-Temperature Routes to Materials for Energy Applications

Daniel E. Morse
California NanoSystems Institute, Univ. of California, Santa Barbara, CA 93106-5100; d_morse@lifesci.ucsb.edu

I. Program Scope:

The objectives of our research have been three-fold: (1) To conduct further molecular and genetic analyses and engineering of silicatein, the self-assembling, structure-directing, silica-synthesizing enzyme we discovered and characterized, to better understand and manipulate in this model system the genetically encoded structural determinants of hierarchical self-assembly and the resultant emergent properties of catalysis and templating of semiconductor synthesis; (2) To use our biologically inspired, low-temperature, kinetically controlled catalytic synthesis method to optimize the nanostructures and performance of anodes and cathodes for high-performance batteries; and (3) To use our biologically inspired, low-temperature, kinetically controlled catalytic synthesis method to further control the structures and properties of the layered cobalt hydroxides, analyzing these structures at the atomic level at DOE synchrotron and neutron diffraction facilities, and analyzing the performance of these materials as a function of structure, seeking to predictively control the their local ordering and the distribution of metal-coordination states, and to understand and optimize the structural basis of their magnetic behaviors.

II. Recent Progress:

A. Genetic Engineering of Silicatein, the Silica-Synthesizing Enzyme Discovered in Sponges:

We conducted further molecular and genetic analyses and engineering of Silicatein, the self-assembling, structure-directing, silica-synthesizing enzyme that we previously discovered and characterized as responsible for the catalytic synthesis of the structure-controlled silica elements in the skeletons of specific sponges (Bawazer et al., 2012). Our aim was both to better understand and to manipulate this model system for the genetically encoded structural determinants of hierarchical self-assembly and the resultant emergent properties of catalysis and templating of semiconductor synthesis.

To accomplish the desired "directed evolution," we conducted genetically engineered, DNA-directed protein expression and enzymatic mineralization on polystyrene micro-beads in water-in-oil emulsions that served as synthetic surrogates of biomineralizing cells. (These surrogates of living cells were needed because the mineral products of the altered enzymes can be toxic to living cells.) After allowing expression of the mutationally altered silicatein genes to produce the new silicatein enzyme variants, and allowing these to catalyze the synthesis of new (non-biological) minerals, the cell surrogates were screened by flow sorting through a high-throughput fluorescence-activated cell sorter, with light-scattering signals utilized to differentially sort the resulting mineralized composites. We demonstrated the utility of this platform by evolutionarily selecting new recombinant silicateins with specific structural and catalytic properties to make semiconductors and a quartz-like, crystalline form of silica never made in living systems. Our demonstration of this bioengineering route to new materials introduced in vitro enzyme selection as a viable strategy for mimicking genetic evolution of materials as it occurs in nature.

We first created a library of millions of randomly mutagenized silicatein gene DNA molecules by randomly recombining the cloned, recombinant genes for 2 different silicatein proteins, the subunits silicatein alpha and beta, and then further enhancing the frequency of additional, random mutations by replicating the mixture of randomly recombined genes using error-prone polymerase chain reaction (PCR). We then introduced these mutagenized silicatein genes into artificial vesicles that served as surrogates for living cells (and surrogates for the natural "silica mineralization vesicles"). The DNA

molecules were anchored to polystyrene microbeads (at a dilution favoring the linkage of <1 DNA molecule/bead) via their 5'-end, leaving the information-encoding length of nucleic acids accessible to enzymes that can transcribe or replicate the gene. Antibodies directed against silicatein proteins also are lined to the beads, to ensure capture of any silicatein protein subsequently made, thus ensuring co-segregation of the mutant genes and their protein products, both linked to the microbeads, as the gene and protein product normally would co-segregate within the same living cells. The beads are then immersed in an aqueous solution containing all the enzymatic, RNA and small molecular components required to enzymatically transcribe the DNA on to the corresponding mRNA, and subsequently translate this mRNA to synthesize multiple copies of the uniquely encoded silicatein protein (either parental or variant, depending on the DNA sequence). This mixture is then emulsified in oil, compartmentalizing each bead-gene to its own oil-bounded aqueous vesicle, which serves as the surrogate of a living cell (method of Tewfik and Griffiths, et al.). The gene-transcription and protein expression reactions yielding silicatein-coated beads were allowed to proceed within the population of millions of vesicles, after which the emulsion was broken by centrifugation, releasing the microbeads, each of which carried, linked to its surface, its display of silicatein proteins and their corresponding encoding gene. These silicatein-displaying beads were then re-emulsified to form a new water-in-oil emulsion that included chemical precursors for mineral synthesis (e.g., either 100 mM tetraethylorthosilicate, as a precursor for silica; or 100 mM titanium bis-ammonium lactate-dihydroxide as a precursor for TiO2), all at neutral pH (see schematic illustration). After allowing time for mineral synthesis at 20 oC, these emulsions were broken, the beads were recovered by centrifugation, and the beads were analyzed (and separated) by rapid, automated flow-sorting, with light-scattering and fluorescence signals used to select those beads of interest for further investigation (Bawazer et al., 2012).

During flow sorting, beads recovered from an emulsion mineralization reaction are hydrodynamically guided past the instrument's laser and interrogated at a defined excitation wavelength (488 nm). A representative population of beads (100,000 beads) is measured; emission intensities through defined band-pass filters and light scattering intensities are acquired from each bead; and the results from all 100,000 measured events are plotted by the instrument. DNA is extracted, replicated by PCR, and cloned from those beads detected to have synthesized minerals of interest, and the cloned, recombinant DNA molecules tested for their ability to code for new (i.e., mutationally altered) silicatein enzymes that prove capable of synthesizing the originally detected minerals again. Mineral composition and crystallinity at this stage are precisely determined by X-ray diffraction (XRD) and electron-dispersive spectroscopy (EDS). Those new silicatein molecules confirmed capable of synthesizing minerals that cannot be made by the parental silicatein were subjected to structural analysis (by sequencing their cloned DNAs, and 3-D modeling of the new proteins), in efforts to relate the altered protein structures of the mutationally altered silicateins to their newly acquired ability to produce new forms of mineral that cannot be made by native silicatein (Bawazer et al., 2012).

Results of these studies showed that the new, mutationally altered silicatein capable of producing cristobalite, a quart-like crystalline form of silica (not produced by the parental enzyme) carried mutations that altered the catalytically active site, whereas the enzyme capable of catalytically producing TiO2 had undergone mutations at both the catalytic site and at secondary sites in the protein. Space-filling models of the engineered proteins help explain their new catalytic activities (Bawazer et al., 2012).

B. Using Biologically Inspired Kinetically Controlled Synthesis To Resolve Atomic-Level Structure and Magnetic Properties of Complex Layered Hydroxides:

The biologically inspired, low-temperature catalytic synthesis method that we developed is based on the kinetically controlled catalytic synthesis mediated by silicatein, as described above. One family of materials conveniently made by this process comprises a group of stably nanostructured cobalt hydroxide-based thin films that exhibit both spontaneous magnetic ordering and photoconductivity. This unique combination of crystallographic and structural orientation with physical properties in the hydrotalcite-like

layered hydroxides thus enables analysis of the correlation between optical excitation of electron-hole pairs and changes in magnetic properties in ways not accessible with materials synthesized by conventional processes. Results of our analyses illustrate the ability of the kinetically controlled catalytic synthesis method to control structure and properties of inorganic materials at the atomic level.

We used the kinetic control afforded by this biologically inspired catalytic synthesis method to control the chemistry and microstructure of the layered cobalt hydroxides and related perovskites (Neilson et al.). By regulating the rate of precursor hydrolysis (through control of the concentration of catalytic ammonia in the diffusing vapor) we can – for the first time – predictively govern the relative proportions of octahedrally and tetrahedrally coordinated cobalt in the final product (Neilson et al., 2011a, b).

These results illustrate the control of structure and properties that we can obtain through the regulated interplay between equilibrium and kinetically trapped local geometries in the synthesis of these layered compounds. Aided by the powerful analytical capabilities of DOE's synchrotron and neutron diffraction user-facilities, we then used this kinetically controlled catalytic synthesis to analyze, resolve and understand the complex magnetic ordering in the disordered cobalt hydroxides through analysis of their local structure (Neilson et at al.). In many ostensibly crystalline materials, unit-cell-based descriptions do not always capture the complete physics of the system due to disruption in long-range order. In the series of cobalt hydroxides that we studied, magnetic Bragg diffraction revealed a fully compensated Néel state, yet the materials showed significant and open magnetization loops. A detailed analysis of the local structure defined the aperiodic arrangement of cobalt coordination polyhedra. Representation of the structure as a combination of distinct polyhedral motifs allowed us to explain the existence of locally uncompensated moments and provided a quantitative agreement with bulk magnetic measurements and magnetic Bragg diffraction (Neilson et al., 2011a, b).

C. Using Biologically Inspired Kinetically Controlled Catalytic Synthesis To Produce High Power Anodes and Cathodes for Batteries and Fuel Cells:

We previously reported our use of the biologically inspired, kinetically controlled catalytic synthesis method described above to inexpensively produce a nanocomposite anode for high-power lithium ion batteries consisting of nanocrystals of Sn grown by a 2-step catalytic process in situ within the interstices of carbon nanotubes (Zhang and Morse, 2012) and the pores of compliant and conductive microparticles of graphite. We extended this approach to produce a high-power, relatively high-voltage, nanocomposite cathode for rechargeable Li-ion batteries (von Bulow et al., 2012). This cathode consists of nanocrystalline (spinel) $LiMn_2O_4$ grown in situ and intimately mixed with well-dispersed, inexpensive multiwall carbon nanotubes (10% w/w; see figure below) This cathode operates at an average voltage of 3.9 v and exhibits good stability and cyclability. It retains 96% of its original capacity after discharge at 10C, >80% capacity after discharge at the very high rate of 20C, and shows complete recovery to 100% capacity after full discharge at 50C (indicating that it suffers little or no damage after this high rate of discharge). The highly faceted spinel produced by kinetically controlled catalytic synthesis method (as opposed to the granular powders typically produced by other methods) apparently creates readily accessible crystallographic channels that facilitate the rapid entry and egress of lithium ions (yielding high power), while the well-dispersed CNTs provide efficient percolation pathways for good conductivity. We also used a variation of our kinetically controlled catalytic synthesis method to grow 3 nm nanocrystals of Pt in carbon matrices to obtain more efficient hydrogen fuel cells (Kong et al., 2013).

III. Future Plans:

The success of the genetic engineering of silicatein summarized above shows that it is possible to mimic and accelerate the process of natural selection that has shaped the diversity of compositions and structures formed by natural biomineralization. We propose in the coming year to extend these efforts to engineer the silicatein enzyme to acquire further new capabilities, including the capacity to synthesize new, non-oxide-containing semiconductors. This will require mutationally inactivating the catalytic hydrolysis site

of the enzyme (to block catalytic introduction of oxygen), in addition to the selection for new functionalities. Future plans for our biologically *inspired* catalytic synthesis include (1) use of our bio-inspired, kinetically controlled catalytic synthesis of nanocrystalline metals in situ in a range of newly developed, high surface area graphene-based carbon matrices for enhanced energy densities, and (2) dynamic analyses during cycling of the electrodes described above by *in situ* measurements using NMR and synchrotron XRD to analyze the mechanisms of ionic and electronic entrance, storage and exit, with the aim of identifying kinetic barriers to these processes that can be addressed by further improvements in design and synthesis.

IV. References cited:

Bawazer, L. A. M. Izumi, D. Kolodin, J. R. Neilson, B. Schwenzer, and D. E. Morse 2012. Evolutionary selection of enzymatically synthesized seminconductors from biomimetic mineralization vesicles. Proc. U.S. Natl. Acad. Sci. 109 (26): E1705-E1714.

Kong, C.S., H.-L. Zhang, F. Somodi and D. E. Morse, 2013. Bio-inspired synthesis of high-performance nanocomposite catalysts for hydrogen oxidation. Adv. Func. Matrls. DOI: 10.1002

Neilson. J.R. J.A. Kurzman, R. Seshadri2, and D.E. Morse. 2011. Ordering double perovskite hydroxides by kinetically controlled aqueous hydrolysis. Inorg. Chem. 50: 3003-3009

Neilson, J.R., D,E. Morse, B. C. Melot, D. P. Shoemaker, J. A. Kurzman, and R. Seshadri. 2011. Understanding complex magnetic order in disordered cobalt hydroxides through analysis of the local structure. Phys. Rev. B 83: 094418 (1-7).

von Bulow, J.F., H.-L. Zhang and D.E. Morse. 2012. Hydrothermal realization of high-power nanocomposite cathodes for lithium ion batteries. Adv. Energy. Mater. 2: 277-389.

Zhang, H.-L. and D.E. Morse. 2012. Transforming large-scale industrially produced carbon nanotubes to high-performance electrode materials for lithium ion batteries. J. Mater. Res. 27: 410-416.

V. Publications acknowledging work supported by this DOE project over the last two years:

Niesz, K, T.Ould-Ely, H.Tsukamoto and D. E. Morse. 2011. Engineering grain size and electrical properties of donor-doped barium titanate ceramics. Cermics Internatnl. 37: 303-311..

Ould-Ely, T., K. Niesz , M. Luger., l. Kaplan-Reinig, K. Niesz, M. Doherty and D. E. Morse. 2011. First large-scale engineered synthesis of BaTiO3 nanoparticles using low temperature bioinspired principles. Nature Protocols 6: 97-104.

Qian, F. and D.E. Morse. 2011. Miniaturizing microbial fuel cells. Trends in Biotechnol 29: 62-69.

Schwenzer, B., J. Hu, and D. E. Morse. 2011. Correlated compositions, structures, and photoluminescence properties of GaN nanoparticles. Adv. Mater. 23(20): 2278-83

Neilson. J.R. J.A. Kurzman, R. Seshadri2, and D.E. Morse. 2011. Ordering double perovskite hydroxides by kinetically controlled aqueous hydrolysis. Inorg. Chem. 50: 3003-3009

Neilson, J.R., D,E. Morse, B. C. Melot, D. P. Shoemaker, J. A. Kurzman, and R. Seshadri. 2011. Understanding complex magnetic order in disordered cobalt hydroxides through analysis of the local structure. Phys. Rev. B 83: 094418 (1-7).

von Bulow, J.F., H.-L. Zhang and D.E. Morse. 2012. Hydrothermal realization of high-power nanocomposite cathodes for lithium ion batteries. Adv. Energy. Mater. 2: 277-389.

Zhang, H.-L. and D.E. Morse. 2012. Transforming large-scale industrially produced carbon nanotubes to high-performance electrode materials for lithium ion batteries. J. Mater. Res. 27: 410-416.

Bawazer, L. A. M. Izumi, D. Kolodin, J. R. Neilson, B. Schwenzer, and D. E. Morse 2012. Evolutionary selection of enzymatically synthesized seminconductors from biomimetic mineralization vesicles. Proc. U.S. Natl. Acad. Sci. 109 (26): E1705-E1714.

Kong, C.S., H.-L. Zhang, F. Somodi and D. E. Morse, 2013. Bio-inspired synthesis of high-performance nanocomposite catalysts for hydrogen oxidation. Adv. Func. Matrls. DOI: 10.1002

Ould-Ely, T., L. Kaplan_Reinig and D.E. Morse. 2013. High rate continuous synthesis of nanocrystalline perovskites and metal oxides in a colliding vapor stream of microdroplets. Adv. Func. Materials (submitted)

Program Title: Electrostatic Driven Self-Assembly Design of Functional Nanostructures

Principle Investigator: Monica Olvera de la Cruz
Department of Materials Science and Engineering, Northwestern University, 2220 Campus Drive, Evanston, IL 60208.
Email: m-olvera@northwestern.edu

Program Scope

The scope of the program is to increase understanding of self-assembly of nanostructures and hence facilitate improvements in design and functionality of the structures by using biomolecules as building blocks. Self-assembly is widely recognized as one of the most efficient methodologies to built novel nano-materials with a varying array of applications and functionalities including electrical, optical, magnetic and sensing. It is crucial to understand the role that electrostatic interactions play during the self-assembly process since most biomolecules are charged. This program shows how electrostatic interactions offer the possibility of designing and generating structures that can be controlled by systematically changing the ionic conditions. Here, we discuss the influence of electrostatics in the self-assembly of cationic and anionic amphiphiles into crystalline membranes and of spherical nucleic acid gold conjugates into three-dimensional crystalline structures.

Recent Progress

Nature uses electrostatic interactions among positively and negatively charged groups to induce the organization of biomolecules into highly complex structures. In particular, amphiphilic molecules that have polar ionizable groups, respond to the pH and the concentration of ions in the solution thereby affecting their physical properties, including their crystallization. Crystalline membranes are essential for many bacteria, bacterial microcompartments, and archaea to survive in extreme environments including high salinity. These organisms take various polyhedral geometries that are characteristic of crystalline closed shells, which we reproduced by co-assembling cationic (3+) and anionic (-1) amphiphiles into vesicles. We demonstrated that these crystalline vesicles exhibit some of the behaviors of highly complex natural membranes, including stability at high salt [1]. We combined TEM with SAXS and WAXS to characterize the co-assembled structures from the mesoscopic to nanometer scale. At low and high pH values, we observe closed, *faceted vesicles with two-dimensional hexagonal molecular arrangements* and at intermediate pH we observe ribbons with rectangular-C packing. Furthermore, as pH increases we observe interdigitation of the bilayer leaflets (Fig. 1).

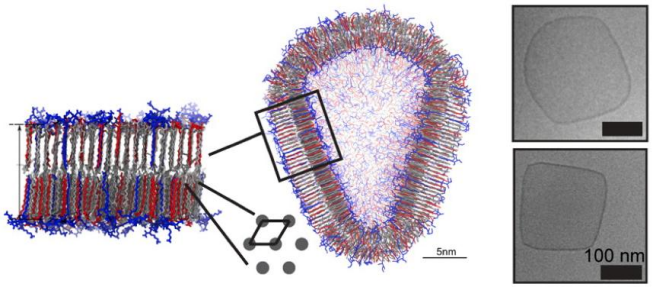

Fig. 1: Atomistic simulations (left), and TEM images (right) of faceted and irregular polyhedra with hexagonal crystalline symmetry, stable in closed shapes and high salt concentration.

Accurate atomistic molecular dynamics (MD) simulations explain the pH-dependent bilayer thickness changes, and also reveal bilayers of hexagonally packed tails at low pH, where only a small fraction of anionic headgroups is charged. Coarse-grained simulations show that the mesoscale geometries at low

pH are faceted vesicles where liquid-like edges separate flat crystalline domains. By coassembling +2 and -1 amphiphiles of various tail lengths into bilayer membranes at different pH values, we recently showed that the crystalline structure is controlled by the competition of the attractions among the polar and among the hydrophobic groups [2]. The pH and the hydrophobic tail length modify the intermolecular packing and the symmetry of their crystalline phase. For hydrophobic tail lengths of 14 carbons (C_{14}), we observe the coassembly into crystalline bilayers with hexagonal molecular ordering via in situ small- and wide-angle X-ray scattering (SAXS and WAXS). As the tail length increases, the hexagonal lattice spacing decreases due to an increase in van der Waals interactions, as demonstrated by atomistic MD simulations. For C_{16}, WAXS shows crystalline molecular ordering corresponding to hexagonal, rectangular-C, or rectangular-P phases depending on pH (see Fig. 2). The stability of the rectangular phases, which maximizes tail packing, increases with increasing tail length. As a result, for very long tails (C_{22}), the possibility of observing packing symmetries other than rectangular phases diminishes. Our work demonstrates that it is possible to systematically exchange chemical and mechanical energy by changing the solution pH value within a range of physiological conditions at room temperature in bilayers of molecules with ionizable groups.

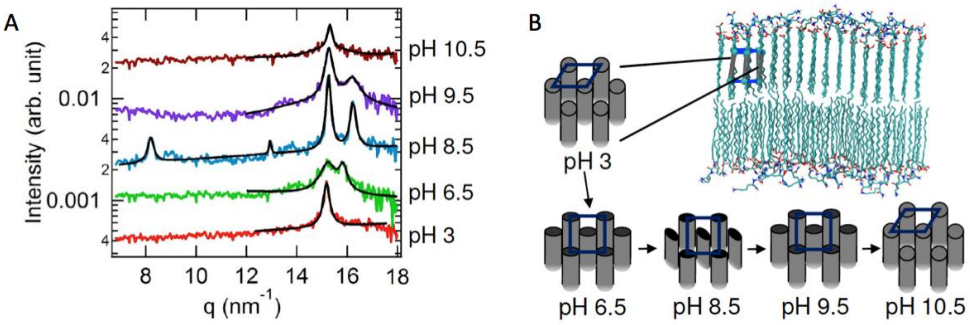

Fig. 2: (A) Wide-angle X-ray scattering data showing the background subtracted scattered intensity versus the scattering vector q for mixtures of anion ***C_{15}-COOH*** *and cation* ***C_{16}-K_2*** *as the pH is increased from 3 to 10.5. (B) Schematic representations for the bilayer model at pH 3, 6.5, 8.5, 9.5 and 10.5. Changes are observed in the packing of the alkyl tails into a hexagonal, a rectangular-C or rectangular-P lattice.*

We have also explored the crystallization driven by the competition of electrostatic repulsions and hydrogen bonding attractions in gold nanoparticles functionalized with nucleic acid. Spherical nucleic acid – gold (SNA-Au) nanostructures have emerged as a major player in this area, due the precise structural control available with DNA linkers. A major obstacle in the assembly of uniform crystalline materials is the predictability and subsequent control of the coalescence dynamics in the superlattice grains. Annealing strategies have shown limited success in grain boundaries coalescence. We developed a coarse grained model (Fig. 3) that elucidates the role of DNA energetics and valency of the functionalized nanoparticle [3]. Though previous experiments and coarse-grained models have investigated the stability of phase diagrams in detail by changing the geometry and binding potential of the SNA-Au building block [4], our model provides a quantitative description of the role of grain boundaries during the crystal growth in these systems. We found that initially, the growth law of isolated faceted bcc superlattices, a(t), is well-described by the power law $t^{1/2}$. At later times, grains coalescence and boundary interactions slow the coarsening dynamics considerably. This slow-growth is shown to be dependent upon the orientation of the crystalline planes between the different aggregates. We describe the coarsening by coalescence via a grain-rotation-induced-coalescence (GRIC) model. Due to the grain boundary interactions, aggregates of larger gold cores have faster coalescence dynamics compared to nanoparticles with smaller gold cores, provided the DNA surface

coverage is constant. This finding provides fundamental new insight into the relationship between nanoparticle size and crystal growth dynamics.

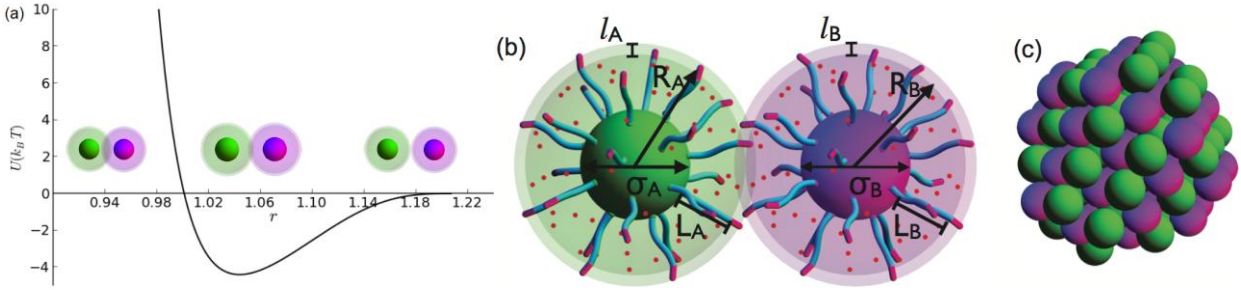

Fig. 3: (a) Total interaction potential U for a pair of SNA particles with $R_{A,B}$ = 14.32 nm, $l_{A,B}$ = 2.97 nm, and □$_{A,B}$ = 10.0 nm. (b) Model colloidal SNA particles used as building blocks of superlattices. The DNA consists of a linker region (blue) and a terminal non-self-complimentary sticky end (pink). The Au core diameter is □, while the model SNA particle has a radius R. The flexible DNA strands lead to an overlap region of width l (light shade). (c) Typical bcc superlattice crystal with its minimum energy shape, which at equilibrium is a rhombic dodecahedron.

The thermodynamic characteristics of SNA-Au conjugates depend critically on interactions between the SNA-Au and the surrounding cationic counterion layer. This ion cloud also determines the binding affinity for complementary nucleic acids, and therefore their self-assembly, as discussed above. Classical density functional theory (DFT) and MD simulations of cations surrounding Au nanoparticles have been carrier out [5]. Recently, we combined MD simulations for the first time with experimental measurements of the cation distribution around the SNA-Au. Using (SAXS) with the isomorphous heavy ion replacement approach, we measured small differences in intensity profiles when SNA-Au particles are dispersed in ionic solutions containing different monovalent ions (Fig. 4); comparing the cation distribution profile with classical DFT, we find agreement between experiment and theory. This work points to a non-uniformity in the radial counterion density in the DNA shells, with an ion cloud that extends consistently with oligonucleotide length. The salt concentration is enhanced up to 8-fold within the DNA shell, depending on bulk concentration.

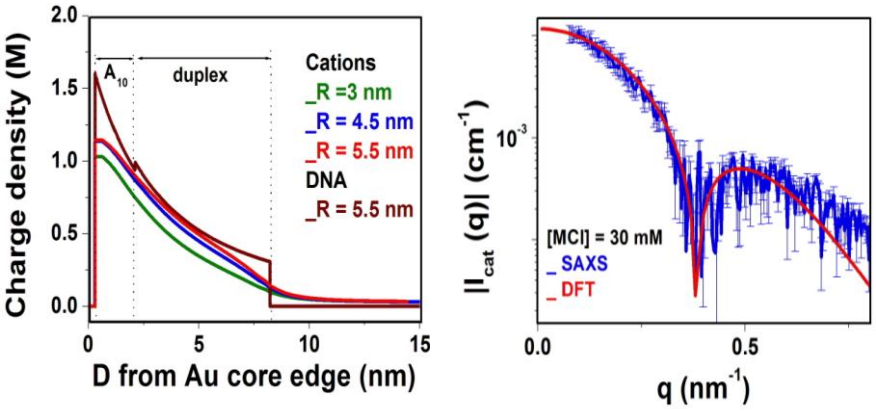

Fig. 4: (left) DFT-derived Na^+ distribution as a function of the distance from the Au core edge (green, blue and red curves) for SNA-Au in 30 mM MCl, and for three different Au core sizes, the. For comparison, the DNA charge density is shown for Au core with radius 5.5 nm (brown curve). (right) Comparisons between the DFT-derived and the SAXS-extracted $|I_{cat}(q)|$ for SNA-Au in 30 mM MCl.

Future Plans

We will use SAXS and the DFT calculations to compute interacting potentials between SNA-Au conjugates, which we will extract from the scattering function. With these potentials we will generate molecular dynamics simulations of the assembly of superlattices of SNA-Au

nanoparticles. We will determine the growth dynamics of various lattices and the kinetic shape of the single crystals for various mixtures of nanoparticles in the presence of monovalent and divalent ions. We aim to construct crystalline membranes of SNA-Au nanoparticles, and study the transport of ions and of small charged molecules through these membranes. In order to further explore the physical properties of crystalline membranes, we plan to study the crystallization of anionic amphiphilic membranes in the presence of divalent cations, and determine their properties including the permeability to water and ions in the various crystalline phases and in the liquid state.

References

1. Molecular Crystallization Controlled by pH Regulates Mesoscopic Membrane Morphology; C-Y. Leung, L. Palmer, B. Qiao, S. Kewalramani, R. Sknepnek, C. Newcomb, M. Greenfield, G. Vernizzi, S. Stupp, M. Bedzyk, M. Olvera de la Cruz, *ACS Nano* **6**: 10901-10909 (2012).
2. Crystalline polymorphism induced by charge regulation in ionicmembranes; C-Y. Leung, L. Palmer, S. Kewalramani, B. Qiao, S. Stupp, M. Olvera de la Cruz, M.J. Bedzyk, *Proc. Natl. Acad. Sci.*, submitted
3. Coarsening Dynamics for Multivalent DNA-Functionalized Colloidal Assemblies; S. Dhakal, K.L. Kohlstedt, G.C. Schatz, C.A. Mirkin, M. Olvera de la Cruz, *ACS Nano*, submitted
4. Modeling the Crystallization of Spherical Nucleic Acid Nanoparticle Conjugates with Molecular Dynamics Simulations; T.I.N.G. Li, R. Sknepnek, R.J. Macfarlane, C.A. Mirkin, M. Olvera de la Cruz, *Nano Letters* **12**(5): 2509-2514 (2012)
5. Local Ionic Environment around Polyvalent Nucleic Acid-Functionalized Nanoparticles; J.W. Zwanikken, P. Guo, C.A. Mirkin, M. Olvera de la Cruz, *J. Phys. Chem. C* **115**: 16368-16373 (2011)

Publications (supported by DOE over last two years)

6. Topological defects in the buckling of elastic membranes; C.M. Funkhouser, R. Sknepnek, M. Olvera de la Cruz, *Soft Matter* **9**: 60-68 (2013)
7. Shapes of pored membranes; Z. Yao, R. Sknepnek, C. Thomas, M. Olvera de la Cruz, *Soft Matter* **8**: 11613-11619 (2012)
8. Mechanical Model of Blebbing in Nuclear Lamin Meshworks; C.M. Funkhouser, R. Sknepnek, T. Shimi, A.E. Goldman, R.D. Goldman, M. Olvera de la Cruz, *Proc. Natl. Acad. Sci.* **110** (9): 3248-3253 (2013)
9. Charge renormalization of bilayer elastic properties; R. Sknepnek, G. Vernizzi, M. Olvera de la Cruz, *J. Chem. Physics* **137**: 10495 (2012)
10. Curvature-driven effective attraction in multicomponent vesicles; M.F. Demers, R. Sknepnek, M. Olvera de la Cruz, *Phys. Rev. E* **86**: 021504 (2012)
11. Nonlinear elastic model for faceting of vesicles with soft grain boundaries; R. Sknepnek, M. Olvera de la Cruz, *Phys. Rev. E* **85**: 050501(R) (2012)
12. Buckling of Multicomponent Elastic Shells with Line Tension; R. Sknepnek, G. Vernizzi, M. Olvera de la Cruz, *Soft Matter* **8**: 636-644 (2012)
13. Platonic and Archimedean geometries in multi-component elastic membranes; G. Vernizzi, R. Sknepnek, M. Olvera de la Cruz, *Proc. Natl. Acad. Sci.* **108**: 4292-4296 (2011)
14. Shape change of nano-containers via a reversible ionic buckling; R. Sknepnek, G. Vernizzi, and M. Olvera de la Cruz, *Phys. Rev. Lett*. **106**: 215504 (2011)

Program Title: " Dynamic Self-Assembly: Structure, dynamics, and function relations in lipid membranes."

Principal Investigator: Atul N. Parikh; co-investigator: Sunil K. Sinha (UCSD)
Mailing Address: 3001 Ghausi Hall, Departments of Chemical Engineering & Materials Science and of Biomedical Engineering, UC Davis, Davis, CA 95616
E-mail: anparikh@ucdavis.edu, ssinha@physics.ucsd.edu

Program Scope. The scope of the program is delimited by two over-arching objectives: *First*, we seek to abstract a physical science based understanding of fundamental rules that determine dynamic and mesoscale self-assembly in lipid bilayer membranes - a versatile class of biologically inspired soft matter. *Second*, we seek to translate these physical principles into design principles for the development of new classes of membrane-based complex materials that exhibit complex, co-operative, and adaptive behavior.

Our approach is primarily experimental; we employ well-defined supramolecular assemblies of lipid amphiphiles (namely, lipid multilamellae, supported lipid bilayers, and giant vesicles) and examine their spontaneous mesoscale organization and dynamic remodeling in response to external fields or perturbations. We study their molecular-level organization and dynamic, mesoscale remodeling under extraneously imposed physical-chemical conditions including (1) interfacial hydration gradients; (2) imposed curvatures; and (4) mechano-chemical perturbations. Interrogating these dynamic reorganizations using spatially- and temporally resolved microscopy and spectroscopy techniques (wide-area and total internal reflection based fluorescence, ellipsometric, infrared vibrational, x-ray reflectivity, neutron spin-echo, and neutron reflectivity) allows a detailed quantitative characterization of structure-dynamics relations in membrane media, over over-arching objective. Building on our results from earlier periods of the program, we have developed a project itinerary organized into following three aims: (**1**): Characterize the mechanism of mesoscale inter-layer coupling of laterally phase-separated domains in stacked lipid bilayers; (**2**) decipher the relations between membrane curvature, molecular shapes, and their effects on phase separation and dynamics in multicomponent fluid lipid bilayers; and (3) characterize real-time effects of mechanochemical perturbations on structure, topography, and dynamics of membrane bilayers.

Recent Progress. Below, we highlight a recent progress on coupled phase separation in liquid-crystalline membrane mesophases.

1. BACKGROUND. Multilamellar lyotropic phases of stacked lipid bilayers exhibiting smectic liquid-crystalline order(*1*) (or membrane multilamellae) are spontaneously produced primarily via hydrophobic forces of lipid-water interactions. A unique feature of such smectic mesophases of stacked-membrane bilayers is that while the constituent lipids exhibit in-plane translational degrees of freedom, their out-of-plane incoherent undulation fluctuations are severely restricted because of the steric spatial confinement they experience with the neighboring layers. It is now well-appreciated that the entropic loss associated with these so-called Helfrich inter-membrane repulsive interactions stabilizes the one-dimensional (1D) smectic order of uniform lipidic mesophases (i.e., 1D positional order). In the past, studies of multilamellar membranes have focused dominantly on uniform systems consisting of single lipids. Biological membrane mesophases and those relevant to practical biomimetic applications, however, are

seldom uniform. Multicomponent mixtures of lipids and proteins, which readily phase-separate into co-existing phases, characterize these functional membrane multilamellae.

RECENT FINDINGS. Using ternary lipid mixtures consisting of unsaturated- (e.g., DOPC, POPC) and saturated lipids (e.g., DPPC, sphingomyelin) doped with cholesterol, we experimentally demonstrated that the phase-separated domains in individual layers of the multilamellar membrane stacks align spontaneously producing columnar mesophases spanning hundreds of lamellae (**Fig. 1**) using time-resolved fluorescence microscopy and X-ray diffraction (Pub. 4).

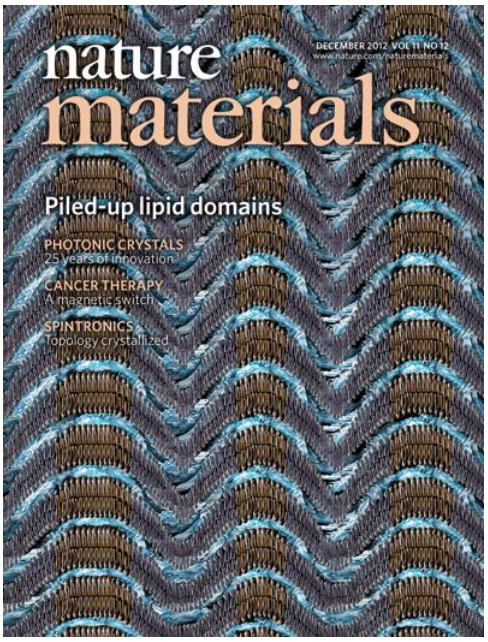

Fig. 1.| A schematic depiction of mesoscale ordering of liquid-ordered domains in liquid-disordered surroundings in co-existing lipid phases in membrane multilayers. (Tayebi, Ma, Vashaee, Sinha, Parikh, Nat. Mater. 2012).

A preliminary analysis of the dynamics of this coupling suggests the existence of co-operative multilamellar "epitaxy" guided not by lipids but by "epistructural tension" of water confined within narrow spaces between the layers. But this hypothesis remains largely unverified. We believe that these results are a major step forward towards developing self-assembly strategies for the long-range serial coupling of functional domains, which can be potentially exploited to align (1) ion-channels to facilitate charge/energy transport, (2) receptors to amplify sensing of target ligand binding, and (3) template the 2- and 3-dimensional crystallization of difficult-to-crystallize membrane proteins relevant in photosynthetic machinery.

EXPERIMENTAL AND THEORETICAL IMPORTANCE OF FINDINGS. From a materials view point, the observations of interlayer mesoscale coupling of intralyer phase separations above suggest new possibilities for designing synthetic material systems recapitulating functional folded membranes such as found in thylakoid membranes of photosynthetic cyanobacteria(*2*) or plant chloroplasts(*3*), and electrocyte cells in electric eels(*4*) for potential applications in photonics, sensing, DNA delivery, and protein crystallization (*5-7*). At fundamental level, the raise several important questions, which require additional experimental and theoretical investigations: (1) Is the observed mesoscale coupling of domain driven by inter-lamellar interactions between the domains or does the ordering of water at the domain interfaces play a role? (ii) if the latter, how is water structured at the lipid-water interfaces? (iii) How does the addition of water-soluble species, namely ions (Ca++) and colloids influence interlamellar periodicity? and (iv) does the interlamellar alignment afford long-range organization of membrane proteins, e.g., ion-channels, which selectively partition within the domains.

Future Plans. Our future plans are to build on the findings highlighted above and others on curvature-dependent phase separation in membrane mesophases (summarized in references). Specific directions for mesoscale coupling highlighted here are briefed below.

(1) Determine the relative roles of hydrophobic mismatch and ordering of interfacial water. The out-of-plane columbar registry of the phase separated domains corresponding to the two phases (which have different bilayer heights) leads to the problem of hydrophobic mismatch for the lipids at the domain boundaries(*8-10*) . Two limiting case scenarios are schematically depicted in Fig. 2.

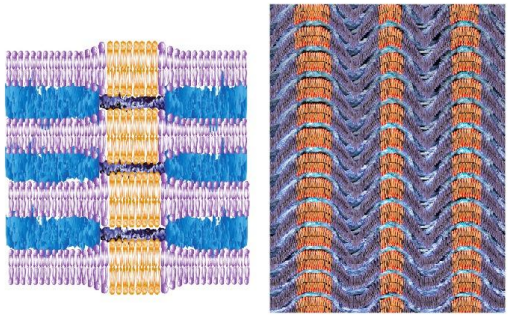

Fig. 2.| a,b, Plausible models for columnar phase-separated membrane mesophases. **a,** single periodicity and two water layer thicknesses, **b,** two periods.

In the first scenario (Fig. 2, left), the thinner fluid phase intercalates a thicker water layer between head groups to compensate for the hydrophobic mismatch, producing a single spatial periodicity for the two co-existing phases. Alternately, water channel of uniform thickness at the aqueous interfaces of both the domain and the surrounding phases should produce two periodicities (Fig. 2, right). We are currently addressing this issue using both X-ray and spectroscopy expts.

(2) Determine the role of ionic and non-ionic solutes and water soluble colloidal particles in the smectic ordering of lipid mesophases. Hydrophobic mismatch intrinsic to phase-separated membrane multilamellae can in principle be reduced by preferential localization of osmolytes in the fluid phase of the mixed smectic liquid crystal. The osmolytes intercalated in the water channels exert osmotic pressure through their thermal Brownian motion, locally expanding the interbilayer spacing and increasing the long-range hydration repulsion between the neighboring bilayers (Fig. 3a). Using ionic (e.g., ca^{+2}) and non-ionic (e.g., sucrose and trehalose) confined in the hydrophilic water channels, we currently explore if the structure such as shown in Fig. 3a can be realized.

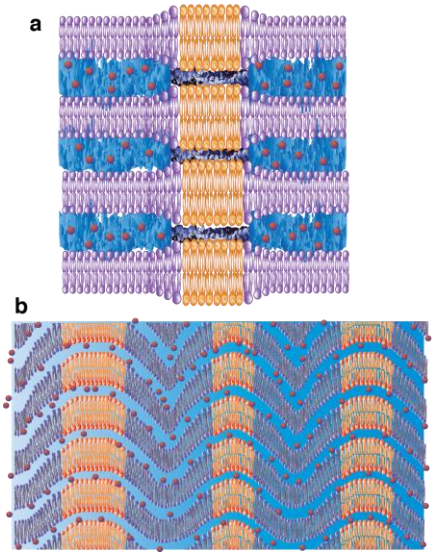

Fig. 3 A schematic depiction of modulation in membrane multilayers using osmolytes. a, Preferential localization of solutes in the fluid phase osmotically swells the water layer. b, uniform organization of solutes producing novel composite structures.

(3) Design and characterize complex structures serially coupling protein function and promote domain-driven two-dimensional crystallization of membrane-proteins. From a biomimetic point of view, the alignment of cholesterol-enriched lo domains in stacked lipid membrane raises additional possibilities of engineering novel material constructs. Here, we seek to explore if ion-channels that colocalize with l_o domains(*11*) (Fig. 4a) and be used to serially couple their transport properties.

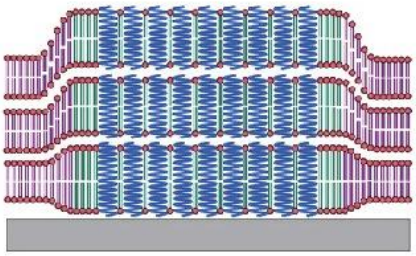

Fig. 4 domains hosting transmembrane proteins or channels (blue) that act in series or serve as a template for membrane protein crystallization. Taken from News & Views by B. Bechinger, Nat. Mater. (2012)(*12*)

We will also explore if conditions can be found in which membrane proteins, which partition preferentially within the l_o domains(*13*) crystallize (Fig. 4).

References

1. Y. K. Levine, A. I. Bailey, M. H. F. Wilkins, Nature 220, 577 (1968).
2. Z. P. Zhang, *et al*, Phy. Rev. A 45, 7560 (1992).
3. A. J. Garcia-Saez, S. Chiantia, P. Schwille, J. of Biol. Chem. 282, (2007).
4. P. I. Kuzmin, et al Biophys J. 88, 1120 (2005).
5. B. Bechinger, Nature Materials 11, 1005 (2012).
6. P. J. Darby, C. Y. Kwan, E. E. Daniel, Amer. J. Physio. 279, L1226 (2000).
7. K. Simons, D. Toomre, Nature Reviews Molecular Cell Biology 1, 31 (2000).
8. E. M. Landau, J. P. Rosenbusch, PNAS 93, 14532 (1996).
9. L. O. Essen, R. Siegert, W. D. Lehmann, D. Oesterhelt, PNAS 95, 11673 (1998).
10. M. Caffrey, Journal of Structural Biology 142, 108 (2003).

Publications acknowledging DOE support (Since 2011, selected)

1. "*Structural Asymmetry in Supported Lipid Bilayers*," G. Chen,1 M. K. Mukhopadhyay, Z. Jiang, Y. Ma, C. M. DeCaro, J. D. Berry, A. M. Brozell, H. Kim, A. N. Parikh, L. B. Lurio, and S. K. Sinha, **Phys. Rev. E**, in review (2013).
2. "*Highly resolved structure of a foating lipid bilayer: Effect of Ca2+ ions and temperature*," Sajal Kumar Ghosh, Yicong Ma, Curt M. DeCaro, Sambhunath Bera, Laurence B. Lurio, Zhang Jiang, Sunil Kumar Sinha, **Biophys. J.,** in review (2013).
3. *"Transient pearling and vesiculation of membrane tubes under osmotic gradients,"* Jeremy Sanborn, Kamila Oglecka, Rachel S. Kraut, Atul N. Parikh, **Faraday Discussions** 161, 167-176 (2013) [+Discussion]
4. "*Long-range inter-layer alignment of intra-layer domains in stacked lipid bilayers*," Lobat Tayebi, Yicong Ma, Daryoosh Vashaee, Gang Chen, Sunil K. Sinha, Atul N. Parikh, **Nature Materials** 11, 1074–1080 (2012). [Cover] [News & Views]
5. "*Osmotic Gradients Induce Bio-reminiscent Morphological Transformations in Giant Unilamellar Vesicles,"* Kamila Oglecka, Jeremy Sanborn, Atul N. Parikh, Rachel S. Kraut, **Frontiers in Membrane Physiology and Biophysics** 3, Art. 120, 1-11 **(2012).**
6. "*Stability of Uni- and Multillamellar Spherical Vesicles*," L. Tayebi, D. Vashaee, and A. N. Parikh, **Chemphyschem** 13, 314-22 (**2012**).
7. "*Substrate Suppression of Thermal Roughness in Stacked Supported Bilayers*," C. M. DeCaro, J. D. Berry, L. B. Lurio, Y. C. Ma, G. Chen, S. Sinha, L. Tayebi, A. N. Parikh, Z. Jiang, and A. R. Sandy, **Physical Review E** 84, (**2011**).
8. *"Reconstituted lipoprotein: a versatile class of biologically-inspired nanostructures,*" Daniel A. Bricarello, Jennifer T. Smilowitz, Angela M. Zivkovic, J. Bruce German, Atul N. Parikh **ACS Nano**, 5, 42-57 (**2011**).

Program Title: Long Range van der Waals-London Dispersion Interactions for Biomolecular and Inorganic Nanoscale Assembly

Principal Investigators: V. A. Parsegian* and W. Y. Ching**
Mailing Address: *Physics Dept. University of Massachusetts-Amherst, Amherst MA, 01003, **Dept. of Physics and Astronomy, Univ. of Missouri-Kansas City, Kansas City MO, 64110
E-mail: *parsegian@physics.umass.edu; **Chingw@umkc.edu
Date of the report: 07/17/2013

Program Scope

The goal of this joint program is to measure directly and to compute accurately electronic properties of nanoscale objects as well as to recognize realistic geometry in order to evaluate the van der Waals-London dispersion (vdW-Ld), electrostatic, and polar components of molecular interactions, operating at distances longer than the interatomic covalent bonds, so as to render tractable the nanoscale and mesoscale material design. The breadth of scope of our endeavors obviously requires a broad expertise provided by our group members in *ab initio* computations, theory of vdW-Ld, electrostatic, and polar interactions, sample preparation, scattering, and spectroscopic measurements.

The main strategy implemented to achieve these goals is to use *ab initio* computational methods to derive molecular interactions, spanning length and time scales that connect atomistic and continuum models, driving nanoscale assembly and alignment. Our earlier work on carbon nanotubes provides *proof of principle* of how careful consideration of electronic structure and bonding, implicit in the electronic spectra, of different materials obtained from *ab initio* quantum theory (UMKC), and electron spectroscopy (CWRU) can be implemented into computations of direct long-range vdW-Ld, electrostatic, and polar interactions (UMass). We now expand and generalize this methodology to include *partial charges* and a whole slew of *new inorganic biologically relevant materials*, such as amorphous SiO_2 (a-SiO_2) glass and $AlPO_4$ (CWRU, UMKC), analyzing in detail the connection between specific features of their electronic properties, the ensuing peaks and bands in optical spectra and finally the resulting strength of long-range vdW-Ld interactions (UMass). Extending the electronic properties of material to partial charge redistribution *in vacuo* as well as charging equilibria in aqueous solutions, biomolecular systems such as oligopeptides, polypeptides and proteins like BSA and collagen, can become parts of rational design based on quantitative knowledge of organizing molecular interactions obtained from detailed second virial coefficient experiments (CWRU) and their analysis in terms of the component long-range interactions (UMass). By bringing the computational and experimental approaches together we can elucidate the interrelation between the *ab initio* optical dispersion spectra and partial charge distribution derived from the electronic structure (UMKC) and the actual interactions measured in ordered molecular arrays of specially prepared samples of double stranded (ds), triple stranded (triplex) and quadruple stranded (quadruplex) DNA through osmotic stress experiments (UMass) in order to understand, control and manipulate the assembly of nanometer-scale heterogeneous structures and/or the conformation of macromolecules.

These new developments lead the way to complete understanding and successful control of long-range interactions between a variety of molecules and molecular aggregates whose material properties can be derived via detailed quantum chemical calculations. The quantitative connection between long-range interaction and material properties will help us to better control and manipulate biomolecular and inorganic nanoscale assembly.

By its very nature our research can only be accomplished through a wide range of expertise in computational materials science (UMKC), molecular force theory (UMass) and a slew of advanced experimental methods (CWRU), and can not be accomplished without extensive and close collaboration between all team members of our partner institutions.

Recent progress

1. Long-range Interactions in the Helix/Coil Transition of Biopolymers and Nanopore Interactions with Polymers (UMass). Papers [#2] and [#3]. Osmotic stress measurements were performed on a range of proteins and polymers, as a precursor to the planned study of ds-DNA oligonucleotides, triplex and quadruplex DNA. These measurements also provide insight into the nature and characteristics of the helix-coil transitions of globular protein molecules that play an important role in the charge distributions, geometries, and solvent interactions influencing long-range interactions in these systems. We showed how long-range interactions in the helix-coil transition of biopolymers couple to external fields, such as the osmotic pressure of the solution with dissolved PEG, in order to bring about conformational phase transitions and how osmotic pressure of a mixture of polymers in equilibrium with a nanopore forces the partitioning of some of the polymer components into the nanopore. This work reveals how an essentially macroscopic concept such as osmotic pressure can modify conformations at a completely different scale be it for a polymer in solution or close to a surface embedded nanopore. This *action through different length-scales* will be used in later developments planned within this program.

2. Role of Single Interatomic Bond Transitions in Long-range Interactions, Excitons in SiO_2 (UMass, CWRU, UMKC). Papers [#4] and [#5]. The presence of narrow excitonic peaks in the optical spectra of some single wall carbon nanotubes motivated us to explore and quantify in detail the possible excitonic effect on the magnitude of the Hamaker coefficients of the long/range vdW-Ld interactions. We have formulated a theoretical approach that shows how change in the dielectric response (interband optical properties) over a sufficiently narrow frequency interval has complicated consequences on the corresponding vdW-Ld interactions. Optical properties of amorphous SiO_2 (a-SiO_2) glass using a near-perfect random network structure have been calculated by the UMKC team. The goal was then to compare the one-electron calculation of optical excitation with the experimentally determined spectra (CWRU), which contain the excitonic peak and then to assess the effect of the excitonic peak in SiO_2 on the vdW long-range interactions calculation. We analyzed in detail the contribution of the exciton peak to all Matsubara frequency terms in the Hamaker coefficient (*Figure 1*). Contrary to the common wisdom, the presence of an additional peak affects the Hamaker coefficient across all of Matsubara frequencies, not just those at energies near the optical peak.

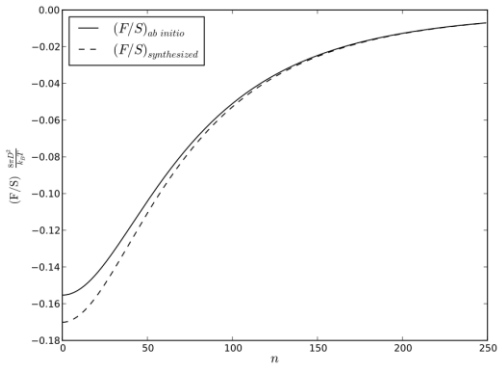

Figure 1 Hamaker coefficient (A_{1v1}) as a function of thermal Matsubara frequency index n.

3. Density Functional Calculation of a Model of Type I Collagen and Development of an Efficient Method Applicable to Large Protein Models (UMKC). Paper [#6]. Collagen molecules are the primary structural proteins for many biological systems. Fundamental knowledge at the atomic level plays an important role for its further understanding. The electronic structure and bonding calculations of a large, realistic model of hetero-structural type I collagen using the density functional theory-based orthogonalized linear combination of the atomic orbital (OLCAO) method has been attempted. Detailed information on density of states (DOS), partial DOS, partial charges on each atom, bond order values, intra- and inter-molecular H-bonding are obtained. We further devised a simplified amino-acid-based potential model, which can be effectively applied to large proteins so as to avoid doing a full self-consistent field (SCF) calculation yet which can retain 90% of the accuracy of the full SCF calculation. This simplified scheme is validated by comparing it to the results obtained from a full SCF calculation. This technique provides a middle ground approach to study complex biomolecular systems at the *ab initio* level. Further applications of this method to large proteins such as capsomere subunits are currently under study.

4. Long-range Interactions between BSA Using Static Light Scattering (UMass, CWRU, UMKC). We formulated a theory of the second virial coefficient (A_2) of the BSA protein based on the decomposition of the total interactions into an electrostatic part and the vdW-Ld part. With minor modifications this theory can be also

applied to DNA oligonucleotides and protein capsids at various buffer conditions. The A_2 can then be conveniently parameterized via the corresponding surface charge and/or surface potential, while the vdW-Ld interactions were parameterized via their Hamaker coefficient, both as functions of ionic strength and pH of the bathing solution. Positive values of A_2 indicate a dominating electrostatic repulsion interaction between the BSA molecules, while the minimum in A_2, obtained experimentally at pH 4.6 and corresponding to the isoelectric point at which the molecules carry no net electrical charges, is due to the dominance of the vdW-Ld interactions. The analysis performed for BSA will allow us to set up a theoretical model that will be later used for A_2 analysis of complex protein aggregates such as empty protein capsids at various solution conditions.

5. Long-range Interactions between 64 SWCNTs (CWRU, UMKC, UMass). Paper [#1]. We reviewed our approach to the *ab initio* electronic structure and optical properties of 64 different single wall carbon nanotubes (SWCNT), of various types and chirality, and their effect on the characteristics of the vdW-Ld interaction between them.

Future plans

1. DNA/DNA (Polynucleotide) Long-range Interactions (UMass). We have made substantial progress in setting up direct measurements of long-range molecular interactions between DNA molecules in ordered arrays, in solutions containing polyvalent counterions, such as cobalt haxammine (CoHex), in order to quantify a first order transition between line hexatic and cholesteric phases. We have been able to detect an upper and a lower critical salt concentration that delineates a closed loop in the phase diagram of the CoHex-condensed DNA. Our finding means that there is a continuity of states between the line hexatic and condensed DNA phases. These two types of phases, associated with different long-range interactions, have always been considered to be completely separate, due to separate mechanisms.

2. Bulk DNA Sample Preparation and VUV Optical Characterization (UMass, CWRU). We learned how to prepare highly ordered samples of concentrated DNA. They will be used for UV spectroscopy on DNA films (CWRU). The samples were prepared by the standard method (A. Rupprecht, Acta Chem Scand 20 494 1966) of wet spinning. This method allowed us to prepare highly concentrated DNA samples with a well defined macroscopic orientation and set DNA density that can be used with different spectroscopic and structural probes such as UV spectroscopy and SAXS. This type of samples can not be obtained commercially.

3. Ab initio Partial Charge Distributions in 1js9 Capsid Proteins (UMKC, UMass). Electrostatic interactions are an important part of the total long-range interaction potential. *Ab initio* spatial partial charge density distribution and surface charging equilibria on the solvent accessible surface of proteins will be calculated and used to compute the electrostatic interaction free energies of capsid proteins. We will start with the charge distribution on the doxorubicin molecule and on a particular virus coat protein (PDB ID 1js9) *in vacuo* and in aqueous solution. (*Figure 2*) on 1js9 and its extended N-tail. These examples pave the way for more realistic calculations of partial charges in the presence of aqueous solvent at various pH conditions and in the presence of counterions. We are also formulating a macroscopic theory of surface charge regulation that will allow us to assess separately the pH and salt effects in solution.

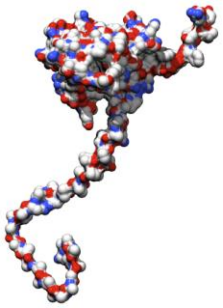

Figure 2 Calculated partial charge distribution (blue neg. and red pos. partial charges) on 1js9 and its extended N-tail.

4. Triplex DNA, Quadruplex DNA Preparations (UMass, CWRU, UMKC). Long-range interactions between duplex DNA *versus* triplex and quadruplex DNA molecules are fundamentally different, the latter being larger than in the duplex case. This could lead to a possibility of quadruplex DNA aggregation even in monovalent salt solutions at physiological conditions, so a comprehensive study of quadruplex DNA will enhance the scientific conclusions of the overall program. We will calculate the electronic structure and optical spectra of these DNA

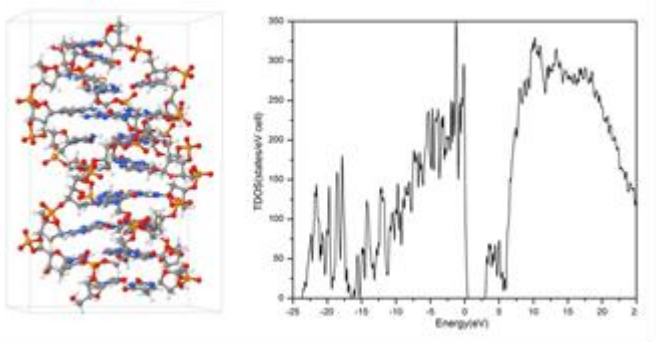

Figure 3 Structure and density of states of triplex DNA.

structures (*Figure 3*) and plan to formulate a theory of vdW-Ld interactions between cylinders of various sizes and explore the effect of their thickness on the long range interactions between them. The problem is complicated because we know from preliminary studies on DNA optical spectra that its optical response is anisotropic, which complicates the calculation of the vdW-Ld interactions. We plan to build upon our prior work and the known formulae for the vdW-Ld interactions between two anisotropic semi-infinite planar regions in order to get the proper formulae for the DNA-DNA interactions at various interaxial separations. This will allow us to assess the importance of the thickness of the molecule in their interactions and potentially formulate a new theory of conformational-transformation driven assembly of biologically relevant polymers.

References (which acknowledge DOE support)

1. R. Rajter, R. H. French, W. Ching, R. Podgornik, V. A. Parsegian, "Chirality-Dependent Properties of Carbon Nanotubes: Electronic Structure, Optical Dispersion Properties, Hamaker Coefficients and van derWaals – London dispersion interactions", RSC Advances, 3 (3), 823 (2013). Published.
2. A. Badasyan, S. Tonoyan, A. Giacometti, R. Podgornik, V.A. Parsegian, Y. Mamasakhlisov, V. Morozov, "Osmotic Pressure Induced Coupling between Cooperativity and Stability of a Helix-Coil Transition". Phys. Rev. Lett. 109, 068101 (2012). Published.
3. R. Podgornik, J.E. Hopkins, V. A. Parsegian, and M. Muthukumar, "Polymers Pushing Polymers: Polymer Mixtures in Thermodynamic Equilibrium with a Pore", Macromol. 45 8921 (2012). Published.
4. Neng Li and Wai-Yim Ching, "Structural, electronic and optical properties of a large random network model of amorphous SiO_2 glass", J. Non-Crystalline Solids (2013). Published.
5. J.E. Hopkins, D.M. Dryden, Wai-Yim Ching, R.H. French, V.A.Parsegian, and R. Podgornik, "Dielectric response variation and the strength of long range van der Waals interaction", in preparation (2013).
6. J. Eifler, P.Rulis, R.Tai and W.Y Ching, "Density Functional Calculation of a 7-2 Heterostructure Model of Type I Collagen and Test for a Simplified Scheme Applicable to Large Protein Models", in preparation (2013).

Other References:

7. R.H. French, N.F. Steinmetz, R. Podgornik, Wai-Yim Ching, V.A. Parsegian, Nanoscale Assembly by Manipulation of Long Range Interactions", Sosman Award Symp., MS&T 2012, Pittsburgh PA, Oct. 7-11.
8. Yingfang Ma, D. M. Dryden, D. Acosta, Lijia Liu, L. DeNoyer, Wai-Yim Ching, N.F. Steinmetz, R. Podgornik, R.H. French, V.A. Parsegian, "Optical Properties and van der Waals-London Dispersion Interactions in Inorganic and Biomolecular Assemblies", MRS 2013 Fall, Boston MA. Submitted.
9. J.C.Hopkins, D.M. Dryden, Wai-Yim Ching, R.H. French, V.A. Parsegian, R. Podgornik, "Dielectric Response Variation and van der Waals London Dispersion Interaction", MRS 2013 Fall, Boston MA. Submitted.
10. S.Yasar, V.A. Parsegian, R. Podgornik, "On the continuity of states between DNA-ordering transitions in mono- and multi-valent salt solutions" , MRS 2013 Fall, Boston MA. Submitted.

Personnel:

UMass: Graduates: S. Yasar, J.E. Hopkins. Sophomore: Kartikeya Nagendra.
UMKC: Postdoc: Sitram Aryal (50%); Graduates: Jay Eifler, Lokendra Poudel; Sophomore: Rex Tai.

Optimizing immobilized enzyme performance in cell-free environments to produce liquid fuels
Grant No. DE-SC0006520

Mithun Radhakrishna, Sanat Kumar
Department of Chemical
Engineering Columbia, New York,
NY 10027
and

Joseph J. Grimaldi, Cynthia H. Collins and Georges Belfort
Howard P Isermann Department of Chemical and Biological Engineering, and
Center of Biotechnology and Interdisciplinary Studies
Rensselaer Polytechnic Institute, Troy, NY 12180-3590

Program Scope:

The increasing demand to find more carbon neutral energy sources has motivated the search for biologically-derived fuel products. The largest concern facing alcohol-based biofuels is the ability to develop an efficient high-yield scalable commercially available production process (1). With the recent discovery of abundant gas resources in the USA through "fracking" technology and recent and expected future drop in energy prices, the challenge for competitive alternate energy sources is more acute (2). Many options that until recently were considered viable, are clearly less so today (3). This quantum change in the US energy mix will force funding agencies such as DOE and energy companies to reevaluate their focus. Limitations on biofuel production using cell culture (*Escherichia coli*(4), *Clostridium(5)*, *Saccharomyces cerevisiae(6, 7)*, brown microalgae(8), blue-green algae(9) and others) include low product (alcohol) concentrations (2-5 vol%)(1) due to feed-back inhibition, instability of cells, low titers and difficulty in scale-up (1)-(10).

Fig 1. Two-step enzymatic reaction to produce i-butanol from ketoisovaleric acid

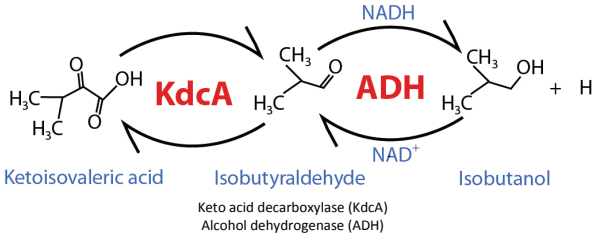

The research funded by this grant for the past two years focused on the bioconversion of acids to aldehydes to alcohol (butanol) using a two-enzyme system. While this enzymatic route offers great promise and excellent selectivity for the production of biofuels, enzymes exhibit slow kinetics, low volume capacity in solution and product feedback inhibition. These limitations have to be overcome so that biofuels can be produced economically. A novel approach is used here to address these limitations. Enzymes synthesized via recombinant DNA technology are immobilized on a solid substrate in order to stabilize them and allow the product to continuously be removed while retaining catalyst. This cell-free enzyme system will be coupled with a separation technique, possibly pervaporation, to constantly remove the desired butanol. Thus we address slow kinetics (genetic mutation, enzyme coupling and removal of inhibitory product), low volume capacity (immobilization and stabilization of enzymes) and product feedback inhibition (product removal) with our approach.

We offer an alternate simplified biofuel production approach to cell culture with the hope of overcoming all three limitations listed above, while speeding up the process considerably and possibly reducing the cost of fuel production. Our semi-*in vitro* partial cell-free scheme requires the following steps (**Fig. 1**):

1. *E. Coli cells:* Production/isolation of two critical enzymes (ketoacid decarboxilase, KdcA, and alcohol dehydrogenase, ADH) using standard fermentation.
2. *Starting Substrate: Streptomyces cinnamonensis* mutants overproduce 2-ketoisovaleric acid to titters of 2.4 g/L (11).

3. *Cell-free:* Simultaneous *in vitro* application of the two enzymes (KdcA and ADH) attached to solid substrates to convert acid (ketoisovaleric acid) to aldehyde (isobutyraldehyde) and then to alcohol (isobutanol, the fuel).
4. *Recovery:* Continuous removal and recovery of isobutanol in order to drive the reactions toward isobutanol (12).

This process is attractive because there are no cells that undergo product feed-back inhibition, enzymes are produced at high titer using standard fermentation *sans* feed-back limitations (step (i) above), protein engineering is used to stabilize the two enzymes to high product titer and high temperature (step (iii)), enzymes are stabilized through immobilization (step (iii)), and the reaction is driven toward product through its continual removal of alcohol (recovery) (step (iv)). We plan to publish three manuscripts where we first optimize the immobilization of two tetramer enzymes, β-galactosidase (control) and ADH, in the first manuscript (13). The other two manuscripts will report on KdcA stabilization using protein engineering (14) and a combination of the two enzymes (KdcA and ADH) into the complete scheme with product recovery.

Research Progress

Fig. 2. Normalized ADH kinetic activity in solution and immobilized passively (just adsorbed) or covalently on non-porous silica, porous SBA-15 and porous methacrylate (resin) particles. (A) ADH covalently attached on 200 (◆) and 100 (▲) nm acid functionalized silica nanoparticles, in solution (■), and nanoparticles with no immobilized ADH (●). (B) ADH passively immobilized on SBA-15 (◆), ADH passively immobilized on SBA-15 after multiple washes (▲), SBA-15 particles with no immobilized ADH (●), ADH free in solution (■). (C) ADH covalently attached to amino functionalized methacrylate resin as a function of bound ADH concentration: methacrylate resin no ADH (●), 3 μg ADH/mg resin (✖), 7 μg ADH/mg resin (▲), 15 μg ADH/mg resin (◆), 17 μg ADH/mg resin (O), equivalent ADH free in solution (■). All absorbance readings were normalized by their initial absorbance.

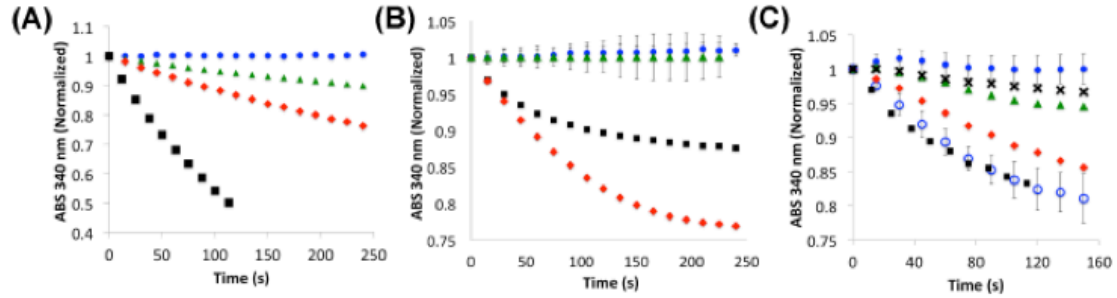

Last year, we demonstrated that the enzyme activity differs when immobilized on either 200 nm and 100 nm mean diameter silica particles. In addition, SBA-15, a mesoporous silica, provided a negative curvature surface in which confinement stabilized the protein and retained its activity. Further studies were performed to test the effect of surface coverage and particle loading. The particle system was tested with a model enzyme, ß-galactosidase, and our two critical enzymes for alcohol production, alcohol dehydrogenase (ADH) and keto-acid decarboxylase (KdcA). This past year, we developed a viable method for immobilizing enzymes with multiple domains on commercial methacrylate resin. When immobilized, the enzyme must exhibit high activity or retain a large fraction of its solution activity and be able to remain immobilized and active through multiple reactions without leaching from the support. Of the four steps listed above, this past year we have:

1. Tested the reaction of a model multi-domain enzyme, β -galactosidase (β -gal), with a simple colorimetric assay ─immobilized on various surfaces to identify the best surface and curvature (concave or convex).

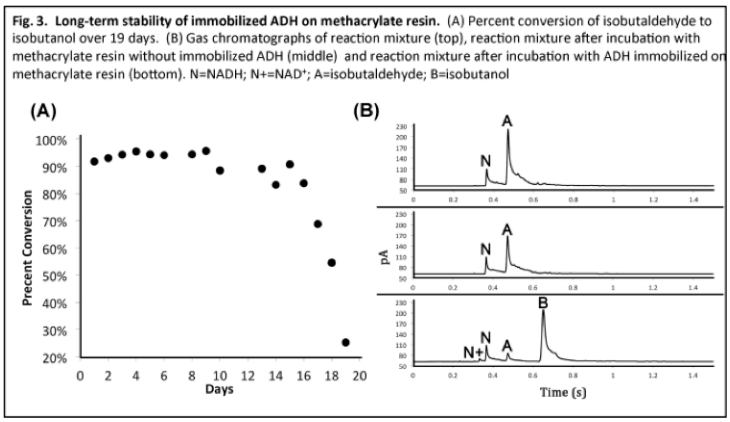

Fig. 3. Long-term stability of immobilized ADH on methacrylate resin. (A) Percent conversion of isobutaldehyde to isobutanol over 19 days. (B) Gas chromatographs of reaction mixture (top), reaction mixture after incubation with methacrylate resin without immobilized ADH (middle) and reaction mixture after incubation with ADH immobilized on methacrylate resin (bottom). N=NADH; N+=NAD+; A=isobutaldehyde; B=isobutanol

2. Immobilize ADH onto the optimal surface obtained from (1) and compared its conversion efficiency with that in free solution for aldehyde to alcohol (**Figs. 2 & 3**).

Production and optimization of keto-acid decarboxylase (KdcA)*:* One key component of the two-stage enzymatic reaction is the first enzyme of the reaction, KdcA, which is not commercially available. We have earlier cloned, overproduced and purified KdcA and successfully tested its activity alone and in combination with immobilized ADH and KdcA in free solution (**Fig. 4**). KdcA is unstable when immobilized and looses its activity.

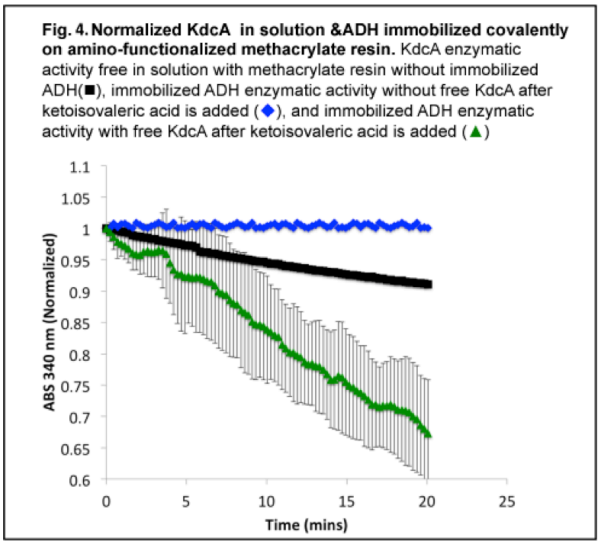

Fig. 4. Normalized KdcA in solution &ADH immobilized covalently on amino-functionalized methacrylate resin. KdcA enzymatic activity free in solution with methacrylate resin without immobilized ADH(■), immobilized ADH enzymatic activity without free KdcA after ketoisovaleric acid is added (◆), and immobilized ADH enzymatic activity with free KdcA after ketoisovaleric acid is added (▲)

Future Plans

Future work will use protein engineering to search for mutations that stabilize KdcA and focus on integrating the system into one process and then recovering i-butanol, the product.

Development of a recovery system for iso-butanol*:* A laboratory scale pervaporation/RO module system and a settling device will be built to study membrane and sedimentation separations of iso-butanol from water.

Simulations

Retention of enzymatic activity upon immobilization is a great challenge due to the structural changes the enzyme undergoes upon immobilization and subsequently losing its activity. It is therefore imperative to understand as to how enzymes interact with variety of surfaces (hydrophobic, neutral and hydrophilic) and different geometries (flat supports, curved surfaces). In the current work, we have tried to understand the physics of protein folding/unfolding and stability of these enzymes on different surfaces and geometries in the framework of the 'Hydrophobic-Polar' (H-P) lattice model through Monte Carlo simulations.

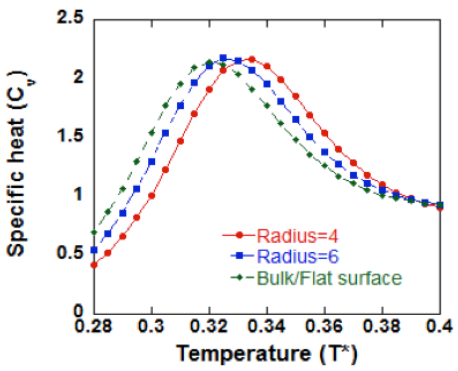

Figure 5: **Simulations:** Specific heat curve of the 64-mer HP protein at different degrees of athermal confinement, at both a flat surface and inside spherical cavities of radius 4 and 6.

Progress

Our results show that, a neutral confinement stabilizes the folded (native) state of the protein against reversible unfolding. Therefore, the folding temperature of the protein shifts to higher temperature for progressively smaller cavities (**Figure 5**). On hydrophobic surfaces, we observe a small stabilization of the protein on flat supports at weak surface hydrophobicity whereas denaturation happens for stronger hydrophobic surfaces due to preferential protein-surface interactions. A hydrophobic confinement always tends to destabilize the protein. Nevertheless, the protein can be still stabilized at weak surface hydrophobicities

relative to that in free solution, due to the entropic dominance of confinement inside such pores (**Figure 6**).

Our simulation results helps to qualitatively rationalize many previous experimental results and most importantly provides us a rationale to explain the experimental findings of our collaborators of increased enzymatic activity of ADH when it is immobilized inside hydrophilic SBA-15 pores and unaffected activity inside weakly hydrophobic PMMA pores. Inside hydrophilic SBA-15 pores, the protein has no energetic propensity to unfold. Further, it is also stabilized as a result of entropic effect due to confinement. In the case of immobilization inside pores, we believe the unaffected activity of ADH is as a result of mutual balance between the entropic and energetic contributions. We believe that the proper tailoring of energetic effects in spherical confinements can be employed to change the activity of the protein at will.

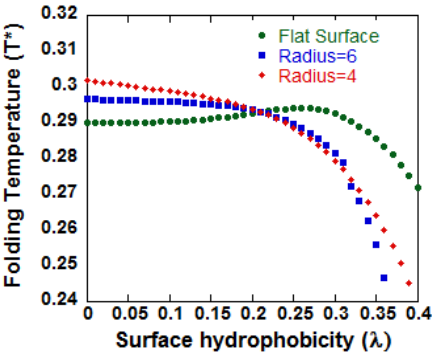

Figure 6: Simulations: Folding (melting) temperature (Tm) of the 64-mer HP protein as a function of surface hydrophobicity (λ) for different degrees of confinement

Future Work

We want to extend the above study for hydrophilic surfaces. Inter-protein interaction between the immobilized enzymes is believed to be one of the major causes for loss in enzymatic activity upon immobilization. We want to investigate mechanisms through which surface properties (hydrophobicity/hydrophilicity) can be modified for different geometries (flat support, inside pores, outside curved surfaces) so that we retain maximum retention of enzymatic activity.

Publications (acknowledging DOE support)

1. Radhakrishna, M.; Sharma, S.; Kumar, S. K., Enhanced Wang Landau sampling of adsorbed protein conformations. *J Chem Phys* **2012,** 136, (11), 114114-114114.
2. Sharma, S.; Berne, B. J.; Kumar, S. K., Thermal and Structural Stability of Adsorbed Proteins. *Biophysical Journal* **2010,** 99, (4), 1157-1165.
3. Radhakrishna, M.; Grimaldi, J.; Belfort, G.; Kumar, S. K., Stability of Proteins Inside a Hydrophobic Cavity. *Langmuir* **2013**.

References:

1. Fischer C, Kleinmarcuschamer D, Stephanopoulos G. 2008. *Metabolic Engineering* 10: 295-304
2. Yethiraj A, Striolo A. 2013. *The Journal of Physical Chemistry Letters* 4: 687-90
3. Tullo A, Johnson J. 2013. *C&EN* 91: 9-13
4. Inui M, Suda M, Kimura S, Yasuda K, Suzuki H, et al. 2007. *Applied Microbiology and Biotechnology* 77: 1305-16
5. Atsumi S, Hanai T, Liao JC. 2008. *Nature* 451: 86-9
6. Lee WH, Seo SO, Bae YH, Nan H, Jin YS, Seo JH. 2012. *Bioprocess and Biosystems Engineering*: 1-9
7. Steen EJ, Chan R, Prasad N, Myers S, Petzold CJ, et al. 2008. *Microbial Cell Factories* 7: 36
8. Wargacki AJ, Leonard E, Win MN, Regitsky DD, Santos CNS, et al. 2012. *Science* 335: 308-13
9. Zhou J, Li Y. 2010. *Protein & cell* 1: 207-10
10. Daugulis AJ, Axford DB, McLellan PJ. 2009. *The Canadian Journal of Chemical Engineering* 69: 488-97
11. Pospíšil S, Kopecký J, Přikrylová V, Spížek J. 2006. *FEMS microbiology letters* 172: 197-204
12. Strathmann H, Gudernatsch W. 1991. *Extractive Bioconversions*: 67-89
13. Grimaldi J CC, Belfort G. *(To be submitted by Aug 1st)*
14. Grimaldi J CC, Belfort G. *(In Prep)*

Project Title: Miniaturized Hybrid Materials Inspired by Nature

Principle Investigator (PI): C. R. Safinya
Co-PIs: Y. Li and K. Ewert
Mailing Address: Materials Department, University of California at Santa Barbara
Santa Barbara, CA 93111
E-mail: safinya@mrl.ucsb.edu

Program Scope

The aims of our research program are to develop a fundamental understanding of the mechanisms underlying lipid- and protein directed assembly, in particular, in elucidating inter-macromolecular interactions in charged systems [1]. The biophysical and physicochemical approaches used in our studies are intended to lead to biomimetic materials with scientific and technological interest.

An important strategy that we will use to achieve our aims is to design functional biomimetic systems based on our understanding of much more complex cellular assemblies. In cells, microtubules (nanometer scale hollow cylindrical biological polyelectrolytes) and their assemblies are critical components in a broad range of functions from providing tracks for the transport of cargo to forming bundles in neurons both to elongate axons and to impart mechanical stability [2]. Previous studies have shown that counterion directed bundling of microtubules (MTs) is an important model system for studies of competing long-range repulsions and short-range attractions [3]. Nevertheless, even in these relatively simple systems our understanding of how assembly occurs remains to be fully understood. For example, while theory and simulations predicts that rigid polelectrolytes should form tight bundles in the presence of counterions, experiments show that the valence of the counterion dictates the observed distinct structures including, tight and loose bundles. More recently, in a series of experiments designed to alter the inter-filament electrostatic interactions through changes in ionic strength, we have discovered that sidearm-directed neurofilament assembly can result in the formation of hydrogels with unexpected and novel properties [4]. (Neurofilaments (NFs), intermediate filaments specific to neurons, consist of three distinct subunit proteins: NF-L (low MW), NF-M (medium MW), and NF-H (high MW), which assemble into a 10 nm core filament with protruding charged sidearms [5-7].) With decreasing ionic strength NF networks transition from a nematic liquid crystal (LC) hydrogel (with parallel filament orientation) to an isotropic hydrogel (with random, crossed filament orientation) and to a reentrant birefringent LC hydrogel (again with parallel filament orientation) [4]. Significantly, these hydrogels exhibit reversibly tunable elastic moduli and remarkable water retention and release properties, which depend on the underlying symmetry of the network (i.e., isotropic versus liquid crystalline).

The projects utilize the broad spectrum of expertise of the PI and Co-PIs in biomolecular self-assembling methods (Safinya, Li, Ewert), custom synthesis (Ewert), and synchrotron X-ray scattering, and electron and optical microscopy characterization techniques (Safinya and Li).

Recent Progress

2D packing of short DNA with non-pairing overhangs in charged membrane–DNA complexes: from Onsager nematics to columnar nematics with finite-length columns

Findings In recent work [9, 14] we described the self-assembling properties of a series of short double-stranded DNA molecules electrostatically adsorbed on membranes (Fig. 1). Employing synchrotron x-ray scattering, we studied ordering on a 2D membrane platform for 11 bp, 24 bp, and 48 bp sDNA rods with single-stranded oligo-thymine (T) overhangs modulating the end-to-end interactions [9]. The DNA ends were designed to enable directed assembly due to controlled competing interactions. These include end-to-end attractions competing with repulsive interactions mediated through different length single-strand thymine nucleotides ends.

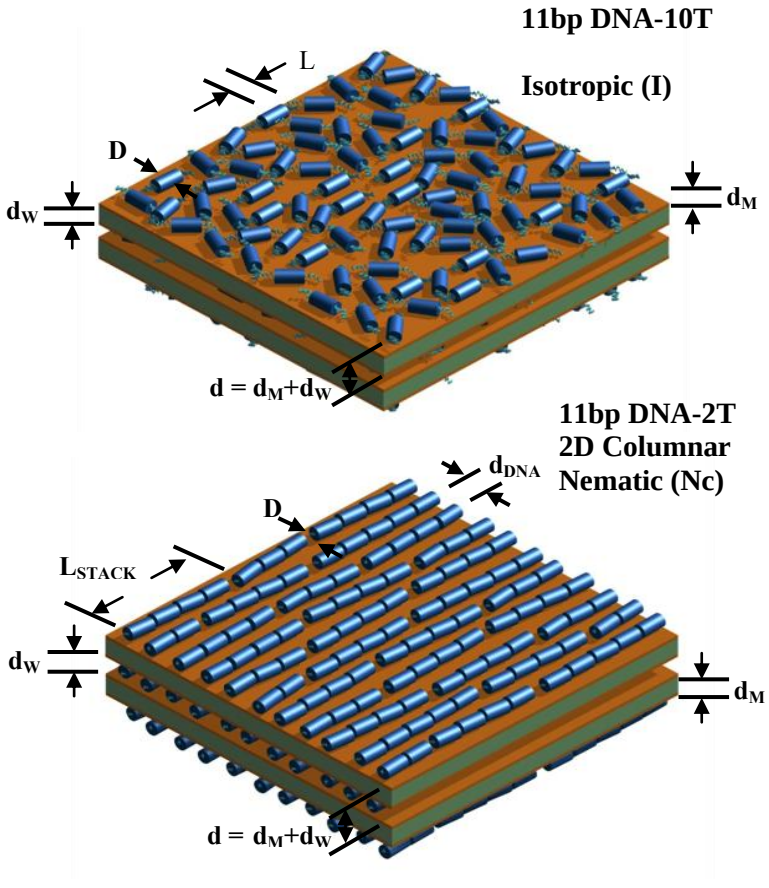

Figure 1. Schematic drawings of the distinct packing phases of short DNA (sDNA) rods (all of which contain non-sticky overhangs) in cationic liposome–short DNA (CL–sDNA) complexes. The complexes are multilamellar assemblies of alternating cationic lipid bilayers of thickness d_M and water layers of thickness d_W. The water layer contains a monolayer of sDNA molecules. The multilamellar unit cell dimension is $d = d_W + d_M$. **(TOP)** The isotropic phase with short-range positional and orientational order, as observed for 11bp DNA-10T (11 bp DNA core with a 10-T non-sticky overhang at each end), with small shape anisotropy length/width = L/D ≈ 1.9. For 48 bp DNA rods with non-sticky ends L/D ≈ 8.16 and one observes the formation of the nematic (N) liquid crystal (LC) phase of sDNA with all rod shaped molecules pointing along the same average direction (picture not shown). Formation of this phase by sDNA rods with sufficiently anisotropic shape is consistent with Onsager's model of LC ordering of anisotropic rods. **(BOTTOM)** A new type of 2D columnar nematic phase, as observed for 11bp DNA-2T rods. The onset of strong DNA end-to-end interactions for 11 bp DNA with very short (2 T) non-sticky overhangs leads to the formation of a distribution of 1D stacks of sDNA rods, which become the building blocks of the nematic phase. The 1D stacks have an average size of ≈ 4 rods, corresponding to an effective length to width ratio L/D ≈ 7.3). d_{DNA} corresponds to the average interhelical spacing. Adapted from [8].

For 48bp and 24bp DNA molecules we find DNA assembly leading to the nematic (N) liquid crystal (LC) phase of short DNA rods with long-range orientational order consistent with the predictions of a well-known model of LC ordering by Lars Onsager. (Onsager showed that that

anisotropic rods (with length L and width w) will exhibit a purely entropic transition from a disordered liquid to the oriented nematic (N) phase when $L/D \geq 4$.) For very short 11bp DNA (where Onsager theory predicts that LC ordering should not occur because $L/D \approx 1.9$ is less than 4, the minimum length to width anisotropy required for LC ordering) our work has led to the unexpected discovery that end-to-end interactions between the rods with 2T overhangs set in dramatically and a new 2D columnar nematic phase (labeled N_C) is found where the building blocks are on average comprised of 1D stacks of four 11bp DNA-2T rods (see Figure 1, bottom).

Significance of Findings Our findings have important implications in the general area of DNA-based assembly in nanotechnology. To date, all DNA-directed assembly/crystallization of colloidal particles (such as metallic or non-metallic nanoparticles with optical and optoelectronic properties) into larger scale materials has been based on recognition through H-bonding of complimentary base pairs. The methods involve joining building blocks together through complimentary (sticky) ends tethered to apposing surfaces, or via non-complimentary projecting domains bridged by an intermediate oligonucleotide with sticky ends. In contrast, the results presented in our paper [8] offer a new direction in DNA-based directed assembly on a two-dimensional substrate platform, where macromolecular building blocks, containing short base pairs tethered to their surfaces, would self-assemble due to end-end stacking interactions. A key point is that the DNA end-end interactions are driven by hydrophobic interactions and will be stable at temperatures where complementary base-pairing H-bonding interactions tend to melt.

Future Plans

(1) Biomimetic hydrogels Following our recent BES-supported experiments [15] we will explore the development of NF-mimicking functional isotropic and liquid crystal hydrogels. The hydrogels will result from the directed assembly of building blocks by custom-synthesized polyampholyte and "polyampholyte-mimicking" linkers. The hydrogels are expected to exhibit salt-responsive tunable elastic moduli and water retention and release properties.

(2) Self-assembly of biomolecules in unilamellar vesicles We have initiated experiments exploring the effects of the confining environment of modestly sized (of order 1000 nm) to extremely large giant unilamellar vesicles (GUVs on the order of 10s of microns mimicking cell dimensions), on the assembling behavior of biological polyelectrolytes. The biopolymers will cover a range of persistence lengths from 100 nm (DNA) and 10^3 nm (intermediate filaments) to 10^4 nm (F-actin from the assembly of G-actin) and a few millimeters (microtubules from the assembly of tubulin). We expect a sharp transition in vesicle shape behavior when the persistence length of the polyelectrolyte crosses the range from being less than the size of the vesicle to larger than the vesicle. The shape, in turn, is expected to feedback and further influence the dynamical self-assembling process. The studies will be conducted both under equilibrium and out-of-equilibrium conditions; e.g., where energy derived from hydrolysable GTP and ATP bonds drive the dynamics, and where we expect distinctly different behavior.

References

1. Safinya, C. R.; et al.: Nanoscale Assembly in Biological Systems: From Neuronal Cytoskeletal Proteins to Curvature Stabilizing Lipids. *Adv. Mater.* **2011**, *23*, 2260-2270.

2. Bray, D. D., Cell Movements: From Moleculse to Motility (Garland, ed. 2, NY, 2001)
3. Needleman, D. J.; et al.: Higher-order assembly of microtubules by counterions: From hexagonal bundles to living necklaces. *PNAS USA* **2004**, *101*, 16099-16103.
4. Deek, J.; Chung, P. J.; Kayser, J.; Bausch, A. R.; Safinya, C. R.: Neurofilament sidearms modulate parallel & crossed-filament orientations inducing nematic to isotropic & re-entrant birefringent hydrogels. *Nature Communications* **2013**, *in press*.
5. Janmey, P. A.; Leterrier, J. F.; Herrmann, H.: Assembly and structure of neurofilaments. *Curr. Opin. Colloid Interface Sci.* **2003**, *8*, 40-47.
6. Beck, R.; Deek, J.; Jones, J. B.; Safinya, C. R.: Gel Expanded–Gel Condensed Transition in Neurofilament Networks by Direct Force Measurements, *Nature Materials* **2010**, *9*, 40-46.
7. Beck, R.; Deek, J.; Choi, M. C.; Ikawa, T.; Watanabe, O.; Frey, E.; Pincus, P. A.; Safinya, C. R.: Unconventional Salt-Switch from Soft to Stiff in Single Neurofilament Biopolymers. *Langmuir* **2010**, *26*, 18595-18599.

Publications (BES-supported, last 24 months, only in print and accepted papers)

8. Bouxsein, N. F.; et al: Two-Dimensional Packing of Short DNA with Nonpairing Overhangs in Cationic Liposome–DNA Complexes: From Onsager Nematics to Columnar Nematics. *J. Am. Chem. Soc.* **2011**, *133*, 7585-7595. DOI: 10.1021/ja202082c.
9. Safinya, C. R.; et al.: Nanoscale Assembly in Biological Systems: From Neuronal Cytoskeletal Proteins to Curvature Stabilizing Lipids. *Advanced Materials* **2011**, *23*, 2260-2270. DOI: 10.1002/adma.201004647.
10. Zidovska, A.; et al.: Block Liposome and Nanotube Formation is a General Phenomenon of Membranes Containing Multivalent Lipids. *Soft Matter* **2011**, *7*, 8363-8369 (Cover of September 21 issue). DOI: 10.1039/C1SM05481C.
11. Leal, C.; et al.: Nanogyroids Incorporating Multivalent Lipids: Enhanced Membrane Charge Density and Pore Forming Ability for Gene Silencing. *Langmuir* **2011**, *27*, 7691-7697. DOI: 10.1021/la200679x.
12. Shirazi, R. S.; et al.: Structural Evolution of Environmentally Responsive Cationic Liposome–DNA Complexes with a Reducible Lipid Linker. *Langmuir* **2012**, *28*, 10495-10503 (Cover of July 17 issue). DOI: 10.1021/la301181b.
13. Beck, R.; et al.: Structures and interactions in bottlebrush neurofilaments: the role of charged disordered proteins in forming hydrogel networks. *Biochem. Soc. Trans.* **2012**, *40*, 1027-1031. DOI: 10.1042/BST20120101.
14. Leal, C.; et al.: Stacking of Short DNA Induces the Gyroid Cubic-to-Inverted Hexagonal Phase Transition in Lipid–DNA Complexes. *Soft Matter* **2013**, *9*, 795-804. DOI: 10.1039/C2SM27018H.
15. Deek, J.; Chung, P. J.; Kayser, J.; Bausch, A. R.; Safinya, C. R.: Neurofilament sidearms modulate parallel and crossed-filament orientations inducing nematic to isotropic and re-entrant birefringent hydrogels. *Nature Communications* **2013**, *in press*.
16. Needleman, D. J.; Ojeda-Lopez, M. A.; Raviv, U.; Miller, H. P.; Li, Y.; Song, C.; Feinstein, S. C.; Wilson, L.; Choi, M. C.; Safinya, C. R.: Ion specific effects in bundling and depolymerization of taxol-stabilized microtubules. *Faraday Discussions* **2013**, *in press*.

Program Title: Assembling Microorganisms into Energy Converting Materials

Principle Investigator: Ozgur Sahin
Mailing Address: Department of Biological Sciences and Department of Physics, Columbia University, New York, NY 10027, USA
E-mail: sahin@columbia.edu

Program Scope

This program aims to investigate and harness the capabilities of biological structures to convert energy from naturally occurring variations in relative humidity (RH). Progress in this direction can potentially lead to new forms of energy converting materials with unique capabilities for harvesting energy from evaporation, storage of energy in environmentally benign and abundant biomaterials, and high work density actuation.

Biological organisms have developed numerous water-responsive structures that convert energy from water potential gradients into mechanical work to power vital biological tasks [1]. Our strategy is to integrate these energy converting biological structures into engineered materials. This approach has the advantage that the key energy converting components are synthesized biologically and can be genetically manipulated. We rely on micrometer-sized spores of *Bacillus* as energy converting biological materials. Spores can change their diameter by as much as 12% in response to changing RH [2, 3]. Our previous experiments [4] revealed that the elastic modulus of spores are on the order of 10 GPa, suggesting that humidity driven changes in spore size must exhibit high energy densities. To investigate the possibility of creating robust and scalable energy conversion materials based on spores, this research program spreads over two main thrusts: 1) development of hybrid structures that can efficiently generate electricity by converting energy from evaporation of water in to sub-saturated atmosphere; 2) understanding how the interaction between water and the nanostructure of spores imposes limits on energy conversion. The result of these studies will demonstrate the potential of biologically based devices and identify challenges and strategies for further progress. We use a combination of experiments with individual spores and with centimeter-scale, spore-based structures created by self-assembly.

Recent Progress

Summary: We have focused our recent efforts to determine the energy density of individual spores. Our initial experiments (see Fig.1) have demonstrated a relatively high energy density, fast response time, and high reversibility of spore based energy conversion. We have used atomic force microscopy (AFM) based experiments to characterize the energy

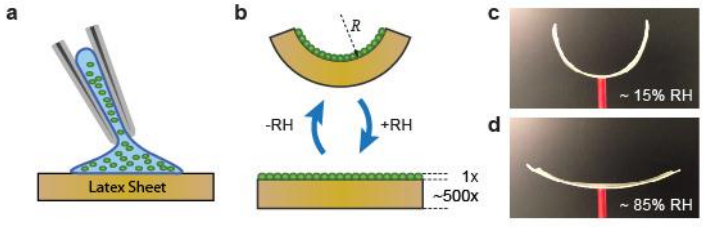

FIG. 1. (a) Scheme depicting the deposition of an approximate monolayer of spores on a rubber latex sheet. (b) Spores induce curvature in response to changing RH. In this demo, the thickness ratio between latex sheet and the spore layer is approximately 500. (c, d) Experimental observation of (b) latex sheet (2 cm x 6 cm x 0.35 mm) coated with a layer of *B. subtilis*. The RH is ~15% in (c) and 85% in (d).

conversion processes of individual spores. Specifically, we have created a thermodynamic cycle, in which the force applied to the spore and the RH level surrounding the spore were cyclically altered to obtain a positive work output in every cycle. These experiments require dynamic control of RH surrounding the spore, application of sufficiently large pressures to deform the spore structure, and precise measurements of the deformation. To meet these requirements, we have developed an environment-controlled AFM system with force sensing cantilevers having sufficiently high spring constants and tip diameters. Our results show that energy densities of spores are orders of magnitude higher than the best synthetic water-responsive materials [5] and conventional actuator materials.

Customization of the AFM setup: Although AFM provides a suitable experimental platform for measuring the energy density of individual spores; there are several technical challenges that we had to address. We have found that changes in RH causes significant drifts in the position of the sample stage of AFM, making it difficult to determine changes in the sizes of spores upon water absorption/release. We have addressed this difficulty by (1) minimizing the volume where RH is controlled and (2) minimizing the duration of RH change. The optimized experimental setup allows us to maintain sample stage drift within approximately 4 nm, while changing the RH surrounding the sample from about 15% to more than 90%.

In addition to the customizations of the environment control of AFM, we also had to tailor the force probe of the AFM for measuring the forces generated by the spores. The high work density of spores result in forces up to 0.1 mN, which is much larger than forces typically encountered in AFM experiments. We have used custom-made AFM nano-indenter probes having high spring constants (up to 1 kN/m) and large tip radiuses ~ 800 nm, which is comparable to the dimensions of individual spores (Fig. 2a).

Experimental results: Using the custom AFM setup, we have measured maximum strain and energy density of spores. The basic experiment involves changing the RH rapidly and monitoring the response of spore diameter while the spore is subjected to external pressure applied by AFM. We found that despite having large spring constants and tip diameters, custom-made AFM nano-indenter probes are able to image spores immobilized on silicon or mica substrates in the tapping-mode (Fig. 2b). Taking advantage of this imaging capability, we selected spores that are not in direct contact with other spores to perform energy density measurements illustrated in Fig. 2c. Once the probe tip is placed on the spore in the contact mode, the spore height can be

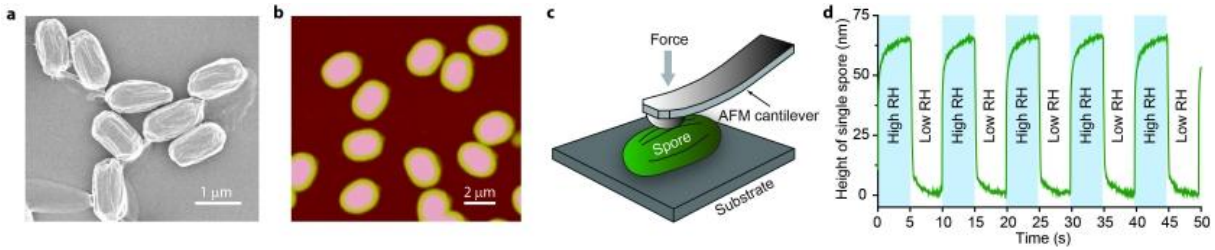

FIG. 2. (a) SEM image of *B. subtilis* on a silicon substrate. (b) AFM image of *B. subtilis* spores on a mica substrate. The resolution is limited because of the large tip radius. (c) Illustration of AFM based probing of individual spores. (d) Strain response of *B. subtilis* to changing RH. Spore diameter is approximately 700 nm.

measured as a function of RH or force. As shown in Fig. 2d, we first measured the overall changes of spore height as RH is cycled between ~ 15% to ~ 90%. The changes in height seen in

Fig. 2d correspond to a strain of ~ 8%. The data also show that the response of spores to changing in RH is relatively fast (less than 1 second and likely limited by rate of change of RH).

To measure work density of spores, we have created a thermodynamic cycle by changing forces and RH levels in four stages illustrated in Fig. 3a. In stage I, the spores rest at low RH air. The AFM probe applies a small force to the spores, just enough to maintain contact. In stage II, the cantilever exerts a predetermined force (loading). The spores respond by reducing their overall height. In stage III, the spores are subjected to high RH while the force is maintained constant. Spores respond to increasing RH by expanding and pushing the cantilever away from the surface. In stage IV, the force is reduced back to zero. The spores expand further due to the reduction in mechanical load. The cycle is completed by lowering the RH to the initial level. Because spores expand against force at stages III and IV, there is a positive work output of the thermodynamic cycle. Fig. 3b shows experimentally measured force vs. height curves as single spores of *B. subtilis* go through the thermodynamic cycle under various maximum pressures. The areas enclosed by the force vs. height curves correspond to the amounts of work done by individual spores, which reaches ~ 0.5 pJ. We determine the energy density of spores by considering the contact mechanics between the spherical tip and the spore (approximated with a cylinder) and estimating the volume of the spore contributing to the mechanical work. Based on this analysis, we observed that spores of *B. subtilis* exhibit energy densities around 10 MJ/m^3.

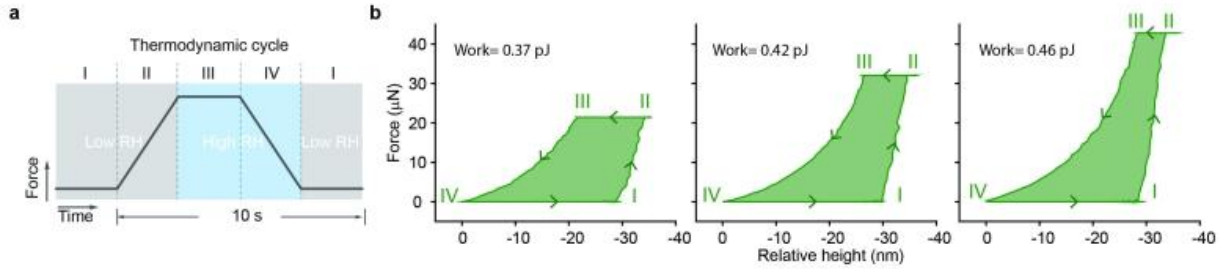

FIG. 3. (a) Illustration of a thermodynamic cycle created by controlling the force and RH (experimental setup is illustrated in Fig. 2c). (b) Force vs. relative-height curves of *B. subtilis* with different peak forces during the thermodynamic cycle.

Discussion of findings: The energy density of spores obtained from measurements on individual spores is orders of magnitude higher than the best synthetic water-responsive materials [5] and conventional actuator materials. These results suggest that spores can potentially serve as building blocks of high energy density stimuli-responsive materials whose applications range from energy harvesting and storage to high performance actuators for robotics.

Future Plans

Correlate variations among the energy densities of different species with their morphology and/or chemical composition.

We are planning to study energy conversion process of spores using different species and mutant spores. For example, previous experiments showed that *B. thuringiensis* exhibit a higher stain than *B. subtilis* [2]. In addition, specific mutations in *cotE-gerE* mutant of *B. subtilis* allow removing a large portion of spore coat, which could increase spore energy density by removing parts that do not contribute to energy conversion.

Measure kinetics of water transport within the spore nanopores with dynamic AFM methods.
We plan to investigate kinetic limits on the power generated by the spores due to water transport limitations. These experiments can teach us about the behavior of water in nanoscale biologically confined environments. We plan to use dynamic AFM methods to study the kinetics of water transport within the spores. Energy dissipation due to transport limitations can affect resonance behavior of an AFM tip in contact with a spore.

Refine energy density estimates by theoretical modeling.
Energy density of spores can be calculated by dividing the work done to the volume contributing to the work. Due to the finite size of tip, the applied pressure is non-uniform within the contact region between large radii sphere tip and spore. We are currently modeling the contact mechanics between the AFM tip and the spore to make a better estimation of energy density.

Develop centimeter scale devices with oscillatory response and investigate the role of transport limitations on the power output and frequency.
We plan to investigate bacterial spore based mechanical oscillators that can cyclically absorb moisture from high RH air and release moisture into dry air while producing a net power output. We will investigate the role of moisture transport limitations on oscillation frequency and power output.

References

1. Fratzl, P. and F.G. Barth, *Biomaterial systems for mechanosensing and actuation.* Nature, 2009. **462**(7272): p. 442-448.
2. Westphal, A.J., et al., *Kinetics of size changes of individual Bacillus thuringiensis spores in response to changes in relative humidity.* Proceedings of the National Academy of Sciences of the United States of America, 2003. **100**(6): p. 3461-3466.
3. Plomp, M., et al., *The high-resolution architecture and structural dynamics of Bacillus spores.* Biophysical Journal, 2005. **88**(1): p. 603-608.
4. Sahin, O., et al., *Physical basis for the adaptive flexibility of Bacillus spore coats.* Journal of the Royal Society Interface, 2012. **9**(76): p. 3156-3160.
5. Ma, M.M., et al., *Bio-Inspired Polymer Composite Actuator and Generator Driven by Water Gradients.* Science, 2013. **339**(6116): p. 186-189.

References acknowledging DOE support

6. Chen, X., Mahadevan, L., Driks, A. & Sahin, O. Spores of *Bacillus* as building blocks of high energy density stimuli-responsive materials and nanogenerators. *Submitted*

Program Title: (Bio)Chemical Tailoring of Biogenic 3-D Nanopatterned Templates with Energy-Relevant Functionalities

Principal Investigator (PI): Kenneth H. Sandhage; Co-PI: Nils Kröger
Mailing Address: 771 Ferst Drive, School of Materials Science and Engineering, Georgia Institute of Technology, Atlanta, GA 30332
E-mail: ken.sandhage@mse.gatech.edu

Program Scope: The overall aim of this research has been to obtain fundamental understanding of (bio)chemical methodologies to enable utilization of the unique 3-D nanopatterned architectures naturally produced by diatoms for the syntheses of advanced catalytic and structural materials attractive for bio-energy conversion and energy storage applications. This research has been conducted in three thrusts:

Thrust 1 (*Mechanistic analysis of in vivo immobilization of proteins in diatom biosilica*) is directed towards elucidating the fundamental mechanism(s) underlying the cellular processes of *in vivo* immobilization of proteins in diatom silica.

Thrust 2 (*Mechanistic analysis of shape-preserving reactive conversion of diatom biosilica into porous, high-surface area inorganic replicas*) is aimed at understanding the fundamental mechanisms of shape preservation and nanostructural evolution associated with the reactive conversion of diatom biosilica templates into porous, high surface area inorganic replicas.

Thrust 3 (*Immobilization of energy-relevant enzymes in diatom biosilica and onto diatom biosilica-derived inorganic replicas*) involves use of the results from both Thrust 1 and 2 to develop strategies for *in vivo* and *in vitro* immobilization of enzymes in diatom biosilica and diatom biosilica-derived inorganic replicas, respectively.

Recent Progress

Thrust 1 Progress: We have previously demonstrated that peptide segments of silaffins that contain pentalysine clusters (PLCs; i.e., five non-consecutive lysines within a stretch of 12-14 amino acid residues) are particularly potent in immobilizing proteins in diatom silica *in vivo* (11). Segments T6 and T7 were the shortest PLC-containing peptides that exhibited high silica-targeting efficacy, and were chosen to investigate the structure-function correlation in PLCs by expressing GFP fusion proteins and analyzing them by fluorescence microscopy of live cells and isolated biosilica. This analysis has revealed the following features of PLC structure are important for silica immobilization (11): (i) lysines need to be post-translationally modified and cannot be replaced by arginines; (ii) the PLC needs to contain at least one phosphoserine residue; and (iii) PLC function is sequence independent. This information is important for further analyses of molecular mechanisms of protein transport to the silica deposition vesicle in diatoms.

Thrust 2 Progress: Recent work has focused on: i) determining the kinetic mechanism of shape-preserving magnesiothermic SiO_2 reduction (leading to highly-porous Si replicas of diatom micro-shells), ii) understanding how shape is preserved during such transformation, and iii) developing a reaction-based method for generating highly-porous Au replicas of diatom microshells (12).

The magnesiothermic reduction of SiO_2 has been conducted at $\leq 750^oC$ via the net reaction:

$$2Mg(g) + SiO_2(s) => 2MgO(s) + Si(s) \quad (1)$$

This reaction yields a product layer comprised of a compact, interwoven mixture of nano-crystalline MgO and Si (7,14,15). The thickening of this product layer followed a parabolic rate law with time (Fig. 1a) and occurred predominantly by reaction at an internal interface (not at the external surface of the MgO/Si

layer). These observations were consistent with magnesio-thermic reduction being controlled by inward magnesium diffusion through the product layer.

Owing to the reaction-induced increase in solid volume, the adherent MgO/Si product layer formed on SiO_2 was in a state of high compression (a residual stress >5 GPa was detected after 1 h of reaction at 750°C by XRD analysis). However, appreciable distortion and cracking were not observed during shape-preserving magnesiothermic reduction at $\leq$750°C. Upon annealing of partially-reacted specimens at 750°C, MgO nanocrystals formed on the specimen surface in increasing amounts with time, to yield a compact and thickening MgO layer on the external surface of the MgO/Si product. The increase in thickness of this MgO layer was inversely pro-portional to the decrease in residual stress (Fig. 1b), which was consistent with stress-induced migration of MgO as a predominant mechanism of stress relaxation and shape preservation.

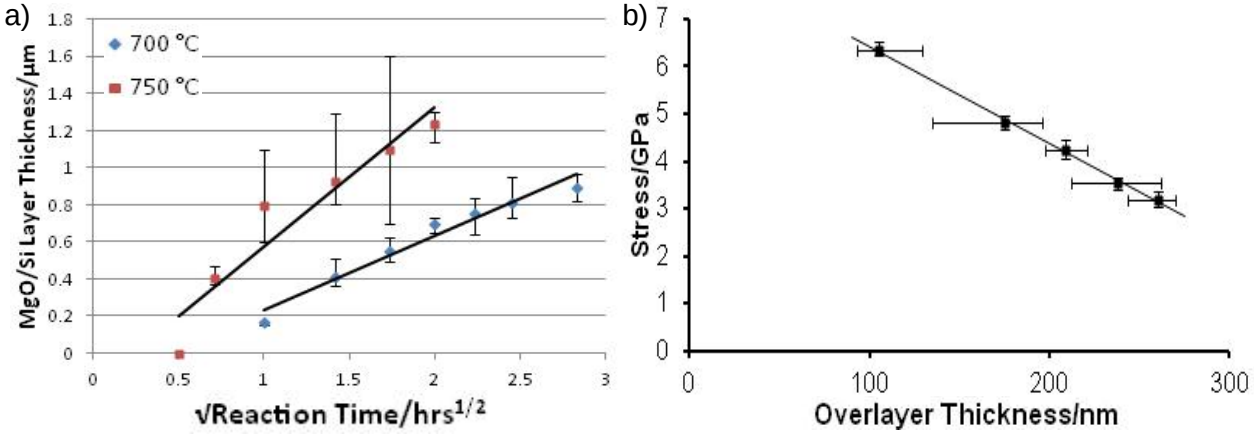

Figure 1. a) Parabolic thickening of the MgO/Si product layer formed on SiO_2 during magnesiothermic reduction at 700 and 750°C. b) Correlation between the relaxation in compressive stress in the MgO/Si product layer, and the thickness of the MgO formed on this product layer, during annealing at 750°C.

Gold is commonly used as a conductive template for enzyme immobilization. Over the past year, a reaction-based process has been developed for converting diatom microshells into highly-porous Au replicas for enzyme loading (in Thrust 3). A series of shape-preserving gas/solid reactions was used to convert diatom silica into high specific surface area (>1300 m^2/g) carbon replicas (1,13). These replicas were functionalized with tin(II) chloride as a catalyst, and then exposed to a silver electroless deposition solution. After carbon pyrolysis, the silver replicas were exposed to an aqueous chloroauric acid solution to displace silver with gold. The resulting Au-bearing specimens retained the diatom microshell morphology and possessed a surface area 10 times higher than previously reported for Au diatom microshell replicas (13).

Thrust 3 Progress: Recent work in this thrust has focused on evaluating catalysis upon flow through powder beds of enzyme-loaded diatom-derived or commercial supports. Glucose oxidase (GOx), a negatively-charged model enzyme, was cross-linked with protamine (PA) to yield a positively-charged hybrid (GOx-PA) with the same specific activity as GOx (16). Negative charges were introduced to surfaces of C microshell replicas (dC) and Au-bearing replicas (dAAS) to allow for electrostatic GOx-PA binding. dC specimens were treated with 2.6 M HNO_3 for 48 h (dC_{Ox}) to generate surface carboxyl groups. The dC_{Ox} supports were then exposed to a dendritic amplification protocol for further carboxyl enrichment (dC_{Ox1Amp}). dAAS specimens were treated with 3-mercaptopropionic acid (MPA) to apply a monolayer with pendant carboxyl groups ($dAAS_{MPA}$). Vulcan carbon exposed to HNO_3 for 48 h (VC_{Ox}), and gold nanoparticles (50-100 nm dia.) exposed to MPA ($AuNP_{MPA}$) were used as commercial supports.

Specific values of surface area (SSA), mesopore volume for pores of 2-50 nm dia. (SMeV[2-50]) or 22-50 nm dia. (SMeV[22-50]), and GOx-PA loading of various templates are shown in Table 1.

Table 1. Specific values of surface area, mesopore volume, enzyme loading, and catalytic activities of diatom silica, diatom-derived replicas, and reference particles. One Unit (1 U) of GOx-PA activity corresponded to 1 µmol glucose consumed per min. n.d.: not determined. b.d.l.: below detection limit.

Sample	SSA (m^2g^{-1})	SMeV[2-50] (cm^3g^{-1})	SMeV[22-50] (cm^3g^{-1})	Enzyme Loading (10^{-3} g enzyme g^{-1} support)	Specific Activity (10^{-3} Ug^{-1} GOx-PA)
$dSiO_2$	1.72	0.005	5.91×10^{-4}	1.9	56.0
dC_{Ox1Amp}	180	0.307	0.0189	63.7	51.3
VC_{Ox}	63.6	0.037	2.29×10^{-3}	12.3	25.3
$dAAS_{MPA}$	64.2	0.052	1.90×10^{-3}	15.7	49.3
$AuNP_{MPA}$	1.17	b.d.l.	1.20×10^{-5}	10.1	20.7

Catalysis trials were conducted by circulating a glucose solution at a constant rate through a powder bed of a given GOx-PA-loaded material. For the first 15 min, a constant rate of glucose consumption was observed for each GOx-PA-loaded support (Fig. 2). This initial rate of glucose reaction, which followed the trend in specific enzyme loading for these supports (Table 1), increased in the order: $dSiO_2$ < $dAuNP_{MPA}$ < VC_{Ox} < $dAAS_{MPA}$ <dC_{Ox1Amp}. When the glucose consumption rate was normalized to the GOx-PA loaded on a given support, the values of specific catalytic activity (far right column, Table 1) were similar and highest (49.3-56.0x10^{-3} Ug^{-1}) for all diatom-shaped supports ($dSiO_2$, dC_{Ox1Amp}, $dAAS_{MPA}$) relative to the reference supports (20.7-25.3x10^{-3} Ug^{-1}). This result indicated that the diatom-derived hierarchical morphology strongly promoted interaction of GOX-PA with glucose relative to conventional supports (13).

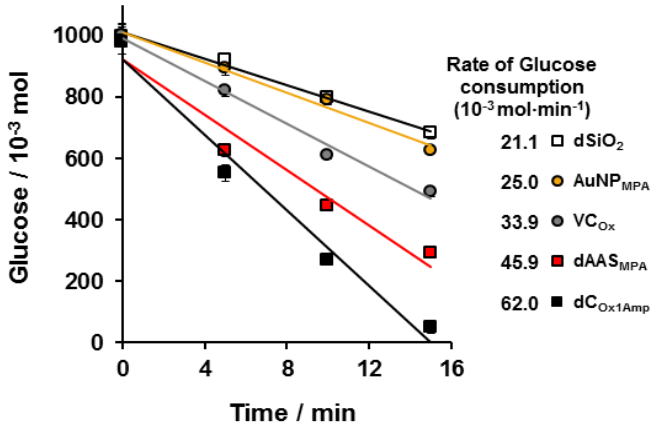

Figure 2. Glucose consumption as a function of time during flow-through catalysis for the first 15 min through powder beds comprised of GOx-PA-loaded microparticles.

Importance of Findings: Nature provides impressive examples of organisms, such as diatoms, capable of forming complex 3-D hierarchically-patterned (nano-to-microscale) inorganic structures with fidelity and scalability under ambient conditions that exceed man-made assembly methods. However, the range of chemistries, particularly inorganic chemistries, formed by living organisms pales in comparison to the rich palette of complex man-made inorganic and inorganic/organic hybrid materials. The present work provides important basic insights into the 3-D shape-preserving *in vivo* and *in vitro* chemical tailoring of diatoms and diatom silica that allow for the synergistic coupling of intricate bio-enabled assembly with non-natural synthetic chemistries to yield 3-D structured materials tailored for enhanced catalysis.

Future Plans: Future proposed research will take advantage of fundamental knowledge gained on, and methods developed for, the shape-preserving chemical conversion of hierarchically-structured biogenic silica from the present project. However, instead of focusing on the generation of highly-porous inorganic replicas for use in catalytic applications, the emphasis will shift towards learning how to convert bio-optical structures (certain diatom micro-shells, butterfly scales) into replicas with attractive infrared

properties for enhanced control of thermal radiation (for heat management applications). With Nils Kröger now at the Technical Univ. of Dresden, Mohan Srinivasarao (Georgia Tech) will join this new proposed effort. Dr. Srinivasarao's expertise in modeling and evaluation of bio-optical structures is well-suited for such research.

Publications Acknowledging DoE Support over the Past Two Years

1. Bio-enabled Syntheses of Hollow, High Surface Area, Micro/mesoporous Carbon Particles with Selectable 3-D Biogenic Morphologies for Tailored Catalysis, Filtration, or Adsorption. Z. Bao, M.-K. Song, S. Davis, Y. Cai, M. Liu, K. H. Sandhage, *Energy Environ. Sci.* **4** (10) 3980-3984 (2011).
2. Direct Patterning of Arbitrary-Shaped Ferroelectric Nanostructures on Platinized Silicon and Glass Substrates. S. Kim, Y. Bastani, H. Lu, W. King, S. R. Marder, K. H. Sandhage, A. Gruverman, E. Riedo, N. Bassiri-Gharb, *Adv. Mater.* **23** (33) 3786-3790 (2011).
3. Live Diatom Silica Immobilization of Multimeric and Redox-active Enzymes. V. C. Sheppard, A. Scheffel, N. Poulsen, N. Kröger, *Appl. Environ. Microbiol.* **78** (1) 211-218 (2012).
4. Syntheses of Nanostructured Cu- and Ni-based Micro-assemblies with Selectable 3-D Hierarchical Biogenic Morphologies. Y. Fang, J. D. Berrigan, Y. Cai, S. R. Marder, K. H. Sandhage, *J. Mater. Chem.* **22** (4) 1305-1312 (2012) (Highlighted in Editors' Choice section of Science, Jan. 20, 2012)
5. Differential Responses of Osteoblast Lineage Cells to Nanotopographically-Modified, Microroughened Ti-Al-V Alloy Surfaces. R. A. Gittens, R. Olivares-Navarrete, T. McLachlan, Y. Cai, S. L. Hyzy, J. M. Schneider, Z. Schwartz, K. H. Sandhage, B. D. Boyan, *Biomater.* **33** (35) 8986-8994 (2012).
6. Biologically-enabled Syntheses of Freestanding Metallic Structures Possessing Subwavelength Pore Arrays for Extraordinary (Plasmon-Mediated) Infrared Transmission. Y. Fang, V. W. Chen, Y. Cai, J. D. Berrigan, S. R. Marder, J. W. Perry, K. H. Sandhage, *Adv. Funct. Mater.* **22** (12) 2550-2559 (2012). (Back Cover)
7. Freestanding Monolithic Silicon Aerogels. K. Chen, Z. Bao, J. Shen, G. Wu, B. Zhou, K. H. Sandhage, *J. Mater. Chem.* **22** (32) 16196-16200 (2012).
8. Differential Responses of Osteoblast Lineage Cells to Nanotopographically-Modified, Microroughened Ti-Al-V Alloy Surfaces. R.A. Gittens, R. Olivares-Navarrete, T. McLachlan, Y. Cai, S.L. Hyzy, J. M. Schneider, Z. Schwartz, K.H. Sandhage, B.D. Boyan, *Biomater.* **33** (35) 8986-8994 (2012).
9. Intergranular W/ZrC Nanocomposites via a Selective Liquid/Solid Displacement Reaction. D. W. Lipke, Y. Zhang, Y. Cai, K. H. Sandhage, *J. Am. Ceram. Soc.* **95** (9) 2769-2772 (2012).
10. The Roles of Titanium Surface Micro/Nano-topography and Wettability on the Differential Response of Human Osteoblast Lineage Cells. R. A. Gittens, R. Olivares-Navarrete, A. Cheng, D. M. Anderson, T. McLachlan, I. Stephan, J. Geis-Gerstorfer, K. H. Sandhage, A. G. Fedorov, F. Rupp, B. D. Boyan, R. Tannenbaum, Z. Schwartz, *Acta Biomater.* **9** (35) 6268-6277 (2013).
11. Pentalysine Clusters Mediate Silica Targeting of Silaffins in *Thalassiosira pseudonana*. N. Poulsen, A. Scheffel, V. C. Sheppard, P. M. Chesley, N. Kröger, *J. Biol Chem.* **288** (28), 20100–20109 (2013).
12. A Low-Temperature Magnesiothermic Reaction Process for the Scalable Production of Porous Silicon for Rechargeable Lithium Batteries. A. Xing, J. Zhang, K. Chen, Z. Bao, Y. Mei, A. S. Gordin, K. H. Sandhage, *Chem. Commun.* Published online on June 20, 2013.
13. Rapid Flow-through Biocatalysis with High Surface Area, Enzyme-loaded Carbon and Gold-bearing Diatom Frustule Replicas. S. C. Davis, V. C. Sheppard, G. Begum, Y. Cai, Y. Fang, J. D. Berrigan, N. Kröger, K. H. Sandhage, *Adv. Funct. Mater.* Accepted on April 5, 2013, in press.

Other Publications

14. Novel, Bioclastic Route to Self-Assembled, 3D, Chemically Tailored Meso/Nanostructures: Shape-Preserving Reactive Conversion of Biosilica (Diatom) Microshells. K. H. Sandhage, M. B. Dickerson, P. M. Huseman, M. A. Caranna, J. D. Clifton, T. A. Bull, T. J. Heibel, W. R. Overton, M. E. A. Schoenwaelder, *Adv. Mater.* **14** (6) 429-433 (2002).
15. Shape-preserving Reduction of Silica Micro-Assemblies into Microporous Silicon Replicas. Z. Bao, M. R. Weatherspoon, Y. Cai, S. Shian, P. D. Graham, S. M. Allan, G. Ahmad, M. B. Dickerson, B. C. Church, Z. Kang, C. J. Summers, H. W. Abernathy, III, M. Liu, K. H. Sandhage, *Nature* **446** (3) 172-175 (2007).
16. Biocatalytic Nanoscale Coatings Through Biomimetic Layer-by-Layer Mineralization. N. R. Haase, S. Shian, K. H. Sandhage, N. Kröger, *Adv. Funct. Mater.* **21** (22) 4243-4251 (2011).

A Plant Nanobionic Approach to Enhance Solar Energy Conversion of Extracted Chloroplasts using Spontaneously Assembled Nanoparticles

Michael S. Strano
Professor of Chemical Engineering
66-566 Department of Chemical Engineering
77 Massachusetts Avenue
Cambridge, MA 02139-4307
Email: strano@MIT.EDU
phone: (617) 324-4323
fax: (617) 258-8224
http://web.mit.edu/stranogroup/

The interface between plant organelles and non-biological nanostructures has the potential to impart the former with new and enhanced functions, and unlike photosynthetic proteins, has been relatively unexplored for energy applications. This nanobionic approach can yield isolated chloroplasts – plant organelles responsible for converting CO_2 and solar energy to glucose – that are more stable to reactive oxygen species ex vivo, possess enhanced photosynthetic activity, and allow real time information exchange via embedded nanosensors for free radicals. We show that cationic or anionic single walled carbon nanotubes (SWNT) have the ability to passively transport and irreversibly localize within the lipid envelope of extracted plant chloroplasts from Spinacia oleracea L. This mechanism extends to poly (acrylic acid) nanoceria (PAA-NC) and their corresponding nanotube complexes (SWNT-NC). Concentration of reactive oxygen species such as superoxide were suppressed to 42 % and 56 % by delivering PAA-NC and SWNT-NC, respectively, inside chloroplasts. Internalized SWNTs and SWNT-NC complexes promoted photosynthetic activity over 3 times higher than controls. The proposed mechanism for this increase is the ability of semiconducting SWNTs to convert solar energy into excitons that can be transferred to the chloroplast electron transport chain, thus improving photosynthetic activity. SWNT chloroplast complexes also allow fluorescent reporting of nitric oxide generation. Nanobionic engineering of extracted plant organelles may contribute to developing biomimetic light-harvesting materials with regenerative properties, enhanced efficiency and prolonged lifetimes.

Scope

Chloroplasts are the ultimate source of chemical energy making virtually all food supplies and fuel on the planet. Theoretical calculations set the limit of chloroplast glucose production efficiency at 12 % [1]. However, harnessing its photosynthetic power for solar energy conversion to liquid fuels remains a challenge. The primary goal of the program is to develop a fundamental understanding of chloroplasts self-repair photosynthetic processes to create biomimetic constructs that interface with synthetic nanomaterials giving them novel and enhanced functions. We have interfaced plant-derived components with nanostructured complexes to synthesize the first photoelectrochemical complex capable of mimicking key aspects of the plant self-repair cycle [2]. In this setup, a solution consisting of photosynthetic reaction centers, phospholipids, scaffold proteins, single-walled carbon nanotubes (SWNTs) and surfactant spontaneously self-assemble into a photoactive complex, wherein the reaction centers are each embedded into a lipid bilayer. Like plant-based self-assembly (Figure 1a), the process is completely reversible [3]. In an alternative study, we synthesized light-harvesting antennas reminiscent of those surrounding the PSII to enhance photo-conversion [4]. The core-shell constructs consisted of large band-gap nanotubes in an outer shell and small, band-gap nanotubes within the fiber core. We took advantage of chloroplasts densely packed arrays of photosystems and antenna complexes with self-assemble and self-repair properties to create the first chloroplast-based biofuel cell [5](Figure 1b). However, under ex-vivo conditions chloroplast photosynthetic rates declined because self-repairing mechanisms are limited. We hypothesized that chloroplast degradation ex-vivo is a consequence of light-induced generation of reactive oxygen species (ROS) and quantitatively showed that dextran-wrapped nanoceria (dNC) can act as a catalytic ROS scavenger whilst preserving chloroplast photoactivity [5]. However, dNC particles were not able to penetrate the chloroplast outer envelope promoting only minor scavenging of photogenerated ROS. Thus we predicted far more effective ROS scavenging by nanoceria

assembled within chloroplast photosynthetic machinery, allowing us to create novel photovoltaic complexes that could become more economically viable solutions to the energy problem

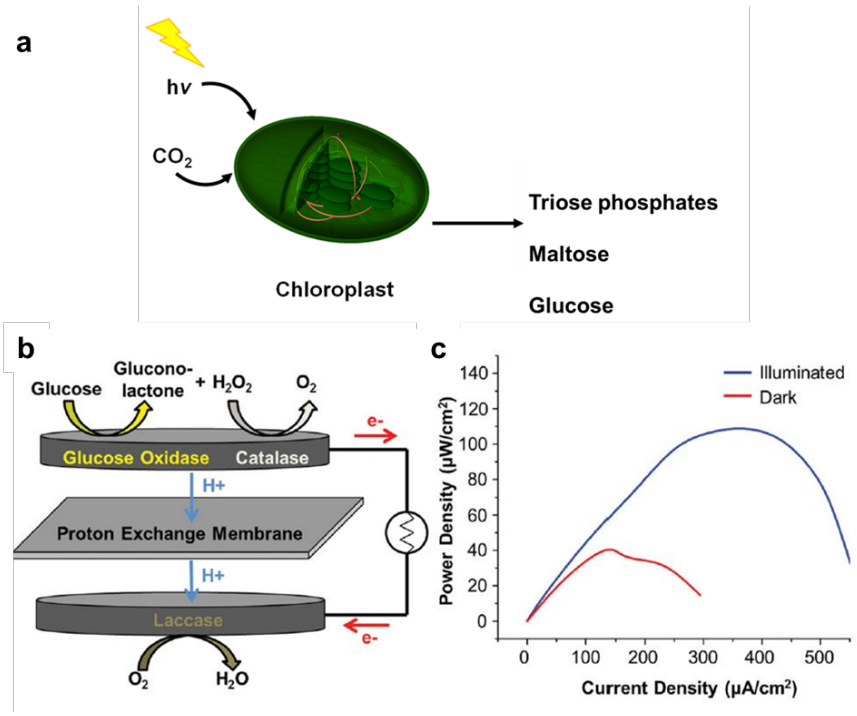

Figure 1| Chloroplast Biofuel cell [5]**. a,** By capturing atmospheric CO2, chloroplasts convert light energy into three major forms of sugars that fuel plant growth: maltose, triose phosphate and glucose. **b,** Photoelectrochemistry of extracted chloroplasts demonstrating photosynthetic yield and electrochemical conversion under illumination. Chloroplasts were incorporated into a biofuel cell that converts the exported glucose into electrons based on a platform developed by Zebda and co-workers [6].

Recent Progress

We developed a concept that is unexplored in the literature. We asked if and how nanomaterials can interface constructively with extracted plant organelles to enable novel or enhanced function. We hypothesized that the assembly of both semi-conducting and metallic nanoparticle complexes within chloroplast photosynthetic machinery has the potential to enhance solar energy capture and conversion through ROS scavenging and novel optical and electronic capabilities. This effort was divided into objectives that attempt to (1) understand a newfound mechanism of transport and spontaneous assembly of nanomaterials inside chloroplasts extracted from spinach leaves; (2) enhance the ability of the chloroplast to scavenge ROS using cerium and carbon-based nanoparticles transported to optimal sites of ROS generation, a bottleneck in extending organelle lifetime; and (3) upregulate the photoactivity and glucose output in chloroplasts via specific nanoparticle assemblies within photosynthetic machinery. These objectives constitute a plant nanobionic approach to generating new constructs for energy research which may contribute significantly to biomimetic energy generation. We utilized single-particle tracking of nIR fluorescent semi-conducting SWNTs to investigate their interaction with isolated plant chloroplasts from spinach leaves. Our group discovered that SWNTs suspended in strongly cationic or anionic coatings were found to traverse and localize rapidly within the chloroplast outer envelope. The process is observed to occur within seconds of nanoparticle interaction with the inner and outer lipid bilayer and is irreversible (Fig. 2a). This novel passive transport mechanism enables the delivery of poly (acrylic) acid nanoceria (PAA-NC) and SWNT-Nanoceria (SWNT-NC) with negative zeta potential to the sites of ROS generation within chloroplast photosynthetic membranes (Figure 2b). SWNT movement through chloroplast membranes occurs via passive mechanisms. We propose that SWNT penetration through the chloroplast lipid bilayer occurs via kinetic trapping by lipid exchange (Fig. 2c).

Glycerolipids, forming the majority of chloroplast outer envelope, wrap around SWNTs as they interact with the membrane. The disruption of the chloroplast membranes leads to lipid adsorption to the hydrophobic SWNT surface. As nanotubes penetrate through the envelopes, they are coated with a layer of lipids that irreversibly binds them to the chloroplast interior. The lipid membrane re-heals after nanoparticle uptake process is completed. This nanoparticle enabled uptake mechanism through lipid bilayers is a novel pathway for material delivery into plant organelles. Although chloroplast lipid membranes have embedded protein precursor translocons and ion channels, they lack the machinery to import key DNA strands, enzymes and inorganic catalysts to develop an independent, free-living and long term functional Engineered chloroplasts

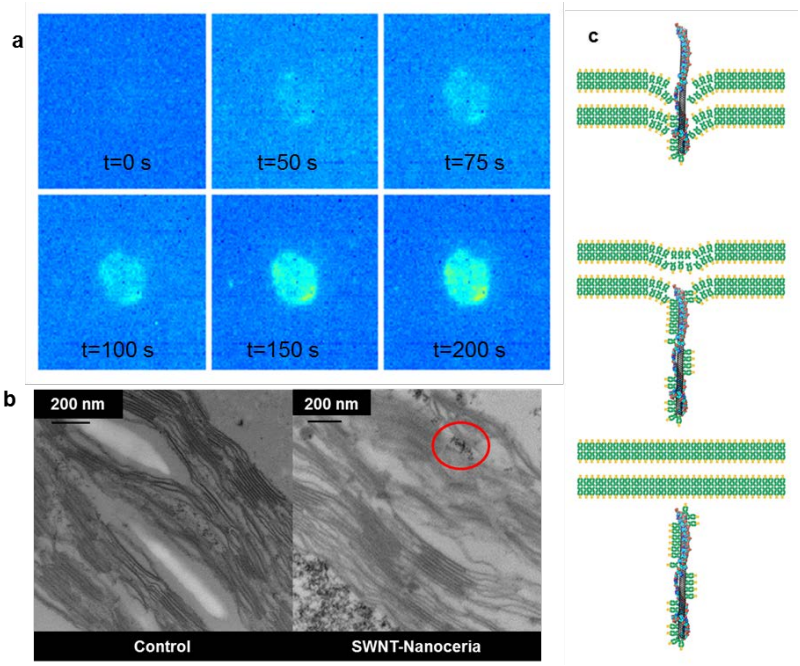

Figure 2 | Mechanism of SWNT trapping by chloroplast lipid bilayer. a, NIR photo stilt indicating rapid penetration of AT15-SWNTs through the lipid bilayers of isolated chloroplasts.
TEM images of SWNT-Nanoceria complex**. b,** Chloroplast TEM cross section, i, after incubation in SWNT-Nanoceria suspension. **c,** SWNT transport through chloroplast double membrane envelope via kinetic trapping by lipid exchange.

via nanomaterials will contribute to the development of a biomimetic light-harvesting biofuel cells with regenerative, enhanced photosynthetic properties, and prolonged lifetimes. PAA-NC and SWNT-NC localization inside chloroplasts significantly downregulates damaging ROS (Fig. 3a). Chloroplast substantial reduction in superoxide concentrations from 31.29 + 1.56 μM down to 12.99 + 0.89 with PAA-NC and 17.62 + 2.57 μM with SWNT-NC, is facilitated by the proximity of nanoparticles to the sites of ROS generation, providing a short pathway for superoxide radicals to react with nanoceria Ce3+ dangling bonds. While chloroplast ROS scavenging by 17 μM PAA-NC declines over time, other PAA-NC concentrations and SWNT-NC maintained significantly lower levels of ROS, with 1.4 and 2.8 mg L-1 SWNT-NC having the maximum impact. Chloroplast enhanced and extended photoactivity by passive assembly with SWNT-NC was evidenced in higher reduction rates of the electron acceptor dye dichloroindophenol (DCPIP) (Fig. 3b). DCPIP intercepts electrons transported from photosystem II to photosystem I in the chloroplast photosynthetic machinery 28. PAA-NC interfaced with chloroplasts had an optimum concentration at 8 μM, showing slightly higher photoactivity for the initial 3.5 hours followed by complete deactivation of photosynthetic electron transport after 6 hours. SWNT-NC particles had the strongest effect on photoactivity with more than three times higher chloroplast DCPIP reduction from light energy harnessing when chloroplasts without nanoparticles were almost inactive. Furthermore, PAA-NC unexpectedly enable isolated chloroplast glucose output in both light and dark conditions (Fig. 3c). After 88 hours of continuous light, chloroplasts assembled with PAA-NC showed a similar total glucose output of 2128.3 + 177 nmol Glc mg Chl-1 to dark PAA-NC chloroplasts, while isolated chloroplasts without nanoparticles showed no significant change in glucose production over this time period. Our results indicate that PAA-NC preserves the biochemical reactions involved in starch to glucose conversion both under light and dark conditions but does not facilitate photosynthesis ex vivo. Nanotechnology has the potential to enable novel and enhanced functional properties in photosynthetic entities for solar energy harnessing. The development of nanobionic chloroplasts is facilitated by the passive assembly of high zeta potential nanomaterials within the photosynthetic machinery.

Future Plans: The vision is to create plant-based photocatalytic complexes with regenerative, enhanced photosynthetic properties, and prolonged lifetimes. Our goal is to understand the mechanisms of how nanoceria and carbon nanotube complexes assembled in the photosynthetic machinery enable chloroplast higher photosynthetic activity and preservation of biofuel production. This nanobionic approach will lead to the development of a new generation of hybrid nanomaterial photosynthetic complexes from the organelle to the whole-plant level. The main objectives of this work will (1) examine how carbon nanotube optical and semi-conducting properties may enhance solar energy harnessing by expanding the chloroplast absorption spectrum; (2) test a novel mechanism of nanoceria preservation of chloroplast biofuel generation by modifying the pH dependent activity of enzymes responsible for starch to glucose conversion; (3) determine the effects of nanoceria and SWNT-Nanoceria as chloroplast scavengers of ROS like hydrogen peroxide and

hydroxyl radical; and (4) explore if and how nanobionics can augment biofuel synthesis at the cellular, organ and organism level.

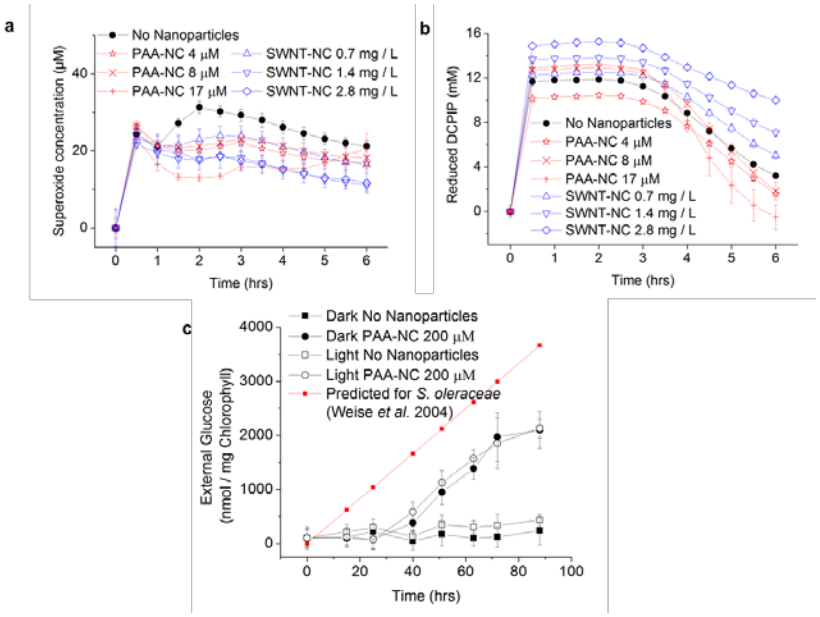

Figure 3 | Nanoceria and SWNT-Nanoceria chloroplast bionics. a, Increased superoxide scavenging by SWNT-NC and PAA-NC at chloroplast sites of ROS generation. **b,** Enhanced photoactivity of isolated chloroplasts assembled with SWNT-Nanoceria was quantified by electron transfer to DCPIP. **c,** PAA-Nanoceria preservation of chloroplast glucose output in both light and dark conditions in comparison to predicted glucose based on extrapolation of initial rates of starch conversion reported by Weise et al. 2004 (red line). Values are averages with respective standard deviations (n = 3).

Publications over 2 years

1. Juan Pablo Giraldo, Sean M. Faltermeier, Thomas P. McNicholas, Ardemis A. Boghossian, Nigel F. Reuel, Andrew J. Hilmer, Fatih Sen, Jacqueline A. Brew, Michael S. Strano. A Plant Nanobionic Approach to Enhance Solar Energy Conversion of Extracted Chloroplasts using Spontaneously Assembled Nanoparticles. Nature Materials, In review. *"We gratefully acknowledge support from the U.S. Department of Energy under grant number ER46488"*

2. Ardemis A. Boghossian , Fatih Sen , Brenna M. Gibbons , Selda Sen , Sean M. Faltermeier , Juan Pablo Giraldo , Cathy T. Zhang , Jingqing Zhang , Daniel A. Heller , and Michael S. Strano. 2013. Application of Nanoparticle Antioxidants to Enable Hyperstable Chloroplasts for Solar Energy Harvesting. Advanced Energy Materials, In press. *"This work was financially supported by a grant from the U.S. Department of Energy (grant no. ER46488)"*

3. Boghossian, A. a, Choi, J. H., Ham, M.-H., & Strano, M. S. (2011). Dynamic and reversible self-assembly of photoelectrochemical complexes based on lipid bilayer disks, photosynthetic reaction centers, and single-walled carbon nanotubes. Langmuir : the ACS journal of surfaces and colloids, 27(5), 1599–609. *"The authors thank a grant from the U.S.Department ofEnergy (grant numberER46488) for support of SPT microscopy utilized in this work"*

4. Boghossian, A. A., Ham, M.-H., Choi, J. H., & Strano, M. S. (2011). Biomimetic strategies for solar energy conversion: a technical perspective. Energy & Environmental Science, 4, 3834–3843. *There is no section for acknowledgments in this paper. We have notified the editor of this problem.*

5. Tvrdy, K., Jain, R. M., Han, R., Hilmer, A. J., Mcnicholas, T. P., & Strano, M. S. (2013). A Kinetic Model for the Deterministic Prediction of Gel-Based Carbon Nanotube Separation. ACS Nano, 7(2), 1779–1789. *"This work was financially supported by the U.S. Department of Energy (Grant No. ER46488)*

6. Rishab, Kevin et al. A Quantitative Theory of Adsorptive Separation for the Electronic Sorting of Single-Walled Carbon Nanotubes. JACS, In review.

Nanoengineering of Complex Materials

Principal Investigator: Samuel I. Stupp
Departments of Chemistry and Materials Science and Engineering
Northwestern University
2220 Campus Drive, Evanston, IL 60208-3108

Program Scope

The goal of this of program is to use self-assembly and molecular design to direct the formation of materials on the nanoscale. One of the strategies used is supramolecular chemistry integrated with other forces in order to learn how to program molecules for self-assembly of soft matter across scales, especially hierarchical structures. A second strategy of interest in the program is the use of biomimetic templating to create unique structures and functions, for example inorganic structures templated by organics or the use of organic templates to create complex nanostructures.

Recent Progress

Pleochroism in Charge-Transfer Assemblies

Intermolecular charge transfer complexes, pairs of molecules that accept and donate electrons, commonly form 1D structures when crystallized. These crystals form as either mixed or segregated stacks in which the donor and acceptor molecules organize in a face-to-face or edge-to-edge orientation, respectively. Strategies for the self-assembly of all-organic materials exhibiting higher dimensionalities of electron transfer are limited. We recently discovered the assembly of 2D supramolecular networks of charge-transfer complexes that form a crystalline architecture.[1] These networks have bidirectional charge-transfer interactions wherein one donor molecule shares electron density with two different acceptors: one acceptor is positioned face-to-face and the other edge-to-face with respect to the donor. The crystals also exhibit pleochroism since their absorption spectra change continuously with the orientation of plane-polarized light (Fig. 1), and interestingly they never extinct between polarizers. Preliminary measurements show that the biaxial polarity stabilizes ferroelectricity along two crystallographic axes at room temperature. This supramolecular network could enable ferroelectrics with polarization of higher dimensionality and optically active electronic memory.

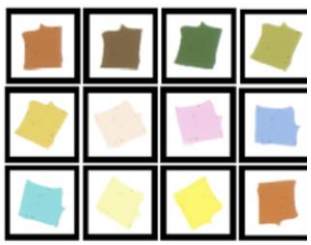

Fig. 1. Polarized optical microscopy of single crystal complexes with parallel polarizers.

Room-temperature organic supramolecular ferroelectric materials

Ferroelectric materials show spontaneous electric polarization that can be reversed by an external electric field and can find potential applications in sensors, photonic crystals, and energy-efficient memories. Organic ferroelectrics have the particular advantage that they can be easily processed into devices and their syntheses are versatile and inexpensive. We recently reported on a new family of organic ferroelectric crystals based on intermolecular charge transfer between electron rich (donor) and electron poor (acceptor) molecules.[2] The donor and acceptor molecules are equipped with hydrogen

bonding motifs to achieve a supramolecular network of charge transfer complexes able to demonstrate ferroelectricity in alternating stacks above room temperature. Very recently, we have initiated a project to develop 1D charge transfer assemblies that can form in solution. The new donor and acceptor molecules contain a short peptide sequence known to form 1D structures. Red solutions were obtained upon mixing donor and acceptor components in a 1:1 ratio and preliminary hysteresis curves of devices using solutions of these molecules suggest the potential for ferroelectric activity.

Long-Range Crystallization in Self-Assembling Filament Networks

In solution, 1D objects, such as carbon nanotubes, filamentous viruses, and rigid molecules, can spontaneously form orientationally ordered domains or networks as a result of their shape. This excluded volume effect is useful in the design of devices, liquid crystals, high-strength materials, and bioactive hydrogels. We discovered that like-charge peptide amphiphile (PA) cylindrical nanofibers self-assemble into large crystalline arrays at surprisingly large distances (up to 320 Å).[3] This crystallization into a 2D hexagonal lattice is spontaneous beyond a given concentration, but interestingly also can be triggered reversibly by ionizing X-rays at lower concentrations. We also discovered an azobenzene-based amphiphile that can self-assemble into highly charged nanofibers in water. Small-angle X-ray scattering (SAXS) shows that these nanofibers form crystalline networks with large inter-fiber spacings up to surprising distances of up to 130 nm mediated by repulsive forces between the charged nanostructures. Solution concentration and temperature can be adjusted to control the packing structure and inter-fiber spacings.

Hierarchical Self-Assembly by Rational Molecular Design

Hierarchical self-assembly of membranes using bio-inspired building blocks has been recently revealed as a path to complex, functional materials. These membranes, which form at the aqueous interface between cationic PAs and anionic hyaluronic acid (HA), exhibit unique structure formation that is dynamic in time. We showed that this hierarchical structure requires strong interactions between PA molecules and polyelectrolyte molecules, suggesting the importance of rapid diffusion barrier formation.[4] Strong attraction can be introduced through specific interactions between the PA and the polyelectrolyte (Fig. 2). SAXS shows that membranes formed in the case of weak PA-polymer interaction display a nanoscale cubic ordering that likely results from clusters of PA nanostructures surrounded by polyelectrolyte chains. We have also found that membrane microstructure and properties can be rationally manipulated by varying the molecular structure of membrane building blocks. Self-assembly of HA with PAs incorporating β-sheet forming residues results in robust membranes that exhibit a dense diffusion barrier, while assembly of HA with PAs lacking β-sheet forming residues results in weak membranes that exhibit long, non-fibrous fingering protrusions. Furthermore, simply increasing the HA molecular weight slows the growth rate of orthogonal nanofibers. Molecular simulations suggest that these findings

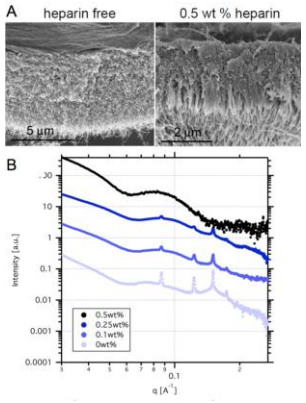

Fig. 2. (A) Scanning electron micrographs of membrane cross-sections of HA/HBPA sacs self-assembled with or without heparin. (B) SAXS patterns of sacs self-assembled with varying concentrations of heparin.

may result from complex relationships between inter-molecular interaction energies and diffusion at very early time points in the membrane formation.

We also recently reported the first example of precise one-dimensional templating of a virus-like nanostructure using DNA as the template. This involved the encapsulation of a linear or circular double-stranded DNA template with pre-assembled mushroom-shaped nanostructures having a positively charged domain into 1D nanostructures of precisely controlled length (Fig. 3). The structure forms by self-assembly of coiled-coil peptides conjugated at opposite termini with poly(ethylene glycol) (PEG) chains and cationic segments to interact with the DNA template. We proposed a model that relates the length of the terminal PEG chains to the nanostructure stiffness. This stiffening counterbalances the natural tendency of the DNA template to buckle or condense into toroids.

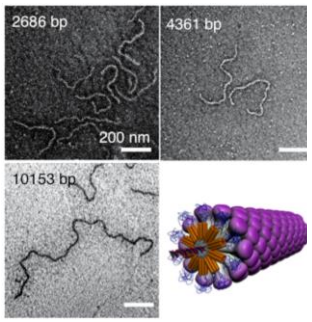

Fig. 3. TEM of solutions of DNA and mushroom-shaped nanostructures shows that the assembly length is determined by the DNA template.

Internal dynamics of supramolecular nanofibers

While applications of functional supramolecular structures are progressing rapidly, questions remain as to the relationship between the unique dynamics profiles through supramolecular assemblies and the consequences of these dynamics in new technologies. We implemented a novel methodology to measure cross-sectional dynamics of a PA nanofiber by employing spin labeling at selected sites of a PA nanofiber and measuring the electron paramagnetic resonance (EPR) spectra of nanofibers doped with each spin labeled PA (Fig. 4). The fitted EPR spectra reveal the rotational diffusion rates of each spin probe as a function of radial position of the spin label. We show that the rotational diffusion rates are commensurate with the strength of intermolecular interactions and exchanging Na^+ counterions with divalent Ca^{2+} counterions increases charge screening and induces stronger intermolecular interactions at an internal site within the nanofiber. This methodology represents the first experimental example of cross-sectional dynamics measurements on a sub-nanometer length scale and can be applied to other supramolecular assemblies to access information about their functional structures.

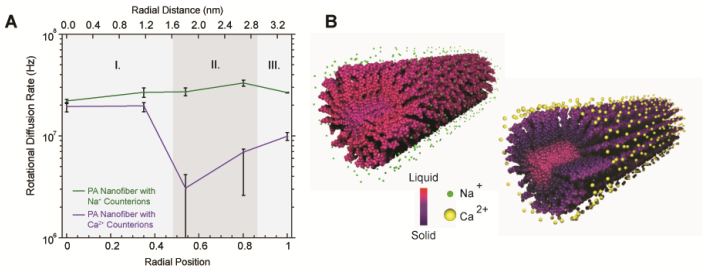

Fig. 4. (A) Rotational diffusion rates extracted from EPR spectral simulations of at each position of the probe. (B) Molecular rendering of PA nanofibers surrounded by Na^+ counterions and Ca^{2+} counterions. Colors indicate the cross-sectional gradient of solid-like (blue) to liquid-like (red) dynamics.

Future Plans

Our future plans for this program include will include: exploring ferroelectric behavior in hydrated materials and solutions, precisely controlling hierarchical

organization within self-assembled materials, and using free radical spin labels and EPR to design linkers control how signals are presented on the surfaces of nanofibers.

References

(1) Shveyd, A. K.; Tayi, A. S.; Rolczynski, B. S.; Sue, A. C.-H.; Cao, D.; Szarko, J. M.; Stern, C.; Sarjeant, A. A.; Wang, K. L.; Kahr, B.; Chen, L. X.; Stupp, S. I.; Stoddart, J. F., Supramolecular networks exhibiting electron transfer in two dimensions. Submitted.
(2) Tayi, A. S.; Shveyd, A. K.; Sue, A. C.-H.; Szarko, J. M.; Rolczynski, B. S.; Cao, D.; Kennedy, T. J.; Sarjeant, A. A.; Stern, C. L.; Paxton, W. F.; Wu, W.; Dey, S. K.; Fahrenbach, A. C.; Guest, J. R.; Mohseni, H.; Chen, L. X.; Wang, K. L.; Stoddart, J. F.; Stupp, S. I., Room-temperature ferroelectricity in supramolecular networks of charge-transfer complexes. *Nature* **2012,** 488, 485-489.
(3) Cui, H. G.; Pashuck, E. T.; Velichko, Y. S.; Weigand, S. J.; Cheetham, A. G.; Newcomb, C. J.; Stupp, S. I., Spontaneous and X-ray-Triggered Crystallization at Long Range in Self-Assembling Filament Networks. *Science* **2010,** 327, 555-559.
(4) Bitton, R.; Chow, L. W.; Zha, R. H.; Velichko, Y. S.; Pashuck, E. T.; Stupp, S. I., Electrostatic Control of Structure in Self-Assembled Membranes. *Small* In press.

Publications Supported By BES (2011-2013)

(1) Matson, J. B.; Zha, R. H.; Stupp, S. I., Peptide Self-Assembly for Crafting Functional Biological Materials. *Curr. Opinion Solid State Mater. Sci.* **2011,** 15, 225.
(2) Tevis, I. D.; Palmer, L. C.; Herman, D. J.; Murray, I. P.; Stone, D. A.; Stupp, S. I., Self-assembly and Orientation of Hydrogen-Bonded Oligothiophene Polymorphs at Liquid-Membrane-Liquid Interfaces. *J. Am. Chem. Soc.* **2011,** 133, 16486.
(3) Aida, T.; Meijer, E. W.; Stupp, S. I., Functional Supramolecular Polymers. *Science* **2012,** 335, 813.
(4) Fry, H. C.; Garcia, J. M.; Medina, M. J.; Ricoy, U. M.; Gosztola, D. J.; Nikiforov, M. P.; Palmer, L. C.; Stupp, S. I., Self-assembly of Highly Ordered Peptide Amphiphile Metalloporphyrin Arrays. *J. Am. Chem. Soc.* **2012,** 134, 14646.
(5) Newcomb, C. J.; Moyer, T. J.; Lee, S. S.; Stupp, S. I., Advances In Cryogenic Transmission Electron Microscopy for the Characterization of Dynamic Self-Assembling Nanostructures. *Curr. Opinion Colloid Interface Sci.* **2012,** 17, 350.
(6) Tevis, I. D.; Tsai, W.-W.; Palmer, L. C.; Aytun, T.; Stupp, S. I., Grooved Nanowires from Self-Assembling Hairpin Molecules for Solar Cells. *ACS Nano* **2012,** 6, 2032.
(7) Velichko, Y. S.; Mantei, J. R.; Bitton, R.; Carvajal, D.; Shull, K. R.; Stupp, S. I., Electric Field Controlled Self-Assembly of Hierarchically Ordered Membranes. *Adv. Funct. Mater.* **2012,** 22, 369.
(8) Ruff, Y.; Moyer, T.; Newcomb, C. J.; Demeler, B.; Stupp, S. I., Precision Templating with DNA of a Virus-like Particle with Peptide Nanostructures. *J. Am. Chem. Soc.* **2013,** 135, 6211.
(9) Sampath, S.; Basuray, A. N.; Hartlieb, K. J.; Aytun, T.; Stupp, S. I.; Stoddart, J. F., Direct Exfoliation of Graphite to Graphene in Aqueous Media with Diazaperopyrenium Dications. *Adv. Mater.* **2013,** 25, 2740.
(10) Stephanopoulos, N.; Ortony, J. H.; Stupp, S. I., Self-Assembly for the Synthesis of Functional Biomaterials. *Acta Mater.* **2013,** 61, 912.

Program Title: Using *in vitro* maturation and cell-free expression to explore [FeFe] hydrogenase activation and protein scaffolding requirements

Principle Investigator: J.R. Swartz
Mailing Address: Department of Chemical Engineering, Stanford University
Stanford, CA 94305-5025
E-mail: jswartz@stanford.edu

Program Scope

Our overall program objective is to elucidate the assembly and activation mechanisms as well as the structural requirements for [FeFe] hydrogenases. This recognizes the extremely important and fundamental function of these enzymes; combining subatomic particles, electrons and protons, to produce a molecule, dihydrogen, important as a chemical feedstock and a potential fuel. To approach this challenge, we have recognized the need to develop key investigational tools while accumulating insights into these amazing catalytic materials.

We are in the first year of our second funding period. The first period provided a well-defined *in vitro* hydrogenase activation system and used that to help elucidate the small molecular weight chemicals required for enzyme activation. However, this activation requires the presence of a cell extract, and we are now working to identify the required factors provided by the *E.coli* extract. In the first period, we also identified an unexpectedly important role for the proximal Fe-S cluster and we showed, surprisingly, that most of the amino acids that form the scaffolding for this cluster as well as the H-cluster active site can be changed while retaining significant activity. We have now essentially completed a 96-well device and protocol for measuring hydrogen production rates to gain the capability for evaluating all possible amino acid changes surrounding these influential Fe-S clusters. We will also use this device to screen libraries of randomly mutated hydrogenases to gain further insights into the structure function relationships that govern activity and other functional attributes such as oxygen tolerance. To more fully elucidate these relationships, the Steve Cramer lab is providing spectroscopic analysis of both the wild type and mutated enzymes. We seek to use this knowledge to produce more useful enzymes, for example, oxygen tolerant hydrogenases, as well as to provide guidance to those seeking to produce inorganic and hybrid mimics that could offer increased durability.

Recent Progress

Identifying Hydrogenase Activation Requirements. While full *in vitro* maturation of CpI was established during the first funding period, a crude cell lysate is required. It was hypothesized that proteins involved in Fe-S cluster assembly and installation were being supplied by the extract. To this end, the *isc* operon, which is responsible for the generation of Fe-S clusters in *E.coli*, was targeted. The genes for the six proteins in the *isc* operon were first cloned, and each protein was expressed, purified, and confirmed to be active. All six proteins were then introduced into the *in vitro* activation reaction and different ratios of the six were explored.

In the absence of cell extract, only 1% activation was achieved with the *isc* proteins; suggesting that the extract is providing additional essential components. This observation is consistent with work conducted to improve *in vivo* hydrogenase expression and activation in *E.coli*. Additional *In vivo isc* operon overexpression (relative to that provided by a Δ*iscR* mutation) failed to increase the activation of the hydrogenase when co-expressed with its maturases *in vivo*. A cell extract enriched with *isc* proteins also failed to improve cell-free hydrogenase expression and maturation.

Upon discovering that the *isc* proteins were insufficient for replacing the cell extract, the crude *E. coli* extract was fractionated to identify the beneficial components. An anion exchange separation produced a fraction that promoted activation, and it contained an SDS PAGE band not present in inactive fractions. This protein band was analyzed by mass spectrometry and determined to be cysteine synthase A, expressed by the *cysK* gene. Interestingly, while this protein is involved in the biosynthesis of cysteine, it also provides cysteine desulfurase activity in *E. coli*. At first, this seemed to be a trivial finding since one of the *isc* proteins, IscS, is a cysteine desulfurase. However, IscS does not confer the same benefits as the fractions containing CysK. Further, previously identified active fractions were tested in the presence of the *isc* proteins to determine if the *isc* proteins work in conjunction with CysK, but no added benefit was observed. Thus, it can be inferred that CysK contributes a different function relative to IscS. The next step is to clone the *cysK* gene and to produce and purify the protein. Different enzymatic assays can then be used to explore its catalytic capability. In addition, the purified protein will be tested for its ability to replace the cell extract. If this is not observed, further fractionation experiments will be conducted in which CysK will be added to each fraction to identify synergistic proteins or other components in the cell extract that promote the activation of apohydrogenase.

Development of a 96-well Hydrogen Production Assay. The objective is to develop a reliable, semi-high throughput method to measure hydrogen production rates using a 96-well format. This is based on a sensor glass that is coated with tungsten oxide (WO_3) and palladium. Catalysis of hydrogen by the palladium reduces the coating to WO_2 which turns blue. Although the concept is simple, reduction to practice was complicated. The final device is pictured in Figure 1. Panel A shows the mounting frame that includes a gas mixing chamber below the mounting surface for the 96-well plate. This allows us to use filter bottom 96-well plates and to inject gases (notice syringes) with known hydrogen concentrations. The hydrogen rapidly diffuses into the 96-well plate and into the space above each well. We can then monitor the rate of blue color formation at various hydrogen partial pressures to calibrate the device. A critical element is the gasket shown on top of a 96-well plate in panel B. We were not able to find a suitable commercial gasket, and we designed, fabricated, and coated a silicone gasket that fits partially into the plate wells and provides significant contact surface to seal against the sensor plate. Finally (panel C), the sensor plate is clamped onto the top using 6 latches that pull down on a force transmittance frame. This was designed for simple operation since it is used within a glove box. Finally, a digital camera sends time lapse images to a computer that records the "blueness" of the spots that form over each well as a function of time.

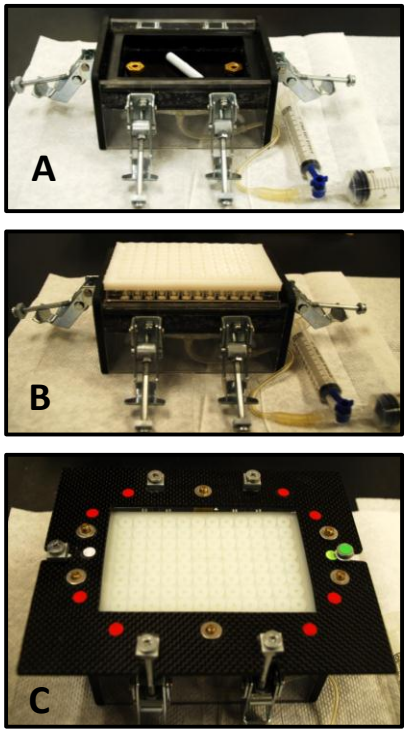

Figure 1: Device for 96-well H_2 production measurements.

Figure 2 shows sample data in which a partially inactivated hydrogenase sample with 135nM CpI was compared to a fresh one with 10nM CpI. Electrons are supplied to the hydrogenase (CpI) from dithionite (DTH) via the *Clostridium pasteurianum* ferredoxin (CpFd). These results indicate that the older hydrogenase had lost most of its activity. After use, the sensor plates are regenerated by oxygen exposure.

This turns out to be a critical part of the protocol, and we are now optimizing the regeneration procedure and further calibrating and optimizing device performance.

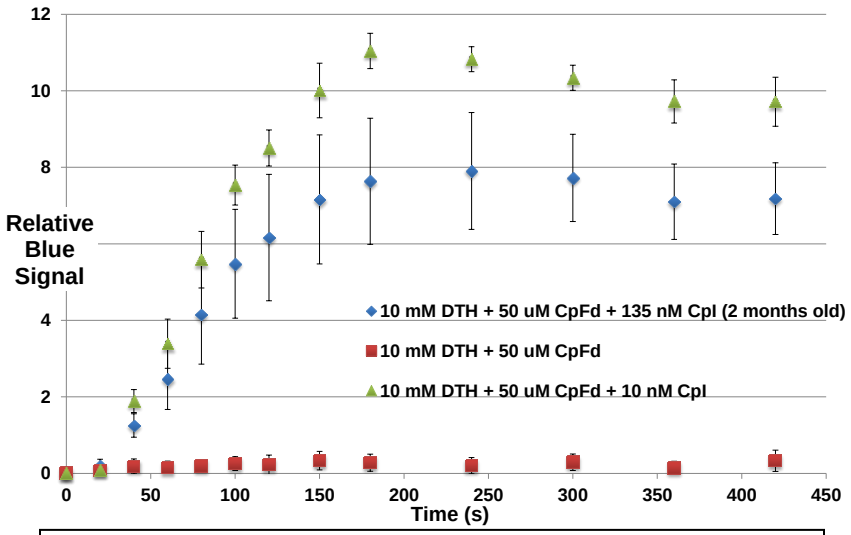

Figure 2: Sample hydrogen production graphs from the 96-well device.

Initial Characterization of Targeted Hydrogenase and Ferredoxin Mutations: An initial alanine screen of 87 sites around the H-cluster and proximal Fe-S sulfur centers showed that the enzyme was surprise-ingly tolerant to such changes. During this survey, other research groups reported that certain Ni-Fe hydrogenases have six cysteines interacting with their proximal Fe-S centers rather than the four cysteines present in [FeFe] hydrogenases. When the extra cysteines were removed, oxygen tolerance was reduced. We therefore did an initial screen to determine how well our *Clostridium pasteurianum* hydrogenase (CpI) tolerated changes within 6.5Å of the proximal cluster. We identified five sites that retained more than 50% hydrogen consumption activity when the native amino acid was changed to cysteine (Figure 3). We are now making the double and triple mutants and will evaluate their oxygen tolerance.

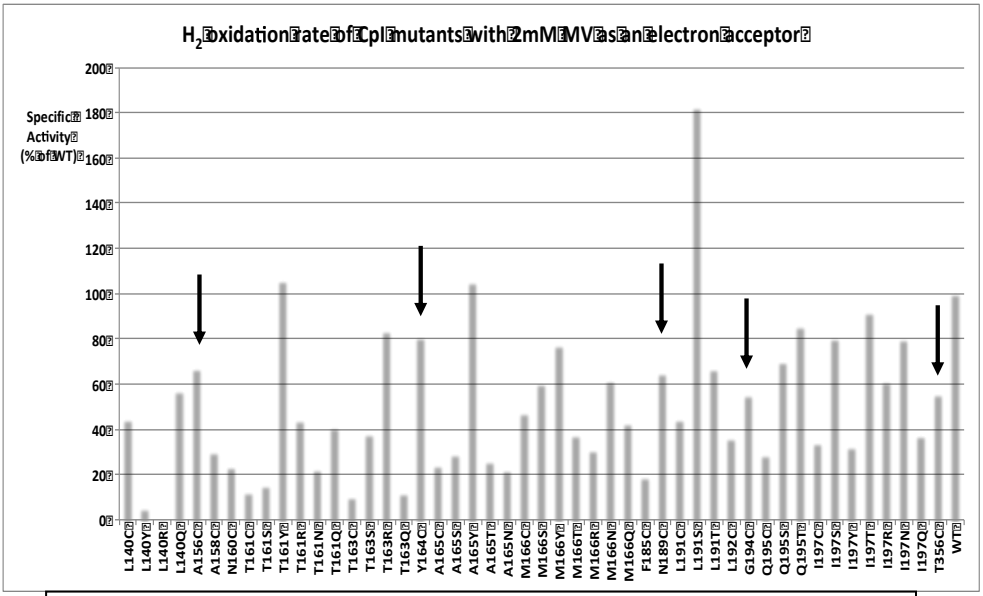

Figure 3: Effects mutating amino acids adjacent to the proximal Fe-S cluster.

Interestingly, mutating the leucine at position 191 to serine nearly doubled activity.

As we learned, it is important to determine oxygen tolerance when the enzyme is operating to produce hydrogen. For these tests, we cannot use dithionite as an electron source since it reacts rapidly with the oxygen. Instead we use NADPH as an electron source and therefore require a ferredoxin NADP reductase (FNR) to transfer electrons to CpFd for delivery to CpI. This is a more natural approach than by adsorbing hydrogenases to electrodes as other groups have done. However, we have observed very low FNR turnover rates in this enzymatic electron transfer pathway, and hypothesize this to be caused by an accumulation of reduced ferredoxin because of the rather low affinity of CpFd to CpI ($k_m \approx 20\mu M$).

In parallel work with the Cramer lab, we have observed that the rate of oxygen binding to the H-cluster is much faster than FTIR evidence of H-cluster damage. It therefore appears that if we can reduce the bound oxygen quickly enough, the enzyme can be protected. This motivates us to increase the affinity of CpFd to CpI. We have used a computer docking model (CusPro) to predict CpFd/CpI interaction surfaces, and have begun to mutate the amino acids on the surface of CpFd that are believed to facilitate docking. So far all single mutations have been well tolerated but have not significantly affected the functional CpFd/CpI interaction as indicated by hydrogen production rates. The docking appears to be favored by ion pairing interactions that help to position CpFd in the right place for hydrophobic interactions to provide the dominant affinity. We will now use the guidance from this model to combine mutations that will enhance the hydrophobic attractions and also improve ion pairing cooperativity. The working hypothesis is that increasing Fd affinity to the hydrogenase will keep the [$Fd^{reduced}$] much lower, that this will increase FNR turnover rates, and that this improved electron supply will help to stabilize the hydrogenase when exposed to oxygen.

Future Plans

1. Identifying unknown hydrogenase maturation factors. We will continue to use *E.coli* extract fractionation to identify proteins or other factors that provide such active support for [FeFe] hydrogenase maturation. The CysK enzyme has already been identified suggesting that our approach will be fruitful. This knowledge will then be used to engineer *E.coli* for improved *in vivo* hydrogenase production and to provide more productive extracts for cell-free production to facilitate the evaluation of large libraries of hydrogenase mutants.

2. Screen targeted and random mutational libraries. Using the 96-well hydrogen production assay device, we will screen libraries in which all amino acid substitutions are evaluated in the 87 site adjacent to the H-cluster and proximal Fe-S center. These will be evaluated for activity as well as oxygen tolerance. We will also target the diffusional channels for mutational analysis to determine their effect on oxygen tolerance, if any.

3. Analyze interesting mutants using FTIR and other spectroscopic methods. The mutants identified in part 2 will then be analyzed by FTIR to assess the impact of the protein scaffolding change on the H-cluster electrostatics. These changes will then be correlated with functional changes to gain a better appreciation of hydrogenase structure function dependencies.

References (which acknowledge DOE support)

1. New Insights into [FeFe] Hydrogenase Activation and Maturase Function. Jon M. Kuchenreuther, R. David Britt, and James R. Swartz. 2012 PlosOne **7**(9): e45850. Diu:10.1371/journalpone.0045850.
2. NRVS and EPR Spectroscopy of ^{57}Fe-enriched [FeFe]Hydrogenase Indicate Stepwise Assembly of the H-cluster. Jon M. Kuchenreuther, Yisong Guo, Hongxin Wang, William K. Myers, Simon J. George, Christine A. Boyke, Yoshitaka Yoda, E. Ercan Alp, Jiyong Zhao, R. David Britt, James R. Swartz, and Stephen P. Cramer. 2013 Biochemistry **52**(5): 818-826. doi:10.1021/bi301336r.

Chemically Directed Self-Assembly of Protein Superstructures and Construction of Tunable Redox Functionalities in their Interfaces

Principle Investigator: F. Akif Tezcan
Mailing Address: University of California, San Diego, Department of Chemistry and Biochemistry, 9500 Gilman Drive, La Jolla, CA 92093-0356
E-mail: tezcan@ucsd.edu

i) Project Scope

The goals of this project are:
1) To elucidate and control the bottom-up assembly of 0-, 1-, 2- and 3D nanoscale protein superstructures/arrays, and to functionalize them toward energy-related applications.
2) To construct redox-active copper centers in the interfaces of protein superstructures.
These goals combined will lead to the chemically controllable self-assembly of well-ordered superstructures under ambient conditions that will be used for light-harvesting and redox catalysis. These structures also will provide a framework for a fundamental understanding of protein self-assembly as well as crystal nucleation and growth.

Proteins are nature's most versatile building blocks, programmed at the genetic level to perform myriad functions and largely responsible for the complexity of an organism. The exquisite, error-free self-assembly of proteins into *ordered yet dynamic* nano- and microscale architectures, such as 1D microtubules,[1] 2D bacterial surface layers (S-layers),[2] 3D virus capsids[3] is a cornerstone of life, and has served as a major inspiration for synthetic supramolecular chemistry and nanoscience.[4] In fact, many self-assembled protein arrays themselves have been widely exploited as well-ordered and genetically/chemically modifiable structural templates in numerous nanotechnological applications.[5-7] Significantly, crystalline protein arrays form the basis of diffraction-based methods for structure determination, and their acquisition generally represents the rate-limiting step in this process. Thus, a bottom-up strategy for arranging proteins into periodic structures would have wide-ranging applications in crystallography and in nanotechnology, where it would allow access to novel biological polymers that incorporate the wide range of chemical functionalities afforded by the proteins.

In contrast to simpler building blocks such as DNA[8] and RNA[9] and peptides, the designed self-assembly of proteins has largely been inaccessible, plagued by the chemical heterogeneity and size of the molecular surfaces required for protein-protein interactions. In order to overcome this challenge, we have exploited the simultaneous directionality, strength and reversibility of metal coordination interactions to assemble monomeric or non-self assembling proteins into discrete (closed) or infinite (open) architectures under thermodynamic control. The resulting assemblies present, by default, metal coordination sites in their interfaces, which can be further engineered for function such as electron transfer and redox catalysis.

This project is a multi-disciplinary effort, which melds the strengths of inorganic chemistry, protein engineering, structural biology and supramolecular chemistry, and combines a wide variety of techniques ranging from protein crystallography, electron (TEM, SEM, cryo EM, in situ liquid EM), fluorescence and atomic force microscopy, and the characterization of metal reactivity and photophysics through an armament of static and time-resolved spectroscopic methods and electrochemistry.

ii) Recent Progress

ii.1) Metal-Directed, Chemically Tunable Assembly of 1-, 2- and 3D Crystalline Protein Arrays: Coordination chemists have had considerable success in exploiting the directionality and reversibility of metal coordination to construct discrete supramolecular assemblies and infinite 1-, 2- and 3D coordination polymers through ligand design.[10-13] In parallel, protein designers have combined protein building blocks within intrinsic symmetries to create ordered protein arrays.[14-16] We have merged design strategies from both approaches. We had observed previously that when Zn^{2+} was added in greater than 1.5-fold molar excess to a designed metal-binding variant of the protein cytochrome cb_{562} (MBPC1), it formed large, heterogeneous aggregates, which we attributed to multiple and indiscriminate modes of Zn-mediated interprotein coordination. Combining the symmetry- and directional bonding-based self-assembly strategies mentioned above, we posited that, if two or more selective Zn coordination sites on the MBPC1 surface could be stabilized in appropriate orientations relative to each other, it should be possible to dictate the self-assembly of the protein into regular, extended arrays through metal coordination. This was accomplished using the construct RIDC3, which incorporated ten computationally prescribed surface mutations

into MBPC1. The mutations stabilized a C_2-symmetric dimer, which could self-assemble upon Zn addition into 1D helical nanotubes, and 2- and 3-D crystalline arrays in a fashion that was predictably controllable by adjusting Zn concentrations and the pH of the solution (Figure 1). All of these assemblies were thoroughly characterized by TEM, cryo-electron microscopy and X-ray crystallography, which yielded an atomic-level picture of the arrangement of RIDC3 molecules in these arrays and the underlying Zn-coordination environments.

This investigation was significant from several points of view: 1) it represented the first time a monomeric protein has been engineered to assemble in a chemically tunable fashion into 1-, 2- or 3D crystalline assemblies. 2) The combined dimensions of these ordered arrays spanned nearly the entire nanometer-micrometer scale (5 nm to 200 □m). 3) The 1- and 2D RIDC3 arrays resembled natural assemblies like microtubules, helical viruses, and S-layers in terms of their shapes, dimensions, structural uniformity as well as their stimuli-responsiveness. These findings highlighted a particular advantage of "metal-directed protein self-assembly", which is its inherently chemically tunable and modular nature. In theory, self-assembling proteins can be chosen based on their built-in functions (*e.g.*, electron transfer for cyt cb_{562}), and/or be functionally augmented through derivatization or through the interfacial metals themselves. These features create a versatile platform for engineering functional biomaterials and for studying the fundamentals of protein self-assembly and crystallization under highly controllable conditions.

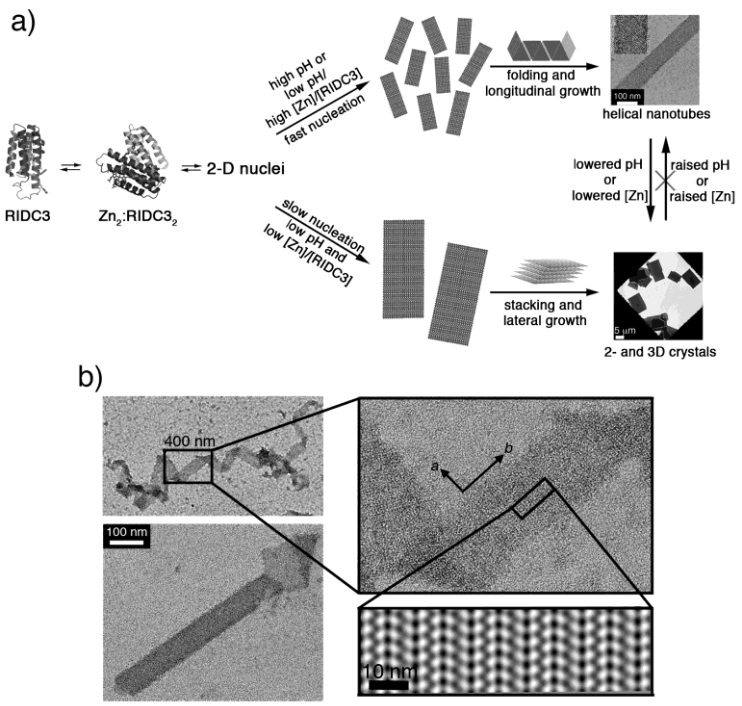

Figure 1. (**a)** Model for Zn-mediated RIDC3 self-assembly under fast and slow nucleation conditions. (**b)** TEM images of a 2D RIDC3 ribbon and a tubular structure with frayed ends, illustrating the interconversion between tubular and sheet-like morphologies. Shown in the right bottom corner is the 2D image reconstruction of a single-layered portion of the ribbon, indicating the molecular arrangement of RIDC3 molecules.

ii.2) Exceptionally Stable, Designed Supramolecular Protein Arrays with Innate Redox Functionalities to Control the Templated Growth of Pt Nanoparticles: The ability to choose proteins as building blocks based on their distinct chemical functions–rather than their existing structural properties–and to program their bottom-up self-assembly into ordered nanoscale arrays would have immense utility in nano- and biotechnology (e.g., in catalysis or sensing). In contrast to top-down nanofabrication strategies, the bottom-up assembly of such protein arrays would ensure a high density of chemical functionalities in a given surface area and lend access to collective properties such as supramolecular stabilization, allostery, cooperativity and self-healing. With these considerations in mind, we investigated the stability of the 1- and 2D RIDC3 arrays and their use as redox-active

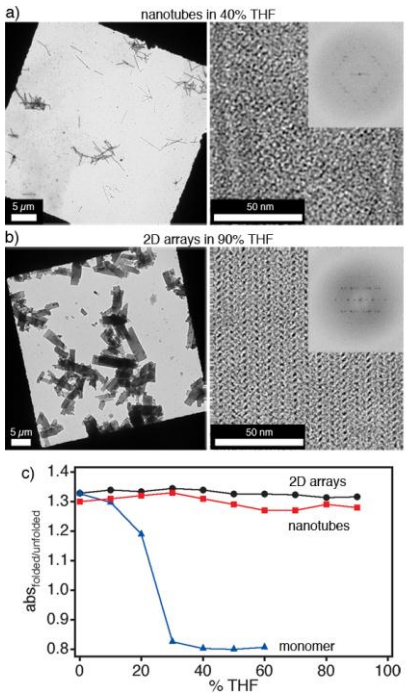

Figure 2. Chemostability of Zn-mediated RIDC3 arrays. Both the 1D nanotubes **(a)** and the 2D arrays **(b)** remain crystalline and well-dispersed in organic solvents (here, THF). **(c)** Whereas the monomeric building blocks readily denature at low THF concentrations when isolated, they are highly stable once arranged into supramolecular assemblies.

templates for inorganic nanoparticle growth. We have found that, owing to their regularity and their density, the 1D RIDC3 nanotubes and the 2D RIDC3 arrays are stable up to 80-90 °C and, in the latter case, retain their crystalline order in up to 100% polar organic solvents (THF, DMF, methanol, isopropanol) for at least 2 months. Impressively, the monomeric RIDC3 building blocks themselves unfold at much lower percentages of organic solvents (for example at 30% THF) (Figure 2), illustrating how supramolecular assembly can stabilize individual protein components, which is crucial for bio/nano-technological applications that center on the specific activity of the protein building blocks.

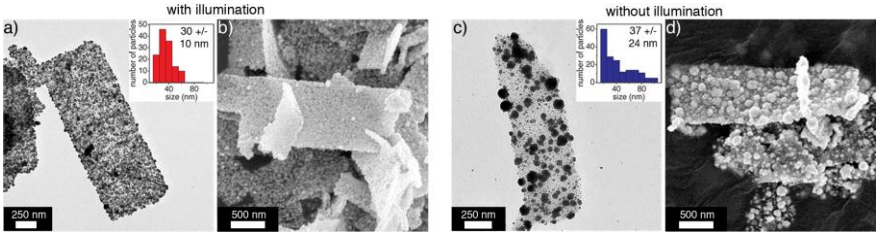

Figure 3. Control of the size and spatial distribution of PtNPs grown on photoredox active RIDC3 templates as characterized by TEM and SEM.

Having established the tunability and stability of Zn-mediated RIDC3 superstructures, we then examined whether these advantages could be coupled with the built-in redox activity of RIDC3 monomers in controlling the templated growth of Pt nanoparticles (PtNPs). We showed that PtNPs can be controllably grown on the RIDC3 arrays surfaces using a variety of conditions including high temperatures (>90 °C) or light-induced electron transfer (Figure 3). Our experiments showed that the reduction of surface-bound Pt(II) to seed the growth of PtNPs is mediated by the heme centers of individual RIDC3 building blocks (thus fulfilling their physiological role as electron transfer agents). To our knowledge, this represents the first example where supramolecular protein architecture with an innate functionality actively controls inorganic material synthesis (rather than acting as a static template).

ii.3) Re-engineering of protein interfaces to render the assembly of protein cages inducible by metal binding: Cage-like proteins such as virus capsids and ferritin fulfill crucial roles as molecular containers of previous/toxic cargo. Their self-assembly, which involves the simultaneous engagement of several protein-protein interaction surfaces, is complex and difficult to study,[17] but this would be greatly facilitated if the assembly process can be chemically triggered. The ability to chemically induce protein cage assembly would also greatly expand their already-diverse applications in nanotechnology. Toward this end, we developed a new methodology that we have termed "reverse Metal Templated Interface Redesign, rMeTIR" which involves the grafting of stable metal coordination motifs into a subunit interface in an existing protein cage, followed by the disruption of the native, complementary non-covalent interactions in this interface. Using rMeTIR, we have rendered the assembly of a ferritin variant, MIC1, responsive to Cu(II) binding (Figure 4), which also enabled us to isolate the monomeric components of ferritin for the first time. Similar to RNA-templated formation of virus capsids, copper ion removal did not disrupt cage architecture after self-assembly. These studies showed that 1) the monomeric subunits were fully folded but highly unstable, showing how nature can assemble highly stable architectures out of unstable building blocks, 2) polar, H-bonding interactions were crucial for the correct orientation of monomeric subunits during self-assembly, and 3) the interior of the cage could be chemically labeled with large functional groups in a uniform fashion.

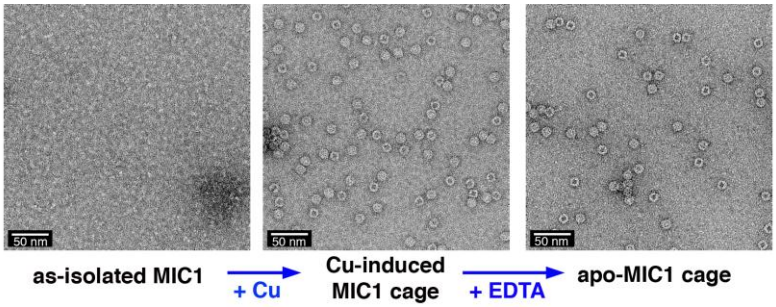

Figure 4. Cu-induced assembly of a reengineered ferritin variant, MIC1.

iii)Future Directions

Our future studies will focus on the following: 1) Understanding the dynamics of RIDC3 self-assembly into 1-, 2- and 3-D arrays and the structural transformations between these architectures. This will be accomplished through a combination of TEM, cryoTEM, SAXS as well as in-situ, liquid EM measurements in collaboration with PNNL scientists. 2) Monitoring, understanding and better controlling the dynamics nanoparticle growth on crystalline protein arrays. These efforts will capitalize on our finding that PtNP growth can be spatiotemporally controlled on RIDC3 arrays (with light, if desired). 3) Incorporating "programmability" into protein self-assembly. This will be accomplished through the construction of DNA-protein chimeras that self-assemble in response to metal binding

and DNA hybridization. 4) Making metal-induced protein cage assembly chemically reversible. This effort will shed further light into the design principles of natural protein cages. 5) Constructing coordinatively unsaturated, interfacial Cu sites in protein assemblies for catalytic O_2 activation and long-range electron transfer.

iv) References

(1) Li, H. L.; DeRosier, D. J.; Nicholson, W. V.; Nogales, E.; Downing, K. H. *Structure* 2002, *10*, 1317.
(2) Sara, M.; Sleytr, U. B. *J. Bacteriol.* 2000, *182*, 859.
(3) Parent, K. N.; Sinkovits, R. S.; Suhanovsky, M. M.; Teschke, C. M.; Egelman, E. H.; Baker, T. S. *Phys. Biol.* 2010, *7*.
(4) Seeman, N. C.; Belcher, A. M. *Proc. Natl. Acad. Sci.USA* 2002, *99*, 6451.
(5) Shenton, W.; Pum, D.; Sleytr, U. B.; Mann, S. *Nature* 1997, *389*, 585.
(6) McMillan, R. A.; Paavola, C. D.; Howard, J.; Chan, S. L.; Zaluzec, N. J.; Trent, J. D. *Nat. Mater.* 2002, *1*, 247.
(7) Lee, Y. J.; Yi, H.; Kim, W.-J.; Kang, K.; Yun, D. S.; Strano, M. S.; Ceder, G.; Belcher, A. M. *Science* 2009, *324*, 1051.
(8) Delebecque, C. J.; Lindner, A. B.; Silver, P. A.; Aldaye, F. A. *Science* 2011, *333*, 470.
(9) Chworos, A.; Severcan, I.; Koyfman, A. Y.; Weinkam, P.; Oroudjev, E.; Hansma, H. G.; Jaeger, L. *Science* 2004, *306*, 2068.
(10) Caulder, D. L.; Raymond, K. N. *Acc. Chem. Res.* 1999, *32*, 975.
(11) Holliday, B. J.; Mirkin, C. A. *Angew. Chem., Int. Ed. Eng.* 2001, *40*, 2022.
(12) Leininger, S.; Olenyuk, B.; Stang, P. J. *Chem. Rev.* 2000, *100*, 853.
(13) Ockwig, N. W.; Delgado-Friedrichs, O.; O'Keeffe, M.; Yaghi, O. M. *Acc. Chem. Res.* 2005, *38*, 176.
(14) Padilla, J. E.; Colovos, C.; Yeates, T. O. *Proc. Natl. Acad. Sci. USA* 2001, *98*, 2217.
(15) Yeates, T. O.; Padilla, J. E. *Curr. Opin. Struct. Biol.* 2002, *12*, 464.
(16) Sinclair, J. C.; Davies, K. M.; Venien-Bryan, C.; Noble, M. E. M. *Nature Nanotech.* 2011, *6*, 558.
(17) Zlotnick, A. *J. Mol. Biol.* 1994, *241*, 59.

v) Publications from last 2 years (citing DOE support)

1. R. J. Radford, J. D. Brodin, E. N. Salgado, F. A. Tezcan (2011) "Expanding the Utility of Proteins as Platforms for Coordination Chemistry, **Coord. Chem. Rev.**, *255*, 790-803.
2. R. J. Radford, M. Lawrenz, P. C. Nguyen, J. A. McCammon, F. A. Tezcan (2011), "Porous Protein Frameworks with Unsaturated Metal Centers in Sterically Encumbered Coordination Sites", **Chem. Comm.**, *47*, 790-803.
3. E. N. Salgado, J. D. Brodin, M. M. To, F. A Tezcan (2011). "Templated Construction of a Zn-Selective Protein Dimerization Motif", **Inorg. Chem**., *50*, 6323-6329.
4. J. D. Brodin, X. I. Ambroggio, K. N. Parent, C. Tang, T. S. Baker, F. A. Tezcan (2012). "Metal-Directed, Chemically-Tunable Assembly of One, Two and Three-Dimensional Crystalline Protein Arrays", **Nat. Chem.**, *4*, 375-382.
5. D. J. E. Huard, K. M. Kane, F. A. Tezcan (2013), "Re-engineering protein interfaces yields copper-inducible ferritin cage assembly", **Nat. Chem. Biol.**, *9*, 169-176.
6. A. Medina-Morales, A. Perez, J. D. Brodin, F. A. Tezcan (2013), "In Vitro and Cellular Self-Assembly of a Zn-binding Protein Cryptand via Templated Disulfide Bonds", **J. Am. Chem. Soc.,** *in revision.*
7. J. D. Brodin, J. Carr, F. A. Tezcan (2013), "Exceptionally Stable Designed Protein Assemblies with Innate Redox Functionalities to Control the Templated Growth of Pt Nanocrystals, **J. Am. Chem. Soc.,** *to be submitted.*

An Investigation into The Effects Of Interface Stress And Interfacial Arrangement On Temperature Dependent Thermal Properties Of A Biological And A Biomimetic Material

Tao Qu, Yang Zhang, and Vikas Tomar
Purdue University-West Lafayette
Email: Tomar@purdue.edu Cell: 317-294-3251

Project Abstract

A significant effort in the biomimetic materials research is on developing materials that can mimic and function in the same way as biological tissues, Reddi (2000; Shin et al. (2003), bio-inspired electronic circuits, Haupt and Mosbach (2000), bio-inspired flight structures, Thakoor et al. (2002; Thakoor et al. (2003), bio-mimetic materials processing, Heuer et al. (1992; Mann (1995; Aksay et al. (1996; Barthelat (2007), and structural biomimetic materials, Gao (2006; Fratzl and Weinkamer (2007; Chen et al. (2008; Meyers et al. (2008) etc. Most structural biological and biomimetic material properties are affected by two primary factors: **(1)** interfacial interactions between an organic and an inorganic phase usually in the form of interactions between an inorganic mineral phase and organic protein network; and **(2)** structural arrangement of the constituents. Examples are exoskeleton structures such as spicule, Mayer and Sarikaya (2002; Aizenberg et al. (2005), nacre, Lin and Meyers (2005), and crustacean, Raabe et al. (2005; Raabe et al. (2006), Fig. 1. A significant effort is being directed towards making synthetic biomimetic materials based on a manipulation of the above two primary factors.

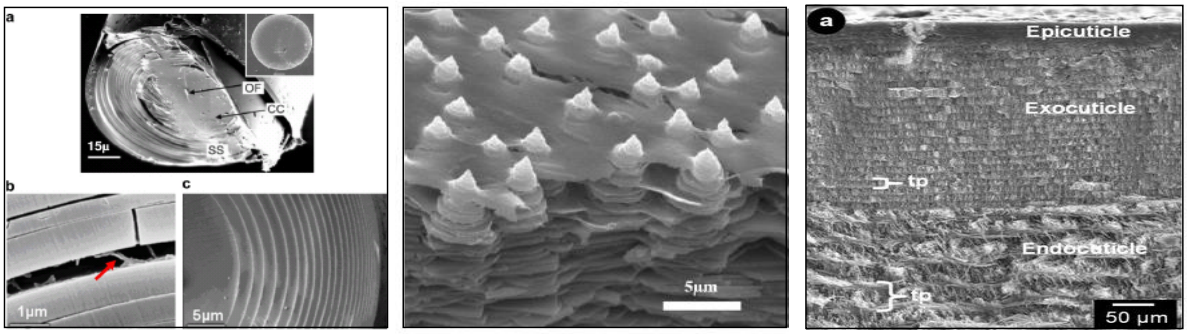

(a) **(b)** **(c)**

Fig. 1: An illustration of three different types of biomaterial morphologies (a) sponge spicule, Aizenberg et al. (2005), (b) aragonite nacre, Lin and Meyers (2005; Tang et al. (2007), and (c) crustacean exoskeleton Raabe et al. (2005)

The proposed research is based on a hypothesis that in synthetic materials with biomimetic morphology thermal conductivity, *k*, (how fast heat is carried away) and thermal diffusivity, *D*, (how fast a material's temperature rises: proportional to the ratio of *k* and heat capacity) can be engineered to be either significantly low or significantly high based on a combination of chosen interface orientation and interfacial arrangement in comparison to conventional material microstructures with the same phases and phase volume fractions.

The following are the main findings of the ongoing research project (started Fall 2012).

METHOD DEVELOPMENT

1. We have established a combined Raman spectroscopy and nanomechanical loading based experimental framework to perform environment (liquid vs. air vs. vacuum) dependent and

temperature dependent (~1000 degree-C) *in-situ* thermal diffusivity measurements in biomaterials at nanoscale to micron scale along with the corresponding analytical theoretic calculations. (Zhang and Tomar, 2013)

2. We have also established a new classical molecular simulation based framework to measure thermal diffusivity in biomolecular interfaces. We are writing a publication currently (Qu and Tomar, 2013) to report the framework and findings in tropocollagen-hydroxyapatite based idealized biomaterial interfaces.

PHYSICAL FINDINGS

1. Analyses using experiments have revealed that in the case of bone thermal conductivity and thermal diffusivity at micron scale shows significant dependence on compressive stress and temperature. Overall, there is a decrease with respect to increase in temperature and increase with respect to increase in compressive stress. Bio-molecular simulations on idealized tropocollagen-hydroxyapatite interfaces confirm such findings. However, simulations also reveal that thermal diffusivity and thermal conductivity can be significantly tailored by interfacial orientation. More importantly, in inorganic materials, interfaces contribute to reduce thermal conductivity and diffusivity. However, analyses here reveal that both can be increased despite presence of a lot of interfaces.
2. Based on significant role played by interfaces in affecting bone thermal properties, a crustacean-exoskeleton system (Fig. 1-c) is examined for thermal diffusivity using the newly developed setup. Special emphasis here is on this system since such arrangement is found to be common in fresh water shrimp as well as in some deep water organisms surviving in environment extremes. Experiments reveal that in such system thermal diffusivity is highly tailorable. More importantly, experiments show that in such materials thermal diffusivity shows an increase as a function of temperature increase contrary to the normal notion in inorganic materials where presence of interfaces leads to reduction in thermal conductivity and consequently thermal diffusivity.
3. Overall, experiments and models have established that in biomaterial interfaces a counterintuitive role of interfaces in mediating thermal conduction as a function of stress and temperature is possible in contrast to inorganic materials where interfaces almost always lead to reduction of thermal conductivity as a function of such factors. More investigations are underway to reveal physical origins of such counter-physical characteristics. Such principles can be significantly useful in developing new and innovative bioenergy and inorganic energy systems where heat dissipation significantly affects system performance.

Student Supported

Yang Zhang (Experiments) and Tao Qu (modeling). Both are PhD students. Tao Qu started on the project in spring 2014 and Yang Zhang has been working since Fall 2012.

Publications in preparation (all supported by DoE-BES with no cross-connection with another funding agency)

1. Zhang, Y. and Tomar, V., 2013, "Micron scale measurements of stress and temperature dependent diffusivity in bone tissue"
2. Zhang, Y. and Tomar, V., 2013, "An investigation of stress dependent transient thermal diffusivity in fresh water shrimp structures"

3. Qu, T., and Tomar, V., 2013, "Classical molecular dynamics based simulations on thermal diffusivity in tropocollagen-hydroxyapatite based biomolecular systems"

Invited Talks

4. Qu, T., Zhang, Y. and Tomar, V., 2013, "Interfacial Biothermomechanics of BioMaterial Interfaces", MRS Fall meeting 2013
5. Qu, T., Zhang, Y. and Tomar, V., 2013, "Interfacial Biomechanics Of Material Interfaces in Tropocollagen and Chitin Based Materials", Thermec Meeting, December 2013

References

Aizenberg, J., Weaver, J., Thanawala, M., Sundar, V., Morse, D. and Fratzl, P. (2005). "Skeleton of Euplectella sp.: structural hierarchy from the nanoscale to the macroscale." Science **309**: 275-278.

Aksay, I. A., Trau, M., Manne, S., Honma, I., Yao, N., Zhou, L., Fenter, P., Eisenberger, P. M. and Gruner, S. M. (1996). "Biomimetic pathways for assembling inorganic thin films." Science **273**(5277): 892-898.

Barthelat, F. (2007). "Biomimetics for next generation materials." Philos. Transact A Math Phys. Eng Sci. **365**(1861): 2907-2919.

Chen, P.-Y., Lin, A. Y. M., Lin, Y.-S., Seki, Y., Stokes, A. G., Peyras, J., Olevsky, E. A., Meyers, M. A. and McKittrick, J. (2008). "Structure and mechanical properties of selected biological materials." J. Mech. Behav. Biomed. Mat. **1**: 208-226.

Fratzl, P. and Weinkamer, R. (2007). "Nature's hierarchical materials." Prog. Mat. Sci. **52**: 1263-1334.

Gao, H. (2006). "Application of fracture mechanics concepts to hierarchical biomechanics of bone and bone-like materials." International Journal of Fracture **138**: 101-137.

Haupt, K. and Mosbach, K. (2000). "Molecualrly imprinted polymers and their use in biomimetic sensors." Chem Rev. **100**(7): 2495-2504.

Heuer, A. H., Fink, D. J., Laraia, V. J., Arias, J. L., Calvert, P. D., Kendall, K., Messing, G. L., Blackwell, J., Rieke, P. C. and Thompson, D. H. (1992). "Innovative materials processing strategies: a biomimetic approach." Science **255**(5048): 1098-1105.

Lin, A. and Meyers, M. A. (2005). "Growth and structure in abalone shell." Mater Sci Eng A **390**: 27-41.

Mann, S. (1995). Biomimetic materials chemistry, Wiley-VCH.

Mayer, G. and Sarikaya, M. (2002). "Rigid biological composite materials: structural examples for biomimetic design." Exp Mech **42**: 395-403.

Meyers, M. A., Chen, P.-Y., Yu-Min Lin, A. and Seki, Y. (2008). "Biological materials: Structures and mechanical properties." Progress in Material Science **53**: 1-206.

Raabe, D., Romano, P., Sachs, C., Fabritius, H., Al-Sawalmih, A., Yi, S., Servos, G. and Hartwig, H. G. (2006). "Microstructure and crystallographic texture of the chitin-protein network in the biological material of the exoskeleton of the the lobster Homarus americanus." Mater Sci Eng A **421**: 143-153.

Raabe, D., Sachs, C. and Romano, P., ;:. (2005). "The crustacean exoskeleton as an example of a structurally and mechanically graded biological nanocomposite material " Acta Mater **53**: 4281-4292.

Reddi, A. H. (2000). "Morphogenesis and tissue engineering of bone and cartilage: Inductive signals, stem cells, and biomimetic biomaterials." Tissue Engg. **6**(4): 351-359.

Shin, H., Jo, S. and Mikos, A. G. (2003). "Biomimetic materials for tissue engineering." Biomaterials **24**(24): 4353-4364.

Tang, H., Barthelat, F. and Espinoa, H. D. (2007). "An elasto-viscoplastic interface model for investigating the constitutive behavior of nacre." J. Mech. Phys. Solids **55**: 1410-1438.

Thakoor, S., Cabrol, N., Lay, N., Chahl, J., Soccol, D., Hine, B. and Zornetzer, S. (2003). "Review: The benefits amd applications of bioinspired flight capabilities." J. Robotic Systems **20**(12): 687-706.

Thakoor, S., Chahl, J., Srinivasan, M. V., Young, L., Werblin, F., Hine, B. and Zornetzer, S. (2002). "Bioinspired engineering of exploration systems for NASA and DoD." Artificial Life **8**(4): 357-369.

Self-Assembly of Pi-Conjugated Peptides in Aqueous Environments Leading to Energy-Transporting Bioelectronic Nanostructures

PI: John D. Tovar
Johns Hopkins University, Department of Chemistry, Department of Materials Science and Engineering, and Institute for NanoBioTechnology, NCB 316, Baltimore, MD 21218
Email: tovar@jhu.edu
Group webpage: http://www.jhu.edu/~chem/tovar/index.html

Program Scope: The design of electronically relevant peptide-based nanomaterials capable of energy migration and interaction with the biotic interface would be the first step towards the transduction of artificial and natural energy currencies for harvesting or transport. This DOE program is concerned with our efforts to synthesize and understand pi-conjugated self-assembling peptides that form one-dimensional electronically delocalized materials under completely aqueous conditions. In the context of peptide-based electronic materials, this poses several challenges. First, the pi-conjugated entities tend to be very insoluble in aqueous environments so careful peptide design must be capable of providing molecular solubility. Second, the cofacial pi-stacking recognized as optimal for energy migration suffers from electrostatic quadrupolar repulsion among the pi-electron clouds and must be compensated for by design with other more enthalpically favorable electrostatic interactions among the peptide hydrogen-bonding arrays.

We developed self-assembling peptides bearing a diverse range of pi-electron structures. These molecules can be triggered to self-assemble into discrete 1-D nanostructures through changing solution pH or even in the presence of cell culture media and other media of high ionic strength. During molecular association and aggregation into the supramolecular nanostructures (Figure 1), the peptide sequences undergo hydrogen bonding and thereby force the pi-electron units into close pi-stacked orientations. The initiation of molecular self-assembly into discrete 1-D nanostructures is achieved through changing solution pH or even in the presence of cell culture media and physiologically relevant calcium ion concentrations. These materials were characterized photophysically using steady-state and time-resolved UV-vis, photoluminescence and circular dichroism. Nanomaterial morphologies were visualized using atomic force, scanning electron and transmission electron microscopies. The resulting nanostructures are under 10 nm in diameter and extend microns in length. This ability to fashion pi-conjugated structures from aqueous environments at this length scale is unprecedented and opens up many possibilities for future research as discussed below.

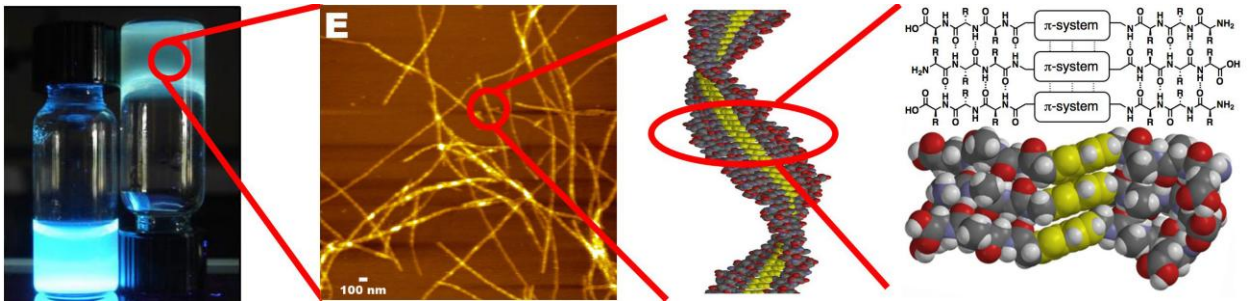

Figure 1: A solution of pi-conjugated (bithiophene) peptides (fluorescent at far left) is triggered to assemble resulting in a macroscopic self-supporting hydrogel comprised of random networks of 1-D nanostructures (center left) that form as molecular components (far right) self-associate into pi-stacked aggregates (center right).

Recent progress. The primary research activities over the past two years have involved getting the preliminary results described at the last Contractor's Meeting to full and complete form for publication. Critical new scientific advances over the past two years of the program include (1) the development of new synthesis strategies to incorporate pi-electron complexity into the peptide frameworks, (2) development of new nanomaterial alignment strategies, and (3) photophysical and electrical measurements within individual nanostructures and within globally aligned macrostructures. Six papers arising from DOE support have been published or accepted, and three others are currently (or will very shortly be) under review. These publications include three invited review/feature article manuscripts.

(1) New synthesis techniques. Our prior synthetic approaches required difficult syntheses of amino acid or diacid containing pi-electron units. We devised two alternative strategies that minimize the need for complex synthetic chromophores and at the same time allow for a much greater diversity of electronic structures (Refs 4 and 9, the former shown in Figure 2). Rather than synthesize the full pi-conjugated segment, we can simply N-acylate a resin-bound peptide with a small portion of an aryl halide and then use on-resin palladium-catalyzed chemistry to "cross-link" two peptide chains leading to an internally embedded conjugated oligomer. This is a much more versatile approach in that smaller and synthetically more tractable fragments are necessary. Using these new strategies, we prepared some of the longest pi-conjugated oligomer sequences yet reported within completely water soluble oligopeptides which will be important for encouraging more effective aqueous energy migration through the resulting supramolecular nanostructures.

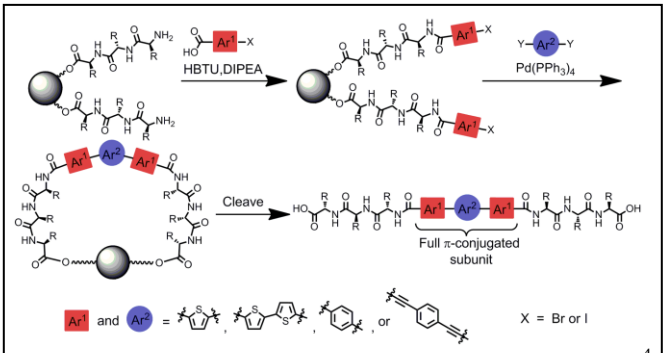

Figure 2: Solid-phase palladium-catalyzed cross-coupling.[4]

(2) Macroscopic alignment of peptide nanostructures. Utilizing a method developed in the Stupp lab at Northwestern, we prepared macroscopic noodle-like hydrogels comprised of globally aligned peptide nanostructures (Figure 3). The chromic properties of the internal pi-conjugated groups can be used in lieu of external dyes and at the same time can impart new functions to the macroscopic noodle structures. The individual aligned features observed in the SEM are on the order of 30-40 nm, suggesting that they are made up of several bundled peptide amphiphile nanostructures whose long axes are coincident with the noodle long axis (or, the direction of solution extrusion). The nature of the molecular aggregation event enforces cofacial interactions among the pi-electron units with the axis of intermolecular delocalization running coincident with the nanomaterial long-axis and subsequently along the noodle long axis, leading

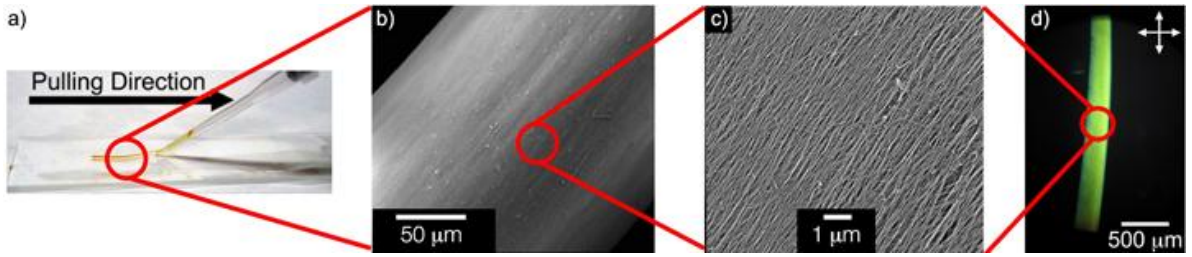

Figure 3: Different size scales to visualize the optoelectronic noodles: Macro (a), meso (b,d) and micro (c). Panel (a) was visualized by naked eye, (b) and (c) with SEM and (d) with a light microscope.[5]

to anisotropic electrical properties in the macrostructure. This work appeared as a cover article in *Advanced Materials*.[1] In a continuation project, we used the noodle fabrication process to prepare aligned matrices of reactive peptides that could be triggered to photopolymerize into conjugated polymer nanomaterials (specifically, based on the diacetylene monomer unit).[2] This gives access to an entirely new class of covalently linked nanomaterials in addition to the extensive library of non-covalent intermolecularly delocalized nanomaterials at our disposal.

Unfortunately, the ability to achieve homogeneous alignment throughout the noodle volume was subject to empirical fickleness. C. M. Schroeder and W. L. Wilson at UIUC were interested in making this process more reproducible and potentially more scaleable. They devised a microfluidic device that allows for controllable assembly and dis-assembly conditions (flow rates, concentrations, etc.) as well as direct in situ spectral profiling of the noodle structures thus formed.[7] The homogeneity of the optical properties is much more evident than with the manual noodle drawing techniques. DOE-supported contributions in this joint effort consisted of material synthesis and discussion of photophysical results, the independent intellectual aspects of device design and implementation were led by the UIUC team.

(3) Photophysical studies of "supramolecular polymorphism". The presence of exciton-coupled pi-electron units within the interior of peptide nanomaterials offers a very rich structure-space to explore static and dynamic spectral properties. The facile tunability of peptide sequences furthers this space. We are finalizing an exhaustive full paper documenting how subtle changes in peptide sequence can rationally influence electronic coupling within the 1-D nanomaterials.[8] We find very clear progressions between classical H-aggregate exciton coupling and excimer-like structures as the steric bulk and/or the hydrophobicity of the amino acid residues are altered at controlled positions along the peptide backbone in molecules of the form HO-DXXX-OPV-XXXD-OH, where X denotes a possible site of variation and OPV is the central embedded styryl chromophore. This "polymorphism" arises from the fact that the molecular design can accommodate several variations in intermolecular electronic coupling among the same chromophore unit just by varying the primary amino acid sequence.

Current research activities. Work over the past several months has focused on two specific subtasks of our award application.

(1) Graphene-based peptide nanostructures. The first involves the development of suitable "2-D" conjugated electronic structures that mimic in part graphene subunits. Multiple reactive groups are being installed to anchor peptides using the synthetic methods developed in our labs previously. We are examining new subunits as well as known subunits known in the literature or supplied in collaborative efforts by interested researchers. The polyvalent peptide presentation as determined in our preliminary research does not impact nanostructure formation as observed photophysically, and we are exploring the morphologies of the resulting materials using electron microscopy. Our synthetic designs for graphene fragments involve the installation of carboxylic acid groups (for amide bond formation to peptide chains) or functionality reactive under palladium catalysis (halides, alkynes). The parent cores are oftentimes known materials, but the C3 symmetries we are targeting for the functionalization chemistries are not.

(2) Biosignal presentation. We have prepared pi-conjugated peptides that express biotin, a well-known ligand for streptavidin protein binding. In our materials, not only can we use the inherent biotin-streptavidin photophysics to characterize the binding, but we also expect modulation of the nanostructure pi-electron delocalization in intramolecular and intermolecular regimes. These investigations will allow us to understand how the abiotic electronic materials can interface with biological systems. The molecules form nanomaterials upon assembly as

observed by TEM, and we are now exploring their response to the biological signal. We have used biotin in the context of photopolymerizable diacetylene peptide molecules that assemble prior to photoreaction, and we anticipate similar studies to examine non-covalent electronic perturbations (e.g., among aggregated oligothiophenes)

Future plans. In addition to our continuing synthetic, optoelectronic and morphological characterization, we plan to initiate studies of internal electric field creation within the nanomaterials by way of heterostructure formation by way of co-assembling (via self-sorting) molecules with different peptide sequences and different pi-electron properties and through photoseparation of photogenerated excitons based on charge transfer mechanisms to pendant electron accepting residues adjacent to the pi-conjugated stacked units buried within the nanomaterials. These two elements were critical components of our recently awarded renewal.

List of papers to acknowledge DOE support: 2011-2013

[1] B. D. Wall,* S. R. Diegelmann,* S. Zhang,* T. J. Dawidczyk, W. L. Wilson, H. E. Katz, H.-Q. Mao and J. D. Tovar, "Aligned macroscopic domains of optoelectronic nanostructures prepared via the shear flow assembly of peptide hydrogels," cover article in ***Advanced Materials***, 2011 (23) 5009-5014. (DOI: 10.1002/adma.201102963) (* contributed equally)

[2] S. R. Diegelmann, N. Hartman, N. Markovic and J. D. Tovar, "Synthesis and alignment of discrete polydiacetylene-peptide nanostructures," in the ***Journal of the American Chemical Society***, 2012 (134) 2028-2031. (DOI: 10.1021/ja211539j)

[3] B. D. Wall and J. D. Tovar, "Synthesis and characterization of pi-conjugated peptide-based supramolecular materials," invited by ***Pure and Applied Chemistry*** (selected conference papers from the 14th International Symposium on Novel Aromatic Compounds, Eugene, OR, July 2011), 2012 (84) 1039-1045. (DOI:10.1351/PAC-CON-11-10-24)

[4] A. M. Sanders, T. J. Dawidcyzk, H. E. Katz and J. D. Tovar, "Peptide-based supramolecular semiconductor nanomaterials via Pd-catalyzed solid-phase 'dimerizations'," in ***ACS Macro Letters***, 2012 (1) 1326-1329. (DOI: 10.1021/mz3004665)
NOTE: correction posted 3 December 2012 (DOI: 10.1021/mz300622w)

[5] J. D. Tovar, "Supramolecular construction of optoelectronic biomaterials," invited by ***Accounts of Chemical Research***, 2013, (46) 1527-1537. (DOI: 10.1021/ar3002969)

[6] S. R. Diegelmann and J. D. Tovar, "Polydiacetylene-peptide one-dimensional nanomaterials," invited as a Feature Article by ***Macromolecular Rapid Communications,*** *accepted.*

[7] A. B. Marciel, M. Tanyeri, B. D. Wall, J. D. Tovar, C. M. Schroeder, W. L. Wilson, "Fluidic-directed assembly of aligned oligopeptides with π-conjugated cores," *revisions requested.*

[8] B. D. Wall, A. E. Zacca, W. L. Wilson, A. L. Ferguson and J. D. Tovar, "Supramolecular polymorphism: Tunable electronic interactions within pi-conjugated peptide nanostructures dictated by primary amino acid sequence," *to be submitted.*

[9] A. M. Sanders and J. D. Tovar, "Solid-phase Pd-catalyzed cross-coupling methods for the construction of pi-conjugated peptide nanomaterials," *submitted.*

Dynamic Self-assembly, Emergence, and Complexity
Principal investigator: George M. Whitesides
Department of Chemistry and Chemical Biology
Harvard University
Cambridge MA 02138
Gwhitesides@gmwgroup.harvard.edu

i. PROGRAM SCOPE.

General Description. The focus of this research program continues to be the study of complex systems, and especially complex systems whose properties manifest themselves in terms of patterns or regular structures, in biomimetic-like motions, or in unusual physical behaviors.

The program has two general goals. i) To build (e.g., in chemical terms, to "synthesize") complex systems, by selecting and characterizing individual components, adding them to the system one at a time, and observing the appearance of unexpected behaviors and phenomena. ii) To use ideas taken from biological systems—themselves prototypically complex—as stimuli for invention in functional materials and structures, robotics, and other areas.

Subprograms, short description. This program has focused on four types of self-assembly involving both static and dissipative systems: **i) Meso-Scale Self-Assembly of Coulombic Crystals.** Contact electrification has been used to form arrays (in 2D) of charged spherical particles, and the assembly of these particles studied as a function of relative charge, shape, and other parameters. This work provides a physics-based model for crystallization and phase-change. **ii) "Entropic" Self-assembly.** Meso-scale particles—even when uncharged—self-assemble when agitated. The mechanism of this self-assembly is not entirely obvious, but is probably related to some of the types of entropic mechanisms for self-organization observed with colloids and macromolecules. **iii) New Materials and Systems:** We have been particularly interested in superhydrophobic paper, as a material for construction of new functional systems, and in Magnetic Levitation as a process enabling 3D self-assembly, and new types of measurements of densities. i**v) Self-organization of Flamelets and Plasmas; Charge Transport by Tunneling.** Flames are prototypical dissipative systems, and systems of flamelets show a variety of self-organizing structures. Tunneling through self-assembled monolayers is finally becoming a system that is convenient and reproducible enough that it is generating reliable data characterizing relationships between the structure of the molecules in the SAM, the SAM, and the junction. **Discontinued areas:** We have largely stopped work on the worm (C. elegans), because—although it is an excellent system to study for physical scientists interested in biological organisms, we have better opportunities elsewhere.

Significance. This research is important for three reasons:

i) It is discovering and developing systems appropriate for a "constructionist" approaches to fundamental studies of complexity and simplicity.
ii) It is providing new tools for materials scientists ("Leegoos," superhydrophobic paper, magnetic levitation.)
iii) It is generating fundamental mechanistic information about processes important in transport of electrical charge (especially tunneling of charge through thin insulating films)

ii. RESEARCH PROGRESS

The following examples illustrate results in the last year. These systems are fully described in papers published during the year, and listed at the end of this abstract.

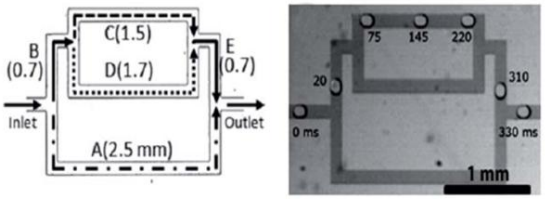

This diagram shows the type of counter intuitive, "complex" but deterministic pattern of paths taken by bubbles flowing in a system of microchannels. The bubbles take the *longest*, rather than the shortest, path through the system.

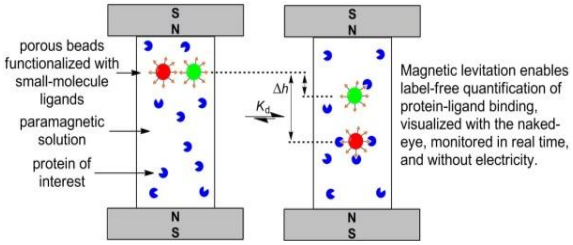

Magnetic levitation (MagLev) provides a new way to estimate densities, and to carry out new types of assays, by balancing magnetic and gravitational buoyancy. In this illustration, adsorption of a protein to a diamagnetic bead suspended in a paramagnetic solution and placed between the poles of two solid-state NbFeB magnets with like poles facing changes the density of the bead sufficiently to provide an easily detectable signal.

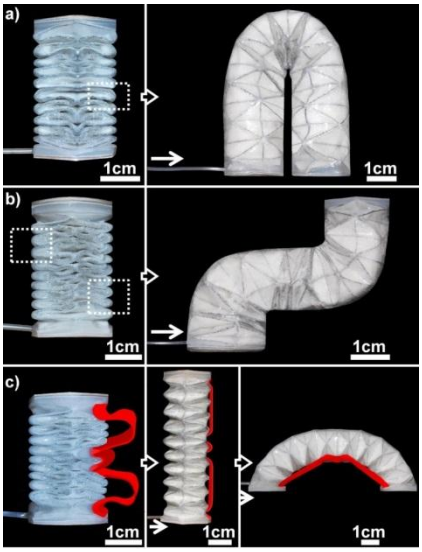

Most machines and actuators are made from rigid structural elements, connected by bearings or joints, and moved by electric motors. We are developing a set of machines and robots that rely on compressed air (~0.5 atm) to actuate structures made of composites of elastomeric polymers and flexible but non-extensible reinforcing agents. These images show an "origami-like" structure modified in several ways to control its motion on pneumatic inflation. In each, the figure on the left—on pressurization—expands into the figure on the right.

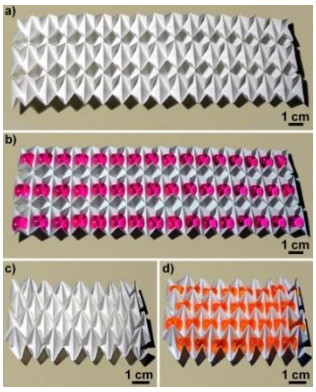

Treatment of paper with a polyfluorinated siloxane (e.g., $C_8F_{13}CH_2CH_2SiCl_3$) yields a remarkable material—omniphobic paper—which is more hydrophobic than Teflon, and unwetted by most hydrocarbons, but still completely permeable to gasses. These picture show that simply folding this "Rf paper" (into an origami-like structure) creates a series of "wells" that contain water containing dyes. This demonstration is of a prototype of a structure to be used as a replacement for 96-well plates in some kinds of experiments.

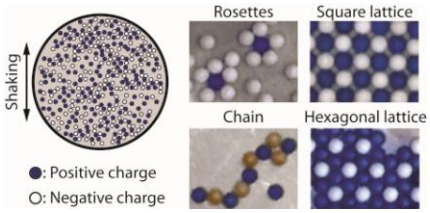

Electrostatic charging of polymeric matter by contact electrification is increasingly well understood. It is now possible to use this kind of charging to create patterns with well-defined structures by self-assembly.

iii. FUTURE PLANS AND CHANGES IN DIRECTION

Contact Electrification: Studies of Mechanisms. We have made substantial qualitative progress in understanding many of the mechanisms of contact electrification involving organic insulators. We are now involved in quantitative studies of rates of charging. These studies are demonstrating that some of the processes that we considered to be single, seem, in fact, to be multiple: that is, there are indications of multiples competing processes. We will continue to disentangle these complex processes (which probably involve competing reactions that lead to charging and discharging). We will continue with fundamental mechanistic studies, with the intention of understanding the multiple processes (ion transfer, corona discharge, electrostatic discharge (sparking)). We will also continue work already started in van de Graaff generators.

Bubbles in Channels. We have a particular interest in erythrocytes and leucocytes moving in blood vessels, and will finish projects already started in this area. Unless, however, we find other uses for bubbles/droplets in microchannels, we intend to stop this work. (We do plan exploratory work in two-phase fluids moving in random porous media—a subject of substantial interest in its own right, and of distant but fundamental relevance to fracing (pressure fracturing.)

Flamelets. The study of systems of small, interacting flames has been exceptionally difficult experimentally, but continuingly attractive as a model system for studying dissipative processes. We believe that we *finally* have a reproducible system, and will begin to examine the behavior of this prototypic dissipative system.

Soft Robotics and Soft Machines. This area is a very rich one—in its materials science, for its emphasis on functional systems in which materials are a major part, and because of its effort to abstract principles from "simple" living systems that can be used—albeit using mechanisms and actuators different than those in biology—in non-living systems.

1 PAPERS PUBLISHED, IN PRESS, SUBMITTED WITH SUPPORT FROM THIS DoE GRANT (2012/2013)

DROPLETS AND BUBBLES

1 "The Magnitude of Lift Forces Acting on Drops and Bubbles in Liquids Flowing inside Microchannels", Stan, C. A., Ellerbee, A. K., Guglielmini, L., Stone, H. A. and Whitesides, G. M. Lab on a Chip, 2012, 13, 365-376.

BIOLOGICAL SYSTEMS

2 "A Microfluidic Device for Whole-Animal Drug Screening using Electrophysiological Measures in the Nematode C. elegans", Lockery, S. R., Hulme, S. E., Roberts, W. M., Robinson, K. J., Laromaine, A., Lindsay, T. H., Whitesides, G. M. and Weeks, J. C. Lab on a Chip, 2012, 12, 2211-2220.
3. "Measuring Binding of Protein to Gel-Bound Ligands Using Magnetic Levitation", Shapiro, N. D., Mirica, K. A., Soh, S., Phillips, S. T., Taran, O., Mace, C. R., Shevkoplyas, S. S. and Whitesides, G. M. J. Amer. Chem. Soc., 2012, 134, 5637-5646.
4. "Using Magnetic Levitation to Separate Mixtures of Crystal Polymorphs", Atkinson, M. B. J., Bwambok, D. K., Chen, J., Chopode, P. D., Thuo, M. M., Mace, C. R., Mirica, K. A., Kumar, A. A., Myerson, A. S. and Whitesides, G. M. submitted 2013

SOFT ROBOTICS AND SOFT ACTUATORS

5. "Elastomeric Origami: Programmable Paper-Elastomer Composites as Pneumatic Actuators", Martinez, R. V., Fish, C. R., Chen, X. and Whitesides, G. M. Adv. Func. Mater., 2012, 22, 1376-1384.
6. "Camouflage and Display for Soft Machines", Morin, S. A., Shepherd, R. F., Kwok, S. W., Stokes, A. A., Nemiroski, A. and Whitesides, G. M. Science, 2012, 337, 828-832.
7. "Robotic Tentacles with Three-Dimensional Mobility Based on Flexible Elastomers ", Martinez, R. V., Branch, J. L., Fish, C. R., Lin, L., Suo, Z. and Whitesides, G. M. Advanced Materials, 2013, 25, 205-212.
8. "Omniphobic "R^F Paper" Produced by Silanization of Paper with Fluoroalkyltrichlorosilanes", Glavan, A., Martinez, R. V., Subramaniam, A. B., Yoon, H. J., Nunes, R. M. D., Lange, H., Thuo, M. M. and Whitesides, G. M. *Adv. Func. Mater.*, In press 2013,
9. "Stretchable, Transparent, Ionic Conductors", Keplinger, C., Sun, J.-Y., Foo, C., Whitesides, G. M. and Suo, Z. G. *Science*, submitted 2013,

ELECTRETS, ELECTROSTATIC CHARGING, AND CHARGE TUNNELING

10. "Analog Modeling of Worm-Like Chain Molecules Using Macroscopic Beads-on-a-String", Tricard, S., Feinstein, E., Shepherd, R. F., Reches, M., Snyder, P. W., Bandarage, D. C., Prentiss, M. and Whitesides, G. M. Phys. Chem. Chem. Phys., 2012, 14, 9041-9046.
11. "A Simple Two-Dimensional Model System to Study Electrostatic-Self-Assembly", Cademartiri, R., Stan, C. A., Tran, V. M., Wu, E., Frair, L., Vulis, D., Clark, L. W., Tricard, S. and Whitesides, G. M. Soft Matter, 2012, 8, 9771-9791.
12. "A Macroscopic Device Described by a Boltzmann-Like Distribution", Tricard, S., Stan, C. A., Shakhnovich, E. I. and Whitesides, G. M. Soft Matter, 2013, 9, 4480-4488.
13. "Statistical Tools for Analyzing Measurements of Charge Transport", Reus, W. F., Nijhuis, C. A., Barber, J. R., Thuo, M. M., Tricard, S. and Whitesides, G. M. J. Phys. Chem. C, 2012, 116, 6714-6733.
14. "Comparison of SAM-Based Junctions with Ga203/EGaIn Top-Electrodes to other Large-Area Tunneling Junctions", Nijhuis, C. A., Reus, W. F., Barber, J. R. and Whitesides, G. M. J. Phys. Chem. C, 2012, 116, 14139-14150.

Multi-Responsive Polyelectrolyte Brush Interfaces:
Coupling of Brush Nanostructures and Interfacial Dynamics

PI: **Y. Elaine Zhu**
Department of Chemical and Biomolecular Engineering
182 Fitzpatrick Hall, University of Notre Dame,
Notre Dame, IN 46556
Email: yzhu3@nd.edu

Program Scope

The overall goal of this project is to, at a molecular level, understand and effectively control the dynamics of probe molecules, neutral or charged, at polyelectrolyte (PE) brush surfaces of tunable brush chain nanostructures and interfacial interactions under varied external stimuli. Specifically, the conformational nanostructures of PE brushes are examined and optimized to consequently enhance interfacial molecular dynamics under varied solution pH, added salts and applied ac-electric fields. With precisely controlled nanostructures of grafted PE brush thin films, the coupling of brush conformations and local counterion concentration of PE brushes in response to solution pH and added salts are investigated. The interfacial dynamics of single probe molecules, neutral versus charged, on weak PE brush surfaces at rest or under nanoscaled ac-electric stimuli is also examined to determine the optimal PE nanostructures and interfacial interaction to effectively enhance interfacial ion and molecular transport. The long-term goal is to establish a new paradigm in molecular design of polyelectrolyte based multi-responsive polymer thin films for efficient ion and molecular transport for energy storage and microfluidic applications.

The experimental methods involve integrated single-molecule imaging and spectroscopic measurements in a microfluidic platform in addition to traditional materials characterization methods such as AFM and light scattering. The project also involves the expertise in the PI's group in polymer brush synthesis and surface modification to molecular design and synthesis of smooth and homogeneous polyelectrolyte thin films for single-molecule experiments.

Recent Progress

We have recently found that the critical solution parameters to control the conformational and phase transition of polymer brushes can be largely shifted by added molecules and macroions, showing a strong dependence of additive molecular size and charge density. The focus of our current activity is to control, characterize, and understand the interaction of nanostructured macroions with PE and biomolecular assemblies in solution and at surface.

- *Effect of macroions on the structure of surface-tethered polyelectrolyte brushes.*

Surface and particle coated by polymer brushes have become important coatings for lubrication and controlled adhesion or components in nanofluidic devices to facilitate efficient transport, however little work has been completed on the molecular-level effects of additives on polymer brush films. Recently, we have found that added small molecules exhibit great effect on the magnitude of the thickness change and conformational transition temperature of neutral thermo-responsive polymer brushes. Currently we have focused on the effect of added macroion on weak PE brushes immersed in aqueous solutions.

As the conformation of PE chain is highly sensitive to local electrostatic environment, we have thus investigated the effect of added macroions on the thickness and conformational transition pH of poly(2-vinyl pyridine) (P2VP), whose coil-to-globule transition (CGT) in dilute solutions has been understood based on our previous work completed in the early stage of this project. In this work, we have focused on polyoxometalate (POM) macroion, $[(MoO_3)_{176}(H_2O)_{80}]Na_{32}$ ($\{Mo_{176}\}$) nanocluster. $\{Mo_{176}\}$ macroion is spherical assemblies of molybdenum transition metal oxides and carries net 32 negative charges uniformly distributed over its well-defined atomic coordination structure of ~3.5 nm in diameter as shown in Figure 1a. By using AFM and contact angle goniometer, we have investigated the change of P2VP brush thickness and surface wettability with added $\{Mo_{176}\}$ macroion. Our earlier work has confirmed the CGT of P2VP brushes occurs over the critical transition pH, pH_{CGT} =2.5 for P2VP brushes of grafting density about 0.1 chain/nm^2.

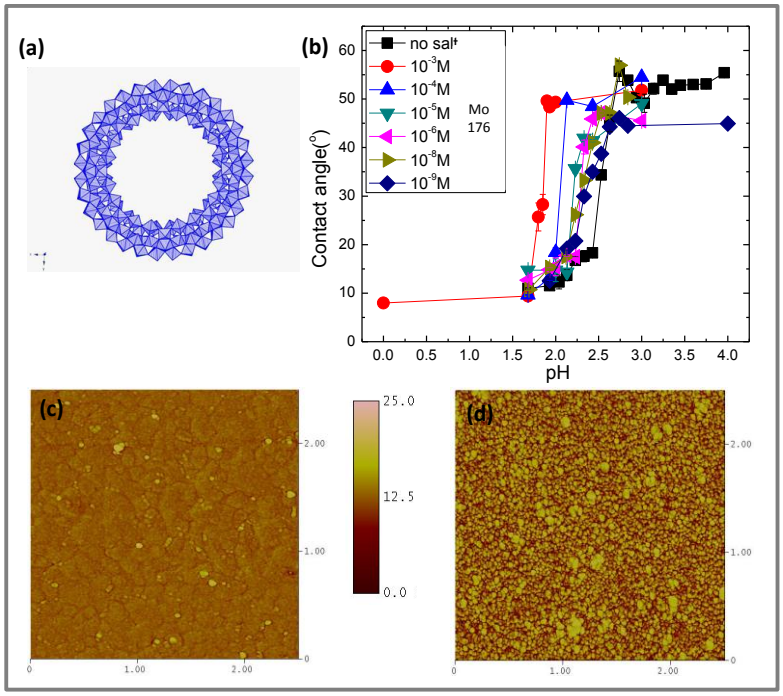

Figure 1. (a) Molecular structure of $\{Mo_{176}\}$ macroion. (b) Water contact angle on P2VP brush thin films against varied pH in solution added with $\{Mo_{176}\}$ macroions, showing the shift of pH_{CGT} to lower pH with increasing macroion concentration, which is opposite to the trend of simple salt effect on pH_{CGT}. which is opposite to the trend of simple salt effect on pH_{CGT}. The contrasting morphology of P2VP brush surfaces without and with macroions as shown in AFM phase image (c) and (d), respectively, indicates the assembly of macroions with P2VP brush chains due to electrostatic attraction.

It is clearly observed in Figure 1b that added $\{Mo_{176}\}$ macroions can significantly lower the pH_{CGT}, whose trend is surprisingly *opposite* to that by adding simple monovalent or divalent salts to P2VP brushes. The unusual effect of macroions on pH_{CGT} in sharp contrast to that of simple ions suggests strong counterion condensation of macroions near PE brush chain. As the morphology of P2VP brush thin films is characterized with $\{Mo_{176}\}$ macroion of increased concentration by AFM, we have confirmed the aggregation of $\{Mo_{176}\}$ macroions with the end segments of P2VP chains at aqueous interfaces, leading to the formation of $\{Mo_{176}\}$-P2VP complexes with resulting increased surface roughness. Such formation of macroion-PE brush complexes can be further explored for molecular design of charge-selective membranes and mechanically reinforced "smart" polymeric coatings for gating, separation and lubrication.

- *Tunable assembly of polyelectrolytes and biomolecules with macroions.*

With stimuli-responsive polyelectrolyte and biomolecules such as lipids, we have explored the processes of their supramolecular assembly on nanoscales. One successful approach we have

recently achieved is to control the nanostructure of hetero-polymeric assembly by POM-based macroions thanks to their unique crystalline ordering.

By using AFM, TEM and light scattering techniques, we have investigated the assembly of P2VP-b-polystyrene (P2VP-PS) diblock copolymers in aqueous solution added with {Mo_{176}} macroions. As shown in Figure 2a, we have observed the self-organization of P2VP-PS into polymer vesicles (polymersomes) with {Mo_{176}} macroions. The presence of embedded {Mo_{176}} macroions is confirmed by the dark rim contrast by TEM as shown Figure 2b. It is sharply contrasted from plain homogenous P2VP-PS polymersomes without {Mo_{176}} macroions. The readily adsorption and assembly of {Mo_{176}} macroions with P2VP-PS polymersomes is contributed to the strong electrostatic interaction between anionic macroions and P2VP blocks. Furthermore, we have found that the size of assembled hybrid polymersomes can be tuned by solution pH and salt concentration as illustrated in Figure 2c-d: the size of macroion-decorated polymersomes can be increased by more than 20 times from its original size by increasing solution pH or simple salt concentration due to pH- and ion-responsive characteristics of P2VP block. More interestingly, we have found that optimal pH and salt concentration are present, allowing the precise control of polymersome swelling. It is also important to note that with embedded macroions, the hybrid polymersome are very stable and well dispersed in solution over several months at least. The applicability of using macroions to form stabilized hybrid polymersome assemblies is demonstrated successfully with other diblock polymers such as PS-b-poly(ethylene oxide) (PS-PEO) and poly(ethylene-oxide)-b-poly(caprolactone) (PEO-PCL).

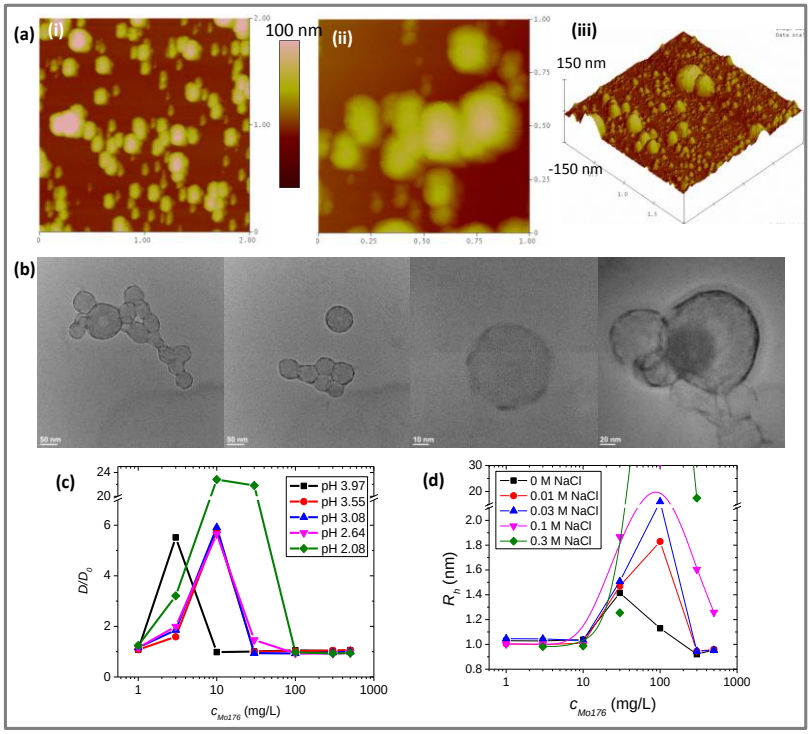

Figure 2. (a) AFM microphaphs of varied scan sizes show the assembly of {Mo_{176}} macroion with P2VP-PS polymersomes in aqueous solution. (b) The presence of macroions in PS-P2VP vesicles is confirmed in dark rims by TEM, also suggesting macroion-enhanced stability and mechanical strength of polymer vesicles. The size of macroion-decorated P2VP-PS polymersomes can be further tuned by varying solution pH and added salt concentration, as shown in (c) and (d), respectively, indicating the preserved pH- and ion-responsive characteristics of macroion-polymersome assemblies.

Additionally, we have explored the same approach to assemble hybrid liposomes using zwitterionic or cationic lipids with {Mo_{176}} macroions. The size of hybrid liposomes decorated with macroions exhibits a similar response to solution ionic environments as macroion-polymersome assemblies.

Future plan:

The exciting and new research development described above will be further pursued. Future plan also includes the investigation of the interaction and dynamics of functional macroions on lipid biomembrane to control the interfacial transport and biomolecule-templated hybrid nanomaterial assembly.

1) *Study the diffusive dynamics and transport of ionic fluorescence probes on P2VP brushes.* In our recent study of the diffusion of fluorescence probe molecules on neutral polymer brushes, we have demonstrated the presence of an optimal brush thickness range for the fastest molecular surface diffusion. Thus we will examine the effect of brush thickness and grafting density on ions and macroions transport through oppositely charged PE brush thin films.
2) *Examine and control the nanocluster assembly at polymer and lipid membrane interface.* With the surprising and exciting observation of POM macroion assembly with polymers and lipid biomolecules, we will continue this work to study the effect of macroion charge density and size on the structural evolution of dynamic self-assembly process of hybrid polymersomes and liposomes. The mechanical reinforcement of macroion-stabilized polymer and lipid vesicles will be examined against macroion concentration. To explore the potential application of macroion-polymer assembly as new membranes for efficient and selective molecule and ion separation, we will also evaluate the selective permeability of small ions through assembled macroion-polymer vesicles of varied polymer chemical composition.

Publications resulting from DoE support in 2011-2013

1) B. Jing, M. Hutin, E. Connor, L. Cronin and Y. Zhu, Polyoxometalate (POM) macroion-induced phase and morphology instability of phospholipid bilayer, *Chemical Sci.* (2013) in press.
2) B. Jing, H. Wang, K.-Y. Lin, P. J. McGinn, C. Na and Y. Zhu, A facile method to functionalize engineering solid membrane supports for rapid and efficient oil-water separation, *Polymer* (2013) in revision.
3) S. Wang and Y. Zhu, Molecular motion at polymer brush interfaces: from simple Brownian diffusion to hydrated lubrication, submitted to *J. Polymer Sci. B* (2013).
4) H. Wang, K. Lin, B. Jin, P. McGinn, Y. Zhu, and C. Na, Magnetic carbon nanotubes for oil-water separation, *Water Research* 47, 4198-4205 (2013).
5) L. C. C. Elliott, B. Jing, B. Akgun, Y. Zhu, P. W. Bohn and S. K. Fullerton-Shirey, Loading and distribution of a model small molecule drug in poly(N-isoproprylacrylamide) brushes: a neutron reflectometry and AFM study, *Langmuir,* 29, 3259-3268 (2013).
6) S. Wang and Y. Zhu, Manipulating single annealed polyelectrolyte chain under ac-electric fields: collapse versus accumulation, *Biomicrofluidics* 6, 024116 (2012).
7) S. Wang, B. Jing and Y. Zhu, Single molecule diffusion on hard, soft and fluid surfaces, *RSC Advances* 2, 3835-3843 (2012).
8) S. Wang and Y. Zhu, Conformation transition and electric potential of single weak polyelectrolyte: Molecular weight dependence, *Soft Matter* 7, 7410-7415 (2011).
9) B. Jing and Y. Zhu, Disruption of supported lipid bilayers by semihydrophobic nanoparticles, *J. Am. Chem. Soc.* 133, 10983-10989 (2011).

Poster Sessions

Biomolecular Materials
Principal Investigators' Meeting

Poster Session I

Monday, August 19, 1:30pm & 5:30pm

1. Directed assembly of hybrid nanostructures using optically resonant nanotweezers
David Erickson, Cornell University

2. Active Assembly of Dynamic and Adaptable Materials: Active Protein Assemblies
George Bachand, Erik Spoerke, Mark Stevens, and Darryl Sasaki, Sandia National Laboratories

3. Active Assembly of Dynamic and Adaptable Materials: Artificial Microtubules
Erik D. Spoerke, George D. Bachand, Mark Stevens, and Darryl Sasaki, Sandia National Laboratories

4. Molecular Nanocomposites—Adaptive and Reconfigurable Nancomposites
Dale L. Huber, Darryl Y. Sasaki, Mark J. Stevens, Carl C. Hayden, Amalie L. Frischknecht, and Paul Clem, Sandia National Laboratories

5. Inducing Artificial Morphogenesis in Soft Synthetic Materials
Anna C. Balazs, University of Pittsburgh

6. Designing Smart, Responsive Communicating Microcapsules from Polymersomes
Daniel Hammer and Daeyeon Lee, University of Pennsylvania

7. Dynamic Self-assembly, Emergence, and Complexity
George Whitesides, Harvard University

8. Dynamics of Active Self-Assembled Materials
Igor S. Aronson and Alexey Snezhko, Argonne National Laboratory

9. Self-Assembly and Self-Replication of Novel Materials from Particles with Specific Recognition
Paul Chaikin, Ned Seeman, Marcus Weck, and David Pine, New York University

10. Actuation of Bioinspired, Adaptive "HAIRS" Powered by Responsive Hydrogels
Joanna Aizenberg and Anna Balazs, Harvard University

11. Protein Biotemplates for Self-Assembly of Nanostructures
Sarah Heilshorn, Nicholas Melosh, Seb Doniach, and Andrew Spakowitz, SLAC National Accelerator Laboratory

12. Bioinspired Hydrogen Bonding-Mediated Assembly of Nano-objects toward Adaptive and Dynamic Materials
Zhibin Guan, University of California, Irvine

13. Surface Mechanical Properties of Bioinspired Architectures
Anand Jagota and Chung-Yuen Hui, Lehigh University

14. Phospholipid Vesicles in Materials Science
Steve Granick, University of Illinois

15. Assembling Microorganisms into Energy Converting Materials
Ozgur Sahin, Columbia University

16. Miniaturized Hybrid Materials Inspired by Nature
Cyrus Safinya, University of California, Santa Barbara

17. Functional, Hierarchical Nanocomposites - Colloidal Liquid Crystal Gels and Liquid Crystal Elastomers
Nicholas L. Abbott and Juan J. de Pablo, University of Wisconsin

18. Dynamic Self-Assembly: Structure, Dynamics, and Function Relations in Lipid Membranes
Atul N. Parikh and Sunil K. Sinha, University of California, Davis

19. Soft-Matter Physics: Directed Self-Assembly of Soft-Matter and Biomolecular Materials
Benjamin Ocko, Antonio Checco, and Masafumi Fukuto, Brookhaven National Laboratory

20. DNA-Grafted Building Blocks Designed to Self-Assemble into Desired Nanostructures
Sanat Kumar, Venkat Venkatasubramanian, Michael Collins, and Oleg Gang, Columbia University

21. Self-Assembling Biological Springs: Force Transducers on the Micron and Nanoscale
Ying Wang, Angel Young, Aleksey Lomakin, and George B. Benedek, Massachusetts Institute of Technology

22. Multi-Responsive Polyelectrolyte Brush Interfaces: Coupling of Brush Nanostructures and Interfacial Dynamics
Y. Elaine Zhu, University of Notre Dame

23. Self-Assembly of Pi-Conjugated Peptides in Aqueous Environments Leading to Energy-Transporting Bioelectronic Nanostructures
John D. Tovar, Johns Hopkins University

24. High Efficiency Biomimetic Organic Solar Cells
Marc A. Baldo and Troy Van Voorhis, Massachusetts Institute of Technology

25. Surface Patterning of Conjugated Polyelectrolytes using Lipid Membrane Domains
D.Y. Sasaki, N. Zawada, S.F. Gilmore, P. Narasimmaraj, M.A.A. Sanchez, J.C. Stachowiak, C.C. Hayden, H.-L. Wang, A.N. Parikh, and A.P. Shreve, Los Alamos National Laboratory

26. Energy and Charge Transfer in Conjugated Systems and Biomolecule Assisted Self-Assemblies

Y.-I. Park, H. Tsai, Z. Liu, M. Cotlet, A. P. Shreve, J. Gao, J. Grey, J.S. Martinez, and H.-L. Wang, Los Alamos National Laboratory

27. Fluorescent Silver and Gold Nanoclusters Tuned for Assembly

J.K. Sharma, H.-C. Yeh, M. Neidig, A. Boncella, R. Rocha, H. Fazelinia, E. Balog, S. Sinha, C. Strauss, H.-L. Wang, A.P. Shreve, and J.S. Martinez, Los Alamos National Laboratory

28. Optical and Electro-optic Modulation of Biomimetically Functionalized Nanocarbon Materials

Myungwoong Kim, Changshui Huang, Yuanchun Zhao, Mark Eriksson, Francois Leonard, Bryan Wong, and Padma Gopalan, University of Wisconsin-Madison

Biomolecular Materials
Principal Investigators' Meeting

Poster Session 2

Tuesday, August 20, 1:00pm & 5:15pm

1. Bioinspired Magnetic Nanomaterials
Surya Mallapragada, Mufit Akinc, Dennis Bazylinski, David Vaknin, Marit Nilsen-Hamilton, Alex Travesset, Monica Lamm, Ruslan Prozorov, Tanya Prozorov, and Klaus Schmidt-Rohr, Ames Laboratory

2. Emergent Atomic and Magnetic Structures
Tanya Prozorov, Ames Laboratory

3. Investigations of Plant Cell Wall Structure using Sensitivity-Enhanced Solid-State NMR Spectroscopy
Tuo Wang, Olga Zabotina, Daniel Cosgrove, and Mei Hong, Ames Laboratory

4. Computational Studies of Programmed DNA Self-Assembly of Inorganic Nanoparticles
Alex Travesset and Chris Knorowski, Ames Laboratory

5. Enzymatic Synthesis of Semiconductors: Directed Evolution of Silicatein, the Silica-Synthesizing Enzyme (and Advantages of Kinetically Controlled Catalytic Synthesis)
Daniel E. Morse, University of California, Santa Barbara

6. Enzyme-Controlled Mineralization in Biomimetic Microenvironments Formed by Aqueous Phase Separation and Giant Vesicles
Christine D. Keating, Pennsylvania State University

7. Molecular Nanocomposites − Complex Nanocomposites
Jeff Brinker, Bryan Kaehr, Hongyou Fan, Eric Carnes, Paul Clem, and Andrew Dattelbaum, Sandia National Laboratories and Los Alamos National Laboratory

8. Material Lessons from Biology: Crystal Engineering via Amplification of Nucleation
Iva Perovic and John Spencer Evans, New York University

9. Material Lessons from Biology: "Borg" Crystal Engineering
Eric Chang, Roland Kroeger, Lara Estroff, and John Spencer Evans, New York University

10. (Bio)Chemical Tailoring of Biogenic 3-D Nanopatterned Templates with Energy-Relevant Functionalities
Kenneth H. Sandhage and Nils Kröger, Georgia Institute of Technology

11. Multicomponent Protein Cage Architectures for Photocatalysis
Arunava Gupta and Peter E. Prevelige, University of Alabama

12. Multicomponent Protein Cage Architectures for Photocatalysis
Trevor Douglas and Bern Kohler, Montana State University

13. Optimizing Immobilized Enzyme Performance in Cell-Free Environments to Produce Liquid Fuels
Joseph J. Grimaldi, Cynthia H. Collins and Georges Belfort, Rensselaer Polytechnic Institute

14. Optimizing Immobilized Enzyme Performance in Cell-Free Environments to Produce Liquid Fuels
Mithun Radhakrishna and Sanat Kumar, Columbia University

15. A Hybrid Biological/Organic Photochemical Half-Cell for Generating Dihydrogen
John H. Golbeck and Donald A. Bryant, Pennsylvania State University

16. A Plant Nanobionic Approach to Enhance Solar Energy Conversion of Extracted Chloroplasts using Spontaneously Assembled Nanoparticles
Michael S. Strano, Massachusetts Institute of Technology

17. Rigid Biopolymer Nanocrystal Systems for Controlling Multicomponent Nanoparticle Assembly and Orientation in Thin Film Solar Cells
Jennifer N. Cha and Dylan Domaille, University of Colorado

18. Modular Designed Proteins Constructions for Solar Generated H2 from Water
P. Leslie Dutton, University of Pennsylvania

19. Using In Vitro Maturation and Cell-Free Expression to Explore [FeFe] Hydrogenase Activation and Protein Scaffolding Requirements
James R. Swartz, Stanford University

20. Nanoengineering of Complex Materials
Samuel I. Stupp, Northwestern University

21. Long Range van der Waals-London Dispersion Interactions for Biomolecular and Inorganic Nanoscale Assembly
Roger H. French and Nicole F. Steinmetz, Case Western Reserve University

22. Long Range van der Waals-London Dispersion Interactions for Biomolecular and Inorganic Nanoscale Assembly
V. Adrian Parsegian and W. Y. Ching, University of Massachusetts-Amherst and University of Missouri-Kansas City

23. Chemically Directed Self-Assembly of Protein Superstructures and Construction of Tunable Redox Functionalities in Their Interfaces
F. Akif Tezcan, University of California, San Diego

24. Electrostatic Driven Self-Assembly Design of Functional Nanostructures
Monica Olvera de la Cruz, Northwestern University

25. Directed Organization of Functional Materials at Inorganic-Macromolecular Interfaces
Aleksandr Noy, Jim De Yoreo, Tony Van Buuren, George Gilmer, and Matt Francis, Lawrence Livermore National Laboratory, Pacific Northwest National Laboratory, and University of California, Berkeley

26. Simulations of Self-Assembly of Nanoparticle Shape Amphiphiles
Sharon C. Glotzer, University of Michigan

27. Programmed Nanomaterial Assemblies in Large-Scale 3D Structures: Applications of Genetically Engineered Peptides to Bridge Nano-assemblies and Macro-assemblies
Hiroshi Matsui, City University of New York, Hunter College

28 Integrating modeling and experiments to design robust self-healing materials
Anna C. Balazs and Kris Matyjaszewski, University of Pittsburgh

29. Experimental Realization of 'Repair-and-Go' using Microencapsulation of Nanomaterials
Todd Emrick, University of Massachusetts-Amherst

30. An Investigation into the Effects of Interface Stress and Interfacial Arrangement on Temperature Dependent Thermal Properties of a Biological and a Biomimetic Material
Tao Qu, Yang Zhang, and Vikas Tomar, Purdue University-West Lafayette

Author Index and List of Participants

Author Index

Participant List

Name	Organization	E-Mail Address
Abbott, Nicholas	University of Wisconsin-Madison	abbott@engr.wisc.edu
Aizenberg, Michael	Harvard University	michael.aizenberg@wyss.harvard.edu
Aronson, Igor	Argonne National Laboratory	aronson@anl.gov
Bachand, George	Sandia National Laboratories, New Mexico	gdbacha@sandia.gov
Balazs, Anna	University of Pittsburgh	balazs@pitt.edu
Baldo, Marc	Massachusetts Institute of Technology	baldo@mit.edu
Belfort, Georges	Rensselaer Polytechnic Institute	belfog@rpi.edu
Brinker, Jeff	Sandia National Laboratories, New Mexico / University of New Mexico	cjbrink@sandia.gov
Bryant, Don	Pennsylvania State University	dab14@psu.edu
Chaikin, Paul	New York University	chaikin@nyu.edu
Checco, Antonio	Brookhaven National Laboratory	achecco@gmail.com
Ching, Wai-Yim	University of Missouri-Kansas City	chingw@umkc.edu
Clem, Paul	Sandia National Laboratories, New Mexico	pgclem@sandia.gov
Click, Tammy	Oak Ridge Institute for Science and Education	tammy.click@orau.org
Crockett, Teresa	U.S. Department of Energy	teresa.crockett@science.doe.gov
de Pablo, Juan	University of Chicago	depablo@uchicago.edu
De Yoreo, James	Pacific Northwest National Laboratory	james.deyoreo@pnnl.gov
Domaille, Dylan	University of Colorado	Dylan.Domaille@colorado.edu
Douglas, Trevor	Montana State University	tdouglas@chemistry.montana.edu
Dutton, P. Leslie	University of Pennsylvania	dutton@mail.med.upenn.edu
Emrick, Todd	University of Massachusetts Amherst	tsemrick@mail.pse.umass.edu
Erickson, David	Cornell University	de54@cornell.edu
Evans, John Spencer	New York University	jse1@nyu.edu
French, Roger	Case Western Reserve University	roger.french@case.edu
Fukuto, Masafumi	Brookhaven National Laboratory	fukuto@bnl.gov
Gersten, Bonnie	U.S. Department of Energy	bonnie.gersten@science.doe.gov
Glotzer, Sharon	University of Michigan	sglotzerkjc@umich.edu
Gopalan, Padma	University of Wisconsin-Madison	pgopalan@wisc.edu
Granick, Steve	University of Illinois, Urbana-Champaign	sgranick@uiuc.edu
Guan, Zhibin	University of California, Irvine	zguan@uci.edu
Gupta, Arunava	University of Alabama	agupta@mint.ua.edu
Hammer, Daniel	University of Pennsylvania	hammer@seas.upenn.edu
He, Ximin	Harvard University	ximinhe@seas.harvard.edu
Heilshorn, Sarah	SLAC National Accelerator Laboratory & Stanford University	heilshorn@stanford.edu
Henderson, Craig	U.S. Department of Energy	craig.henderson@science.doe.gov
Hong, Mei	Iowa State University	mhong@iastate.edu
Huber, Dale	Sandia National Laboratories, New Mexico	Dale.Huber@sandia.gov
Hui, Chung Yuen	Cornell University	ch45@cornell.edu

Jagota, Anand	Lehigh University	anj6@lehigh.edu
Keating, Christine	Pennsylvania State University	keating@chem.psu.edu
Kini, Aravinda	U.S. Department of Energy	a.kini@science.doe.gov
Mallapragada, Surya	Ames Laboratory	suryakm@iastate.edu
Markowitz, Michael	U.S. Department of Energy	mike.markowitz@science.doe.gov
Martinez, Jennifer	Los Alamos National Laboratory	jenm@lanl.gov
Matsui, Hiroshi	CUNY-Hunter College	hmatsui@hunter.cuny.edu
Morse, Daniel	University of California, Santa Barbara	d_morse@lifesci.ucsb.edu
Noy, Aleksandr	Lawrence Livermore National Laboratory	noy1@llnl.gov
Ocko, Ben	Brookhaven National Laboratory	ocko@bnl.gov
Olvera de la Cruz, Monica	Northwestern University	M-Olvera@northwestern.edu
Palmer, Liam	Northwestern University	liam-palmer@northwestern.edu
Parikh, Atul	University of California, Davis	anparikh@ucdavis.edu
Parsegian, Adrian	University of Massachusetts Amherst	parsegian@physics.umass.edu
Podgornik, Rudolf	University of Massachusetts Amherst	podgornik@physics.umass.edu
Prevelige, Peter	University of Alabama Birmingham	prevelig@uab.edu
Prozorov, Tanya	Ames Laboratory	tprozoro@ameslab.gov
Radhakrishna, Mithun	Columbia University	mithun.150887@gmail.com
Safinya, Cyrus	University of California, Santa Barbara	safinya@mrl.ucsb.edu
Sahin, Ozgur	Columbia University	sahin@columbia.edu
Sandhage, Kenneth	Georgia Institute of Technology	ken.sandhage@mse.gatech.edu
Sennett, Michael	U.S. Department of Energy	michael.sennett@science.doe.gov
Shreve, Andrew	University of New Mexico	shreve@unm.edu
Snezhko, Oleksiy	Argonne National Laboratory	snezhko@anl.gov
Spakowitz, Andrew	Stanford University	ajspakow@stanford.edu
Spoerke, Erik	Sandia National Laboratories, New Mexico	edspoer@sandia.edu
Steinmetz, Nicole	Case Western Reserve University	nicole.steinmetz@case.edu
Strano, Michael	Massachusetts Institute of Technology	strano@mit.edu
Stupp, Sam	Northwestern University	jill-johnson@northwestern.edu
Swartz, James	Stanford University	jswartz@stanford.edu
Tezcan, Faik	University of California, San Diego	tezcan@ucsd.edu
Thiyagarajan, Thiyaga	U.S. Department of Energy	p.thiyagarajan@science.doe.gov
Tomar, Vikas	Purdue University	tomar@purdue.edu
Tovar, John	Johns Hopkins University	tovar@jhu.edu
Travesset, Alex	Ames Laboratory	trvsst@ameslab.gov
van Buuren, Anthony	Lawrence Livermore National Laboratory	vanbuuren1@llnl.gov
Vo, Thi	Columbia University	tdv2101@columbia.edu
Wang, Hsing-Lin	Los Alamos National Laboratory	hwang@lanl.gov
Wang, Ying	Massachusetts Institute of Technology	ywang09@mit.edu
Whitesides, George	Harvard University	gwhitesides@gmwgroup.harvard.edu
Zhu, Yingxi (Elaine)	University of Notre Dame	yzhu3@nd.edu